ISTANBUL TECHNICAL UNIVERSITY ★ GRADUATE SCHOOL OF SCIENCE ENGINEERING AND TECHNOLOGY

NUMERICAL ANALYSIS OF PRESTRESSED ANCHORED PILE WALL: SHORING SYSTEM IN FRONT OF HISTORIC BUILDING IN HILTON ISTANBUL BOMONTI HOTEL AND CONFERENCE CENTER PROJECT

M.Sc. THESIS

Ece AKTAN

Department of Civil Engineering

Soil Mechanics and Geotechnical Engineering

Thesis Advisor: Assoc. Prof. Dr. Musaffa Ayşen LAV

MAY 2014

ISTANBUL TECHNICAL UNIVERSITY ★ GRADUATE SCHOOL OF SCIENCE ENGINEERING AND TECHNOLOGY

NUMERICAL ANALYSIS OF PRESTRESSED ANCHORED PILE WALL: SHORING SYSTEM IN FRONT OF HISTORIC BUILDING IN HILTON ISTANBUL BOMONTI HOTEL AND CONFERENCE CENTER PROJECT

M.Sc. THESIS

Ece AKTAN
501091334

Department of Civil Engineering

Soil Mechanics and Geotechnical Engineering

Thesis Advisor: Assoc. Prof. Dr. Musaffa Ayşen LAV

MAY 2014

İSTANBUL TEKNİK ÜNİVERSİTESİ ★ FEN BİLİMLERİ ENSTİTÜSÜ

ÖNGERMELİ ANKRAJLI KAZIKLI DUVAR NÜMERİK ANALİZİ: HILTON ISTANBUL BOMONTI HOTEL VE KONFERANS MERKEZİ PROJESİ KAPSAMINDA YER ALAN TARİHİ BİNA ÖNÜ İKSA SİSTEMİ

YÜKSEK LİSANS TEZİ

Ece AKTAN
501091334

İnşaat Mühendisliği Anabilim Dalı

Zemin Mekaniği ve Geoteknik Mühendisliği Programı

Tez Danışmanı: Doç. Dr. Musaffa Ayşen LAV

MAYIS 2014

Ece AKTAN, a M.Sc. student of ITU Graduate School of Science Engineering and Technology student ID **501091334**, successfully defended the thesis entitled "**NUMERICAL ANALYSIS OF PRESTRESSED ANCHORED PILE WALL: SHORING SYSTEM IN FRONT OF HISTORIC BUILDING IN HILTON ISTANBUL BOMONTI HOTEL AND CONFERENCE CENTER PROJECT**", which she prepared after fulfilling the requirements specified in the associated legislations, before the jury whose signatures are below.

Thesis Advisor :	**Assoc. Prof. Dr. Musaffa Ayşen LAV** İstanbul Technical University	.....
Jury Members :	**Assoc. Prof. Dr. Aykut ŞENOL** Istanbul Technical University	.....
	Assoc. Prof. Dr. Ayşe Edinçliler BAYKAL Bogazici University	.....

Date of Submission : 05 May 2014
Date of Defense : 28 May 2014

To my mother,

FOREWORD

I would like to appreciate honory my advisor Assoc. Prof. Dr. Musaffa Ayşen LAV. I consider all her ideas, time contributions and also her experience. As well as sincere appreciation goes to my advisor for her encouragement and constructive criticisms during the thesis.
I also want to thank the members of my master graduate committe for their guidance and suggestions.
Special thanks go to Zetaş's design manager M.Sc. civil engineer Önder AKÇAKAL for his help.
I would also like to acknowledge my co-workers at IC İçtaş Construction for their friendship and support.
Finally I would like to thank my mother Nil Soysal for all her love and support.

May 2014

Ece AKTAN
(Civil Engineer)

TABLE OF CONTENTS

Page

ABBREVIATIONS

ASSHTO	**:** American Association of State Highway and Transportation Officials
ASTM	**:** American Society for Testing and Materials
BS	**:** British Standards
CAD	**:** Computer Aided Design
DIN	**:** Deutsches Institut für Normung
FEM	**:** Finite Element Modelling
FHWA	**:** Federal Highway Administration
HSM	**:** Hardening Soil Model
ISRM	**:** The International Society for Rock Mechanics
NAVFAC	**:** Naval Facilities Engineering Command
OCR	**:** Overconsolidation Ratio
PLT	**:** Point Load Test
SPT	**:** Standard Penetration Test
USACE	**:** The United States Army Corps of Engineers

LIST OF TABLES

Page

LIST OF FIGURES

Page

NUMERICAL ANALYSIS OF PRESTRESSED ANCHORED PILE WALL: SHORING SYSTEM IN FRONT OF HISTORIC BUILDING IN HILTON ISTANBUL BOMONTI HOTEL AND CONFERENCE CENTER PROJECT

SUMMARY

One of the most significant research subjects in geotechnical engineering is deep excavation support systems. Deep excavation support systems are used to provide a safety work area and to prevent the failure of surrounding structures during foundation construction. These excavation support systems can be built as permanent structures or temporary structures. Within the scope of this thesis, it is dwelled on prestressed anchored walls that are widely used also in our country. The subject of this thesis is the investigation of a shoring system that will be built to support a deep excavation near an adjacent structure and see the effect of some parameters on the behavior of the shoring system. The shoring system was built as a temporary system due to time of the construction.

In this thesis, an actual case study was examined by using a finite element method program Plaxis 8.2. A prestressed anchored pile wall used as an excavation support system for the foundation construction of 7-storey car park as a part of Hilton Istanbul Bomonti Hotel and Conference Center. The depth of the excavation was 26 m and there was a historic building adjacent to excavation. Plaxis 8.2 software was used to model the behavior of the wall and the ground during the staged excavation.

In the first chapter, a general information about the importance of deep excavation systems is given and the scope of the study is described.

A detailed review of lateral earth pressures is presented in the second chapter. Different types of calculation methods for lateral earth presssures acting on braced cuts and anchored walls are given in detail in addition to classical lateral earth pressure calculation methods.

In the third chapter, a detailed literature review of prestressed anchored wall is given. All elements forming a prestressed anchors are firstly represented. The determination criterias for sizing a prestressed anchored pile wall is given in detail according to the standards and codes. The failure mechanisms that may occur in prestressed anchored walls are also given in this chapter. The failure of a prestressed anchored wall may occur as a result of wrong sizing of the structural elements so that the sizing criterias are given in detail. The creation of a prestressed anchored pile wall starts with the determination of the lateral forces acting on the wall due to the lateral earth pressure, surcharge loads, water loads if ground water exists and earthquake loads. Mostly, earthquake loads are ignored while supporting the deep excavation with temporary systems to avoid unnecessary high costs. Moreover, the contruction stage and installation phases of a prestressed anchored pile wall is given step by step in chapter three. During a deep excavation, as long as the foundation works started, the deep excavation support elements must be protected to corrosion. The requirements for corrosion protection of prestressed ground anchors are also given in this chapter. It is

wanted that a shoring system does not make large deformations especially if it is built near an important structure. Therefore, the shoring system must be observed until reaching the bottom of the deep excavation. For this purpose, some instruments were placed just behind the shoring wall to observe the lateral movements that will occur during the deep excavation. The investigated area given in this thesis was observed with inclinometers, thus a a detailed information about the inclinometers is given in this chapter as well. A prestressed anchored pile wall is an active retaining system which means that the ground anchors are loaded at the end of each construction stages. The anchor loading criterias are summarized at the end of chapter three.

Finite element modelling in geotechnical engineering was elucidated in the fourth chapter. Moreover, it was given a detailed information about the finite element software Plaxis 2D in this chapter and also the Hardening Soil Model that was used to model the behavior of the ground in front of historic building is given.

Following the literature research done in the previous sections, a case study is given in chapter five. In the case study, deep excavation for the foundation of 7-storey car park located in front of historic building included in Hilton Istanbul Bomonti Hotel and Conference Center is discussed. During this study, major design considerations are conceived. The deep excavation support system was selected as mini piled prestressed anchored wall according to the preliminary design and a numerical analysis was carried out by using finite element software Plaxis version 8.2. The idealized soil profile recommended in the geotechnical evaluation report was used in the design and the Hardening Soil Model was used for modeling. During the deep excavation, instrumental measurements and regular observations were carried out carefully and it was decided to the revise the shoring system project to prevent the occurance of some problems. The revised project was remodelled by Plaxis 8.2 and the outputs for the calculations were also given in this chapter. After that a cost analysis was done to compare the old and the revised projects. As well as in the fifth chapter, influence of some soil strength properties, structural properties and soil-structure interface properties were also investigated and the results were interpreted by graphs obtained from Plaxis calculations. First of all, back-calculations were carried out by changing the modulus of elasticity and the internal friction angle values and lateral displacements obtained for each model were given with graphs. After that for the same geometry model, back-calculations were done according to different interface reduction factor values and it was seen that the interface reduction factor is a characterictic property that takes different values according to the type of soil and structure. Also in this chapter, the effect of anchor bonded length, the inclination of the anchor with horizontal, the effect of nominal strand diameter and the horizontal spacing of ground anchors were investigated and the Plaxis results were given with graphs.

In last chapter, the work carried out in the thesis was summarized with specific conclusions and recommendations for future studies were given as well.

ÖNGERMELİ ANKRAJLI KAZIKLI DUVAR NÜMERİK ANALİZİ: HILTON ISTANBUL BOMONTI HOTEL VE KONFERANS MERKEZİ PROJESİ KAPSAMINDA YER ALAN TARİHİ BİNA ÖNÜ İKSA SİSTEMİ

ÖZET

Geoteknik mühendisliğinin en önemli inceleme alanlarından biri de derin kazı destekleme sistemleridir. Temel inşaatı sırasında güvenli bir çalışma ortamı sunabilmek ve çevre yapıları kazı esnasında oluşabilecek olan etkilerden koruyabilmek amacıyla derin kazı destek sistemleri kullanılmaktadır. Bu destekleme sistemleri kalıcı ya da geçici olarak inşa edilebilirler. Bu tez kapsamında, ülkemizde de oldukça yaygın olarak kullanılan öngermeli ankrajlı destek sistemleri üzerinde durulmuştur. Bu tezin konusu, önemli bir yapı kenarında gerçekleştirilen bir derin kazının desteklenmesi amacı ile inşa edilen bir iksa sisteminin araştırılması ve bazı parameterelerin iksa sisteminin davranışı üzerindeki etkilerinin araştırılmasıdır. İnşaat süresinin kısa olması sebebi ile inşa edilen iksa sistemi geçici özelliktedir.

Bu tezde, Plaxis 8.2 sonlu elemanlar programı kullanılarak bir vaka analizi yapılmıştır. Bu çalışma kapsamında tarihi bir bina önünde oluşturulan iksalı kazı geoteknik mühendisliği uygulamalarında yaygın olarak kullanılan bir sonlu elemanlar programında modellenmiş ve çeşitli parametrelerin iksa sistemi üzerindeki etkileri araştırılmıştır.

İlk bölümde derin kazı destekleme sistemlerinin önemine değinilmiş ve bu tezin kapsamı hakkında bilgi verilmiştir.

Yanal toprak basınçları ikinci bölüm kapsamında detaylı bir şekilde incelenmiştir. Klasik toprak basıncı hesaplama metotlarına ek olarak destekli kazılarda ön tasarım hesapları için geliştirilen çeşitli toprak basıncı dağımlarına da detaylı olarak verilmiştir. Derin temel çukurlarını desteklemek amacıyla oluşturulan iksa sistemlerinin boyutlandırılması sisteme etkiyen bütün yüklerin belirlenmesi ve zemin cinsine ve destekleme sistemine en uygun görünür basınç diyagramının belirlenmesi ile gerçekleştirilir. Belirlenen toprak yükleri ile sisteme etkiyen sürşarj yüklerinin birlikte etkisi göz önünde bulundurularak iksa sistemi elemanlarına gelecek kesit tesirleri hesaplanır ve buna göre iksa elemanlarının boyutlandırılması yapılır.

Üçüncü bölümde öngermeli ankrajlı duvarlar hakkında geniş bir literatür çalışmasına yer verilmiştir. Öngermeli ankrajlı iksa duvarını oluşturan yatay ve düşey destek elemanları, bu elemanların seçimi ve boyutlandırılması ve öngermeli ankrajlı duvarların imalat aşamaları, imalat süresince ankraj elemanlarının korunması ve uygulanan testler hakkında geniş kapsamlı bir literatür çalışması yapılmıştır. Öngermeli ankrajlarla oluşturulmuş bir iksa duvarında yenilme şekillerinin çoğu, elemanların yanlış boyutlandırılmaları sonucu meydana gelmektedir. Bu nedenle bu bölümde, ankraj elemanlarının boyutlandırılması hakkında standartlara atıfta bulunularak geniş yer verilmiştir. Derin kazılarda meydana gelebilecek deplasmanların sınırlandırılması amacıyla kullanılan öngermeli ankrajların tasarımında güvenli ankraj boyunun tayini oldukça önemlidir. Öngermeli ankrajlarda

ankraj kök boyu ve serbest boyunun tayininde ankrajların boyutlandırılması potansiyel kayma düzleminin yeterli miktarda gerisinde kalacak şekilde yapılmalıdır. Bununla birlikte bu bölümde, öngermeli ankrajların kök boyunun belirlenmesinde zemin sürtünmesinin ve zeminin kohezyon durumunun da belirleyici olmasına değinilmiştir. Öngermeli ankrajlı bir iksa duvarının inşaası öncelikle toprak basıncı, sürşarj yükleri, yeraltı suyunun mevcut olduğu durumlarda hidrostatik basınç ve deprem kuvvetleri gibi duvara etkiyecek olan yanal kuvvetlerin belirlenmesi ile başlar. Genel olarak, geçici iksa sistemleri söz konusu olduğunda daha ekonomik bir tasarım açısından deprem kuvvetleri dikkate alınmamaktadır. Yine üçüncü bölüm kapsamında, öngermeli ankrajlı bir iksa duvarının oluşturulmasında kazı aşamaları ve ankrajların yerleştirilmesi sırasıyla verilmiştir. Temel çukurunun desteklenmesi için yapılmış olan bir derin kazı destek sisteminin, kazı çukuru açık kaldığı sürece dış etkilere maruz kalabileceği düşünülüp sistem elemanlarının korozyona karşı korunması önemlidir. Bu nedenle, öngermeli ankrajlı bir perde duvar elemanlarının korozyona uğramaması için alınacak önlemler üçüncü bölüm kapsamında yer bulmuştur. Bir derin kazı destekleme sisteminin özellikle de yakınlarında tünel, bina gibi önemli bir yapı bulunuyorsa büyük deformasyonlar yapmaması istenir ve tasarım buna göre yapılır. Derin kazı boyunca kazının her kademesinde deneyimli mühendislerce belirlenen zaman aralıklarında kazıda oluşan deformasyonların izlenmesi gerekmektedir. Böylece sistemin periyodik olarak gözlenmesi sağlanarak, kazı boyunca meydana gelebilecek herhangi bir sorunun önceden tespit edilip gerekli önlemlerin alınması sağlanır. Bu amaçla iksa duvarının arkasına deplasmanların izlenmesi için birtakım gözlem aletleri yerleştirilmelidir. Bu tez kapsamında incelenen alana ait yanal deplasman takibi inklinometre cihazlarıyla gerçekleştirilmiş olduğu için bu bölümde inklinometre gözlem aletlerinden bahsedilmiştir. İnklinometre kuyularının tesis edilmesi ve ölçüm alınması hakkında kısa bir bilgi verilmiştir. Öngermeli ankrajlı kazıklı duvar aktif bir iksa sistemi olup, her kademede oluşturulan ankrajlar belirlenen yüklerde yüklenerek sistem aktif hale getirilmektedir. Son olarak bu bölümde, öngermeli ankrajları aktif hale getirmek için uygulanan yükler ve testler ile de ilgili bilgiye yer verilmiştir. Öngermeli ankrajlı sistemlerde her bir ankrajın aldığı yük, yükleme deneyleri ile kanıtlanır.

Diğer pek çok mühendislik probleminde olduğu gibi geoteknik mühendisliğinde de incelenen bir problemin daha basit ve anlaşılır bir hale getirilmesi için sonlu elemanlar ya da sonlu farklar metotlarından faydalanılmaktadır. Basit zemin yapıları için çoğunlukla bir boyutlu modeller yeterli olurken, çok tabakalı zemin profillerinin incelenmesi, istinat yapıları ve derin kazılar gibi daha karmaşık problemlerin çözülmesinde modelleme, iki veya üç boyutlu modelleme teknikleri kullanılarak gerçekleştirilmektedir. Bu tez çalışması kapsamında tarihi bir bina önünde gerçekleştirilen derin kazının modellenmesi Plaxis iki boyutlu sonlu elemanlar programı düzlemsel gerilme koşullarında kullanılarak gerçekleştirilmiştir. Bu nedenle dördüncü bölüm dahilinde, geoteknik mühendisliğinde sonlu elemanlar metodu ve modelleme tekniği hakkında bilgi verilmiştir. Daha sonra bu tez kapsamında yapılan çalışmalar boyunca kullanılan Plaxis 2 boyutlu sonlu elemanlar programı hakkında geniş bir bilgiye yer verilmiştir. Ayrıca tez kapsamında ele alınan vaka analizinin modellenmesinde kullanılan gelişmiş zemin modeli Hardening Soil Model hakkında da detaylı bilgi verilmiştir. Hardening Soil Model'de zemin rijitliği gerilme seviyesine bağlı olarak artan basınçla birlikte artmaktadır. Ayrıca bu modelde, zemini tanımlamak için programa girilen zemin mukavemet parametreleri ve elastisite modülü Mohr Coulomb Model'den farklı olarak derinlik boyunca artırılarak kullanılmaktadır.

Önceki bölümlerde yapılan literatür çalışmalarının ardından, beşinci bölümde bir vaka analizine yer verilmiştir. Vaka analizi olarak Hilton İstanbul Bomonti Hotel ve Konferans Merkezi Projesi içinde yer alan tarihi bina önünde konumlandırılacak 7 katlı otoparkın temel inşaatı için yapılan destekli kazı sistemi ele alınmıştır. Bu tez kapsamında, başlıca tasarım ilkeleri ve ilgili standartlar göz önünde bulundurularak nümerik bir çalışma yapılmıştır. Bu bölüm kapsamında öncelikli olarak incelenen kesitin yer aldığı proje tanıtılmış, daha sonra proje için hazırlanmış geoteknik değerlendirme raporunda yer alan sondaj bilgileri, arazi ve laboratuvar deneyleri ile arazi için oluşturulan idealize zemin profiline yer verilmiştir. Geoteknik değerlendirme raporundan elde edilen bilgiler ışığında, yapılan ön tasarım çalışmaları sonucunda kazı destek sistemi olarak öngermeli ankrajlı mini kazıklı iksa duvarının uygun olduğuna karar verilmiş ve yatay toprak basıncına göre her bir ankraj noktasındaki kesit tesirleri hesaplanmıştır. Elde edilen maksimum kesit tesirlerine göre, sistemin ön boyutlandırılması yapılmıştır. Daha sonra, uygun iksa sistemi olarak kararlaştırılan derin kazı destekleme sistemin modeli, iki boyutlu Plaxis versiyon 8.2 sonlu elemanlar programında oluşturulmuştur. Tasarım parametreleri olarak geoteknik raporda önerilen idealize zemin profiline ait parametreler kullanılmış ve zemin modeli olarak da Hardening Soil Model seçilmiştir. Kazı süresince, inceleme konusu arazide her bir kazı kademesini takiben yerinde gözlemler ve aletsel okumalar yapılmıştır. Kazı süresince çevre ile etkileşimin iyi gözlenmesi ve düzenli olarak aletsel okumaların alınması sonucu, oluşabilecek problemler önceden tespit edilmiş ve projede revizyon yapılmasına karar verilmiştir. Revize edilmiş projenin modeli de Plaxis sonlu elemanlar programı versiyon 8.2 ile yapılmış olup sonuçlar beşinci bölümde verilmiştir. Daha sonra eski ve yeni projeler arasında birim fiyat tablosundan yararlanılarak bir maliyet karşılaştırılması yapılmıştır.

Ayrıca bu bölümde, sonlu elemanlar programında girilen bazı parametrelerin iksa sistemi üzerindeki etkisi de araştırılmıştır. Bu amaçla, zemin mühendislik özelliklerinin, zemin/yapı arayüz elemanının ve yatay destek elemanları olarak kullanılan öngermeli ankrajların özelliklerinin iksa sisteminin rijitliği üzerindeki etkileri diğer parametrelerin sabit tutulması koşulu ile aynı geometri model üzerinde araştırılmıştır. İlk olarak zeminin elastisite modülü ve içsel sürtünme açısı değerleri değiştirilerek, Plaxis sonlu elemanlar programı ile geri analizler yapılmış ve elde edilen sonuçlara göre; bu mühendislik parametrelerinin iksa sisteminde meydana gelen deplasmanlar üzerindeki etkileri araştırılmıştır. Daha sonra arayüz azaltma faktörünün yanal yüke maruz kazık elemanındaki deplasmanlar üzerindeki etkisi Plaxis sonlu elemanlar programı kullanılarak araştırılmış; elde edilen sonuçlar sunularak arayüz elemanının kazığın yapıldığı malzeme ve zeminin cinsine göre karakteristik bir değer aldığı anlaşılmıştır. Son olarak ankraj kök boyunun, ankraj yerleştirme açısının, ankraj tendon çapının, ankraj yatay aralığının yanal deplasmanlar üzerindeki etkisi yine Plaxis sonlu elemanlar programı kullanılarak araştırılmış ve elde edilen sonuçlar grafikler ile sunulmuştur.

Son bölümde, tez kapsamında yapılan çalışma özetlenmiş; ileriki çalışmalar için yararlanılması açısından sonuç ve önerilere yer verilmiştir. İksa sistemi tasarımında, sistemde oluşabilecek deplasmanların önceden tahmin edilmesinde sonlu elemanlar metodunun önemine değinilmiş ve kazı boyunca yapılan aletsel gözlemlerin tasarımın yeniden değerlendirilmesi ve gerektiği takdirde revize edilmesine olanak sağladığına değinilmiştir. Ayrıca derin kazıların modellenmesinde, zemin ve yapısal özelliklerin değişiminin sistemdeki etkileri de ileriki çalışmalara ışık tutması açısından neden-sonuç ilişkisi çerçevesinde verilmiştir.

1. INTRODUCTION

Nowadays, many engineering structures such as skyscrapers, tunnels, infrastructures, roads, dams etc. need to be supported by retaining systems to resist both the horizontal and vertical loads. It is significant that during a deep excavation or an infrastructure construction such as tunnels and pipelines etc., it must be taken some precautions to prevent the failure of surrounding structures such as buildings and roads. The failure of the surrounding structures may occur as settlement of the ground or lateral displacement. To avoid both the settlement and the displacement problems and to make the safest design, the ground and the groundwater conditions, distance between the construction site and the adjacent structures, duration of the excavation must be examined in detail. Displacements occured in soil or rock in a deep excavation support system are affected from groundwater conditions, soil properties, geological and topographical features, excavation method and the duration of the deep excavation and also the type of support system. These effects may all be considered during the design phase and it is known that the creation of an appropriate solution is in the field of application of geotechnical engineers.

Firstly, geotechnical investigations must be carried out for the investigation area to determine the soil or rock properties and then a detailed geotechnical report must be prepared by an experienced geotechnical engineer. In the report, all the borings and the field and laboratory tests should be given in detail to give the information about the investigated site.

Secondly, the design process starts. The safest and the most economical ground model should be designed by the geotechnical engineer. Sheet pile walls, reinforced concrete walls, diaphragm walls, soil nailed walls, bored piles, struts etc. can be chosen as deep excavation support systems. Mostly, ground anchors and struts can also be used together with these systems to provide a lateral support. It is noted that in the design it must be considered that the ground anchors are classified as permanent and temporary ground anchors according to their service life. It is also noted that the designed system must be economical. The geotechnical engineer

should avoid unnecessary sizing of the structural elements. An another important issue in the construction of braced excavations is that the noise and the environmental pollution. There should be taken some precautions to prevent dust cloud during drilling processes.

The subject of this study is prestressed ground anchors used as lateral support in braced excavations. In a deep excavation supported by using prestressed anchors, the shoring wall is fixed to the earth by ground anchors and these anchors carry the tensile forces develop as a result of soil or rock mass and hydrostatic pressures and external loads. The prestressed anchors transfer the tensile forces behind the potential failure surface of soil or rock. In addition, prestressed anchors helps to counteract the moment forces that may cause the failure of the system. This study undertaken on a case study constructed as a prestressed anchored pile wall has two aims: the first one is modelling a deep excavation support system by using a finite element software and the second purpose is to investigate the effect of some soil and structural properties by back calculations. In geotechnical engineering so many methods are developed to make deformation and stability analysis. In this study, a two-dimensional finite element method is carried out to investigate the behavior of prestressed anchored pile wall. Plaxis software version 8.2 is used to model and analyze the geotechnical problem given as a case history within this thesis.

During the thesis, a detailed literature review on lateral earth pressures develop in braced excavations and prestressed ground anchors is presented. After that with a case study displacements occur in prestressed anchored pile wall are investigated within the scope of this thesis. Furthermore, instrumental observations are also given that are very important in geotechnical engineering due to check the accuracy of the assumptions, to check the compability of the design with the site application and to get any displacements occur in the retaining structure during the deep excavation under control. According to the geotechnical site investigations, a preliminary design was carried out and then the model of the investigated section was created in the finite element programme. Also, the effect of some parameters and the structural properties are also investigated with a serial numerical analysis by using the finite element software Plaxis version 8.2.

2. LATERAL EARTH PRESSURES

Lateral earth pressure occurs when soil particles at rest are forced by an excavation, shrinkage or expansion that cause movements in the soil. Stability analysis of retaining structures is done under various load assumptions and these assumptions are really important because a wrong in load assumption may cause undesirable situations such as noneconomical design or an unstable structure. Lateral loads accepted for shoring systems are determined according to the soil properties, depth of excavation, importance of the structure that will be built, economy, displacement tolerance etc.

As indicated in the preceding paragraph lateral earth pressures develop while a lateral stress is applied onto the retaining wall. Lateral earth pressures are defined with a coefficient that is obtained from the ratio of horizontal effective stresses to vertical effective stresses. The coefficient of earth pressure is obtained by using some empirical correlations for different types of earth pressures. In this chapter, both the lateral earth pressure types and also classical and advanced earth pressure theories are explicated in detail.

2.1 Earth Pressure at Rest

At rest pressure is defined as the resultant pressures in all dimensions are equal to zero. Earth pressure at rest occurs when the wall(sheet pile wall, retaining wall, bottom wall etc.) has no lateral movement. The coefficient of earth pressure at rest K_o, can also be expressed as the ratio of horizontal stress and vertical stress.

$$\sigma'_h = K_o \times \sigma'_v \quad \textbf{(2.1)}$$

σ_h': Effective horizontal stress

σ_v': Effective vertical stress

Jaky's expression is widely used to calculate K_o value for coarse grained soils

$$K_o = 1 - sin\varphi \text{ (Jaky, 1944)} \quad \textbf{(2.2)}$$

φ: Internal friction angle of soil

The coefficient of earth pressure at rest in overconsolidated soils $K_{o,OC}$ is computed by using Schmertmann's expression

$$K_{o,OC} = 0.5 \times (OCR)^{0.5} \quad \textbf{(2.3)}$$

OCR: Over consolidation ratio

In cohesive soils, K_o can also be computed by using Terzaghi's expression according to linear elastic theory

$$K_o = \upsilon/(1-\upsilon) \quad \textbf{(2.4)}$$

υ: Poisson's ratio

K_o values change according to the type of soil. In general, for sandy soils it is in the range of 0.40 to 0.50; for normally consolidated clays it is in the range of 0.55 to 0.65; for overconsolidated clays it can be greater than 1 and lastly for heavily overconsolidated clays K_o value can be greater than 2.

Lateral earth pressure at rest is generally used in the design of rigid structures such as cantilever walls; however it is not used in flexible retaining structures such as anchored walls. In this thesis, a flexible shoring system is modelled with ground anchors near an important building so that the preliminary design was done by considering not to move the adjacent building. Therefore, hand calculations were done according to K_o to stay in the safe zone.

2.2 Active and Passive Earth Pressures

Active and passive earth pressures can be explained by the retaining wall movements. When the wall moves away from the backfill soil, the lateral pressure decreases and lateral strain expansion occurs as a result. Otherwise, passive earth pressure develops when the wall moves towards the backfill soil. Passive earth pressure causes increase in pressure as a result of compressive lateral strains. Coulomb's (1773) and Rankine's (1857) earth pressure theories still form the basis of earth pressure calculations today. In both theories, lateral earth pressures are calculated by using the equilibrium theory of plasticity. The equilibrium theory of plasticity can be best explained by Mohr-Coulumb failure envelopes.

2.2.1 Active and passive earth pressures according to Coulomb wedge theory

Coulomb Wedge Theory (1776) is the earliest solution method for the calculation of lateral earth pressures. The soil is assumed to be an isotropic, homogeneous and cohesionless material in this theory. Coulomb Wedge Theory can be used when there is an inclined cohesionless backfill behind a retaining wall. There is a friction between the wall and the backfill soil that is represented by δ. The wall friction angle δ is generally assumed to equal 1/3φ or 2/3φ where φ is internal friction angle of backfill. The wall friction angle δ can be taken as zero for the systems exposed to dynamic loading. It is considered that when the wall moves forward in active state and the triangular shaped wedge behind the retaining wall slips downward (Figure 2.1).

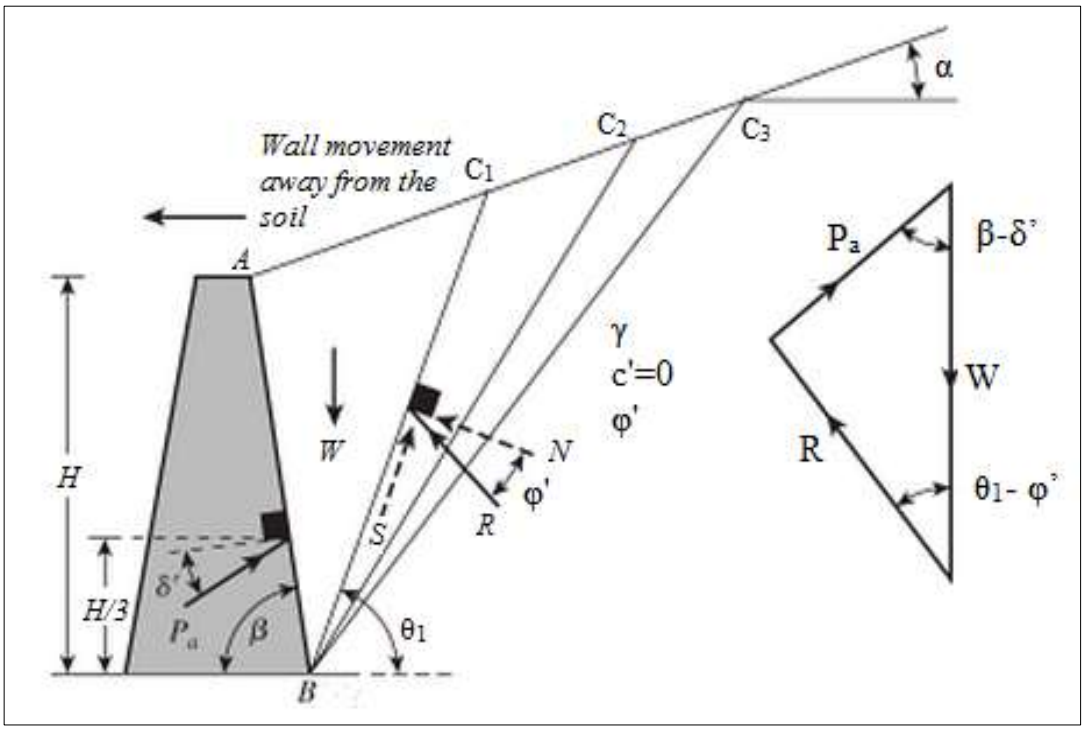

Figure 2.1 : Coulomb's active earth pressure (Das, Braja M., 2007).

The coefficient of active earth pressure K_a is calculated as:

$$K_a = \frac{sin^2(\beta+\varphi)}{sin^2\beta\, sin(\beta-\delta)\left[1-\sqrt{\frac{sin(\varphi+\beta)sin(\varphi-\alpha)}{\sin(\beta-\delta)\sin(\alpha+\beta)}}\right]^2} \quad \textbf{(2.5)}$$

α: Slope angle above retaining wall

β: Angle of retaining wall from horizontal

φ: Angle of resultant force with normal force

δ: Angle of friction between the wall and backfill

The active earth pressure P_a is calculated as:

$$P_a = \frac{1}{2}\gamma H K_a \quad \textbf{(2.6)}$$

H: Height of the backfill

γ: Unit weight of soil

In passive case, it is assumed that the retaining wall moves towards to the soil as shown in Figure 2.2. The coefficient of passive earth pressure K_p is calculated as:

$$K_p = \frac{sin^2(\beta-\varphi)}{sin^2\beta\, sin(\beta+\delta)\left[1-\sqrt{\frac{sin(\varphi+\delta)sin(\varphi+\alpha)}{\sin(\beta+\delta)\sin(\beta+\alpha)}}\right]^2} \quad \textbf{(2.7)}$$

The passive earth pressure P_p is given as:

$$P_p = \frac{1}{2}\gamma H K_p \quad \textbf{(2.8)}$$

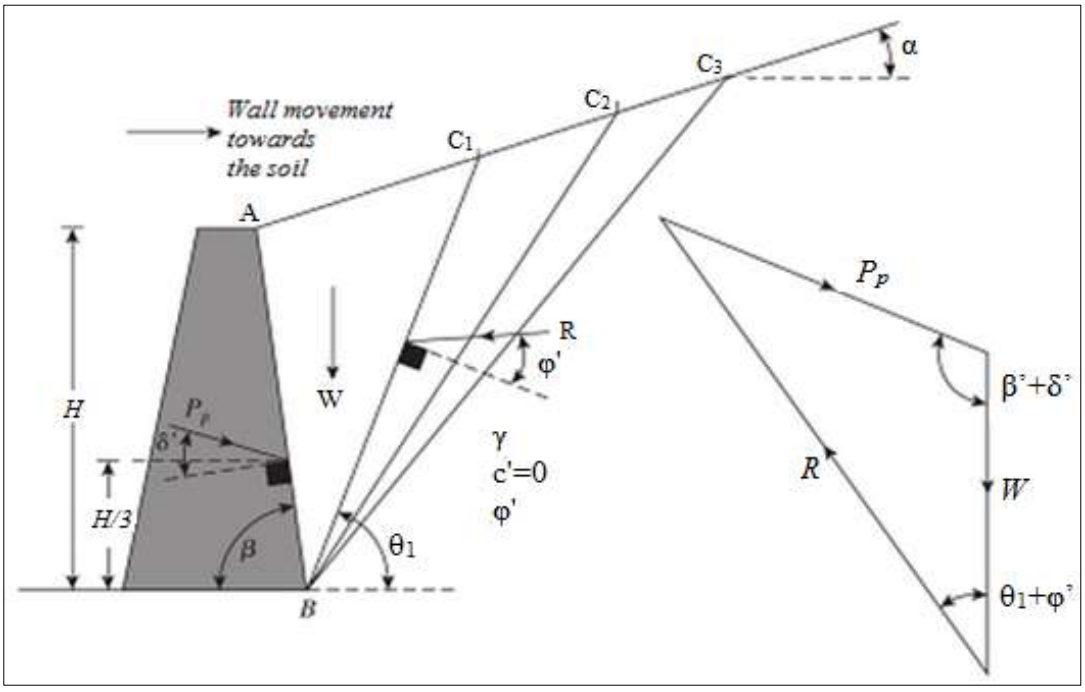

Figure 2.2 : Coulomb's passive earth pressure (Das, Braja M., 2007).

2.2.2 Active and passive earth pressures according to Rankine theory

Assumptions for Coulomb theory are also valid for Rankine theory. Rankine theory is a simplified method of Coulomb theory. The main difference between these two theories can be summarized as:

- In Rankine theory the backfill is accepted as horizontal which means the angle α equals to zero.
- In Rankine theory it is assumed that the backfill side of the supporting wall is not horizontal that means the angle θ equals to zero.
- In Rankine theory, friction between the wall and the backfill soil is neglected; so that the angle δ is assumed to be zero.

Shear strength of soil effects in opposite direction as a result of lateral expansion of soil, so that a shear resistance occurs in soil. This case causes a decrease in lateral earth pressures in fact lateral earth pressures fall under pressure at rest. When a lateral movement which enhances the shear resistance of soil occurs, earth pressure holded in soil will minimize. The minimum lateral earth pressure condition based on the shear strength of soil is called as "active earth pressure". In other words, Rankine active earth pressure develops when retaining structure makes displacements by lateral expanding of the soil to the excavated part of soil, and causes collapse failure (Figure 2.3).

The coefficient of active earth pressure according to Rankine theory is given in the Equation 2.5

$$K_a = tan^2(45 - \varphi/2) \quad \textbf{(2.9)}$$

Rankine active earth pressure for the conditions c≠0 and φ≠0 is;

$$\sigma_a' = \gamma' z K_a - 2c'\sqrt{K_a} \quad \textbf{(2.10)}$$

c: Cohesion of soil

z: Depth

The depth z_o where the active earth pressure σ_a equals zero is given as:

$$z_o = 2c/\gamma\sqrt{K_a} \quad \textbf{(2.11)}$$

Tensile stresses appear between the soil surface and this level. In the soil surface (z=0), the maximum tensile stress is calculated by the equation 2.12 (Kumbasar and Kip, 1999).

$$\sigma_a = -2c/\gamma\sqrt{K_a} \quad \textbf{(2.12)}$$

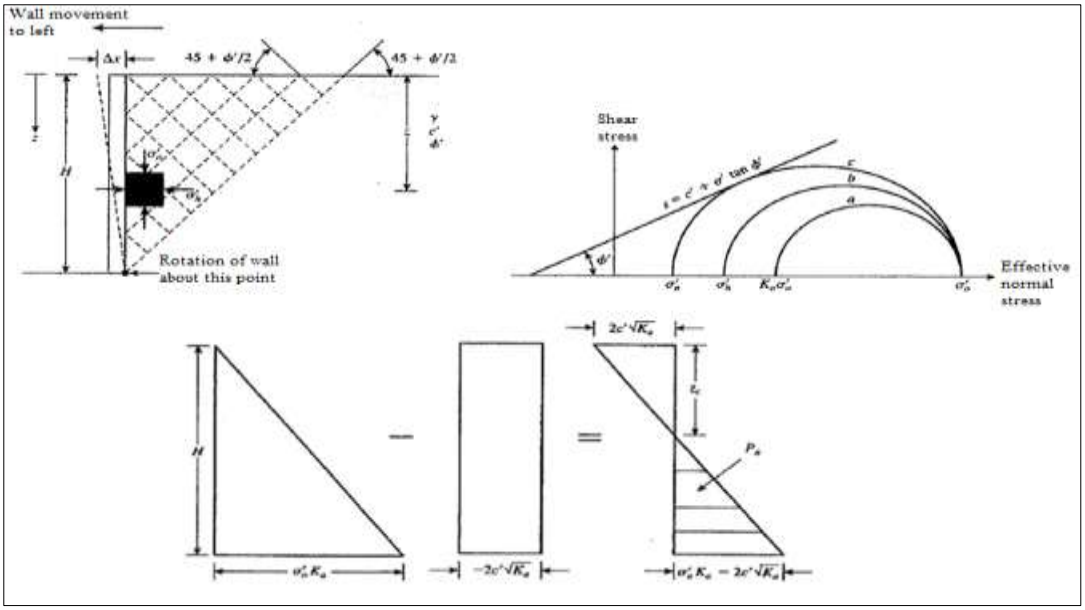

Figure 2.3 : Rankine active pressure for cohesive soils (Das, Braja M., 2007).

Displacement amounts needed to produce active earth pressure at a height of H are given in Table 2.1. As can be seen from Table 2.1 wall displacement amounts changes with respect to the type of backfill material. As well as the height of the retaining wall is effected on the amount of wall movements. Wall displacement amount for active state is in the range of milimiters or centimeters (Özgen, 1984).

Table 2.1 : Displacement amounts required to produce active state (Ranjan, G., and Rao, A.S.R., 2005).

Soil Type	Amount of translation at top
Cohesionless (dense)	0.001H~0.002H
Cohesionless (loose)	0.002H~0.004H
Cohesive (stiff)	0.01~0.02H
Cohesive (soft)	0.02~0.05H

Rankine passive earth pressure develops when retaining structure moves opposite site of excavated area and compressing the soil behind the wall (Figure 2.4).

The coefficient of Rankine passive earth pressure is given in the equation 2.13.

$$K_p = tan^2(45 + \varphi/2) \quad \textbf{(2.13)}$$

Rankine passive earth pressure for the conditions c≠0 and Φ≠0 is;

$$\sigma_p' = \gamma' z K_p + 2c'\sqrt{K_p} \quad \textbf{(2.14)}$$

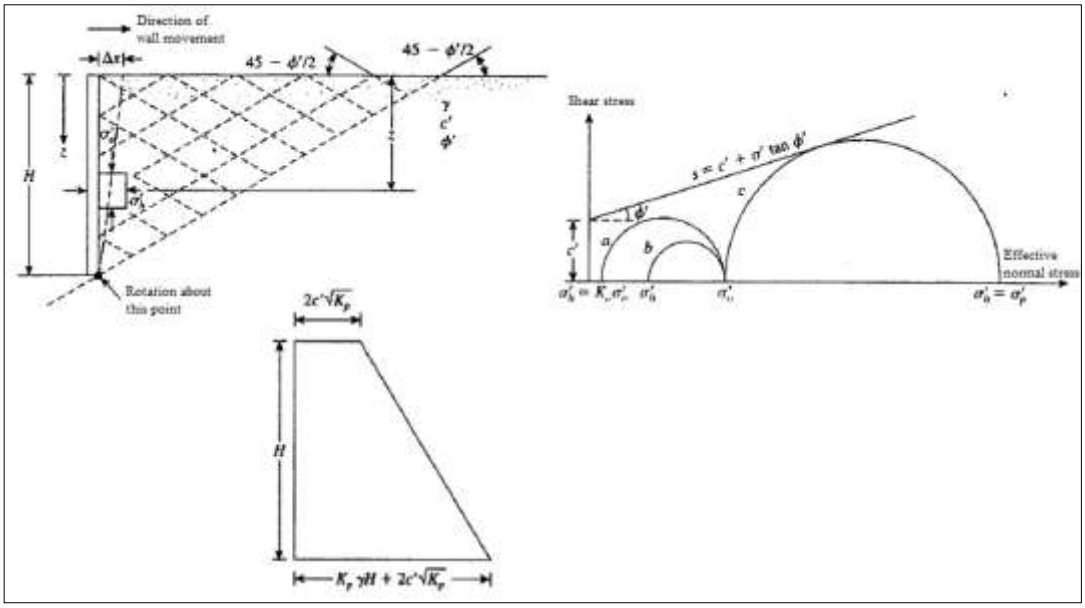

Figure 2.4 : Rankine passive pressure for cohesive soils (Das, Braja M., 2007).

In Table 2.2, displacement amounts needed to produce passive earth pressure at a height H are given. It can be said that the displacement amounts necessary to develop passive earth pressures are larger than for active earth pressures. Wall displacement amount for passive state is in the range of centimeters or decimeters (Özgen, 1984).

Table 2.2 : Displacement amounts required to produce passive state (Das, Braja M., 2007).

Soil Type	Amount of translation at top
Loose sand	0.01H
Dense sand	0.005H
Soft clay	0.05H
Stiff clay	0.01H

2.2.3 Earth pressures due to surface loads

Vertical loads on the backfill surface of the ground cause an increase in earth pressure acting on retaining structure. Surface loads can be considered as the buildings located adjacent to shoring system, vehicular loads, material storage on the ground surface near retaining system. Surface loadings can be classified into two groups: uniformly-distributed loads and concentrated loads such as point loads, line loads, strip loads, triangular loads or ramp loads. According to Rankine theory, a constant active lateral earth pressure occured as a result of uniform surcharge loading

can be added to the main earth pressure. The surcharge load caused by uniform loadings can be calculated by the equation 2.15.

$$\sigma = K_a \times q \tag{2.15}$$

where K_a is the coefficient of active earth pressure and q is uniform surcharge load. Surcharge loads occured as a result of point loads, line loads, strip loads, triangular loads or ramp loads behind the retaining structure can be calculated according to the elasticity theory.

2.3 Earth Pressures Acting on Braced Excavations

Coulomb and Rankine earth pressure theories are generally used for laterally unsupported rigid retaining structures. On the other hand, lateral earth pressure acting on a braced excavation support system could not been calculated by using the classical methods. This is because the support systems in braced excavations are fixed at the top but the diplacements at the bottom of the walls are free. For example, for a minipiled wall, minipiles are fixed at the top with cap beam construction and free at the bottom. Therefore, simply it can be said that in a braced excavation lateral earth pressures do not increase linearly and the pressure envelopes are not triangular-shaped as given in the classical Rankine and Coulomb earth pressure theories. On the contrary, the lateral presssure envelopes are generally parabolic-shaped and nonlinear distribution for every excavation stages. In this section, lateral earth pressure envelopes according to some assumptions done for simplificating the calculations are given for various types of soil.

In the design, earth pressure calculations for a braced excavation are carried out considering both the fixed vertical structural elements and also the lateral support structures. It is known that the changes in lateral deformations induce the development of lateral earth pressures in backfill material. The state of the lateral earth pressure changes according to the retaining wall movements and the direction of the movement as indicated above. The lateral supporting elements may show large displacements; however the vertical retaining elements that are fixed at the bottom show very small displacements. This behavior such of a retaining system is modelled by considering both the at rest and active earth pressure coefficients. The at rest condition is shown by initial stresses in a geotechnical analysis. If the geotechnical

analysis is carried out by using a finite element software, it can be easily seen the development of lateral earth pressure changes during the construction stages of the braced excavation and there is a nonlinear change in the lateral pressure distribution.

For supporting a braced excavation, apparent earth pressure envelopes are developed by various researchers. Terzaghi and Peck recommended a trapezoidal pressure distribution for cohesionless soils(for sands) shown in Figure 2.5(a) and then this envelope is developed for dry or moist sands; however if there is water on the excavation level, water must be pumped out down to the bottom of the excavation. Note that in Figure 2.5(a), the symbol δ represents the friction between the wall and soil. The modified pressure envelope shows an uniform earth pressure distribution as in Figure 2.5(b) and the active earth pressure for sands is given as:

$$P_a = 0.65 \times \gamma \times H \times K_a \qquad \textbf{(2.16)}$$

The active earth pressure coefficient K_a in this equation is calculated with the following formula:

$$K_a = tg^2\left(45 - \frac{\varphi}{2}\right) \qquad \textbf{(2.17)}$$

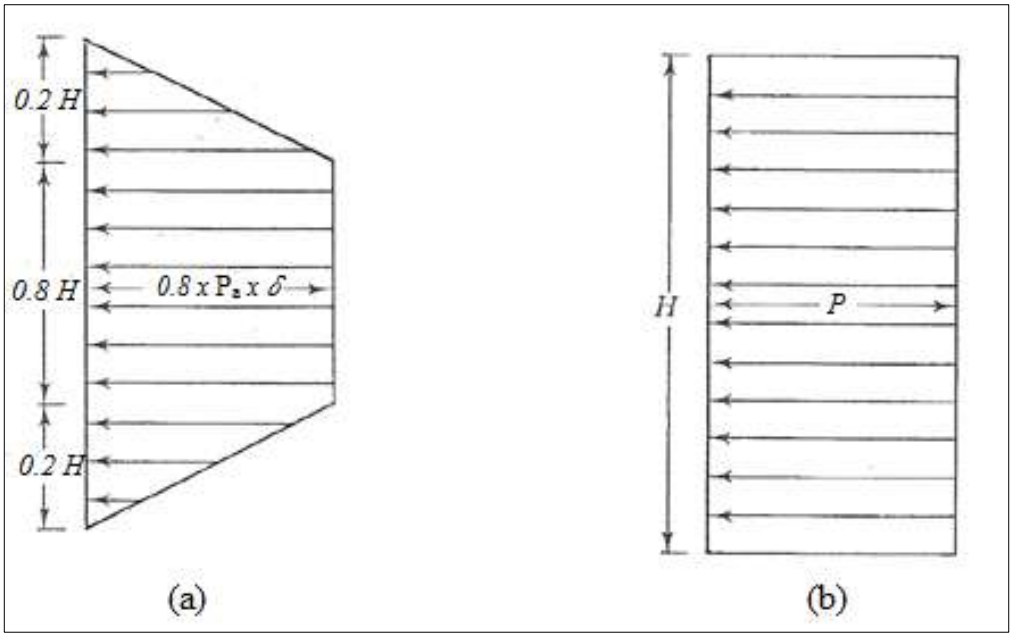

Figure 2.5 : Apparent earth pressure envelope for cohesionless soils (Terzaghi and Peck, 1967).

The recommended apparent earth pressure diagrams for braced excavations supported with ground anchors in sandy soils are trapezoidal-shaped (FHWA-IF-99-

015, 1999). The detailed information for multi-level anchored walls is given in chapter 3.

For cohesive soils Terzaghi and Peck recommended pressure envelopes as shown in Figure 2.6. As the value of the active earth pressure reaches the value of the unconfined compression strength, excavation without a support comes to failure limit. It is known that unconfined compression strength equals two times of cohesion, then the equation becomes

$$2c = \gamma \times H_c - 2c \quad \textbf{(2.18)}$$

$$H_c = 4c/\gamma \quad \textbf{(2.19)}$$

H_c: Critical height

c: Undrained cohesion (φ=0)

γ: Unit weight of clay

It is assumed that the soil does not fail before reaching the critical height H_c. The soil is accepted as stable when $\gamma H_c/c=4$ and this ratio is called as the stability number.

In clayey soils, the first thing that must be checked is the stability number. For soft to medium clays,the stability number $\gamma H_c/c$ is greater than 4 and the active earth pressure is given by the equation 2.20. It is assumed that if $0.3\gamma H$ gives greater pressure value then this value is accepted as lateral earth pressure.

$$P_a = \gamma \times H \times \left[1 - \left(\frac{4c}{\gamma H}\right)\right] \quad \textbf{(2.20)}$$

For stiff clays, $\gamma H/c \leq 4$ and the active earth pressure is given with the following equation:

$$P_a = (0.2 \sim 0.4) \times \gamma \times H \quad \textbf{(2.21)}$$

Shoring systems' lifetime became effective in the development of pressure envelopes. The coefficient 0.2 is used for temporary situations which has a more tolerance of displacement, otherwise 0.4 is preferred. Nonetheless, the active earth pressure can be calculated by using the coefficient 0.3 as an average value for stiff clays:

$$P_a = 0.3 \times \gamma \times H \quad \textbf{(2.22)}$$

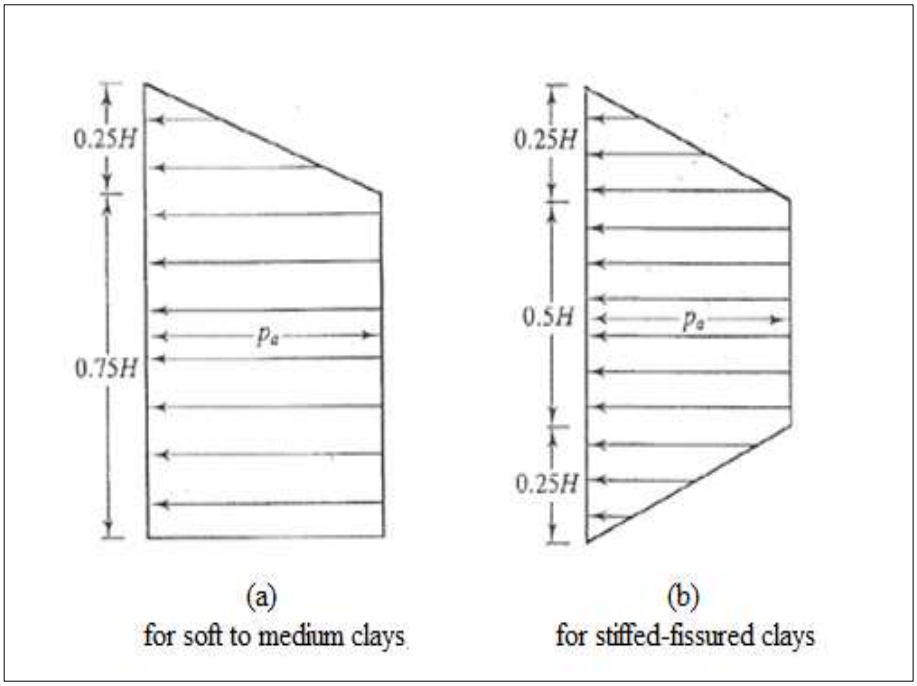

Figure 2.6 : Apparent pressure envelopes for cohesive soils (Terzaghi and Peck, 1967).

According to Tschebotarioff(1973), the lateral earth pressure for cohesionless soils has a trapezoidal shape as in Figure 2.7(a) and is estimated as:

$$P_a = 0.25 \times \gamma \times H \quad \textbf{(2.23)}$$

Tschebotarioff(1973) was also developed pressure envelopes both for temporary and permanent shoring systems in clayey soils as shown in Figure 2.7(b) and Figure 2.7(c). Lateral earth pressure acting on a temporary support in stiff clays can be estimated from the equation 2.24.

$$P_a = 0.3 \times \gamma \times H \quad \textbf{(2.24)}$$

The lateral earth pressures acting on a permanent support in medium clays can be estimated from the equation 2.25. It is clear from the equation that the coefficient taken for the permanent walls is greater than the coefficient taken for temporary walls.

$$P_a = 0.375 \times \gamma \times H \quad \textbf{(2.25)}$$

According to GCO(1990) Review of Design Methods for Excavations, it is seen that Tschebotarioff(1973) method may be more appropriate while the depth of the excavation exceeds about 16 m.

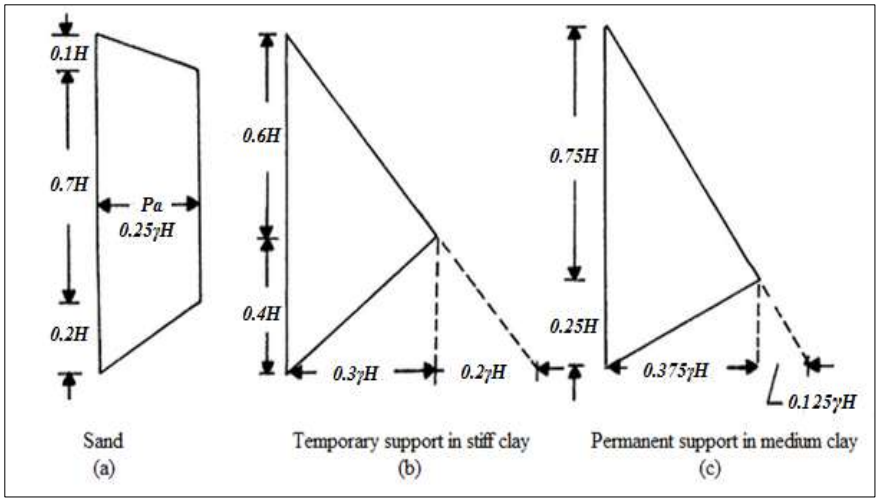

Figure 2.7 : Apparent earth pressure diagrams for different types of soils(Tschebotarioff, 1973).

Figure 2.8 shows the apparent earth pressure diagrams recommended by Navfac(1982) for anchored walls. As can be seen in Figure 2.8, the active earth pressures have greater values than the envelopes obtained for braced cuts. The reason for this situation is there will be less deformations in anchored walls. The rectangular pressure envelope as shown in Figure 2.8(a) is used for cohesionless soils with the coefficient 0.4 in dense sands and with the coefficient 0.5 in loose sands respectively. The equations for the dense and loose sands are given in the following equations respectively.

$$P_a = 0.4 \times \gamma \times H \quad \textbf{(2.26)}$$

$$P_a = 0.5 \times \gamma \times H \quad \textbf{(2.27)}$$

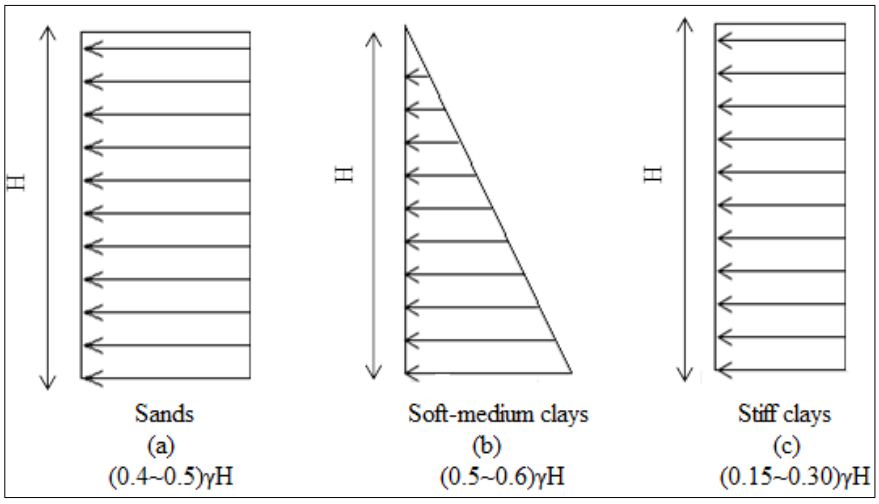

Figure 2.8 : Apparent earth pressure diagrams recommended from Navfac (1982).

For soft to medium sands Navfac(1982) recommends a triangular shaped pressure envelope as shown in Figure 2.8(b) and the active earth pressure can be calculated as:

$$P_a = (0.5\sim0.6) \times \gamma \times H \quad \textbf{(2.28)}$$

For stiff to hard clays Navfac(1982) recommends a rectangular-shaped earth pressure diagram as in Figure 2.8(c) and the active earth pressure is calculated as follows:

$$P_a = (0.15\sim0.30) \times \gamma \times H \quad \textbf{(2.29)}$$

The coefficients given for stiff to hard clays are relevant to the cohesion of soil. If the stability number $\gamma H_c/c$ is greater and equal to 4; then the coefficient 0.30 is recommended to use. In the contrary case; it is recommended to use the coefficient 0.15.

In brief, the estimation of the lateral forces acting on the vertical retaining element is very important in design phase. Lateral earth pressure behind the retaining wall changes according to the surcharge loads, ground water conditions, wall displacements and the type of construction method and as well as the presence of neighbouring structures. Hence the calculations are determined to be carried out according to the active earth pressure coefficient or at rest coefficient. While a neighbouring structure is located 2H away the retaining wall where H is the excavation depth or there is not an infrastructure near the excavated area then the lateral earth pressure calculations are carried out according to the active earth pressure. In such cases the designer must be careful in the selection of the lateral earth pressure coeficient, in fact the higher values of the earth pressure coefficient may cause uneconomical and unsafe system construction if it's unnecessary (Bozkurt, 2010). If any movement is allowed on the retaining wall, then at rest pressure develops. For example, calculations should be carried out according to the at rest pressures for the retaining systems built on uncompressible soils such as rocks or on piled foundations, excavations for tunneling etc (Özgen, 1984). Another important issue is that the engineer should clearly understand the difference between the behaviors of flexible retaining systems and rigid retaining systems because the type of wall also affects the design. For example, in the standards allowable limits for the horizontal wall displacements are given for flexible retaining walls constructed in very deep excavations.

3. PRESTRESSED ANCHORED WALL DESIGN

As the depth of the excavation increases, it is both noneconomical and difficult to support the excavation with rigid retaining structures. In such situations flexible support systems are developed. One of these flexible retaining systems is anchored walls. Anchored walls in rocks can be designed as fully cement injected and non-prestressed or fixed in bonded part of anchor and prestressed. The advantageous of non-prestressed rock anchors corresponding to prestressed rock anchors is low cost and short-time construction. In this chapter, prestressed anchored wall is given in detail.

The calculation steps of a prestressed anchored wall can be defined as follows (Sabatini, 1999)

i. Project criterias must be determined at first. These criterias are the construction method, geometry of the site, purpose of the project, design life of the shoring system.

ii. Both laboratory and in-situ tests must be carried out to determine the soil properties.

iii. Apparent earth pressure envelope must be determined according to the type of soil to calculate the lateral earth pressures. In addition to this, surface loads and water load must be determined.

iv. Horizontal anchor spacings as well as vertical anchor spacings must be determined.

v. Bending rigidity of the vertical retaining structure must be determined and also the dimensions of the vertical element must be determined.

vi. Slope of the anchor must also be determined according to the foundation of the superstructure, site soil conditions, limit conditions of the shoring system and if any infrastructures such as tunnels etc.

vii. According to the calculated forces acting on the anchors, the components of the anchor must be determined.

viii. The embedded depth of the vertical support element must be calculated and then the passive earth pressure must be calculated also.

ix. The stability analysis of the prestressed anchored wall must be checked and if it is unstable the anchor element or the other supporting elements such as vertical piles and beams must be resized.

x. Lateral and vertical displacements must be predicted approximately. Since this prediction helps to revised the design if it is sufficient.

xi. The tests conducted on prestressed anchors must be determined and load values of the performance tests and proof tests must be determined also.

xii. The other supporting elements such as bracing beams must be dimensioned according to the anchor loads.

3.1 Classification of Prestressed Anchors

Prestressed ground anchors are classified according to the various properties such as design life and the method of construction used in the installation of the anchors.

3.1.1 Classification of anchors according to service life

Service life of the anchor is very important in the design of an anchored wall. Since the lateral earth pressures, anchor loads, the material used in the installation of anchors, type of the anchor test and safety factors are all change according to the service life. In general it can be said that if the service life of the anchors is 2 years then it is called as temporary anchors, if it is not it is called as permanent anchors. It should be noted that the service life of a temporary anchor can be decrease according to the soil conditions and the construction quality. Service life of a prestressed ground anchor should be between 18 to 36 months according to ASSHTO (1996). In temporary anchors corrosion is not a problem. However in permanent anchors the service life is more than 2 years so that corrosion and protection of the shoring elements must be taken into account.

3.1.2 Classification of anchors according to the drilling method

Anchor hole drilling must be carried out in the custody of an experienced geotechnical engineer due to increase the efficiency of work, to protect the stability of hole, to control the water pressure if exists ground water etc. In this case, the selection of the most suitable drilling method is very important. Drilling for a ground anchor can be carried out by the methods rotary, percussion, rotary/percussive, or by using auger. Percussion drilling methods are used in rocks. Auger drilling is preferred in soft soils such as clayey soils. Ground anchor installation varies depending on the type of soil and the method used in drilling also effects the friction resistance between the soil and grout. In general, in rocks and firm to hard cohesive soils, fast and economical straight shaft gravity-grouted anchor is used (Figure 3.1(a)). Anchors used in Thrace formation are generally installed by this method. In coarse-grained granular soils, straight shaft pressure-grouted anchor is preferred (Figure 3.1(b)). Another type of anchor is post-grouted anchor as shown in figure 3.1(c) is used generally in cohesionless soils and also stiff cohesive soils (Littlejohn, 1980). Underreamed anchors shown in Figure 3.1(d), are not preferred like as other types; however can be used in firm to hard cohesive soils.

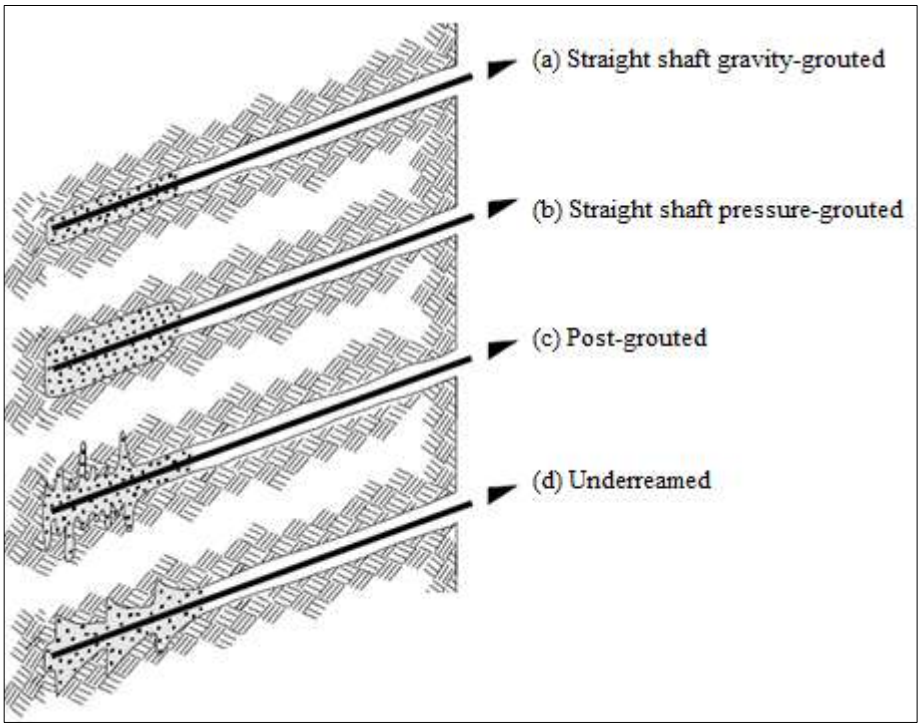

Figure 3.1 : Main types of grouted ground anchors (FHWA-IF-99-015, 1999).

3.2 Parts of a Prestressed Anchor

A prestressed anchor includes 3 main parts: the anchorage, the bonded length and the unbonded length (Figure 3.2). In shortly, the bonded parts carry the prestressing loads, the unbonded parts transfer the loads from anchorage to bonded part and the anchorage provides the connection between the anchor and the retaining system.

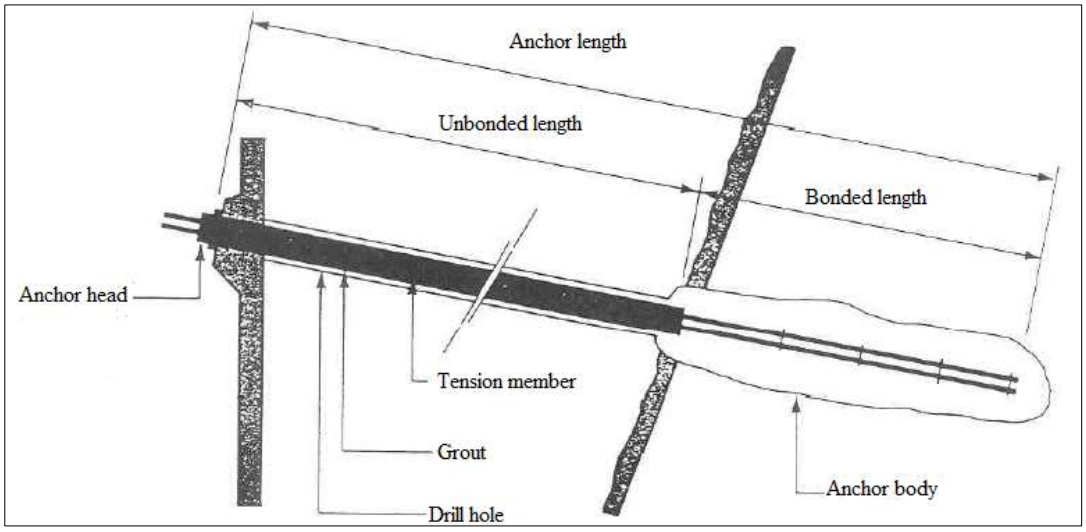

Figure 3.2 : Parts of a ground anchor.

Prestressing force is transfered from the anchorage that is formed from the the combination of anchor head, bearing plate and trumpet to the ground. The unbonded length of an anchor can be defined as the distance between the anchor head and the bonded length. Prestressing load applied to anchor and the additional forces occur as a result of the movement of the ground are transferred to the bonded length by unbonded length of anchor. In general it can be said that the minimum length of unbonded part of anchor is chosen as 4.5 m for strand tendons in rocks and soils and 3 m for bar tendons. It is noted that the unbonded length of a ground anchor can be calculated by using the proof test results carried out in the construction site:

$$L_{fs} = A_t \times E_s \times \Delta e/T \qquad \textbf{(3.1)}$$

In the equation given above, A_t is the cross-section area of the anchor, E_s is the modulus of elasticity of the tendon, Δe is the elastic strain of the tendon in maximum load and T is the maximum test load.

The bonded length of the anchor transmits the force coming from unbonded length to the soil or rock. In general, it can be said that the length of this part cannot be less

than 3 m in rocks. In addition to this, an increase of bonded length after 10 m does not effect the load transfer so that it is not necessary to built it more than 10 m (BS 8081). It must be noted that the bonded part of a prestressed ground anchor must be placed behind the potential failure plane in the design. Another significant point for the installation of bonded part is that the installation should be carried out into the same type of soil or rock because any decrease of rock quality may induce critical decreases in the load capacity of anchor. In Table 3.1, minimum bonded lengths for cement grouted rock anchors is given.

Table 3.1 : Bonded lengths for cement grouted rock anchors (Littlejohn and Bruce, 1971).

Type of rock	Minimum anchor bonded length [m]	Range [m]	Source
Very hard rock	3.0		Sweden: Nordin (1966)
	3.0		Italy: Berardi (1967)
		4.0 to 6.5	Canada: Hanna and Seeton (1967)
	3.0	3.0 to 10.0	Britain: Littlejohn (1972)
		3.0 to 10.0	France: Fenoux et al. (1972)
		3.0 to 8.0	Italy: Condi (1972)
	4.0		South Africa: Code of Practice (1972)
Soft rock	6.0		South Africa: Code of Practice (1972)
Chalk	5.0		France: Bureau Securitas (1972)
	5.0		USA: White (1973)
	3.0	3.0 to 6.0	Germany: Stocker (1973)
	3.0		Italy: Mascardi (1973)
	3.0		Britain: Universal anchorage Co. Ltd. (1972)
	3.0		Britain: Ground Anchors Ltd. (1974)
	3.5		Britain: Associated Tunnelling Co. Ltd. (1973)

The anchorage transmits the prestressing force from the prestressing tendon (bar tendon or strand tendon) to the bearing plate and anchor head is located on the horizontal waler beams or vertical retaining structures. The anchorage components for a strand tendon are shown in Figure 3.3. It must be noted that the geotechnical engineer should check the cleanliness of the surface between the bearing plate and the anchorage components must compliant in terms of type, unit, number of holes of wedge plate, surface state, etc., and all in correct position.

Figure 3.3 : Anchorage components for a strand tendon.

3.3 Components of a Prestressed Anchor

3.3.1 Grout

Grout is a binding element which is a mixture composed of cement, water, and possibly admixtures, transferres the loads on the strand tendon to the ground. By the help of the adherence between the strand tendon and the grout the load on the strand tendon is transferred to the ground; and then transferred to the ground by friction between the grout and the ground. Strength of the cement used for grouting should be higher. For example according to the BS 8081; 28-day compressive strength of 100mm x 100mm cube samples must be a minimum of 40 MPa. In addition to this, the ratio between the water and the cement is important. According to DIN 4125, w/c must be between 35% and 70%; and according to BS 8081 w/c must be between 35% and 60%. In low permeable cohesive soils and rock anchors w/c asked not to exceed 45%. Furthermore, cement type must be compatible with pre-stressed tendons. Known around the selection of the type of cement materials, such as the presence of carbonic acid or sulfates will be considered. Sulphate resisting cement used in the case of risk.

3.3.2 Tendons

Tendon materials can be steel bar or strand tendons. Both of them can be used for soil and rock anchors in slope stabilisation, and excavation support applications.

Generally in practice, tendons are produced with a diameter of 0.5 inch (12.70 mm) or 0.6 inch (15.24 mm). Strand tendons consist of multiple seven wires that are

corrugated in helical twist shaped. The general properties of strand tendons that are mostly used in deep excavation support systems are given in Table 3.2.

Table 3.2 : General properties for strand tendons (ASTM A416, 1997).

Nominal Diameter		13 mm (0.5 inch)		15 mm (0.6 inch)	
Type	Unit	Normal	Super	Normal	Super
Mean diameter	mm	12.5	12.8	15.2	15.5
Mean cross-sectional area	mm^2	93	99	139	140
Unit weight	kg/m	0.74	0.78	1.1	1.1
Minimum breaking load	kN	165	184	244	261
Modulus of elasticity	GPa	195			

3.3.3 Spacers and centralizers

Both centralizers and spacers can be produced from plastic, steel or a material that does not give harm to the prestressing steel. In the manufacture of both centralizers and spacers, wood material must not been used because wood languishes with water. Both of the spacers and the centralizers are used in the fixed part of the anchor.

Centralizers are used for placing and centralizing the strand tendon in the well.

Spacers are used for seperating the tendons form each other and ensure the penetration of the injection and also improve the adherence between the injection and the tendon.

3.3.4 Grout tube

Grout tubes are used for injecting the grout into the well with a pressure of 10 or 20 Bar. The diameter of the tube is 0.02 m.

3.3.5 Sheat

Sheath is used for preventing corrosion of the tendons.

3.3.6 Anchorage wedges

Anchorage wedges as shown in Figure 3.4 are used to fix the anchors. By the help of anchorage wedges, tendons are fixed to the wedge plate. The diameter and the length of the wedges change according to the nominal strand diameter. For instance, for 0.6 inch tendons wedge diameter varies between 15~15.3 mm and the length of the wedge is 46 mm.

Figure 3.4 : Anchorage wedges.

3.3.7 Bearing plate and wedge plate

Both bearing plate and wedge plate are used for fixing the anchors (Figure 3.3). Prestressing loads are transferred from the jack to the anchor with bearing plates. In addition, reaction forces of the ground are transferred to the strands with bearing plate. Bearing plates must be choosen as nondeformable under deflection and must also carry the characteristic load capacity of the anchor. Wedge plates must allow prestressing of strand tendon; adjustment or removal of the anchor loads and reapplication of prestressing loads as well as like bearing platesi wedge plates must carry the characteristic load capacity of strand tendons (Enar, 2010).

3.4 Potential Failure Mechanisms of Ground Anchors

It is important to design ground anchors under overloading conditions. Overloading conditions may occur because of the following reasons:

I. During load testing tendon may break out because of excessive loads on the anchor.
II. If the excavation sequence is not followed
III. Building of new structures close to the excavation
IV. Surcharge of buildings, traffic surcharge

In addition to the failure mechanisms given above also the failure of the anchorage system may be ensued from the combination of these reasons. The failure mechanisms of a ground anchor are shown in Figure 3.5.

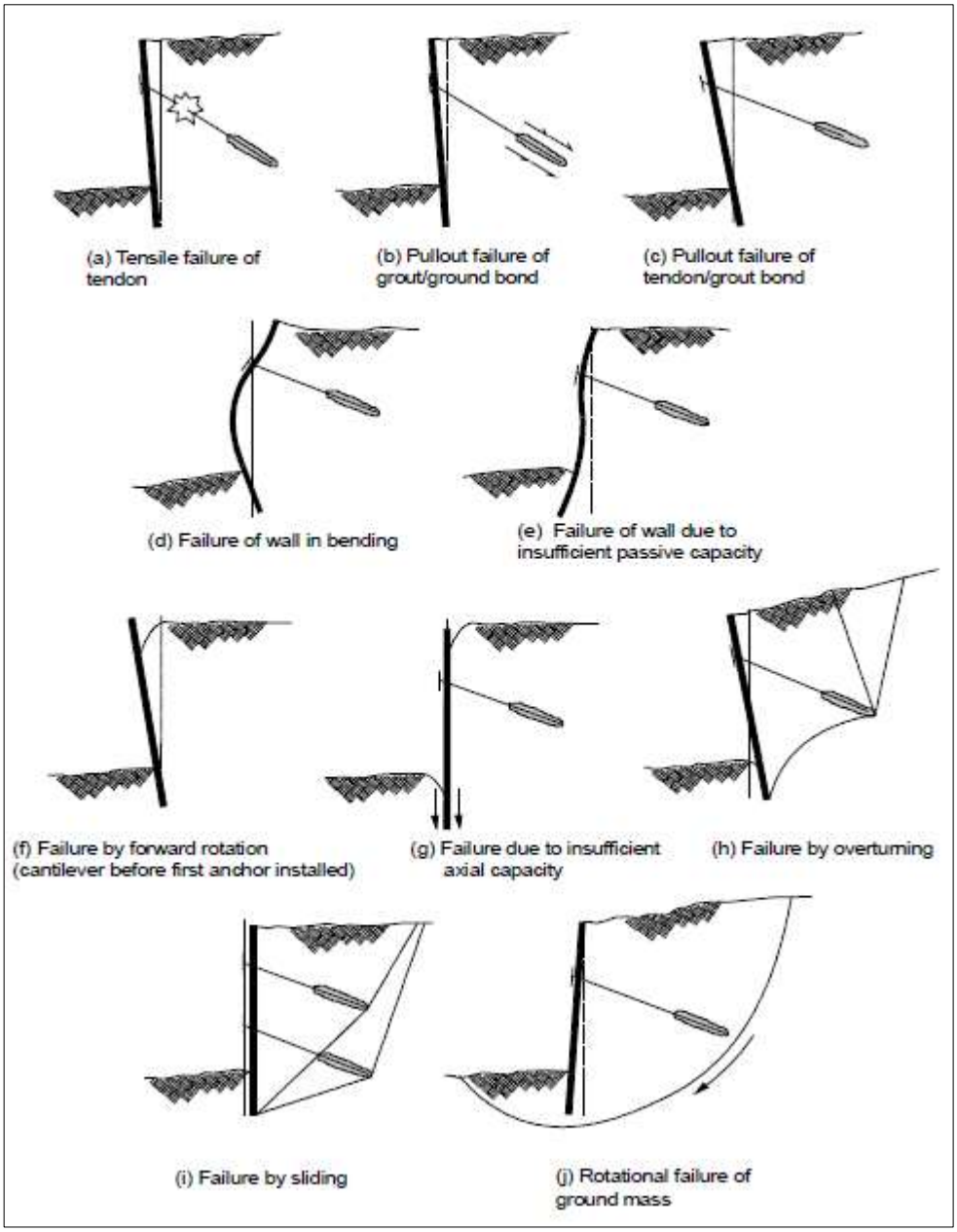

Figure 3.5 : Potential failure conditions to be considered in design of anchored walls (FHWA-IF-99-015, 1999).

3.4.1 Failure of tendon

If an excessive load is applied to the steel tendon, it may cause the failure of the steel tendon. The designer must consider this risk in the design. According to FHWA-IF-99-015 standard, in temporary structures the design load of the anchor must be 80% of the break load of the anchor. However, in permanent structures, this value is taken 60%. Furthermore, in the design of steel tendons, some safety factors are accepted: for temporary structures this value is between the range of 1.4~1.6 and for permanent structures the factor of safety is taken as 2.0.

3.4.2 Failure of the friction between the ground and the grout injection

Friction resistance is related with the cohesion of soil and the vertical stress. When the load applied to the anchor is greater than the friction resistance between the soil and the grout, anchor may pull out.

3.4.3 Failure of the friction between the anchor and the grout

The friction between the anchor and the ground is provided with the adhesion. Adhesion can be defined as the relationship between the grout and rough tendon. Friction resistance occurs because of the movement of the anchor changes according to the magnitude of force applied to the anchor, roughness of the anchor tendon and also the amount of movement.

3.4.4 Failure of the surface elements

The vertical retaining structures also known as the surface elements can be installed angularly. These elements are loaded both vertical and horizontal forces. The most critical phase of these vertical retaining elements occurs after both the first and the last excavation steps. After the first excavation step there is any horizonral supporting element is intalled to the ground so that all the horizontal earth pressures are carried by the vertical retaining structures. And also after the last excavation step, all the horizontal forces are mobilised and assumed as a design load. The reasons of the failure of a vertical supporting element can be both exceeding the bending moments and shearing forces.

3.4.5 Analysis of the external stability

For prestressing ground anchors the external stability analysis contains both the analysis of the collapse failure and the analysis of base failure. In the analysis of the external stability of an anchored wall, it is assumed that the the potential failure surface passes behind the anchor and below the bottom of the anchored wall.

3.4.5.1 Overall stability failure

Overall stability failure means that the anchored wall system fails as a whole. This type of failure is calculated differently for anchored wall with single level of ground anchors and anchored wall with multiple levels of ground anchors. Anchored wall with single level of ground anchors is analysed by Sliding Wedge Force Equlibrium

Method (Figure 3.6). It is assumed that the critical potential failure surface passes in front of the fixed anchor zone. The active and the passive forces acting on the wall are calculated. The free body diagram can be drawed for easy calculation and then by using the anchor force the loads on the system are calculated.

The force that keep the system balanced is calculated until the greatest force is gotten by using the following formula:

$$P_{REQ} = \frac{1}{2}\gamma H^2 \left[\frac{(1+\xi)^2}{tan(\propto)} - K_{pmob}\xi^2 \left(sin(\delta_{mob}) + \frac{cos(\delta_{mob})}{tan(\propto - \emptyset_{mob})}\right)\right] tan(\propto - \phi_{mob}) \quad \textbf{(3.2)}$$

ξ: The ratio of embedded depth to the height of wall, d/H

α: Inclination of potential failure surface

δ_{mob}: Mobilized interface friction angle

ϕ_{mob}: Mobilized friction angle of soil

K_{pmob}: Mobilized passive earth pressure coefficient of soil

The maximum force is then distributed to the anchor as axial force and to the vertical retaining element as bending moment.

It is more difficult to do this analysis in anchored walls with multiple ground anchors. Simply, The Ordinary Method of Slices (Fellenius, 1936) or The Simplified Bishop Method of Slices (Bishop, 1955) are used for the analysis. Both of the Ordinary method of slices and the Simplified Bishop method of slices seperate the circular slip into slices and equation is written for each slice. The basic assumption of the Ordinary Method of Slices also known as "Fellenius Method" is neglecting the forces on the sides of the slice (Figure 3.7). In this method, the normal force on a determined slice is calculated by using the sum of the forces acting on vertical direction. Factor of safety aganist to shear is calculated by summing the moments about the center of the slip circle. In The Simplified Bishop Method, a circular slip surface is also assumed and the interslice forces are assumed as horizontal (Figure 3.8). Once the forces on vertical direction are summed. To calculate the forces on the base of the slice, the resultant equation is combined with the Mohr-Coulomb equation and also with the safety factor definition.

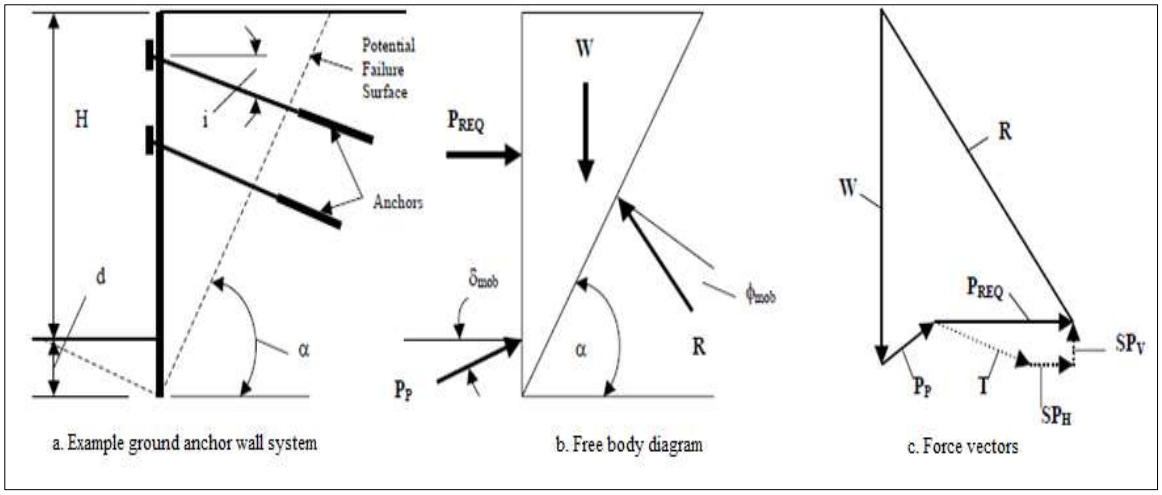

Figure 3.6 : Sliding wedge force equlibrium method for anchored wall with single level of ground anchors (FHWA-IF-99-015, 1999).

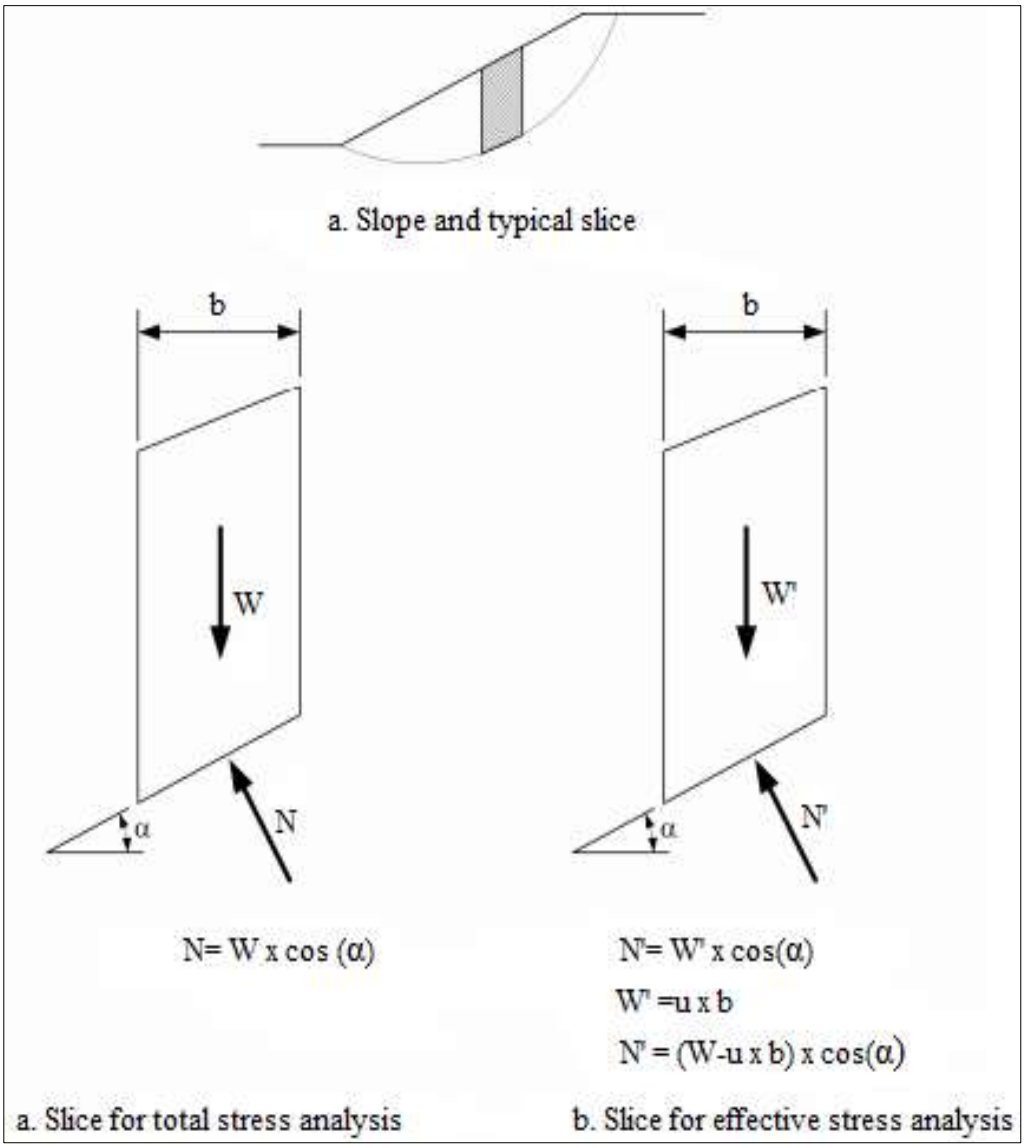

Figure 3.7 : Typical slice and forces for ordinary method of slices (USACE-EM 1110-2-1902, October 2003).

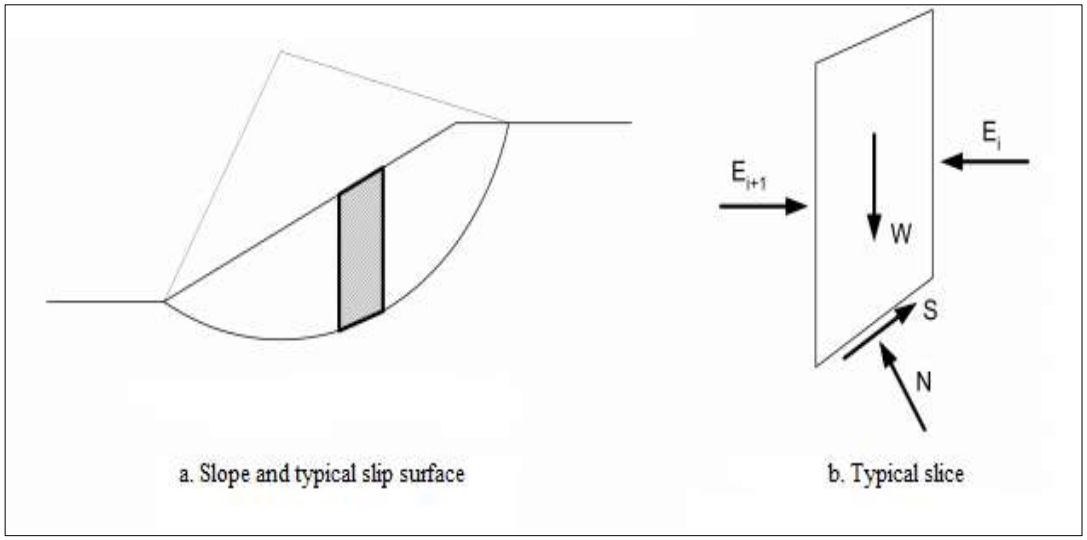

Figure 3.8 : Typical slice and forces for simplified Bishop method (USACE-EM 1110-2-1902, October 2003).

In the analysis of overall stability failure, the earthquake effects are also considered and the safety factors 1.3 and 1.1 are used respectively. If the deep excavation is carried out near a critical structure such as a building, bridge or road etc., minimum 1.5 must be used as a factor of safety (AASHTO, 1996).

It should be noted that the parameters change according to the life of the retaining structure. Soil parameters in drained conditions are used for the permanent structures; however in the external stability analysis of the temporary structures both drained and undrained conditions must be considered and the one which gives the most risky result is used.

3.4.5.2 Base failure by heave

This type of failure occurs in soft and weak cohesive soils such as stiff clays. Vertical loads on a weak soil below the excavation level reduce as a result of the excavation of the soil in front of the supporting wall. In that case, critical settlements occur and heaving starts from the excavation base.

There are various methods to examine the base failure by heave. All of the methods including Terzaghi Method, Bjerrum Method, Eide Method and Slip Surface Method assume a circular failure mechanism occur around the retaining wall element and the factor of safety of this mechanism can be calculated as bearing capacity calculations. Generally, safety factor aganist to base failure by heave is greater than 1.5.

3.5 Forces Acting on the Retaining Structure

To make a realistic design all of the forces acting on the retaining wall including lateral earth pressure, earthquake, surcharge, water loads etc. must be considered. The lateral earth pressure calculation was explained in detail in chapter 3.

3.5.1 Surcharge loads

Surcharge loads acting on retaining structures result from the traffic loads, loads of the surrounding structures etc. The lateral force caused by surcharge loads varies with the height of the excavation and also depends on the earth pressure coefficient.

In general, the surcharge load which spreads over an area of horizontal uniformly can be calculated as follows:

$$\sigma_h = K \times q \tag{3.3}$$

3.5.2 Water loads

Retaining walls are designed for stopping the hydrostatic pressure on the back of the wall. To prevent this hydrostatic pressure behind the wall, the installation of the sufficient drainage is necessary. It is noted that the water pressure increases with increasing depth below the GWT. Weep hole drains can be used to reduce the water pressure behind the wall. Weep holes should be installed with weepingpipes. If weep holes are installed without using weepingpipes, there may occur the block of the hole due to the sedimantation of rock.

3.5.3 Earthquake loads

Earthquake loads must be considered when making a seismic design. The lateral earth pressure acting on a retaining structure during earthquake is analysed by using the Mononobe-Okabe Theory which is an enhancement of the Coulomb Wedge Theory. The Mononobe-Okabe Theory was developed for granular cohesionless soils and in the theory liquefaction is neglected. For a six-month design of a flexible retaining system, the earthquake loads can be neglegted in order to make an economical design.

3.6 Sizing of a Prestressed Ground Anchor

3.6.1 Determination of anchor length

The length of an anchor is the combination of the free anchor length and the fixed anchor length. The free length of the anchor is determined according to the location of the critical potential failure plane behind the retaining wall. The angle of the critical potential failure plane from the horizontal depends on the internal friction angle ϕ and equals to "$45^o+\phi/2$". As a general rule, the free anchor length is extended a minimum distance of 0.2H or 1.5 m from the back of the critical potential failure surface (Figure 3.9). It is noted that the minimum anchor length must be chosen 3 m for bar tendon and 4.5 m for strand tendon.

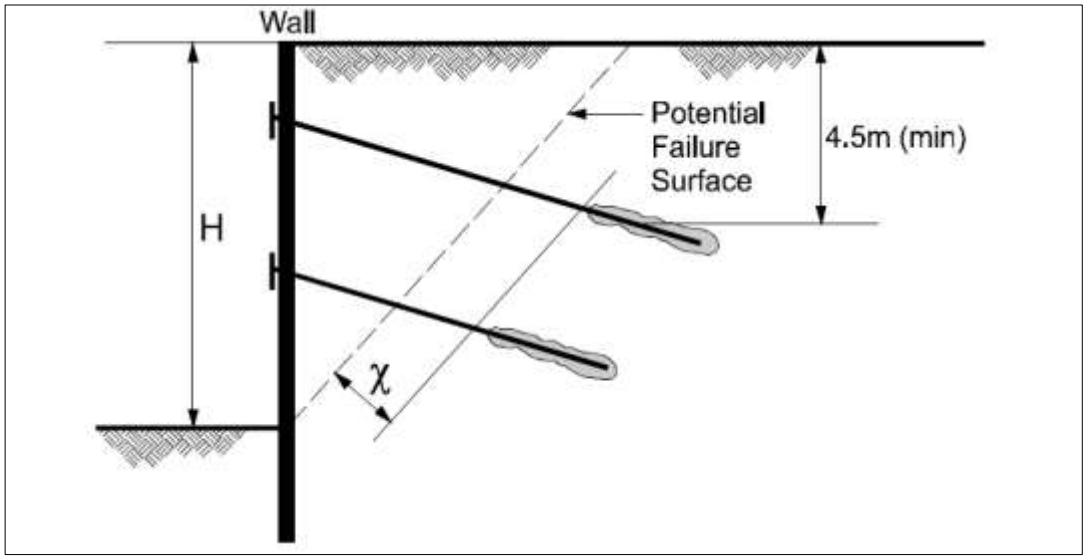

Figure 3.9 : Determination of the free length of prestressed ground anchor (FHWA-IF-99-015, 1999).

The fixed anchor length must be located beyond the critical failure surface in the retained soil mass. It is noted that in the determination of the fixed anchor length, the friction resistance of soil is important. In cohesive soils, the friction force between the fixed anchor zone and the soil is calculated by the following formula:

$$T_f = \pi \times D \times L \times \propto \times c_u \qquad \textbf{(3.4)}$$

c_u: Undrained cohesion (kPa)

α: Adhesion factor

D: Diameter of the fixed anchor zone (m)

L: Fixed anchor length (m)

The adhesion factor decreases with the increasing cohesion in cohesive soils. In general, it can be said that in stiff clays that has undrained cohesion greater than 100 kPa, the adhesion factor can be taken as 0.45 (Xanthakos, 1991).

In cohesionless soils, the fixed anchor capacity T_f can be calculated by the following equation:

$$T_f = \sigma_v \times \pi \times D \times L \times tan\varphi \quad \textbf{(3.5)}$$

σ_v: Effective vertical stress (kPa)

φ: Internal friction angle of the soil (^{o})

Unit friction capacity q_s is also used in the calculation of T_f:

$$T_f = q_s \times \pi \times D \times L \quad \textbf{(3.6)}$$

When calculating the anchor capacity by using the unit friction capacity, the factor of safety must be taken minimum 2.5 in soil anchors and 3.0 in rock anchors (AASHTO, 1996). In rock anchors, the unconfined compression strength q_u can be used to calculate the fixed anchor capacity:

$$T_f = (0.1\sim0.25)q_u \text{ (Ou, 2006)} \quad \textbf{(3.7)}$$

In hard rocks, 10% of the unconfined compression strength is used; however, in slightly weathered rocks 25% of the unconfined compression strength is used.

The fixed anchor length is recommended to be 3.00 m in soil anchors and 4.60 m for rock anchors. In Turkey, ground anchors are installed by using auger or pneumatic systems and the average drilling diameter is 120 mm. The fixed anchor length is generally chosen as 8 m. Anchor performance tests which are carried out in Thrace formation, it is observed that 60~70 tons loads can be easily tested.

In addition, ultimate load transfer values for different types of soils are given in Table 3.3. These values can be used to calculate the anchor bonded length. The estimated transfer load capacity for 1 m bonded length is 100 kN/m for loose sands and 190 kN/m for dense sand according to the Table 3.3.

Table 3.3 : Possible ultimate load transfer values for preliminary design phase of ground anchors in different soil types (FHWA-IF-99-015, p.71).

Soil Type	Relative density/Consistency (SPT ranges corrected according to overburden pressure)	Estimated ultimate transfer load [kN/m]
Sand and gravel	Loose (4-10)	145
	Medium dense (11-30)	220
	Dense (31-50)	290
Sand	Loose (4-10)	100
	Medium dense (11-30)	145
	Dense (31-50)	190
Silt	Loose (4-10)	70
	Medium dense (11-30)	100
	Dense (31-50)	130
Silt-clay mixture with low plasticity or fine micaceous sand or silt mixtures	Stiff (10-20)	30
	Hard (21-40)	60

3.6.2 Determination of anchor spacing

When selecting the vertical and horizontal anchor spacings, the designer must consider the site conditions, optimum number of ground anchors and their loads, type of the retaining wall and its flexural capacity and also the location of ground anchors themselves. To determine the horizontal anchor spacing, the shear forces for each anchor must be calculated at first. And then the loads calculated for each anchor are multiplied with the horizontal anchor spacing to obtain the axial loads on each anchor. The group effect of the anchors should be avoided in the design because it reduces the load carrying capacity of the anchored wall system. Moreover, according to the FHWA-IF-99-015, the horizontal anchor spacings must be chosen greater than 1.2 m to avoid group effects that reduce the anchor load capacity. The distance between the anchor bonded length and the foundation of the adjacent structure is recommended to be greater than 3 m. If the adjacent structure's foundation is shallow foundation then the distance must be greater than or equal to 4.5 m (Akbaş, 2010).

The location and the interval of the vertical retaining element should also be considered in design. In general, the ground anchors are located between the vertical retaining elements.

3.6.3 Determination of anchor inclination

The inclination of a ground anchor must be kept small as possible. In general, ground anchors are installed at an angle of 10^{o}~15^{o} with the horizontal. This inclination provides that the grout reaches more easily into the anchor bond zone. The inclination of the ground anchor can also be up to 45^{o} to prevent the failure of installation pipes and tunnels of surrounding structures.

3.6.4 Determination of strand tendon

In design, to provide the required anchor capacity the number of strands should be changed. Since the diameter of the strand is standard so that it cannot be changed. 7-wire low relaxation super strands with a diameter of 0.5" (13 mm) or 0.6" (15mm) are used in general site applications. For 0,6" (15 mm) diameter prestressing steel strands, the allowable tensile capacity is 260.7 kN and in the calculations this value is multiplied by a factor of safety 0.6 and taken as 156 kN approximately. For 3x0.6" strands, allowable capacity can be taken as 469 kN and for 4x0.6" strands, the allowable capacity can be taken equal to 626 kN in the calculation by considering the factor of safety (FHWA-IF-99-015, p.78).

3.7 Installation of Prestressed Ground Anchors

The following steps are followed during a prestressed anchored wall design:

- Excavation for the first stage ground anchors is carried out and then the anchor points are marked according to the spacings given in the project.
- Drilling machine is set at the inclination angle as defined in the project (Figure 3.10). Drilling method must be determined by the geotechnical engineering as inducing minimum crumble and also as preventing the failure in the anchor hole. Secondly, drilling method must be chosen as not decreasing the capacity of anchor. At the end of the drilling operation, holes must be cleaned with air compressor and if it is necessary drilling must be repeated again. The deviation tolerence from the inclination is ±2 degrees during drilling and the change of the position of the anchor is acceptable for 75 mm in all directions (Enar, 2010).

Figure 3.10 : Drilling for the anchor

- During drilling process, preperations for ground anchors are carried out. Total length of the ground anchor is the sum of the unbonded part and bonded part. Note that also an additional length for prestressing the anchor must be left. This additional prestressing length should be determined due to the jack length. For the investigation site, ground anchors are installed with 0.80~1.25 m prestressing lengths. The strands used in anchored walls are generally chosen as 0.6'' nominal diameter strand.

- Insulation for the prestressing anchors is also an important point. To prevent the grout injection into the unbonded part polyetilen foam or pitch material should be used. Due to low cost, polyetilen foam is mostly preferred in the applications as shown in Figure 3.11. Anchors must be placed into the hole maximum in 8 hours later after the completion of the drilling process due to prevent failures in the hole. Before the installation of the anchor the hole, grout injection is carried out to clean the hole and to fill the cracks in the ground. This will prevent the anchor failures that may occur during the construction.

Figure 3.11 : Preperations for ground anchors

- Cement grout without aggregate is used in anchor grouting. Technical specifications given for the water/cement ratio must be taken into consideration during the preperation of the cement grout. Grout injection process is carried out two times (Figure 3.12). The first grout injection is carried out as pressurized manner during the anchor placement into the hole. This is called as the primary grout. The primary grouting continue until the excess grout is vomitted from the hole. As mentioned in FHWA-IF-99-015, for cohesionless soils anchor capacity increases with increasing pressure. Before the initial set of the cement grout, the second grout injection process is carried out. Secondary grouting increases the anchor capacity especially in highly-weathered rocks and in coarse-grained or fine-grained soils.

Figure 3.12 : Grout injection for anchors

- While waiting for the initial set of the cement grout, reinforced concrete beam construction is carried out as shown in Figure 3.13. In the figure, it is seen that spiral reinforcement is placed around the anchor. The maximum load is firstly given the anchor head by the jack, and this pressure may cause occuring of cracks in the concrete. These spiral reinforcements are used in the waler beam construction to prevent the occurance of cracks by distributing the jack load.

Figure 3.13 : Waler beam assembly for ground anchors

Required time for the initial set the cement grout is approximately 7 days, but this period can be decreased by using some accelerating admixtures for grout. This chemical addmixtures should not contain any materials that can damage the prestressing steel and the grout material. The chemical addmixtures should not contain chlorite, sulphate and nitrite more than 0.1% of its mass (Enar, 2010). In the investigated area, the desirable strength of the cement grout is 21 MPa and Sika Dry Mix-CL is used for providing rapid setting and hardening of cement grout. Thus, the prestressing of ground anchors can be done in 3~4 days instead of waiting 7 days.

- The most significant point in the construction of the anchored pile wall is that all the ground anchors installed to the ground must be prestressed to be activated. Before prestressing ground anchors, firstly components of the

anchor such as bearing plate, wedge plate and wedges must be placed as shown in Figure 3.14. Wedge plates must be cylindirical-shaped and must be placed with no inclination. Hence the inclination of the anchor should be provided with square-shaped bearing plate.

Figure 3.14 : Preperations for anchor testing

- Prestressing loads should not exceed 80% of the characteristic tensile strength of the tendons. The hydraulic stressing jack used in the anchor testing must be calibrated in every six months and the calibration certificate must be kept available. Since the sheets for anchor testing are prepared with reference to the calibration certificates. In Figure 3.15, strand stressing hydraulic jack for anchor testing is shown. There is a support box under the jack to lift the jack until it is located completely. In the investigated area strand stressing hydraulic jack GP-9018/72 is used. At the beginning of stressing procedure, a support aparatus can be used until the anchor takes the first load. After that, anchor can be stand itself and there is no need to use a support aparatus. In temporary ground anchors prestressing load adjusted for testing the anchor is applied by following the loading stages 0.10P, 0.25 P, 0.50P, 0.75P, 1.0P-1.25P respectively. Here P represents the design load of the ground anchor. At all loading stages it must be waited 60 seconds approximately and until the last loading stage measurements are taken from the hydraulic jack. At the last loading stage, it must be waited for 5 minutes and readings from the

hydraulic jack are taken in the minutes 0, 0.5, 1, 3 and 5. Whether the difference between the readings taken at 0.5 minutes and 5 minutes, then it should be waited 45 minutes to see is the elongation of the strand continues or not. After the observation of the elongation of the ground anchor, if there is not a failure in the anchor lock-off will be applied to fix the anchor onto the bearing and wedge plates with wedges. The amount of the lock-offload is chosen by the geotechnical engineer but it generaly in the range of 0.50~1.00P. The ground anchors used in the investigation area mentioned in this thesis are locked to 1.1 times of the design load to prevent the hydraulic head loses. For instance, for the second staged anchors the maximum applied prestressing force is 1.25 times of the design load and equal to 375 kN and the lock-off load is 1.1 times of the design load which is equal to 330 kN. Another significant point in prestressing the anchors is the amount of prestressing load. If the prestressing load is greater than the load capacity of the anchor or the prestressing force is greater than the lateral earth pressure, then the lateral earth pressure behind the wall will increase, even passive earth pressure may develop and induce the system failure.

Figure 3.15 : Testing of ground anchors

3.8 Determination of the Vertical Retaining Element

3.8.1 Determination of the cross-section of vertical retaining element

The vertical retaining elements are designed taking into account of the lateral earth pressures acting on the structure, surcharge loads, water loads and also the seismic loads. Once the wall bending moments are calculated from the anchor loads. For the calculation of anchor loads 2 methods are provided by FHWA: The Tributary Area Method and The Hinge Method. It is noted that the calculation differs for single-level wall and multi-level wall. In multi-level anchored systems, the vertical retaining elements (piles, diaphragm walls etc.) shall be considered as a continuous beam and each anchor point is considered as an imaginary support. Mini piles were used as vertical support elements in this thesis and thought as a continuous beam that transfer loads coming from prestressed ground anchors to the earth. In the design, anchors are considered as fixed support elements that carry shear forces and bending moments. The calculation of wall bending moments for a multi-level retaining wall is shown in Figure 3.16. On the assumption of the vertical retaining element as a continuous beam, the maximum wall bending moment and the shear force equal to "$M_{max}=\frac{1}{2}Pl^2$" and "$Q_{max}=\frac{1}{2}Pl^2$" respectively. Here "P" is the maximum ordinate of the apparent pressure envelope and "l" is vertical anchor spacing.

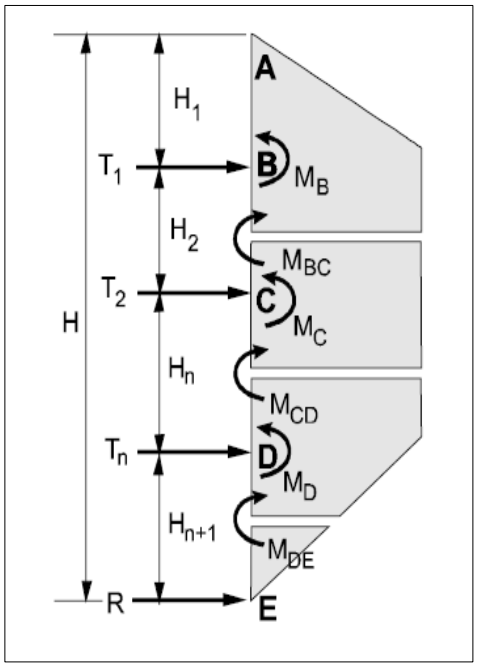

Figure 3.16 : Calculation of wall bending moments using tributary area method in multi-level wall (FHWA-IF-99-015, 1999).

The maximum ordinate of the apparent earth pressure diagram p_e is calculated as follows:

$$p_e = \frac{0{,}65\left\{tan^2\left(45-\frac{\phi}{2}\right)\right\}\gamma H^2}{H-\frac{H_1}{3}-\frac{H_3}{3}} \quad \textbf{(3.8)}$$

If there is ground water problem or surcharge load, these loads must be added to the diagram to get the total lateral force acting on the retaining wall. Surcharge loads act to the wall uniformly and can be calculated as:

$$p_s = q_s \times K_a \quad \textbf{(3.9)}$$

Then the total load acting on the wall is the sum of pe and ps:

$$p = p_e + p_s \quad \textbf{(3.10)}$$

Wall bending moment M_B is calculated as:

$$M_B = \frac{13}{54} \times H_1^2 \times p \quad \textbf{(3.11)}$$

Horizontal anchor loads are calculated as follows:

$$T_1 = \left(\frac{2}{3}H_1 + \frac{1}{2}H_2\right)p \quad \textbf{(3.12)}$$

$$T_2\left(\frac{1}{2}H_2 + \frac{1}{2}H_n\right)p \quad \textbf{(3.13)}$$

Horizontal load of the last anchor is calculated as:

$$T_n\left(\frac{1}{2}H_n + \frac{23}{48}H_{n+1}\right)p \quad \textbf{(3.14)}$$

The total lateral earth pressure is carried both with horizontal anchor loads and reaction force at subgrade of the excavation. Reaction force is expressed as:

$$R = \left(\frac{3}{16}H_{n+1}\right)p \quad \textbf{(3.15)}$$

In this thesis, a mini-piled prestressed anchored wall is investigated. Working principle and installation of small-diameter (less than 450 mm) mini piles are similar with large-diameter (greater than 450 mm) bored piles. However, mini piles can be more advantageous and cost-effective than bored piles when working in narrow areas and bedrock. Mini pile drilling machines take small space so that while there is a lack of space for construction, this type of vertical retaining elements are preferred.

Mini pile construction must be carried out under the control of experienced geotechnical engineers. Pile holes must be measured to check the depth of the hole and must provide the necessary conditions as indicated in the project. (Figure 3.17).

Figure 3.17 : Mini pile installation.

There may occur a fast and disproportional increase in vertical displacements in mini piles after 12 m (Sütçüoğlu, 2010). It may be quite difficult to obtain a continuous pile more than 12 m long. Concrete placement can be a problem for small diameter mini piles whether they built in high lengths. In such cases, mini-piled walls are built in multiple stages.

Another important issue in mini pile installation is discharge of water since there is ground water in the pile hole. In the contrary case, at lower construction stages there may be encountered with empty piles. It is also important to use concrete vibrator equipment during concrete pouring. The use of the concrete vibrator is very important because long-time applications may cause segregaton of concrete. Therefore, concrete pouring of mini piles should be carried out under the control of an experienced engineer. Concrete pouring for minipiles is shown in Figure 3.18. After the completion of mini pile construction, mini piles are connected to each other with cap beam at the top level. The sizes of the cap beam should be determined according to the design and the diameter of the pile.

Figure 3.18 : Concrete casting for mini piles.

3.8.2 Determination of the embedded depth of the vertical retaining element

The carry of lateral loads changes during the excavation. At first construction stage, the designer makes the assumption that all the lateral forces are carried by the vertical retaining element and also the passive resistance at the base of the excavation. In other stages, the lateral forces are distributed to the ground anchors and at the final excavation stage, these lateral forces are carried with the passive resistance. The passive resistance at the base of the excavation is related to the soil properties, wall deflection and the embedded depth and this passive resistance is calculated by using a method developed by Broms in 1965 (Figure 3.19). Case (a) in Figure 3.19 shows the general pile model and the assumption for the method. The pile width is assumed to be equal to b. For cohesionless soils in drained conditions, a triangular passive resistance is assumed to occur at a depth of D. However, for cohesive soils in undrained conditions, a rectangular passive resistance is assumed to occur under 1.5 times of the pile width b. Once the type of soil must be determined since the calculation changes depending on the cohesion of the soil. The calculated passive resistance must be greater than the lateral force acting on the embedded depth of the pile. If it is not, the length of the embedded depth can be changed.

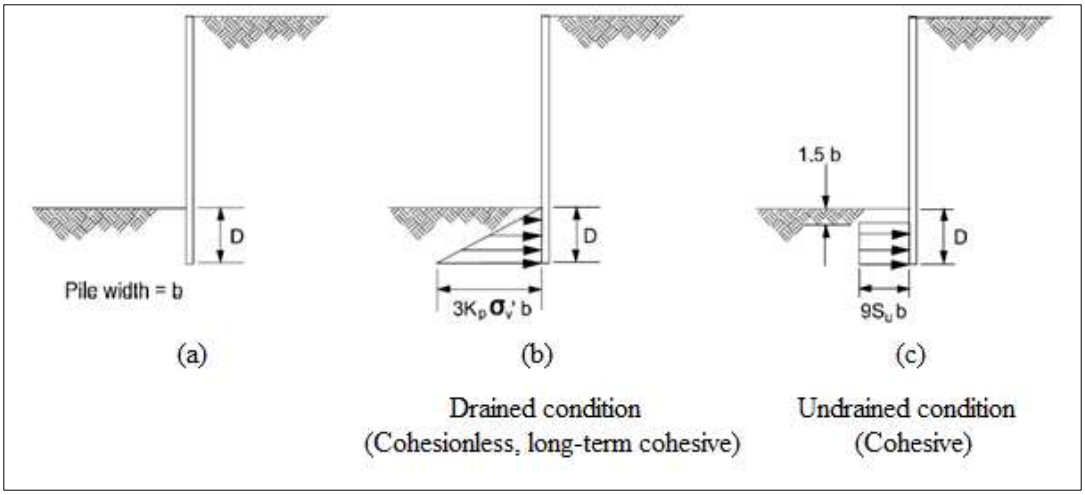

Figure 3.19 : Calculation of the ultimate passive resistance by Broms Method (FHWA-IF-99-015,1999).

3.9 Corrosion Protection of Prestressed Ground Anchors

Corrosion of prestressed ground anchors is a very serious problem since it affects the service life of the anchor. Corrosion problem occurs as a result of the reaction of metal and oxygen. There are so many factors affecting the rate of corrosion: type of the soil, water content, redox potential, soluble salts and aeration. The type of soil is related with both the resistivity of soil and the acidity (the measurement of pH) of the soil. Sandy soils are high up on the resistivity scale and therefore considered the least corrosive. The soils with pH less than 4.0 are defined as 'extremely acidic'; as well as soils with pH greater than 10 defined as 'very strongly alkaline'. It is recommended that the pH range in soils 5~10 for the application of metallic reinforcement structures (FHWA-NHI-09-087, 2009). In general, it can be said that the rate of corrosion increases with the increasing water content. The rate of the corrosion is maximum at an intermediate water content (65% saturation). The values under 65% water content do not permit corrosion failure since the water content is not enough for the reaction. However, at high water contents corrosion rate is also low because inadequate amount of oxygen. Soluble salts such as chlorides and sulphates also decrease the soil resistance aganist to corrosion.

To prevent the corrosion of a ground anchor, some cautions must be taken at the beginning of the installation. Cautions to be taken against to corrosion may vary depending on the parts of an anchor. For example, in the anchor head, a concrete or a steel cover filled with grout can be used. In addition to, anchor head

can also be painted againist to corrosion. In the unbonded anchor length, the protection aganist to corrosion can be provided by using grout or coating and in the bonded length protection is provided by using centralizer or coating.

3.10 Observation of the Retaining Wall Movements

Deformation of the retaining structures continues both during and after the excavation. To observe these deformations some instrumentation methods were developed. For monitoring lateral deformations slope inclinometers (Figure 3.20) and rod extensometers are used. In addition to this, for monitoring the vertical deformations, horizontal inclinometers, both rod and magnet extensometers, sondex, settlement point and settlement cells are used. By the help of these field instrumentation methods, the engineer can check the safety of the retaining structure. The engineer can check the ground movements that may affect the surrounding structures and can also observe that the ground anchors performing as designed.

Figure 3.20 : Slope inclinometer.

The most widely used in these methods in Turkey is inclinometers. Inclinometers are placed to measure the lateral displacements occur during the deep excavation. Installation of the inclinometers must be carried out before the excavation and it must be noted that the depth of the inclinometer hole must be deeper than the excavation base. Inclinometers consist of 4 main parts: a probe casing with gravity-sensing transducer, a probe with double wheel placed into a steel pipe to carry the gravity-

sensing transducer, a readout device and an electrical cable to connect the probe with readout unit (Figure 3.21). To observe the horizontal deformations, the probe of the inclinometer is lowered into a borehole. According to the scale on the cable, readings are taken in each unit during driving up the cable and also the slope of the probe is measured. By using both the angle of the slope and the length of the probe, lateral deformations in each stage can be calculated. Inclinometer measurements are generally defined with graphs.

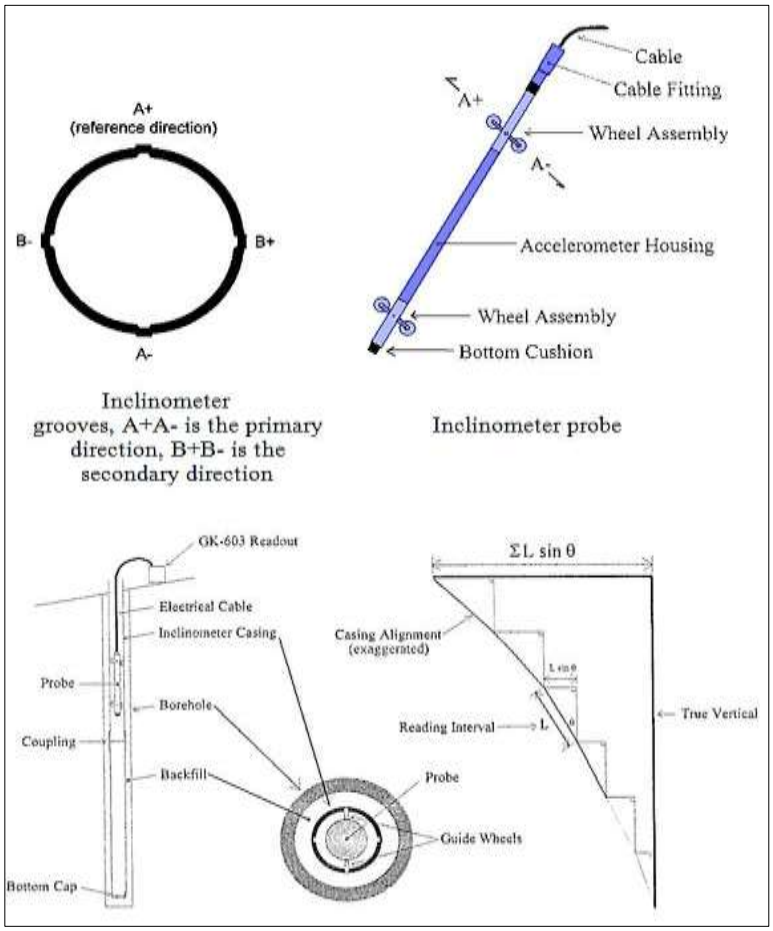

Figure 3.21 : Principal of conventional inclinometer operation [1].

The most commonly used graphs to evaluate the inclinometer measurements are cumulative displacements graph, incremental displacements graph, displacement-time graphs and absolute position graphs. For instance, cumulative displacements graph's horizontal axis shows the displacements in mm and the vertical axis shows the depth in m. In addition, while excessive lateral movements are observed in the ground, the reading frequency from the inclinometers should be increased. Inclinometers may be damaged from the external factors such as anchor hole drilling

and become unusable. In this case, a new inclinometer should be constituted into the related section to observe the lateral displacements.

Within the scope of this thesis the significance of inclinometer measurements was found. Inclinometer instruments IK-6 and IK-7 are placed in front of the Historic Bomonti Brewery before starting the deep excavation. The first readings are taken in 19.05.2010. Inclinometer readings both for IK-6 and IK-7 are given in Appendix F. For the inclinometer IK-6, the wall displacement above the excavation level is measured as in the range of 4~5 mm. The movements observed along the inclinometer hole is in the range of 1~2 mm and this value is taken as the reference mesasurements for the next readings. Besides the inclinometer IK-6, the wall displacement amount is measured as in the range of 5~6 mm above the excavation level. For the inclinometer IK-7 observed movements along the inclinometer hole is also in the range of 1~2 mm as in IK-6. It is seen that the first readings are in the range of allowable limits. During the excavation inclinometer readings were taken after all excavation levels and thus the deep excavation was kept under control as indicated in chapter 5.

The lateral deformations occured behind the retaining structure increases with the excavation depth. The lateral deformations occured in soft clays are larger than the deformations in sandy soils. The lateral deformations can be expressed in the interval $\delta_h(\%) = (0.2\sim0.5)H_e$ depending on the excavation depth (Ou, 2006). Researches performed on greywackes show that the average lateral deformations of a tied-back wall is in the order of $0.1H_e\%$.

The vertical deformations of a retaining structure occur as a settlement at the top of the excavation or heaving at the base of the excavation. The settlements occur on the top of the excavation is dangerous for the adjacent structures. The vertical deformations develop depending on the lateral deformation behind the retaining structure and increases with the increasing lateral deformations. It can be said that the vertical and lateral deformations in soft clays are equal to each other. Furthermore, a research on deep excavations carried out by Mana and Claugh (1981) shows that a relationship between the vertical and the lateral deformations:

$$\delta_v = (0.5\sim0.75)\delta_h \quad \textbf{(3.16)}$$

δ_v: Vertical deformations

δ_h: Horizontal deformations

3.11 Load Testing of Ground Anchors

Prestressed ground anchors must be tested after the installation according to various standards. In general, load tests on prestressed ground anchors can be classified into 3: proof tests, performance tests and creep tests.

3.11.1 Proof tests

The proof tests is the The prestressed ground anchors are tested by incrementally loading and unloading. It is noted that the application method of this test is different for permanent ground anchors and temporary ground anchors. In permanent ground anchors, 150 percent of the design load must be tested. On the other hand, in temporary ground anchors, 125 percent of the design load must be tested.

3.11.2 Perfomance tests

Performance test is carried out on prestressed ground anchor by incremental loading and unloading. The performance test is used for checking the capacity of prestressed ground anchor, observing the load-deformation behavior, causes of the anchor failure, proofing the current unbonded length is equal to or greater than the designed length.

3.11.3 Creep tests

The extended creep test is carried out for evaluating the creep deformations. This test lasts in about 8 hours. In cohesive soils with a plasticity index greater than 20 or liquid limit greater than 50, minimum two ground anchors must be subjected to extended creep test.

3.12 Lock-off Load of Ground Anchors

The lock-off load is the load that is immediately adjusted to the anchor head when prestressing is carried out successfully. The load in the anchor is reduced to a specified load which will be determined by the geotechnical engineer. The lock-off load must be adjusted to the anchor when the load testing procedure ends in success.

4. FINITE ELEMENT METHOD AND PLAXIS 2D

In geotechnical engineering, finite element method, FEM, is mostly used in design and analysis for the investigation of the behaviors of rock and soil. Both in theory and practice it is known that the behavior of the ground cannot be known correctly. This is because of the ground is a very complex material because of exhibiting anisotropy and being nonhomogeneous. However, FEM gives the most realistic results if the soil strength and deformation characteristics are entered correctly. Hence, the measurements carried out both in site and laboratory are very important to get the correct datas of soil and rock.

It is hard to take in consideration of all parameters in the analysis of a geotechnical problem because there are so many factors affecting the analysis. The finite element method, FEM, consists of modeling the wall and the soil as made of small elements and assigning to the elements properties which control their behavior. Beam elements are usually chosen to represent the wall while brick elements are used for the soil. A typical input for the FEM is the mesh description including the geometry of the elements for the wall, the anchors, the soil, the models for the wall material and water, boundary conditions, and the surcharge loads.

The steps for the finite element modelling in geotechnical engineering can be summarized as follows:

i. Identification of the geotechnical problem and determination for the type of analysis (Slope stability analysis, deep excavation analysis, retaining wall analysis, soil settlement analysis, analysis of seepage problems and seismic analysis etc.)

ii. Creation of the idealized soil profile (benefit from the geotechnical report and professional experiences)

iii. Determination of the most suitable soil model for representing the realistic behavior of soil or rock masses

iv. Creation of the geometry model and determination of the boundary conditions

v. Specification of the initial conditions

vi. Determination for the contruction stages

vii. Generation of the mesh

viii. Perform of the analysis (Calculation phase)

ix. Evaluation of the results (Outputs for the calculation results)

Most of the programmes used in geotechnical analysis and design run according to the finite element method. In finite element method, a huge area is divided into small areas or finite elements and all these elements are connected to each other by nodes.

There are so many programmes developed to solve geotechnical problems. In this study, two-dimensional Plaxis version 8.2 was used to analyze a deep excavation. On the other hand, in reality, all the geotechnical problems are 3-dimensional which means that the stresses in a soil spread in three directions. Generally, geotechnical analysis are carried out by using simplified methods instead of using 3-dimensional analysis. Therefore, in a deep excavation analysis, a cross-section in vertical direction is taken from the soil and this vertical cross-section is assumed to be constant along the investigated area. Thus, such a problem like this can be evaluated by using two-dimensional analysis in a vertical plane as perpendicular to the excavation axis.

Note that a geotechnical model must include the soil interfaces, geotechnical structures, construction stages and the loads on the ground. In Plaxis version 8.2 programme all these informations can be entered. A general information about Plaxis 2D software is given below.

4.1 Plaxis 2D

Plaxis 2D is a two-dimensional finite element software developed in 1987 at Delft University of Technology used in the stability and deformation analysis of any geotechnical problem. Plaxis 2D recommends two different types of modelling: plane strain and axisymmetric model. Plane strain modelling is used for uniform cross-sectional geometries; however axisymmetric modelling is used for circular

structures with an uniform radial cross-sectional geometry such as tunnels. Displacements and strains in z-direction are supposed to be zero in plane strain modelling; on the other hand normal stresses in z-direction are considered (Plaxis 2D Reference Manual, 2011).

One of the most significant process in finite element modelling is to create mesh because to perform a finite element calculation, the geometry model must be divided into finite elements. In finite element analysis, 6-node triangular elements or 15-node triangular elements are used to define mesh. 15-node element usage gives detailed analysis for the problems; on the other hand it takes long time. Stresses, strains and pore water pressures are calculated in these points. In this study 15-node triangular elements are used. Mesh density is a significant parameter for finite element analysis. In Plaxis software, there are 5 options for global coarseness: very fine, fine, medium, coarse and very coarse. Mesh density decreases from 'very fine' to 'very coarse'. On the other hand, the time for mesh generation extends. Generally, high frequencies give more accurate results; however, the cost of the analysis increases. In addition, the number of elements, the number of nodes and also the number of stress points increase while the coarseness is set from very coarse to very fine. In most cases, 'medium' option is chosen. Errors may be occured due to selecting the unsuitable global coarseness during mesh generation. This may be because two or more points are positioned at very close distances; so that the program suggests enlarging spacing between the points or may be the mesh is too fine. In Plaxis software, mesh generation is carried out automatically but the average element size which is a representation of refinement degree for the mesh can be controlled by global refinement or local refinement. So that in a such cases, the mesh can be regenerated by using lower coarseness, global or local refinement. To select 'refine global' from mesh menu provides one level increase of global coarseness. In other words, the global coarseness is set to medium from coarse and the mesh is generated automatically again. Moreover, local element size factor can be changed by clicking on the geometry point. The local element size factor is set to 1.0 for each geometry point and can take acceptable values in the range of 0.05~0.5. Generally, it can be said that setting the global coarseness to 'medium' is sufficient for the accuracy of the analysis. It must be born in mind that material sets must be assigned to all soil and structural elements before generating mesh.

In Plaxis analysis, both the soil and structural elements are defined from the 'materials' menu. Structural elements are modelled with the commands 'plate', 'anchors' and 'geogrids'. 'Plate' command is used to model piles, diaphragm walls and foundations. Soil nails and ground anchors are defined with 'anchors' command. 'Geogrids' command is used for grouted bodies. The interaction between the structural element and soil is defined with the command 'interfaces'. Interfaces are created similar to geometry line. Interfaces must be created at both sides of the geometry line to allow a complete interaction between the soil and the structure. Interfaces at both sides of the geometry line are seperated with positive-sign and negative-sign. These mathematical signs are meaningless as physical and they are just used for seperating the sides of the interface. Therefore these signs do not affect the calculations. The roughness of the interaction between the soil and the structure is modelled by an interface strength reduction factor "R_{inter}". The input value for R_{inter} is generally less than 1 and in Table 4.1, suitable values for the interaction between different types of soil and structure are given.

Table 4.1 : R_{inter} values for different types of soil and structure (Bae, 2007).

Type of Soil/Structure	R_{inter}
Sand/Steel	2/3
Clay/Steel	0,5
Sand/Concrete	1,0~0,8
Clay/Concrete	1,0~0,7
Soil/Geogrid	1
Soil/Geotextile	0,9~0,5

As can be seen from Table 4.1, the interface reduction factor takes different values for different types of soil and structure. The foundations and vertical retainnig elements are modelled in Plaxis 2D by using 'plate' elements. The input parameters for plate elements are flexural rigidity EI, normal stiffness EA, element thickness d and the Poisson's ratio υ. In two-dimensional analysis the rigidity of the plate elements are for 1 meter width. Flexural rigidity of the plate element is expressed by the calculation of the elasticity modulus of the material E that the plate element is made up of and the moment of inertia of the plate element, I. It is clear that the flexural rigidity of the plate element changes due to the material of the plate element to be manufactured. Thus this also affects the lateral load carrying capacity of the

plate element that is subjected to lateral forces. The behavior of vertical plate element under lateral forces is controlled by an interface reduction factor, therefore it is very important issue to take the right parameter for defining the interaction between the plate element and the soil. To define anchors, the normal stiffness EA and the horizontal spacing between the anchors are entered.

Plaxis 2D suggests linear elastic model and nonlinear models (Mohr-Coulomb, soft soil model, hardening soil model, soft soil creep model and jointed rock model) for modelling soil. It is also possible to develop another model to define the material by selecting the user-defined model.

In this study, the deep excavation support system in front of Historical Bomonti Brewery was simulated as plane strain and an elasto-plastic multi yield surface. Hardening Soil Model was used to define the behavior soil. Weathering degree of greywacke units decreases with increasing depth due to weather conditions and time. In addition the modulus of elasticity of these greywacke units increases by depth. To describe this type of soil, HSM is more suitable than other models. The Hardening Soil Model is detailed in 4.1.1.

4.1.1 The hardening soil model

A soil model is used for representing the real behavior of soil in a numerical analysis. To understand a soil model, it must be known that the real behavior of a soil/rock in nature. It is known that when a force is applied on a material, there will be deformations due to the internal stresses occur in the material. In perfectly elastic materials, when this load is removed, the material will return to its original shape. This rule prevails for isotropic, homogeneous elastic materials, also known as Hooke's Law. There is an elastic stress-strain relationship according to Hooke’s law. However, in nature materials behave differently which means they represent a nonliner elasticity modulus. Contrary to isotropic materials, the modulus of elasticity takes different values according to the stress directions in anisotropic rock materials. Only a very hard, dense, crystalised and spaceless, igneous and metamorphic rock materials exhibit an ideal elastic behavior.

The Hardening Soil Model is an advanced hyperbolic soil model and based on the Mohr-Coulomb failure criterion; however the hardening soil model differs from the Mohr-Coulomb model with its approximation of stiffness. The Hardening Soil Model

requires both classical and Mohr-Coulomb failure parameters and in addition it also requires some other parameters to define the soil stiffness. Hence, with these soil stiffness parameters, the hardening soil model makes possible to get a better approach to real behavior of soil. In Mohr-Coulomb model, 5 parameters are entered to describe the soil: elasticity modulus (E), poisson's ratio (υ), cohesion (c), internal friction angle (φ) and dilatancy angle (ψ). Moreover, elasticity modulus that is used to represent the stiffness of soil is constant along the depth in Mohr-Coulomb model. The input parameters to define the soil with Hardening Soil Model are listed below:

c_{ref}: (effective) cohesion

φ: (effective) angle of internal friction

ψ: angle of dilatancy

E_{50}^{ref}: secant stiffness at 50% stress level in standard drained triaxial test

E_{oed}^{ref}: tangent stiffness for primary oedometer loading

m: power for stress-level dependency of stiffness

E_{ur}^{ref}: unloading /reloading stiffness (default $E_{ur}^{ref}=3E_{50}^{ref}$)

υ_{ur}: poisson's ratio for unloading-reloading (default $\upsilon_{ur}=0.2$)

p^{ref}: reference stress for stiffness (default $p^{ref}=100$ stress units)

K_o^{NC}: K_o value for normal consolidation (default $K_o^{NC}=1-\sin\varphi$)

R_f: failure ratio q_f/q_a (default $R_f=0.9$)

$\sigma_{tension}$: tensile strength (default $\sigma_{tension}=0$ stress units)

$c_{increment}$: increase of cohesion per unit of depth (default $c_{increment}=0$)

Besides the parameters stated above, some other additional parameters can be used to define the soil behaviour in the Hardening Soil Model. The alternative parameters given below can be entered by clicking 'use alternatives'.

C_c: compression index

C_s: swelling index or reloading index

e_{init}: initial void ratio

Alternative stiffness parameters can be evaluated by using both the stiffness parameters and the initial void ratio. It must be noted that changing the value of the compression index C_c will also make a change in E_{50} and E_{oed}. Furthermore, while the value of the swelling index C_s changes then E_{ur} will also change.

The Hardening Soil Model is more advantageous to Mohr-Coulomb Model. In Mohr-Coulomb Model a constant modulus of elasticity is used to define the soil. Indeed in the Hardening Soil Model, the stiffness depends on the stress level. The Figure 4.1 shows the hyperbolic stress-strain relation in primary loading for a standard drained triaxial test. As can be seen in Figure 4.1, the secant modulus parameter E_{50} is obtained by a triaxial strain curve at 50% of the ultimate shear strength q_f. E_{50} is used instead of the initial modulus E_0 for primary loading in Hardening Soil Model. It is hard to determine the value of secant modulus E_{50} by experiments. In Hardening Soil Model the parameter m to express the stress dependency amount is given as:

$$E_{50} = E_{50}^{ref} \left(\frac{c\,cot\varphi - \sigma_3' \sin\varphi}{c\,cos\varphi + p^{ref} sin\theta} \right)^m \qquad \textbf{(4.1)}$$

where c and φ are cohesion and internal friction angle, respectively. In Plaxis, the value for m can be taken as 1.0 for soft soils and and for other soils the m value varies between 0.5~1.0. Here E_{50}^{ref} is a reference stiffness modulus corresponding to the reference stress p^{ref}. In Plaxis, p^{ref} can be taken 100 kN/m^2. As can be seen in the formula, E_{50} depends on effective confining pressure σ_3' in a triaxial test.

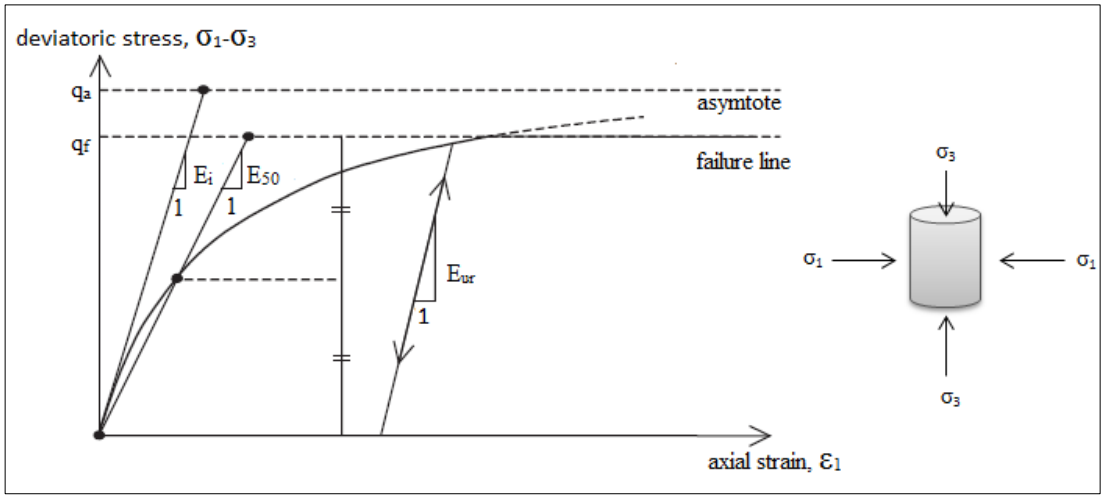

Figure 4.1 : Hyperbolic stress-strain relation in primary loading for a standard drained triaxial test (after Schanz et al., 1999).

For normally consolidated clays, the use of E_0 is more realistic because there is a wide range for the elastic behavior. On the other hand, in sandy soils and normally consolidated clays, a non-linear behavior is observed immediately when loading is started. Thus, the use of secant modulus E_{50} is more realistic for modelling the behavior of this type of soils.

In Hardening Soil Model, oedometer stiffness modulus E_{oed} is used to define the stiffness for 1D compression and defined for a reference stress p_{ref}, as:

$$E_{oed} = E_{oed}^{ref} \left(\frac{c\,cot\varphi - \sigma_1' \sin\varphi}{c\,cos\varphi + p^{ref} \sin\varphi} \right)^m \quad \textbf{(4.2)}$$

It is known that the ground material throws out water and air inside of its particles under a constant pressure and then compressed. The oedometer modulus is used to model the ground behavior at compression. Definition of the tangent stiffness for primary oedometer loading E_{oed}^{ref} at a reference stress p_{ref} is shown in Figure 4.2.

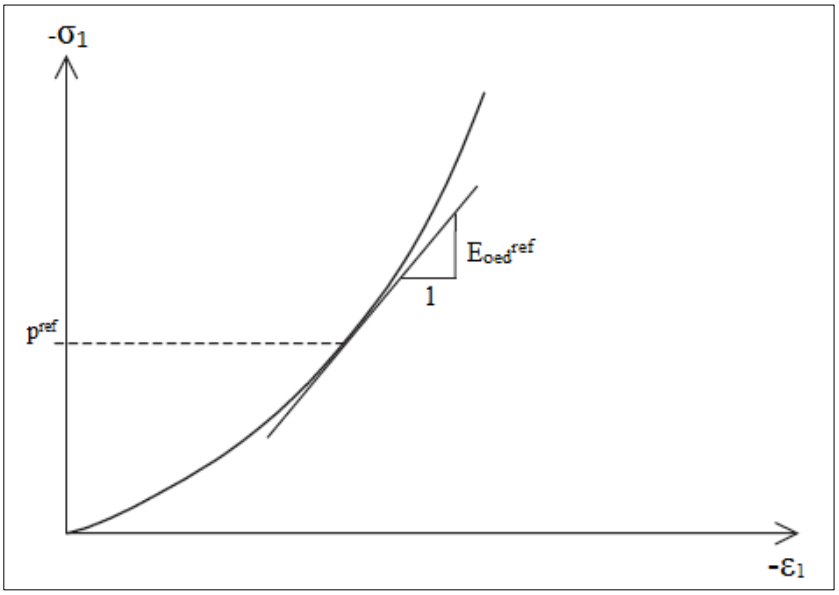

Figure 4.2 : Definition of E_{oed}^{ref} in oedometer test results (Plaxis Material Models Manual, 2011).

It must be taken into account that $\boldsymbol{\sigma_1'}$ is considered as primary loading and used instead of $\boldsymbol{\sigma_3'}$.

For unloading and reloading stress paths, unloading/reloading stiffness modulus E_{ur} is used and defined for a reference stress p_{ref}, as:

$$E_{ur} = E_{ur}^{ref} \left(\frac{c\,cos\varphi - \sigma_3' \sin\varphi}{c\,cos\varphi + p^{ref} \sin\varphi} \right)^m \quad \textbf{(4.3)}$$

In Plaxis Material Models Manual (2011), it is suggested that E_{ur}^{ref} can be estimated to be three times E_{50}^{ref}:

$$E_{ur}^{ref} = 3E_{50}^{ref} \quad \textbf{(4.4)}$$

It can be clearly said that with these three different modulus of elasticity parameters, E_{50}^{ref}, E_{ur}^{ref} and E_{oed}^{ref}, the soil stiffness is identified much more accurately so that the modelling of the soil deformations are carried out more sensitive.

The Hardening Soil Model is developed based on the Duncan and Chang(1970) hyperbolic model. The hyperbolic soil model based on the assumption of stress-strain curves of soil that are obtained from the triaxial test results are approxiamately hyperbolic-shaped. The inelastic stress-strain behavior of soil is represented with different modulus of elasticity values for loading and unloading conditions in the hyperbolic model. The Hardening Soil Model depends on the theory of plasticity and the volumetric strains. The yield cap that allows the preconsolidation pressure is to be taken into consideration was firstly added to the model in Plaxis Version 7. The shear yield surface which is controlled by the triaxial modulus and the cap which is controlled by the oedometer modulus are shown in Figure 4.3.

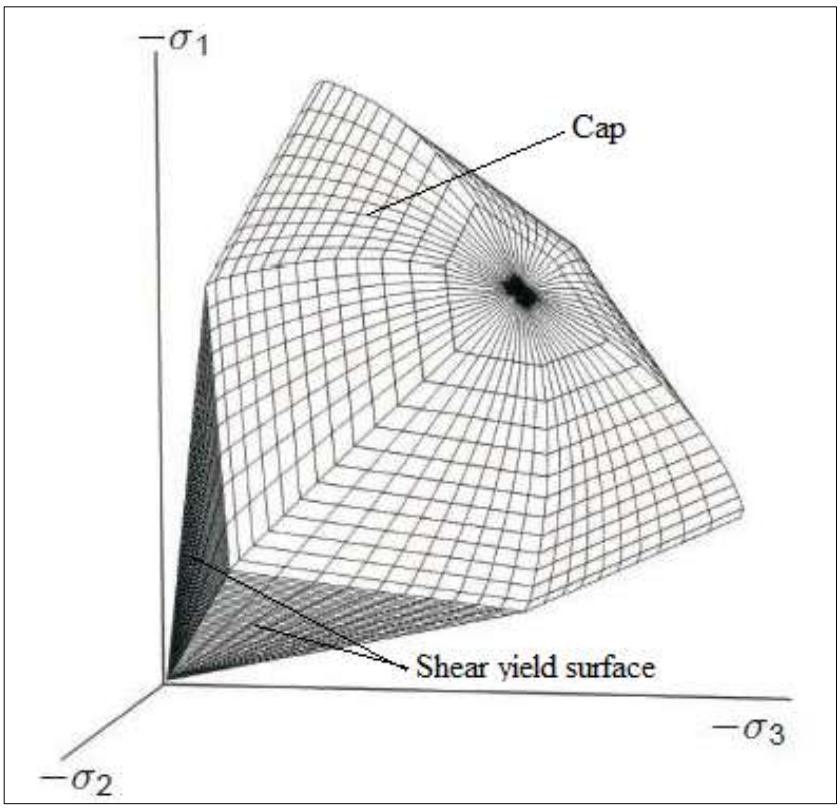

Figure 4.3 : Shear yield surface and cap surface of Hardening Soil Model.

The yield cap surface spreads as a function of preconsolidation pressure. The input for the initial preconsolidation pressures are defined as initial stresses in Plaxis. This means that the initial conditions are taken into account for soil deformation problems in the initial stress generation. Shortly, it can be said that E_{50}^{ref} controls the magnitude of the plastic strains related to the shear yield surface and Eoedref controls the magnitude of the plastic strains occured as a result of cap yield surface as shown in Figure 4.3.

Soil sample has a tendency to compact while a normal stress is applied. As a result of the tendency to compaction, an interconnection mechanism is resulted between the soil particles and thus the movement of the particles is limited. Therefore, a volume expansion in the soil occurs during shear deformations develop. This type of soil behavior is called as 'dilatancy' and the dilatancy of soils is represented by the angle of dilatancy in Plaxis software. The angle of dilatancy, ψ, is used to model irreversible plastic volumetric plastic strain incremements in the volume of the soil sample during plastic shearing. In sandy soils, the dilatant behavior depends both on the internal friction angle and relative density. The angle of dilatancy takes smaller values corresponding to the angle of internal friction. In clayey soils, the angle of dilatancy is assumed to be equal to 0. Plaxis recommends the equation 4.5 for the angle of dilatancy.

$$\psi = \varphi - 30^o \qquad \textbf{(4.5)}$$

This equation is acceptable for non-cohesive soils such as sand and gravel with $\varphi > 30^o$. The positive values for dilatancy angle means that for drained situations, volume change in soil sample continues during the development of shear deformations. However, this is not a realistic assumption because deformations occur without a change in volume at constrant pressure after a critical value. The dilatancy angle can take negative values only for loose sands, but in most cases, it is assumed to be equal to 0.

The Poisson's ratio, υ, is measured from the ratio of lateral strain to axial strain during a triaxial compression test with axial loading. The maxium value for the Poisson's ratio is 0.5. For cohesionless soils, Poisson's ratio varies from 0.25 to 0.35 and for cohesive soils, it varies from 0.40 to 0.50. The Poisson ratio is an important parameter to define the water saturation of rock materials in geotechnical

engineering. In fact, the degree of water saturation increases due to the value of Poisson's ratio approaches to 0.5. Table 4.2 shows a general range of Poisson's ratio for granular soils. In Plaxis, Poisson's ratio for unloading/reloading is used as an advanced parameter for the Hardening Soil Model. The range of 0.30~0.40 is recommended for loading conditions; on the other hand, the range of 0.15~0.25 is recommended as approximate for unloading conditions (Plaxis Material Models Manual, 2011). In Plaxis, for the Hardening Soil Model the Poisson's ratio for unloading/reloading is given as 0.20 as a default value.

Table 4.2 : General range for Poisson's ratio of granular soils (Das, Braja M., 2008).

Soil Type	Poisson's ratio υ [-]
Loose sand	0.20~0.40
Medium dense sand	0.25~0.40
Dense sand	0.30~045
Silty sand	0.20~0.40
Sand and gravel	0.15~0.35

K_o value for normal consolidation is represented with K_o^{NC}. On the contrary of Mohr-Coulomb Model, this value doesn't depend on Poisson's ratio and given with the equation 4.6 as a default.

$$K_o^{NC} = 1 - sin\varphi \quad \textbf{(4.6)}$$

The failure ratio, R_f, is the ratio between the ultimate deviatoric stress q_f and the asymptotic value of shear strength q_a. The value of the failure ratio is always less than 1, and is in the interval of 0.75 and 1.0 (Duncan and Chang, 1970). In Plaxis, R_f is assumed to be equal 0.9 as default.

5. CASE STUDY

5.1 Introduction

The deep excavation in Hilton Istanbul Bomonti Hotel and Conference Center Project was supported by a retaining wall to prevent the failure of surrounding structures and to make a safe excavation during the construction of the foundation. The excavation height varies between 15 m and 30 m. The shoring system was designed with different support systems: soil nails, prestressed anchors and struts. In this study, the section in front of Historic Bomonti Brewery which is protected by the ministry of culture and tourism was examined in detail and by backanalyses the most suitable elasticity modulus for this section was tried to be obtained. The shoring system adjacent to Historic Bomonti Brewery was decided to built as prestressed anchored pile wall. The vertical forces in front of the historic building were supported by using mini piles and the lateral forces were supported by using prestressed ground anchors. The diameter of the mini piles was chosen as 25 cm and the space between the centers of the mini piles was 50 cm. The surcharge load of the historic building with 3 floors was taken as 45 kPa.

The investigated area has a characteristic greywacke formation of Istanbul which is also known as Thrace formation. Thrace formation is commonly seen in European side of Istanbul, especially in Ikitelli, Cebecikoy, Besiktas, Levent, Sisli, Sariyer, Arnavutkoy, Ortakoy, Ayazaga and Gaziosmanpasa (Figure 5.1). This type of soil mostly contains sandstone, claystone and mudstone.

The soil parameters were determined from both the laboratory and the in-situ tests. However in real applications, these parameters cannot be used because the design made by using these parameters may cause the fail of the shoring system. Thus, the designer must choose the right parameters from the experiences gained before.

In this chapter, deep excavation support system of Historic Bomonti Brewery included in Hilton Istanbul Bomonti Hotel and Conference Center Project was presented. As well as the effect of some input parameters were also investigated. For

this project, informations about the soil exploration results, location of the region and geological structure of the site were all taken from the geological report prepared by Enar Engineers Architects&Consultants(2007).

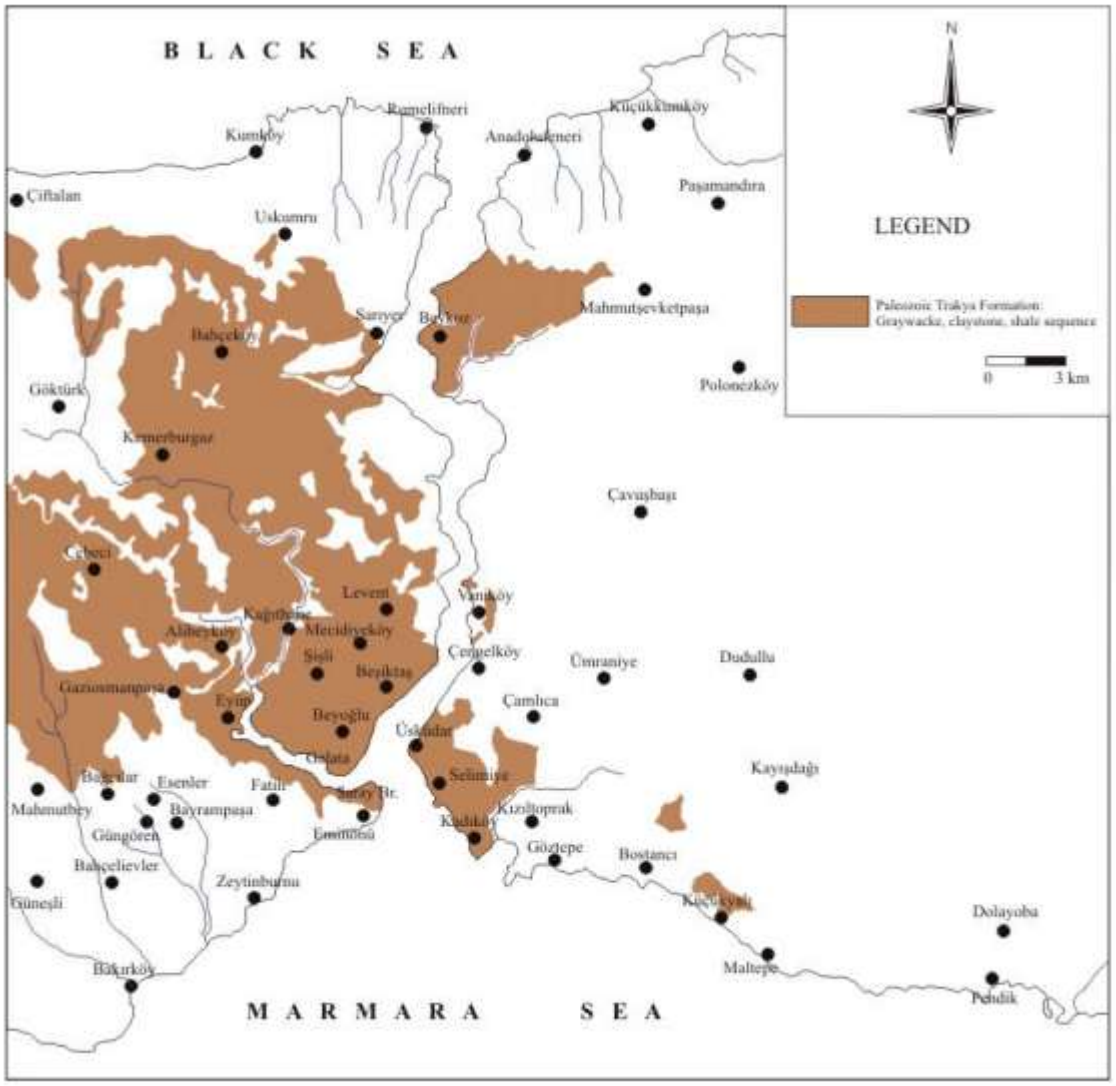

Figure 5.1 : Map showing the location of the greywackes (Modified from Ketin, 1991).

5.2 Project Description

Hilton Istanbul Bomonti Hotel and Conference Center Project is being built at the old Bomonti Brewery site, located in Sisli, traditionally one of the main residential and increasingly commercial density centers in Istanbul.

The project is scheduled to consist of three main uses as a 5-star hotel, office floors with high design standards and a convention center when completed and a fourth

use in the current historical buildings to be called the Historic Bomonti Brewery. A small scaled brewery museum and entertainment area is planned to be placed in and around the renovated historic buildings. Some datas related to the project are as follows:

- The total construction area is 166.016 m^2
- The total area of the historic buildings is 12.715 m^2
- The total area of the new buildings is 153.300 m^2
- The total number of the hotel rooms is 830
- The total number of the hotel floors: 35
- The total number of the lodge floors: 7
- The foundation level is +71.50 m
- The ground level (hotel entrance level) is +96.40 m
- Tower top level is +239.50 m
- The totel height of the tower from the ground level is +143.10 m
- The total construction height from the foundation level is +168.00 m

Key plan and cross section of the investigation area are given in Appendix C. As well as renders for Hilton Istanbul Bomonti Hotel and Conference Center Project can be seen in Appendix D.

5.3 General Geology and Soil Properties

In the region, bedrock is made up of exposed carboniferous period rock Thrace formation that can be seen in most of foundation excavation. Thrace formation is made up of the alternation of sandstone, claystone and mudstone and also seen both in European and Asian sides of Bosphorus. Layers of the artificial fill is seen on the surface of parcel and the thickness is 6 m. Thickness of the fill is almost between 1.5 and 2.0 meters. Under this layer, rocks that have various weathering levels are observed. By the help of the core samples, it can be seen that weathering is going on to the depth of 10~15 meters. Rock units are oxidized as a result of weathering and also the color of these units has been changed.

The colors of the unweathered sandstone is grizzly and light gray and the color of the weathered sanstone that has a middle thick layer is yellow. Mudstone and claystone layers are gray and dark gray at depth, and in weathered layers these units are thin-layered and green olive colored. Generally, weathering of rocks decreases to deeper and medium-weathered and highly-weathered rocks can be seen both in volcanic dyke boundaries that cut the units and fault and shearing zones notwithstanding the depth.

Although there are some differences, layers located in north-northwestern part of the investigation area are sloped to east, and layers in the middle of the investigated area are sloped to west. The inclination angle varies between 20^{o} and 85^{o}.

5.4 Field and Laboratory Works

In the investigation area, there are 8 drillings with a totally length of 170 m were carried out to determine the engineering properties of the ground. The rotary technique is used as drilling method (Figure 5.2). 8 drillings(rotary) were done in the investigation area by Temeltas Co. and during drilling, Craelius type 500 boring machine was used and core samples were taken by using core drilling machine type T76 with double tubes. From these samples TCR and RQD values were determined.

Rock layers in the investigation area can be divided into 4 according to their weathering properties:

- Highly weathered
- Moderately weathered
- Slightly weathered
- Fresh

Highly weathered rocks lose their rock property and looks like gravelly clay. Highly weathered rock units have a color of yellow-brown-olive green, and looks like broken into pieces, discontinuities are generally filled with clay and behaves like poor rock. Total core recovery (TCR), solid core recovery (SCR) and rock quality designation (RQD) values are shown in the following table (Table 5.1).

Table 5.1 : Rock parameters of highly weathered rock units.

Rock parameter	Minimum %	Maximum %	Average %
Total core recovery (TCR)	20	80	42
Solid core recovery (SCR)	0	60	20
Rock quality designation (RQD)	0	17	4

Figure 5.2 : Rotary drilling in Hilton Istanbul Bomonti Hotel and Conference Center

5.4.1 Soil borings

The number and the places of the borings are determined according to the properties of the investigation site and also the properties of the planned structure such as the type of building, number of floors etc. If the boundaries of the structures that will be built in the investigated site are known, the selection of the boring logs can be done easily. However in most cases, the limitations of the structures are not clear at the beginning. Generally, it is recommended that for the areas larger than 1000 m^2, borings should be drilled in the corners and also in the middle of the planned structure. It should not be forgotten that the sampling methods change according to the type of the ground.

In the investigated site, to determine both the physical and mechanical properties of rock in the laboratory conditions, rock drilling and sampling were performed at regular intervals at the boreholes to designate the stiffness or consistency of both the fill material and weathered rock material. T76 type double-tube core barrel was used for taking core samples and water is used as drilling fluid. Boring logs for the general of the construction site are given in Appendix B. Within soil exploration studies, a number of 8 soil borings with a total length of 170 m were conducted at the construction site. The summary of the borings conducted in the site is given in Table 5.2.

Table 5.2 : Soil exploration borings (Enar, 2007).

Boring No.	Boring Depth [m]	Boring Top Elevation [m]	GWT. [m]	Fill Thickness [m]	Rock Top Elevation [m]
SK1	20.00	81.57	-	3.0	78.57
SK2	20.00	86.53	-	4.5	82.03
SK3	20.00	91.20	-	7.5	83.70
SK4	20.00	96.25	-	3.0	93.25
SK5	20.00	96.80	-	3.0	93.80
SK6	28.00	99.80	-	1.5	98.30
SK7	20.00	103.40	-	3.0	100.40
SK8	22.50	104.00	-	4.5	99.50

It is seen that the thickness of the artifical fill layer in the general of the site varies between 3.0~7.5 m. Soil boring SK-4 with a depth of 20 m was conducted in front of Historic Bomonti Brewery to investigate the soil profile. A Heterogeneous fill layer with a thickness of 3 m was encountered on the surface. Under this layer, there is highly-weathered rock layer that consists of the alteration of sandstone-siltstone-claystone. Based on the soil borings it can be said that weathering of rocks decreases with increasing depth.

5.4.2 Seismic refraction test

In addition to the soil borings, seismic refraction tests were carried out at the site. Seismic refraction tests were conducted on the investigated site.

By this method, pressure (longitudinal) wave velocity (V_p) and shear (transverse) wave velocity (V_s) were measured. An American Geometrics brand Smart-Seis

Seismograph with 12 channels was used during the tests. A hammer with a weight of 10kg, which strikes on an iron plate, was used as a seismic source, and P and S geophones were used for measurements. Longitudinal (V_p) waves records were taken by hitting a 10kg hammer vertically on an iron plate at the soil surface and shear (V_s) waves were taken by hitting the hammer horizontally on the iron plate placed at the wall of a hole.

Time-distance (t-x) diagrams were drawn with respect to the longitudinal and transverse velocity records, and with the seismic velocities dynamic soil parameters were determined. The modeling of the soil layers from ground surface to depth was made by computing the time-distance (t-x) diagrams. Thereby, the seismic V_p and V_s wave velocities were calculated and the thickness of soil layers and dynamic soil parameters were determined.

During the refraction tests that were conducted on the site, the travel times of the seismic waves were recorded for each geophone. According to the dimensions of the site spacing between the geophones were selected as 4.0 m for SRM1 and SRM3 and the offset distance of the geophones intervals was selected as 2.0 m. In addition, geophone intervals were selected as 3.0 m and the offset distance was selected as 1.5m.

Seismic refraction method is used to examine both the pyhsical and dynamic soil properties of rock or soil. By using the seismic wave velocities with some correlations, the physical property unit weight of soil and the dynamic properties which are the poisson's ratio, the dynamic elasticity modulus and the shear elasticity modulus, soil amplification A_o, and the vibration period of the ground T_o can be calculated.

The depth of the soil layers determined after seismic evaluations and geomechanical-geodynamical properties of the layers are summarized in Table 5.3. The relationship between the Poisson's ratio and seismic velocities V_p and V_s is given in the following equation:

$$V_s = V_p \times \sqrt{\frac{1-2\upsilon}{2-2\upsilon}} \qquad \textbf{(5.1)}$$

Table 5.3 : Soil parameters calculated according to the seismic refraction test results (Enar, 2007).

SRM No	V_p [m/s]	V_s [m/s]	D [m]	E_d [kg/cm^2]	G_d [kg/cm^2]	γ [g/cm^3]	υ [-]
SRM1	434	228	3.7	1923.3	734.4	1.41	0.31
	3157	1624	>3.7	161553.7	61190.9	2.32	0.32
SRM2	328	192	3.1	1203.6	485.6	1.32	0.24
	2386	1052	>3.1	66046.3	23941.2	2.16	0.38
SRM3	643	279	3.35	3358.4	1213.3	1.56	0.38
	2974	1507	>3.35	137798.4	51910.8	2.29	0.33

D: Depth of soil layer

E_d: Dynamic elasticity modulus

G_d: Dynamic shear modulus

The seismic refraction method can be used to determination of the top of rock elevation. From the seismic refraction test results, it is seen that a loose layer with a thickness of 3.10~3.70m and has longitudinal wave velocity V_p=328~643 m/s and transverse wave velocity V_s=192~279 m/s is the upper layer. This unit is artificial fill layer encountered during soil exploration borings. After the artificial fill layer, there is a competent unit called as Thrace formation (greywackes) that has V_p=2386~3157 m/s and V_s=1052~1624 m/s.

5.4.3 Physical tests

Physical tests are performed on different sized borehole core samples to determine the dry unit weight, saturated unit weight and effective porosity according to the standard TS699. During the physical tests any of the borehole samples show dissolution property in water. A capacity 500 ^oC drying oven and a weighing instrument with a sesitivity of 0.01 g are used. Distilled water was used to determine the porosity. The process for the physical tests is summarized as follows:

Samples firstly kept in oven 24 hours and then dry weight(W_1) was determined.

At cooling stage of the samples, they were put in distilled water and after that water is wiped with a wet cloth and then weighed again to determine W_2.

Right after this process, these saturated samples were put in distilled water again to determine the total volume (V_T).

The number of the sample and soil parameters obtained from the tests are shown in Table 5.4. Lastly, by using the formulas given below, the parameters given in Table 5.4 were calculated.

$$\gamma_{dry} = W_1/V_T \quad \textbf{(5.2)}$$

$$\gamma_{sat} = W_2/V_T \quad \textbf{(5.3)}$$

$$n = 100 \times (W_2 - W_1)/V_T \quad \textbf{(5.4)}$$

As can be seen from the Table 5.4, dry unit weight of the rock varies between 2.45 and 2.72 g/cm^3 and the highest value for the porosity is obtained for the sample SK6 which is the closest sample to the surface. This means that the thickness of the weathering zone is greater than 6 m.

Table 5.4 : Soil parameters obtained from physical tests (Enar, 2007).

Sample No	Depth [m]	γ_{dry} [g/cm^3]	γ_{sat} [g/cm^3]	n [%]
SK1	14.50	2.72	2.74	2.10
	19.50	2.70	2.72	1.40
SK2	8.50	2.59	2.60	6.50
SK3	18.50	2.62	2.67	4.90
SK4	17.50	2.56	2.60	3.70
SK6	6.00	2.45	2.55	9.30
SK8	8.50	2.60	2.63	3.60

Strength of a rock material refers to resistance against external forces. While the applied forces exceed the strength of rock material, failure of the rock material is occured. Experiments carried out in the laboratory to determine the rock material strength are given as follows.

5.4.4 Determination of the uniaxial compressive strength

The uniaxial compressive strength tests are carried out on standard samples according to ISRM suggested methods for rock characterization testing and monitoring in 1985. Uniaxial compressive strength of rock materials is used in many design formulas and is also can be used as an index property to select the suitable excavation technique. There were 3 uniaxial compression tests conducted on the rock samples that are obtained from the borings in ITU Faculty of Mines Rock Mechanics

Laboratory. UCS test results are summarized in Table 5.5. According to the ISRM standards, it can be said that SK1 shows generally a high strength rock profile. As can be seen from the Table 5.5, SK3 and SK6 have compressive strength smaller than 250 kg/cm^2, thus these borings said that the rock profile belong to these borings shows a low strength. In addition, for SK3 it can be said that the layer is more weathered.

Table 5.5 : Uniaxial compressive strength test results (Enar, 2007).

Boring No	Boring Depth [m]	Height of the sample [cm]	Diameter of the sample [cm]	Failure load [kg]	Compressive strength [kg/cm^2]
SK1	14.50	10.92	5.40	11350	495
	19.50	10.12	5.40	14050	613
SK3	18.50	9.98	5.40	3100	135
SK6	6.00	9.73	5.40	3825	170

5.4.5 Determination of the point load strength

ISRM (1985) suggested methods for rock characterization testing and monitoring is used also in point load tests. The PLT is an indirect method for measuring the compressive or tensile strength of rock materials. The PLT results are used with some correlations to obtain the uniaxial compressive strength of rock, q_u. If the rock is heterogeneous and anisotropic, at least 10 samples should be used for the experiment. In the examples of irregularly shaped samples and blocks, the equivalent diameter is wanted to be desirably about 50 mm and the loading is done as in the others. In anisotropic rocks, to determine the upper and lower values of the rock strength, loading should be done both perpendicullar and parallel to the plane of the anisotropy. It is known that the best values can be obtained where the core axis is perpendicular to the weakness plane. In Table 5.6, PLT results are given. I_s is the uncorrected point load strength and I_{s50} is the corrected point load strength index for 50 mm-diameter core. The uncorrected point load strength is calculated by the equation 5.5.

$$I_S = \frac{P}{D_e^2} \qquad \textbf{(5.5)}$$

P: Applied platen load at failure (kg)

D_e: Equivalent core diameter (cm)

Table 5.6 : Soil parameters according to point load test results (Enar, 2007).

Boring No	Depth [m]	Equivalent core diameter, D_e [cm]	Failure load [kg]	Point load index, I_s [kg/cm^2]	Correction factor, K_{plt} $[D_e/50]^{0.45}$	I_{s50} $[I_s x K_{plt}]$ [kg/cm^2]
SK1	10.00	5.40	200	7	1.04	7.28
	14.50	5.40	1400	49	1.04	50.96
	19.50	5.40	2100	72	1.04	74.88
SK2	8.50	5.40	100	4	1.04	4.16
SK4	17.50	5.40	1200	41	1.04	42.64
SK8	8.50	5.40	800	28	1.04	29.12

According to I_{s50} values, rock classification can be done easily. I_{s50} values range between average 5 and 7.5 MPa for SK1, therefore the rock has very high strength in this boring. In borings SK4 and SK8, it can be said that the rock has moderate strength. On the other hand, SK2 has a point load strength index less than 1 MPa, which means that the rock sample taken from this boring is very weak.

5.5 Idealized Soil Profiles

The soil profile in the Bomonti site is determined from both the laboratory tests and in-situ tests. In boreholes, it is seen that the upper layer of the soil is formed from landfill and the lower layer is formed from Thrace formation. The fill in the upper layer has a heterogeneous structure and contains particles with a size of clay and gravel. The thickness of the landfill varies between 1.50 m and 7.50 m. The engineering parameters recommended for these two layers are summarized in Table 5.7.

Table 5.7 : Engineering parameters for landfill and Thrace formation (Enar, 2007).

Soil type/Engineering parameter	Landfill material	Thrace formation
Natural unit weight of soil (γ_n, kN/m^3)	19	22
Internal friction angle (φ, ^{o})	30	37.5
Modulus of elastisity (E, MPa)	5	40
Modulus of vertical subgrade reaction (k_v, kN/m^3)	10000	70000
Modulus of horizontal subgrade reaction (k_h, kN/m^3)	5000	40000
Rock quality designation (RQD, %)		<25%

The view of the greywacke units in the investigation area which are also known as Thrace formation is given in Figure 5.3.

Figure 5.3 : Greywacke units in the investigation area

All in all, it can be said that the rock layers observed in the general of the contruction site don't have potentials of settlement, swelling and collapsing failure. The investigated area is in liquefiable region according to the potential earthquake magnitude; however, soil and rock layers composing the land parcel are not liquefiable.

5.6 Design Parameters for Earthquake

The investigation area is depicted as 2nd degree earthquake region. Design earthquake parameters shall be considered for the project site is given in Table 5.8. There is a relationship between the seismic zone and the effective ground acceleration coefficient A_o. The Bomonti Brewery site is located in Sisli, Istanbul and the seismic zone for this county is 2; so that A_o is equal to 0.30. The characteristic spectrum periods are identified according to the local soil type. There is also a relationship between the local site class and the characteristic spectrum

periods; thusly for Z1 site class, the characteristic spectrum periods T_A and T_B are 0.10s and 0.30s, respectively.

Table 5.8 : Design parameters for earthquake

Property for Eartquake Design	Parameter
Ground Type	A
Local Site Class	Z1
Earthquake Magnitude	7.00 < M < 7.50
Effective Ground Acceleration Coefficient, A_o	0.30
Characteristic Spectrum Periods	T_A=0.10 s, T_B=0.30 s

The parameters given in the table above were used in the earthquake resistant design of the structure that will be built as a 5-star hotel in the Bomonti Brewery site. By using the datas obtained from the geotechnical investigations and previous experiences, model of the investigated area was created in finite element software Plaxis version 8.2 and then a numerical analysis was carried out to make decisions about the project. The retaining wall modelled in this thesis is constructed as a temporary support system; hence it isn't designed against earthquake.

5.7 Finite Element Modelling of Deep Excavation In front of Historic Bomonti Brewery

When a force acts on a rock material internal forces (stresses) aganist to external forces are generated and thus these internal forces cause deformations in the shape and the dimensions of rock material. In the scope of thesis, the behavior of greywackes that is a type of sedimentary rocks is also investigated during a deep excavation. In general, unweathered greywackes' bearing capacity is high. On the other hand, whether the depth of the excavation is higher than 3 meters, it is called as "deep excavation" and must be supported (Sağlamer, 1985). The foundation base elevation of the car park is +70.30 m and the surface elevation is +96.40 m, approximately. Hence, a deep excavation support system must be built.

The finite element analysis is undertaken with Plaxis software version 8.2. Plaxis 8.2 has 4 parts for modelling: Input, Calculation, Outputs and Curves. Any seismic analysis is included in the scope of thesis due to temporary retaining wall design.

5.7.1 Determination of soil properties

Idealized soil profile recommended in geotechnical report prepared by Enar Engineers Architects & Consultants(2007) are used to model the deep excavation support system for the foundation construction of seven-storey car park of Hilton Istanbul Bomonti Hotel and Conference Center Project in front of Historical Bomonti Brewery.

According to the geotechnical report and site observations there is no water in the construction site. Hence, in the analysis ground water was discounted. It can also be said that the calculations are carried out according to the total stresses. This means that the effective stresses will be equal to the total stresses at the end of the calculations. In soil borings, there is a fill layer with a thickness of 3 m in the investigated area; however, this artificial fill layer is removed before the deep excavation support system contruction starts. Therefore, in the Plaxis analysis there is only one soil profile is based on.

5.7.2 Determination of drainage conditions

In Plaxis modelling, material type can be selected as drained, undrained or nonporous. When it comes to a fast excavation, the behavior of soil in cohesive soils is defined as undrained soil behavior. In undrained conditions, stress application occur fastly so that this causes excess water pressure development in soil. If the excavation is carried out slowly which also means that the application of the stresses is carried out in a slow rate, the behavior of soil is defined as drained. This means that excess pore pressures are negligible. The rate of the excavation depends on so many factors such as the site conditions, soil or rock properties, climate conditions, the type of the excavation support system, the performance of the drilling and excavating machines, economical conditions, and also the time given by the contractor of the project. Therefore a suitable excavation time should be defined and during the excavation the behavior of soil should be assumed to be partially drained. Drained conditions are assumed to be valid for sandy and granular soils and undrained conditions are assumed to be valid for clayey soils in practice. In addition, partially drained conditions are assumed to be valid for soils which behavior is as cohesive soils and silty soils. In this thesis, calculations are carried out due to the

drained conditions for the investigated area due to there is no ground water flow so that the water pressures are negligible.

5.7.3 Preliminary design

In the preliminary design, the duration of the deep excavation, the site conditions, safety of the system, applicable building standards and codes, previous experiences, the adjacent structures and if exists infrastructures, and also the budget of the company are considered by using the recommendations given in the geotechnical evaluation report. The geotechnical engineer should design the safest and the economical model for the investigated area.

Construction of large and deep excavations changes the equilibrium state of the foundation soil and groundwater and also affects the adjacent structures and the environment significantly. So that a detailed geotechnical investigation must be carried out to determine the soil properties and existing structures current state around the excavation. For a safe design, one of the most important point is to determine the right coefficient of earth pressure in the preliminary calculations. To design a rigid retaining wall and to provide the security of the adjacent structures, raised earth pressure coefficients can be used. The lateral earth pressure that will act on the wall at the end of the construction is then calculated according to the pressure envelopes developed for braced excavations. Sizing of the retaining wall is carried out due to the reaction forces: shear forces and bending moments.

The retaining wall built in front of historic building is a temporary deep excavation support system due to the type of the project. In the preliminary design, the lateral earth pressures, water pressures, earthquake loads, traffic surcharge loads or the loads of adjacent structures must be considered. The supporting wall must be designed as to carry the lateral forces such as lateral earth pressure, water pressure and surcharge loads without being deformed and buckling. It must be noted that the earthquake loads are not considered for the investigation area indicated in this study because of designing a temporary support system.

In the case study given in the scope of thesis is related to the deep excavation support system built 2 meters away from a historic building for the foundation construction of a 7-storey car park. Therefore, to protect the historic building from settlements the retaining wall must be calculated according to at rest coefficient, K_o. In the

preliminary design, considering cost, time, applicability and the surrounded structures mini-piled anchored wall is found as more appropriate. Mini piling is advantageous for restricted areas with high load capacity. The mini pile construction is determined to be carried out in 2 stages because concrete casting may be a problem while the length of the mini pile increases. There may occur a fast and disproportional increase in vertical displacements in mini piles after 12 m (Sütçüoğlu, 2010). In the investigated area considering all these limitations for mini piles, the mini piles wall was built in 2 stages and the spacing between the piles were taken as 50 cm. The preliminary calculations for support elements are given in Appendix G. The calculations are carried out according to tributary area method as mentioned in chapter 3. For cohesionless soils, the apparent earth pressure envelope produces a total earth load that is approximately 1.3 times greater than Rankine's assumption, equal to $0.65K\gamma H^2$. According to the analysis of limit equilibrium, a uniform horizontal surcharge qK is applied to the wall face. According to the calculations the maximum moment for the vertical retaining element is the moment of span and equals to 58 kNm/m. In Table 5.9 moment capacities for various diameter mini piles are given.

Table 5.9 : Preliminary calculations for mini piles

Pile diameter [cm]	Steel		Concrete		ρ_{min}	ρ_m	m_r	M_r [kNm]
	Class	f_{yd} [Mpa]	Class	f_{cd} [Mpa]		$\rho_{min}f_{yd}/0,85f_{cd}$		$0,25*m_r*\pi*D^3*0,85f_{cd}$
25	420	365	C25	17	0,01	0,258	0,13	22,61
30	420	365	C25	17	0,01	0,258	0,13	39,06
45	420	365	C25	17	0,01	0,258	0,13	131,83

The spacing between the mini piles is selected as 0.50 m to prevent material erosion; thus the body moment will be 29 kNm/m. This means that Φ25 mini piles are suitable.

The lateral support was determined to be provided by prestressed ground anchors which are installed as active anchors by adjust prestressing force. Unlike the prestressed ground anchors, soil nails are known as passive anchors which means that the soil nail element don't carry load itself; however, the load transfer occurs while the retaining system built with soil nails moves to the backfill soil. There may

be large deformations are needed on the wall which is supported by soil nails in order to achieve the maximum load carrying capacity. So that the prestressed ground anchors are used in such cases to reduce these large deformations into acceptable amounts. The ground anchors are pretensioned towards the backfill soil, thus elastic stresses occur (Öncü, 2009). It may be hard to make calculations for each construction stage; thus the design is carried out according to the maximum lateral forces as indicated in chapter 3. The maximum lateral forces obtained by hand calculations are for unit width; hence these forces are calculated by the horizontal spacings between the anchors and thus excepted forces acting on the prestressed ground anchors are obtained. The type of the strand tendon and the number of the strands are determined by considering the excepted forces acting on the prestressed ground anchors. In practice, close-pitch placement of ground anchors with low capacity is preferred instead of sparse placed high capacity ground anchors. As mentioned in chapter 3, generally 0.5 inch and 0.6 inch strand tendons are used in geotechnical applications. The design is carried out by 0.6 inch strand tendons as can be found easily in the market. The shoring system should be connected back by prestressing ground anchors to prevent settlements may occur in historic building. The maximum prestressing force for the first stage anchors is approximately 365 kN which that is obtained by taking 125 percent of the calculated design load. Assuming that the load transfer rate is controlled by the weathering rock layer which is formed from sandstone-siltstone-claystone, as mentioned in chapter 3, FHWA(1999) recommends the load transfer rate for the preliminary design is 100 kN/m. Also assuming the factor of safety equals to 2, then the maximum bonded length is calculated as

$$Maximum\ bonded\ length = 365 \times 2/100 = 7.3\ m \qquad \textbf{(5.6)}$$

Minimum allowable bonded length for anchors installed in rock is 7.5 m as mentioned in the literature review of this thesis. Therefore, for the safety anchor bonded length is chosen as 8 m for the first staged anchors. The allowable anchor capacity for ASTM A416 G-270 3x0.6" type anchors is 547 kN and ASTM A416 G-270 4x0.6" type anchors is 730 kN with a safety factor 0.7(FHWA-IF-99-015, 1999). Thus it is larger than the maximum design load of 365 kN. In addition, for the second stage ground anchors, the maximum prestressing anchor load is calculated as 506 kN/m. It is decided to use 4x0.6" for the second stage for safety design. The cross-

section of the deep excavation in front of historic building is given in Figure 5.4. The first-staged of the excavation was designed with 14 m mini piles supported horizontally by 3x0.6 inch ground anchors and the second-staged excavation was designed with 19 m mini piles supported horizontally by 4x0.6 inch ground anchors. The embedded depth for the first mini pile iwas determined to be constructed as 4.5 m and for the second mini pile the embedded depth was determined to be built as 3.5 m.

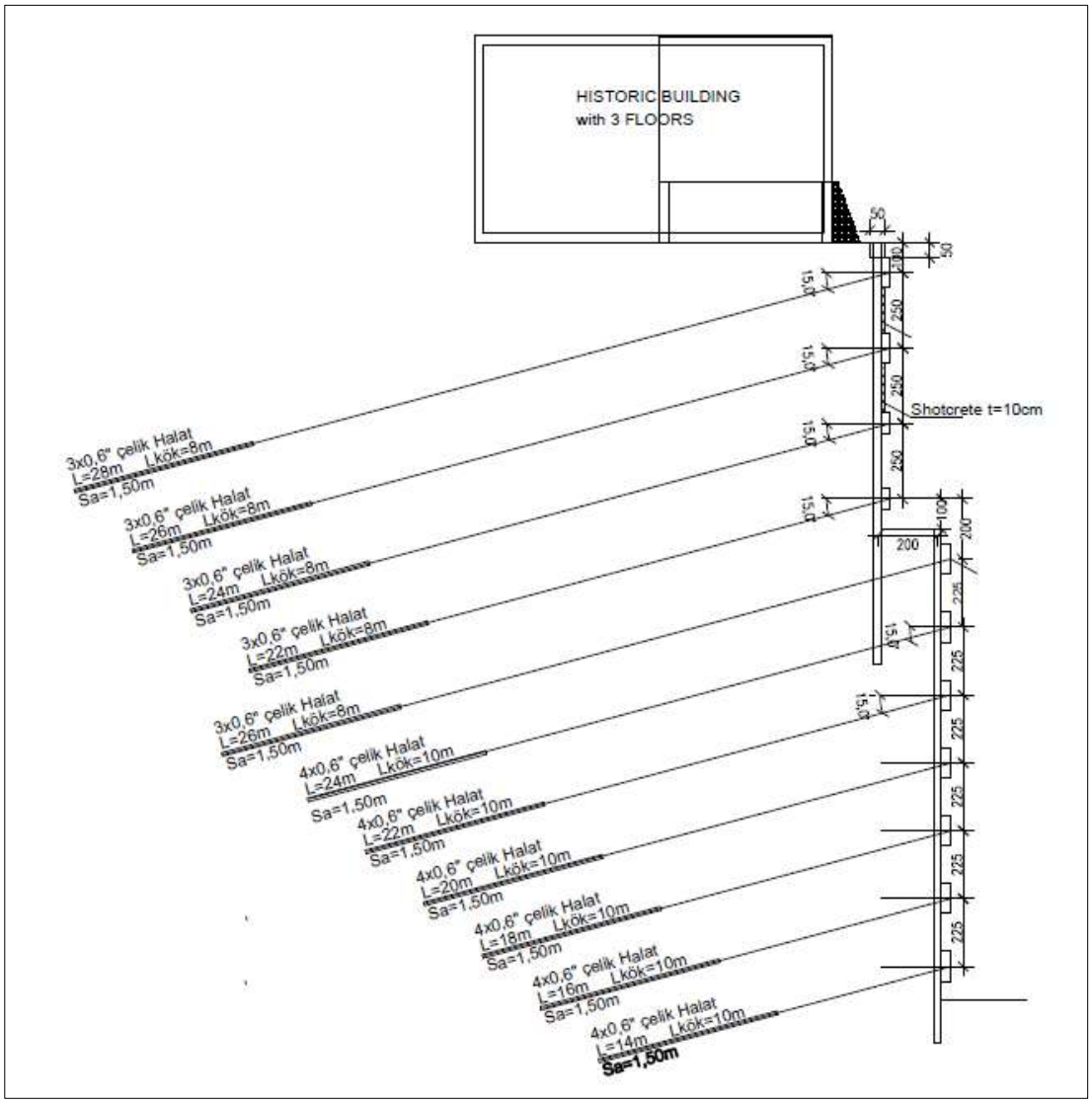

Figure 5.4 : Design cross-section of in front of historical building.

It is noted that the system is hyperstatic because the static equilibrium equations are insufficient to determine both the internal forces and reactions. Hence the solution will be more accurate while the static analysis of the continuous beam is carried out with a reinforced concrete design software.

5.7.4 Plaxis input and mesh generation

Plaxis input contains the generation of both finite element mesh and initial conditions. Firstly, Plaxis 8.2 Input is openned to start modelling. In Plaxis analysis, the first step for the calculation is to create the geometry model of the investigated area. Firstly, dimensions for the model which determined in the preliminary design are entered from general settings in input menu. The type of modelling is set to 'plane strain' and 15-noded element is chosen for finite element meshing. In Plaxis software, staged-construction analysis can be carried out as in real so that in the geometry model all of the construction stages are defined by the command 'geometry line'. Then both the structural elements and also the surcharge loads are entered if exists. After coordinate input has finished, boundary conditions are applied with 'standard fixities' command. The boundary conditions of the geometry model must be chosen wide enough not to affect the results of the geometry model. By default the bottom of the geometry model is fixed in all directions (d_x=0, d_y=0) and the vertical sides are fixed only in one dimension, horizontal dimension (d_x=0, d_y=free). In addition, the top surface of the model is free in all directions. The boundary conditions can be seen at the sides of the geometry model and at the bottom of the geometry model in Figure 5.5.

The vertical support structures such as piles, diaphragm walls, foundations and footings are defined by 'plate' command. Lateral support of the retaining system is provided with active anchors. In Plaxis software, ground anchors are modelled with the combination of geogrids and node-to-node anchors. The unbonded parts of ground anchors are defined with node-to-node anchor and the bonded parts are defined with 'geogrids' command. The surcharge of Historic Bomonti Brewery is entered by the command 'Distributed load-load system A'.

After the geometry model creation has finished, material properties are entered with the command 'materials'. First of all, the soil layers are assigned. The hardening soil model is used to simulate the elastoplastic behavior of soil. HSM is chosen due to a realistic approximation to stress-strain relationship and also convenient for modelling two hardening mechanisms: Plastic shear strains in granular soils or in overconsolidated cohesive soils such as overconsolidated clays and also compressive plastic strains in soft soils. In the model; parameters recommended by Enar Engineers Architects & Consultants are used (Table 5.9). There are 14 soil clusters

defined in the model; and in the site observations it is seen that there is only one type of soil profile so that in the analysis there is one cluster type. The soil is cohesionless; but to improve calculation performance, Plaxis recommends to use small cohesion. Hence c_{ref} is taken as 1 kN/m^2. In addition to Mohr Coulomb failure parameters c, φ, ψ; other basic and advanced parameters are entered to define soil stiffness. To describe the interaction between the pile and the soil, an interface element was formed. The strength reduction factor R_{inter} is used to define the interface element. Plaxis recommends to extend the interface as 1 meter just below the end of the plate element. Thus, the plate element is not fixed to the soil from the end point and the deformations are set to be free. The input parameters for the Hardening Soil Model are given in Table 5.10.

Table 5.10 : Soil data set parameters for HSM.

Hardening Soil		**1 greywacke**
Type	**Unit**	Drained
γ_{unsat}	[kN/m³]	22.00
γ_{sat}	[kN/m³]	22.00
k_x	[m/day]	0.001
k_y	[m/day]	0.001
e_{init}	[-]	0.50
e_{min}	[-]	0.00
e_{max}	[-]	999.00
c_k	[-]	1,00E+15
E_{50}^{ref}	[kN/m²]	40000.00
E_{oed}^{ref}	[kN/m²]	40000.00
power (m)	[-]	0.50
c_{ref}	[kN/m²]	1.00
φ	[°]	37.50
ψ	[°]	7.5
E_{ur}^{ref}	[kN/m²]	120000.00
$\nu_{ur}^{(nu)}$	[-]	0.200
p^{ref}	[kN/m²]	100.00
$c_{increment}$	[kN/m²]	0.00
y_{ref}	[m]	0.00
R_f	[-]	0.90
$T_{strength}$	[kN/m²]	0.00
R_{inter}	[-]	0.95
δ_{inter}	[m]	0.00
Interface permeability		Neutral

Note that it is recommended to avoid apex points that are plastic points in which the allowable shear stress is zero. In material data sets for soil and interfaces menu, to avoid apex plastic points, advanced hardening soil parameters option should be

chosen and then tension cut-off should be selected. Thus, the large number of apex points is prevented and the iteration procedure will be carried out fastly.

To define structural elements piles, prestressed anchors and the foundation of historic building, flexural rigidity EI and axial stiffness EA are used. Parameters EA and EI that are used in axial capacity and bending moment calculations of concrete piles are defined as:

$$EA = E\pi r^2 \quad \textbf{(5.7)}$$

$$EI = E\frac{\pi r^2}{4} \quad \textbf{(5.8)}$$

The input parameters are for unit width, for this reason it must be noted that the results can be obtained by dividing the spacing between piles.

The spread foundation of the adjacent building is also modelled by using plate element with a thickness of 0.35 m and a height of 1.20 m in order to provide a surcharge load that distributes uniformly. The material parameters for defining the plate elements (mini piles and foundation) are given in Table 5.11.

Table 5.11 : Material parameters for mini pile and historic building's foundation.

No.	Identification	EA	EI	w	n	Mp	Np
		[kN/m]	[kNm²/m]	[kN/m/m]	[-]	[kNm/m]	[kN/m]
1	MP_Φ25@0.5m	4.99E6	11500.00	1,3	0.15	1,00E+15	1,00E+15
2	Foundation	1.2E6	107187.5	5,17	0.15	1,00E+15	1,00E+15

Beam elements must be defined with interface elements to obtain a realistic soil-structure behavior before mesh generation. Interface elements provide a better transfer of structural elements' forces to the soil and a better model of deformation. Lateral support of the retaining system is provided with active anchors. For prestressed anchors, axial stifness EA values must be entered to determine anchor loads and displacement values. Prestressed ground anchors are designed with their bonded and unbonded parts. In Plaxis software, ground anchors are simulated with the combination of geogrids and node-to-node anchors. The material parameters for the prestressed ground anchors' unbonded and bonded parts are given in Table 5.12 and Table 5.13.

Table 5.12 : Material parameters for anchors' unbonded lengths.

No.	Identification	EA	|Fmax,comp|	|Fmax,tens|	L spacing
		[kN]	[kN]	[kN]	[m]
1	Anc_3x0.6"@1.5m	109449.00	1,00E+15	1,00E+15	1,5
2	Anc_4x0.6"@1.5m	145932.00	1,00E+15	1,00E+15	1,5

Table 5.13 : Material parameters for anchors' bonded lengths.

No.	Identification	EA	n
		[kN/m]	[-]
1	Groutbody_3x0.6"@1.5m	123870.00	0.00
2	Groutbody_4x0.6"@1.5m	147462.00	0.00

The behavior of ground anchors was chosen as elastic behavior because during the anchor test, the recoverable movement of the anchor is measured. Anchor elongations should be in the range of the elongation limits that were calculated by the geotechnical engineer. It is not wanted to test the anchors up to the yield point; so that the anchors behave as elastic.

After accomplishment of the geometry model as shown in Figure 5.5, from mesh menu element distribution was set to medium for global coarseness and then the mesh was generated. The geometry of the model can be drawen by the help of the tools in the software and also can be drawen by a CAD programme and then exported to the Plaxis software. Material sets must be assigned to all soil and structural elements before mesh generation otherwise the mesh is not generated. The mesh density in a finite element model is an important topic because of its relationship to accuracy and cost. As the mesh density increases, the numerical accuracy is improved, while the computational cost goes up. The generated mesh with significant nodes is shown in Figure 5.6. The geometry model is divided into small elements with 15-noded elements by generating mesh. All the stresses, deformations and also the pore pressures are calculated at these nodes. At the beginning, any of the elements defined in model were activated and the effective stresses were increasing uniformly throughout the depth in accordance with the behavior at rest (K_o condition).

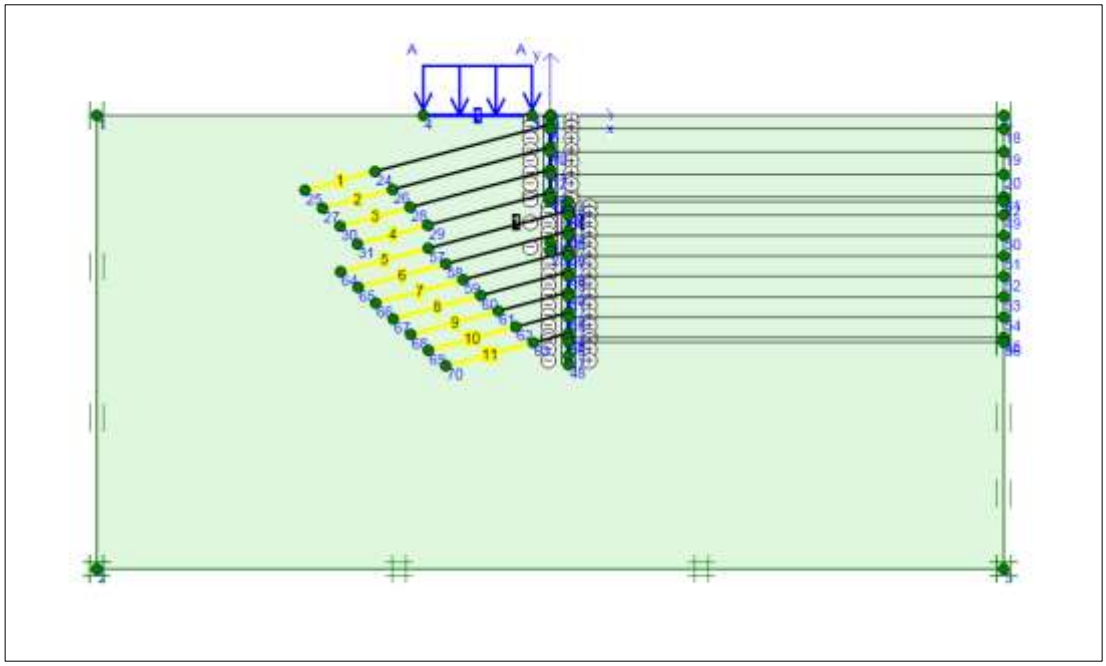

Figure 5.5 : Geometry of the model.

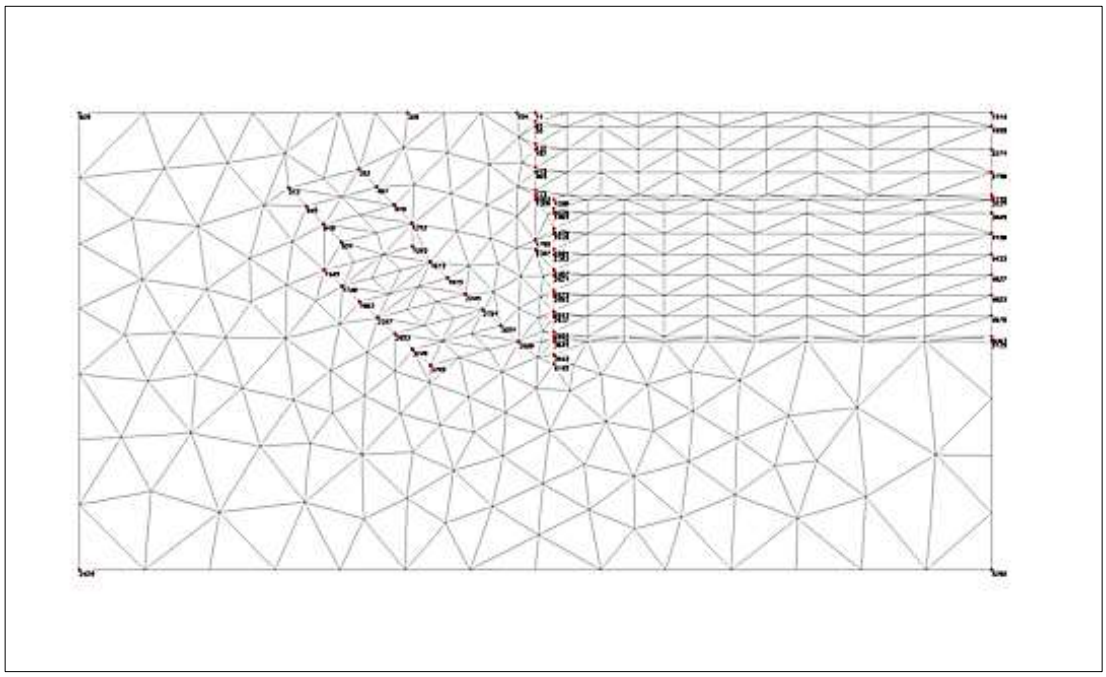

Figure 5.6 : Plot of the mesh with significant nodes.

The Plaxis Input is completed by generating the initial conditions. Water pressures and initial stresses are generated in initial conditions window, respectively. There is no need to enter groundwater conditions in the analysis because there is any groundwater flow in the construction site. K_o-procedure box appears while clicking the 'generate initial stress' button. The default value for K_o is accepted as in Jaky's formula (K_o=1-sinφ=1-sin 37.5^o=0.39) and the total multiplier for soil weight, ΣM-

weight is equal to 1.000 which means that the total weight of the soil is applied for initial stress generation.

5.7.5 Plaxis calculations

While the generation of initial stresses has been completed, 'calculation' mode is run. Loading input is chosen as 'staged construction' and the calculation type is set to 'plastic'. So that the staged construction analysis is carried out as plastic analysis. Calculation phases are defined for the model according to the construction stages. Totally 27 phases are defined for the analysis. In all phases the excavated soil cluster is deactivated and the structural elements which are installed at that phase are activated. After this process, the model is updated and this process is followed for each level until the final excavation level which is indicated in the figures as phase 27 is reached. Weight of soil is activated with K_o-procedure at 'initial phase'. In Plaxis software, lateral forces occured in the interaction zone behind the retaining wall are considered. Plaxis software does not make a distinction between the active and passive earth pressures. Plaxis calculates different earth pressure coefficients for all construction phases corresponding to the wall displacements. In addition, it is known that both the vertical and the horizontal stresses increase with increasing depth which is related through the earth pressure coefficient K. It should be kept in mind that if the excavation support system allows the soil to move, even slightly, then a great deal of the lateral earth pressure will reduce and this is active case where some of the lateral earth pressure is compensated by the slight movement of the retaining wall element. The passive earth pressure occurs only on the embedded depth of the plate element and generally, it must be avoided the development of the large passive earth pressures because passive earth pressure may induce large deformations in the system due to occurance of shear failure in soil. It can be said that the calculations carried out by Plaxis software is done by this logic.

The first phase is named as 'initial stage' and at initial stage displacements are set to zero and intermediate steps are deleted. The surcharge loads and the foundation support of the adjacent structure are activated at initial stage. Hence the construction elements 'Distributed Load System A' and 'Plate' are selected for the initial stage and the program is updated for passing the other phase.

In staged construction analysis, prestressing of ground anchors is an important process. It should not be forgotten that prestressing forces are adjusted per meter. In the analysis, the anchor forces calculated in the preliminary phase can also be used; however in the investigated project, the anchor loads are chosen by considering the ultimate bearing capacity of one tendon. Pulling capacity of one strand tendon is accepted as approximately 15 tons, hence for first stage anchors which have 3x0.6" strand tendons are loaded to 30 tons and the second stage anchors with 4x0.6" strand tendons are loaded to 45 tons per anchor. In Plaxis, prestressing is performed per meter, hence prestressing loads divided into horizontal anchor spacing are entered. It must be noted that the extended part of a prestressed ground anchor is its unbonded part. So that the prestressing force is adjusted only for node-to-node anchor in the calculation phase.

5.7.6 Plaxis output

In the Plaxis software, the calculation type was selected as 'plastic' to make stress and deformation analysis so that the outputs will be related to this type of analysis. Plastic calculation results can be taken in detail by running Plaxis 'output' after the completion of the calculations. In Table 5.14, preliminary design loads for prestressing the ground anchors before calculation phase and anchor loads at the end of Plaxis calculations are shown. The anchor loads can be seen by double clicking on the unbonded part of the anchor in the programme. These loads are for 1 m; thus it is multiplied by the horizontal anchor spacing to obtain the anchor design load. As indicated in chapter 3, temporary anchors are prestressed 125 percent of the design load. Therefore, test loads given in Table 5.14 were calculated according to the coefficient 1.25. Ground anchors are prestressed 0.7 times of the allowable tensile capacity. The allowable prestressing force for ground anchors with a diameter of 15 mm strand for 3 strands is 547 kN and for 4 strands is 730 kN with a factor of safety 0.7 (FHWA-IF-99-015, 1999). It is seen from the table that the prestressed anchors don't exceed the allowable prestressing force capacity because the first 4 anchors which have 3 strands carry maximum 384 kN and the remained anchors that have 4 strands carry maximum 650 kN prestressing force.

Table 5.14 : Anchor design loads.

Anchor No	Vertical spacing [m]	EL. [m]	Total Length [m]	Horizontal spacing [m]	Anchor load [kN/m]	Design load [kN]	Test load [kN]
Initial stage	0	+96,00					
1	1,00	+95,00	28	1,50	198,240	297,360	371,700
2	2,50	+92,50	26	1,50	204,380	306,570	383,213
3	2,50	+90,00	24	1,50	205,240	307,860	384,825
4	2,50	+87,50	22	1,50	199,880	299,820	374,775
5	2,00	+85,50	26	1,50	291,880	437,820	547,275
6	2,25	+83,25	24	1,50	326,540	489,810	612,263
7	2,25	+81,00	22	1,50	330,340	495,510	619,388
8	2,25	+78,75	20	1,50	336,720	505,080	631,350
9	2,25	+76,50	18	1,50	344,500	516,750	645,938
10	2,25	+74,25	16	1,50	347,400	521,250	651,563
11	2,25	+72,00	14	1,50	301,310	451,965	564,956
Excavation-13	1,00	+71,00					

The deformed mesh is shown in Figure 5.7. The deformed mesh is an exaggerated deformed shape of the geometry model after all construction stages completed. The maximum horizontal displacement occured in beam was calculated as 4.0 cm approximately as a result of the Plaxis calculations (Figure 5.8). Besides, the maximum lateral wall displacements for anchored walls built in sands is 0.002H, where H is the height of the wall (FHWA-IF-99-015, 1999). It is known that in almost such deep excavation problems, even if just small deformations occur. The important point is that these displacement values stay in permissible limits. The excavation height in front of Historic Bomonti Brewery is approximately 26.00 m; thus the maximum allowable wall movement is 26m x 0.002= 0.052m= 52mm and 39.62 mm is within the permissible limits. One of the most significant point in finite element analysis is that the location of the maximum displacements. From the Figure 5.8, it is seen that that the maximum displacements occur at the range of 18~20.00m; on the other hand inclinometer measurements given in Appendix F show that the maximum displacements occur at the range of 10~12 m. So that the results obtained in finite element analysis should not always be trusted. The horizontal displacements value in beam is shown in Figure 5.9. It is seen from the figure 5.9 that the maximum displacement occured approximately in the middle of beam which was installed for the second excavation stage.

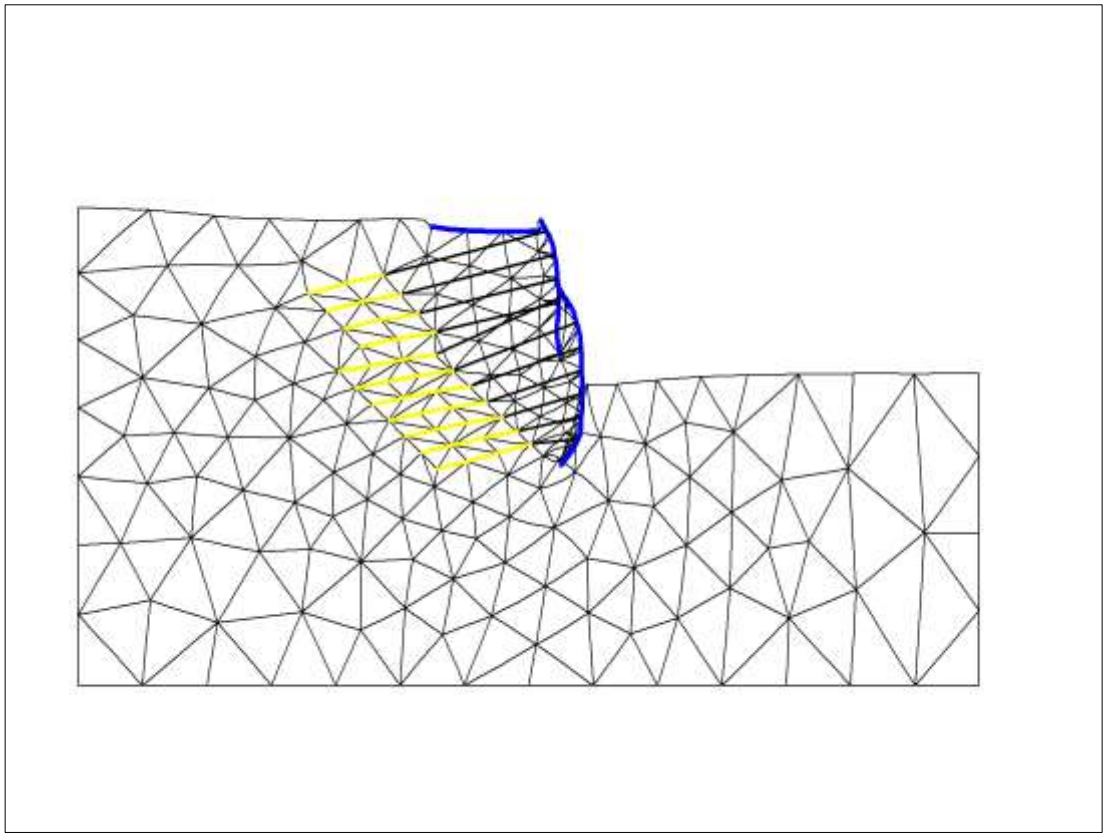

Figure 5.7 : Plot of deformed mesh - step no: 92 - (phase: 27).

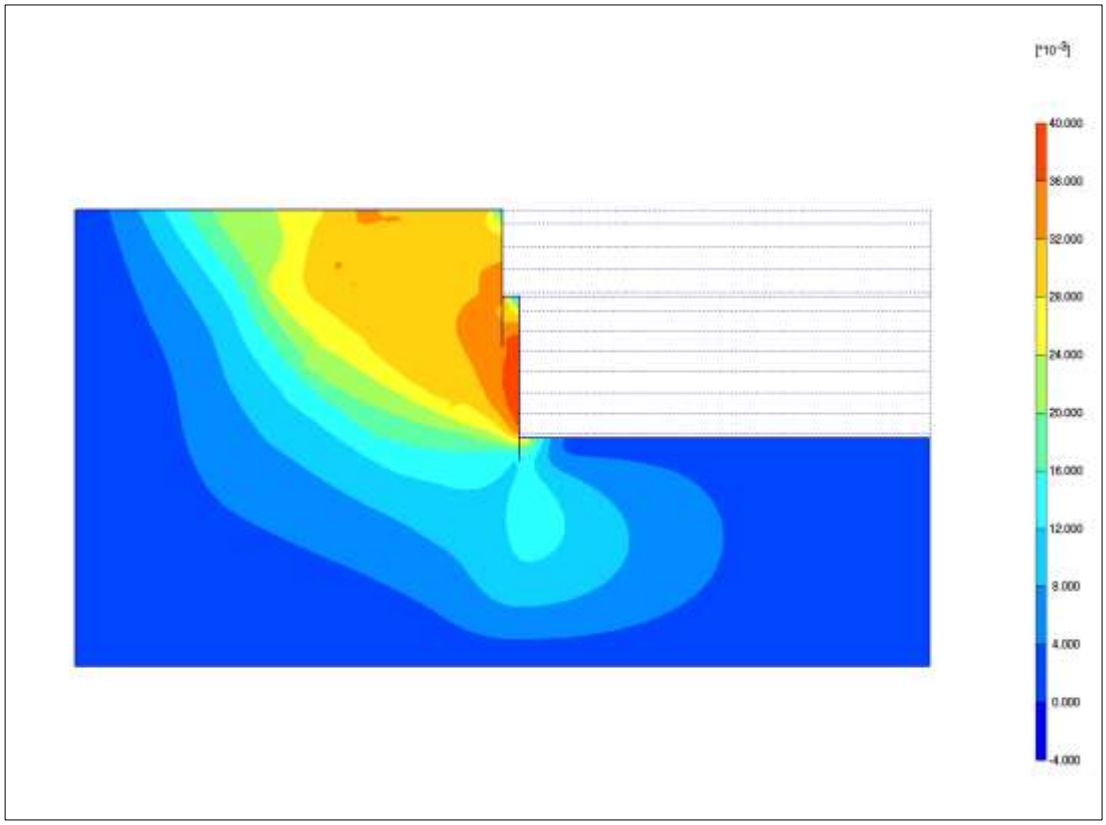

Figure 5.8 : Plot of horizontal displacements (shadings)- step no: 92 - (phase:27).

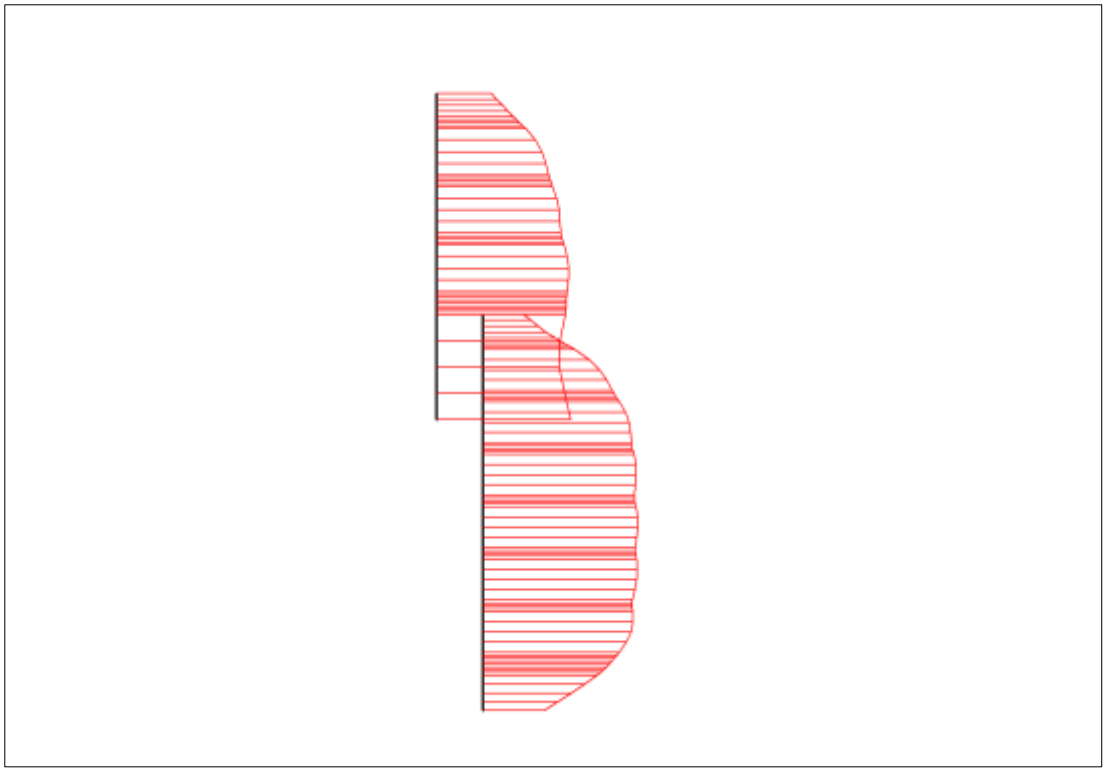

Figure 5.9 : Horizontal displacements in beam extreme value $39.62*10^{-3}$ m (phase: 27).

With Plaxis software, stresses both in horizontal and vertical directions at all points can be calculated. Plaxis software makes the calculations within the frame of elastoplastic behavior of ground. This means that while the stresses occur in ground reaches the elastic limits, plastic irrecoverable deformations occur and after a point fail may occur. In braced excavations, lateral forces in backfill soil decreases wtih increasing lateral displacements of the shoring wall. When the wall moves through the excavation, the at rest pressure changes into the active earth pressure. However, when the lateral earth pressure inreasses unexpectedly as a result of water loads, seismic loads or tensile forces may occur as a result of coming across different types of soil which is not realized in soil borings, the elastic behavior may convert to plasic behavior and then fail of the shoring system may occur. Mohr-Coulomb plastic points are shown in Figure 5.10 as red squares and these points occured above the elastic limit defined in Mohr-Coulomb failure mechanism. As a result of the analysis, Mohr-Coulomb plastic points are centered around the bottom of the excavation. Also from the Figure 5.10, it is clear that the embedded depth of the mini pile is enough because the plastic points are not dense around these area. Also Mohr-Coulomb plastic points are useful for checking the coarseness of mesh. For instance, in a small

model, the plastic Mohr-Coulomb points may reach the boundaries of the geometry model. In such cases it should be used a larger model (Plaxis 2D Reference Manual, 2011).

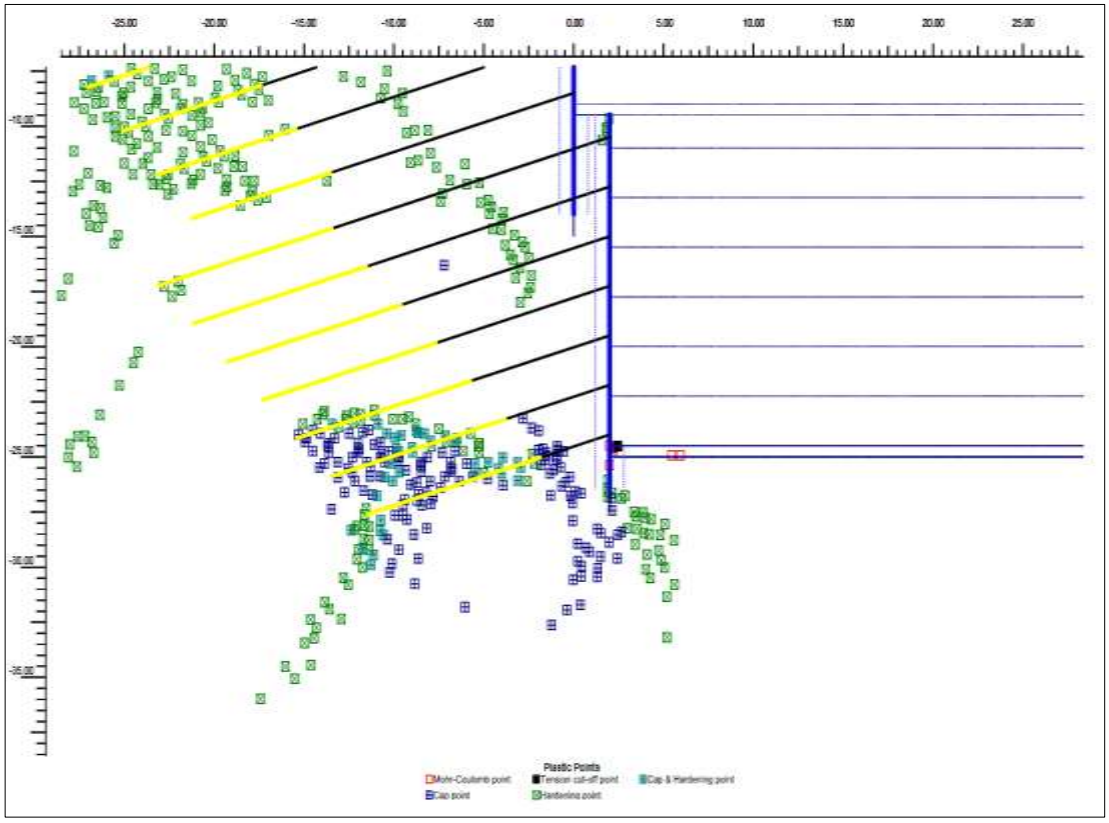

Figure 5.10 : Plot of plastic points- step no: 92 - (phase:27).

Tension point which is represented by tension cut-off in plastic points is only seen at the end of the excavation just next to the vertical plate element. Tensile strength is a mechanical property of rock material and defined by the ultimate strength in tension. Generally, for cohesionless soils, tensile strength is negligible. However, low tensile strength is caused because of the microcracks in the rock material. Rock may fail under a tension stress with a small strain through existence of these microcracks. Tension points which are black squared shapes in Figure 5.10 represents the plastic points which rock fails in tension. Cap and hardening points occur as a result of using HSM as material model and generally represents the previously reached stresses. The cap points are used for representing the stress of points equals to the preconsolidation stress and showed with dark blue squares. Hardening points are used to show the stress points on the shear hardening envelope and showed by using green squares.

5.7.7 Calculation for reinforced concrete elements

Wall shear forces and bending moments are shown in Figure 5.11 and Figure 5.12, respectively. Calculation for vertical retaining elements (mini piles) should be calculated benefit from both the shear forces and bending moments in beam.

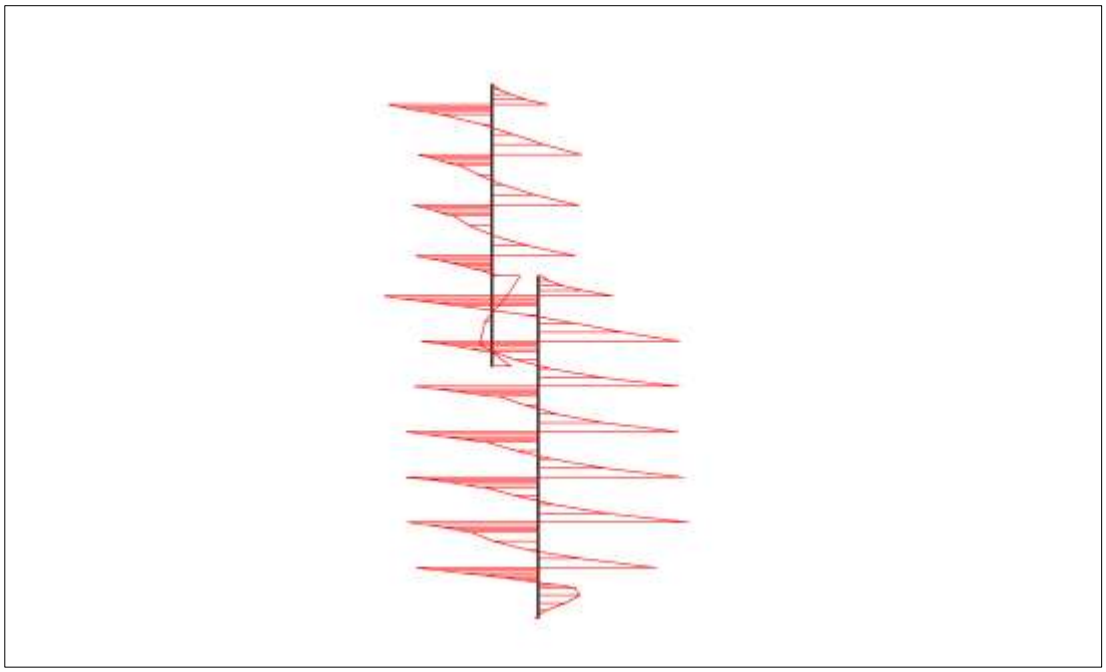

Figure 5.11 : Shear forces in beam extreme value 188.06 kN/m (phase:27).

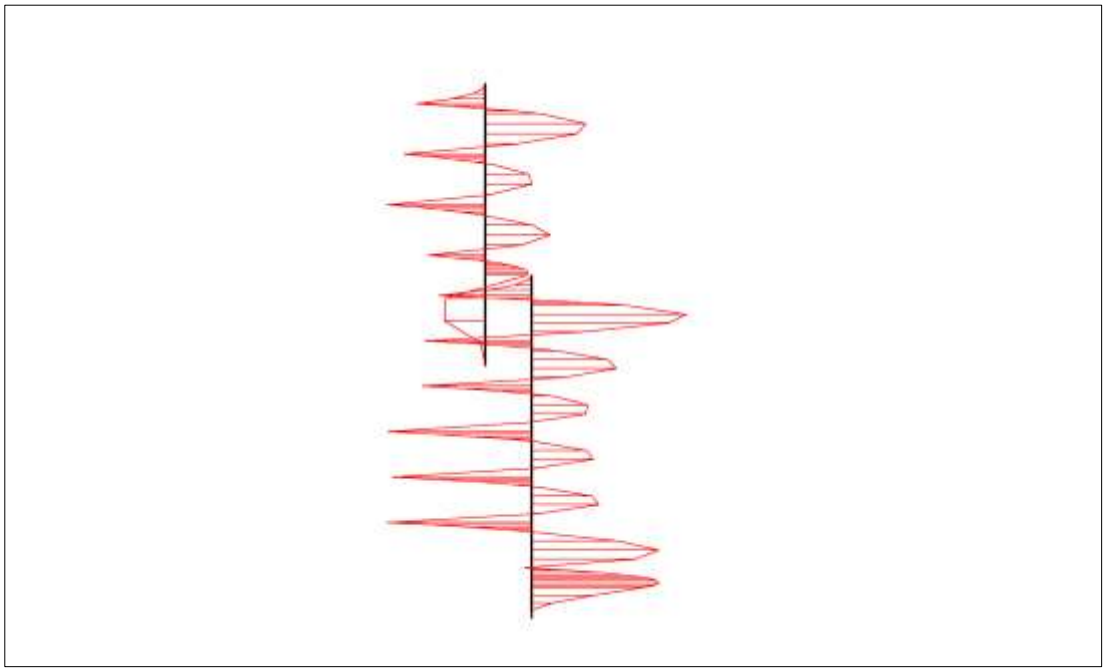

Figure 5.12 : Bending moments in beam extreme value -58.86 kN/m/m (phase:27).

In this study, mini piles were selected as vertical support elements. Mini piles offer an economical solution to temporary support problems. Besides, in narrow sides minipiling is more advantageous to work. To determine the pile reinforcement, bending moment carriage is an important consideration. Internal forces according to Plaxis calculations must be converted to unit width value and must be increased with the coefficient 1.6. Mostly, pile stiffness is more important than bearing capacity of the pile, hence reinforcement ratio is suggested to be between $\rho_{min}= 0.01 \leq \rho \leq \rho_{max}= 0.03$ (Celep, 2007). The longitudinal reinforcement calculation for mini piles is given in Table G.1 in Appendix G. The stirrup reinforcements are placed due to shear forces. According to the calculations the cracking shear resistance for spirral columns $V_{cr}=0.58*f_{ctd}*b_w*d=37.52$ kN is smaller than the designed factored shear force $V_d=94.03$ kN. This means that calculation for shear forces is necessary. Just like in beams and columns, stirrup densification is suggested for plastic hinge regions occured as a result of pile failure. The plastic hinge regions are the sections that have the maximum moment. Especially, in fixed-headed piles, stirrup densification is done in pile-cap beam connection parts. According to the reinforced concrete calculations, longitudinal rebars and links are designed for mini pile as 5ϕ18 and ϕ8/10, respectively (Appendix G).

Mini piles are connected to each other in the upper parts with cap beam. Cap beam encloses the mini piles and keep the displacements that may occur on the top of the pile under control. Cap beam is designed as 50 cm in width and 50 cm in height and the amount of steel reinforcement is limited due to minimum reinforcement ratio in concrete beam design 0.8% (Appendix G). It must be noted that retaining wall construction in front of Historic Bomonti Brewery was carried out in 2 stages so that 2 cap beams were built for mini piles at all levels. The required number of longitudinal steel bars is calculated as 10 and the diameter of the bar is 16 mm.

Waler beams are designed to ensure mini piles work together and to transfer anchor loads to ground. Placement and number of waler beams are determined according to the maximum anchor force and considered that the load is accepted to have a uniform distribution as in a continuous beam. Waler beams are designed as 70 cm x 35 cm. Reinforcing bars for doubly reinforced rectangular waler beam are chosen as 2x5ϕ18 for longitudinal rebars and ϕ10/15 for stirrups (Appendix G).

5.8 The Problems Encountered During Deep Excavation

The deep excavation for the seven-story car park started 2 meters in front of historical building and continued to the depth of 26 m. During the deep excavation in front of The Historic Bomonti Brewery, some problems were encountered.

Inclinometer measurements and inclinometer placement plan are given in Appendix F. As shown from the inclinometer graphs, displacements were remained in a few milimeters between the dates 31.05.2010 and 06.08.2010. However readings taken in 06.08.2010 show that there was an upsurge for the inclinometer IK-7 and reached up to 20 mm. In that time the excavation level is at the 5^{th} stage. After 3 days later in 10.08.2010, readings were retaken from the same inclinometer hole and it was seen that the displacements were reached to 25 mm. There made an observation in the construction site and it was seen that creep movements occured in upper stages of anchors. As a protection, 1.5 m depth weep hole drillings were carried out between the 4^{th} and the 5^{th} waler beams to discharge the leakage water. Moreover, as an immediate protection due to the site observations and continuening increase in the deformations, the upper anchors's creeps were replaced with new ones and then the anchors were prestressed again by the help of an aerial lift and also the new installed ground anchors which grout setting was completed were prestressed (Figure 5.13).

Figure 5.13 : Re-stressing of the unloaded ground anchors

After taking measures summarized above, the deformation read from IK-7 was stopped. Then it is allowed to continue excavating the ground in pieces up to 6th anchor level.

The inclinometer measurements taken from the inclinometer IK-7 in 23.08.2010 shows that there was 5 mm increase in the deformations. To follow and to keep the deformations under control, additional readings are taken from the inclinometer. During this process, site observations were carried out in 25.08.2010 and some cracks that are parallel to the direction of the deep excavation were observed both in the historic building and the lean concrete which was casted for the mobilisation site in front of the historic building and lean concrete casted inside floors of the building. Site observations continued during the same day and it was seen that the cracks was found to proceed in a short time. In addition, inclinometer readings were taken from both IK-6 and IK-7 in the same day and it was seen that there was 2 mm increase in the deformations. Some microcracks were observed in waler beam's concrete surface as well. This increase in displacements may be occured due to some reasons. At that point, The Historic Bomonti Brewery was a masonry structure and it was thought that the foundation excavation for the 7-storey car park didn't cause the sudden failure of this building. The structural remediation works for the historic building was planned to be started with foundation excavations of existing buildings so that all the measures mensioned below were taken to prevent any irreparable damage of the historic building.

It is known that almost all rock excavations induce vibrations on the ground and on the adjacent structures. It was known that the settlement cracks in the historic building didn't cause an immediate failure of the building; however the progression of these cracks should be prevented. These vibrations may be high while using rock blasting and may be low while using mechanical techniques. To speed up the excavation process, four excavators with hammer worked in front of the historic building at the same time and the broken materials were removed without obeying the staged excavation and prestressing the anchors. Due to four excavators' working at the same time and emptying the soil in front of historical building, some cracks were observed on the walls and on the floors of the historical building. For this reason, backfilling was carried out with removed soil immediately. It was considered that the retaining system may be affected from the vibrations caused by four

excavators' working together at the same time. To prevent the failure of the system due to the machine vibrations, it was decided to avoid the working of multiple excavators with hammer should not be concentrated in the same area as shown in Figure 5.14.

Figure 5.14 : Multiple excavators with hammer working together in front of the historic building.

Figure 5.15 shows the graphite schist layers that were seen during the excavation at 7^{th} stage. From the borings this graphite schist layer was not recognized between these layers. Hence, it should be kept in mind that the ground is a composed of different formations. So that soil boring should be carried out carefully and the slope of the boring, number of borings and boring places should be determined carefully. In the investigated area it was made 8 borings to define the soil properties; however ground material may contain different types of soil formations inside. In addition, it mustn't be forgotten that rock is an anisotropic material which is nonhomogeneous and shows different mechanical behaviors in different directions according to the type of loading. The graphite schist layers are one of the most problematic layers in the excavation which have blackish dark gray-black colored, crumbly, have weak-to-moderate strength, medium-very weathered and fragmented. These layers are very sensitive to external factors such as water; can behave like a clayey soil under water. In addition, the uniaxial compressive strength of these layers are low as 16~50 MPa

and RQD varies between 0~62% (Akgün, H., and Koçkar, M. K., 2004). This shearing zone may also cause de-stress and sliding movement in the shoring system.

Figure 5.15 : Graphite schist zones between the 7th and 8th waler beams.

In addition, crackmeters were placed vertically to the cracks in historical building in 26.08.2010 to observe the development of cracks that had been already occured in previous time on the historic building walls and also to observe the progress of the cracks on the lean concrete casted inside of the historic building which were parallel to the direction of excavation. Crackmeters are designed for monitoring the movement progress of the surface cracks. Crackmeters are composed of 2 plates which are placed on each other. A typical crackmeter is shown in Figure 5.16. There is a square shaped signboard on the top plate and a calibrated milimetric scale at the bottom plate. The crack propagation is measured by the movement of the upper plate sliding on the lower plate starting from zero milimeters. Fixing of the crackmeters is carried out by using adhesives or by screwdriving. Usage areas of crackmeters are tunnels, masonry structures, dam construction, monitoring of surface cracks. It was observed that any horizontal movement in the crackmeters placed to monitor the development of cracks in historic building in 26.08.2014 with date of 31.08.2010. Moreover, inclinometer readings were taken more frequently and it was seen that the lateral movement was stopped with the date of 30.08.2010. Thus, the deep excavation was got under control by taking immediate measures.

Figure 5.16 : Crackmeter.

Secondly**,** during the construction stages greywacke formations were weathered and rock falls occured. This may be caused as a result of weather conditions or the slope direction of the greywacke units. To ensure a safety work, shotcrete with a 10 cm thickness was applied between the waler beams (Figure 5.17).

Figure 5.17 : Shotcrete application between the waler beams for safety work.

5.9 Revised Project After Undesirable Movements

After the observation of undesirable displacements occured in the shoring system, project was also revised together with the precautions given in the previous section 5.8. It was decided to built a reinforced concrete wall by installing additional anchors between the waler beams at 7th and 8th construction stages as shown in Figure 5.18. Graphite schist layers as shown in Figure 5.15 given above caused the formation of shear zones. Hence, it was considered that the bonded lengths of the anchor might be in the weak zone; so that the additional anchors lengths' were extended to 30 m with 10 m bonded length.

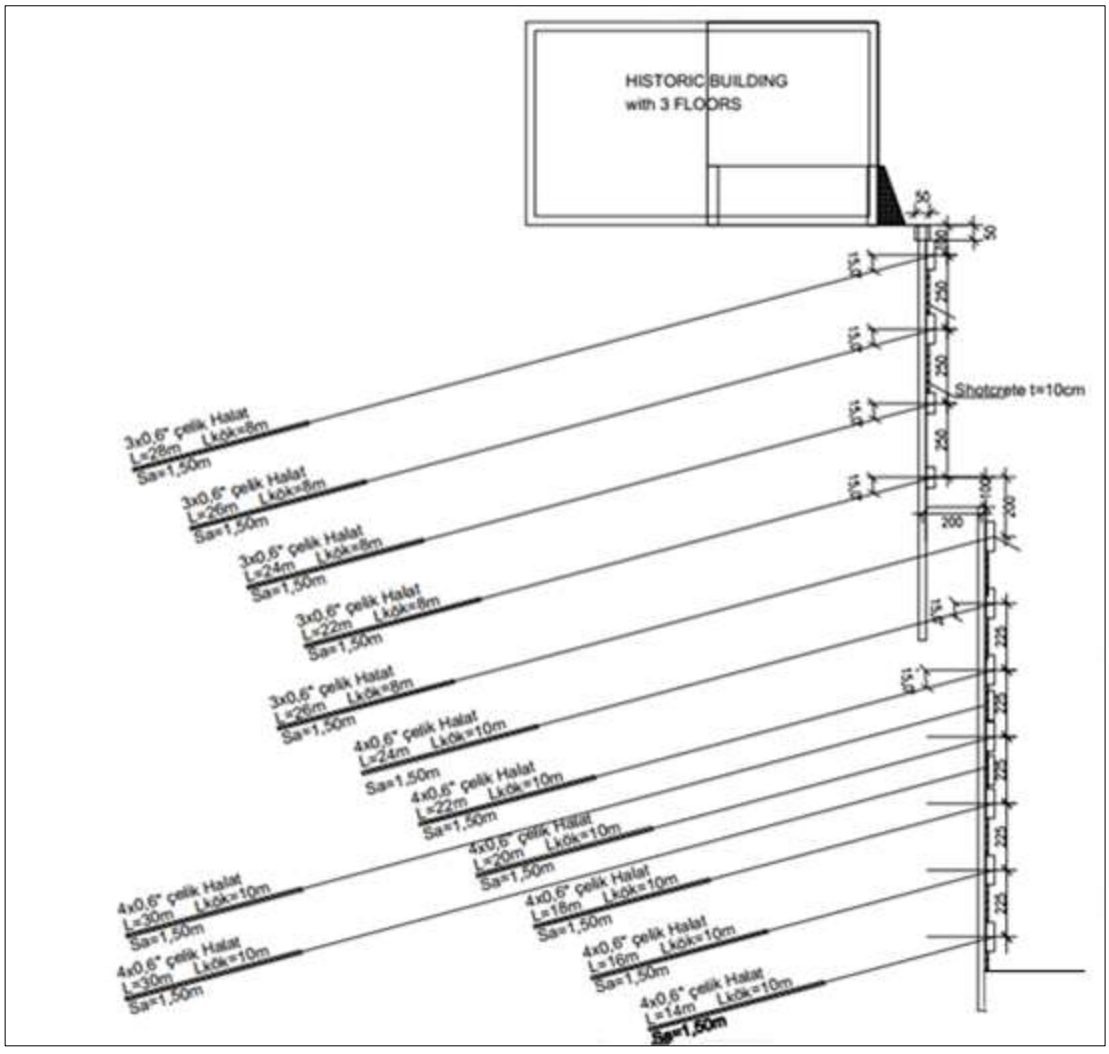

Figure 5.18 : Revised design cross-section of in front of historic building.

The revised project was also created in Plaxis software version 8.2. According to the new calculations, plot of the horizontal shadings is shown in Figure 5.19 and Figure

5.20 shows that the maximum horizontal displacements occur approximately 6 meters above the excavation bottom.

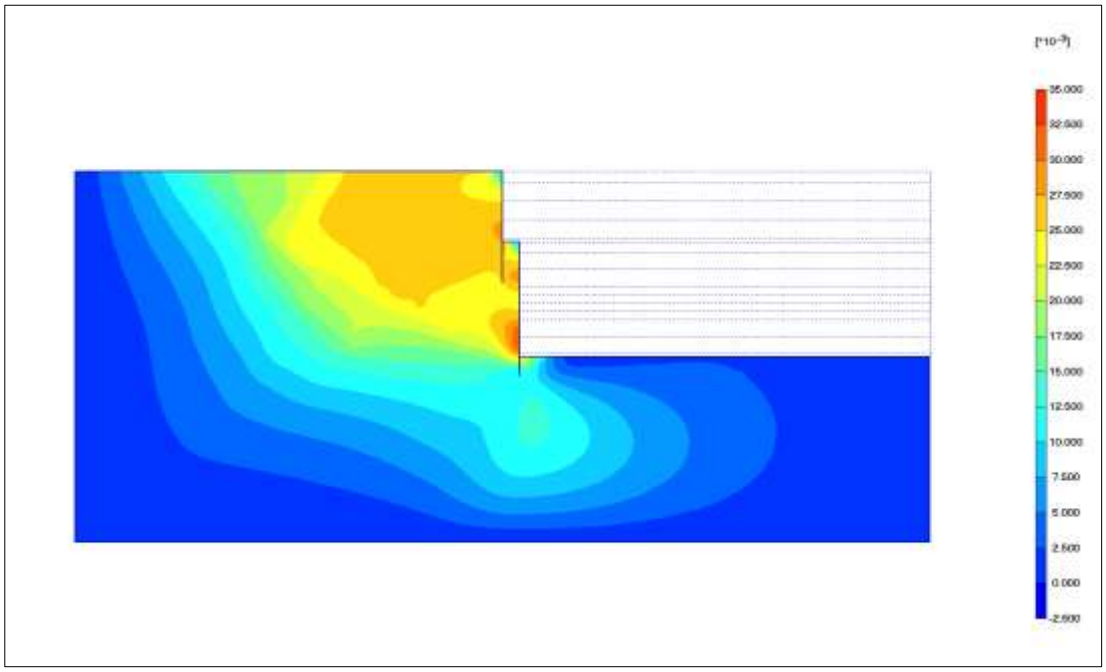

Figure 5.19 : Plot of horizontal displacements (shadings) - step no: 147 (phase:31).

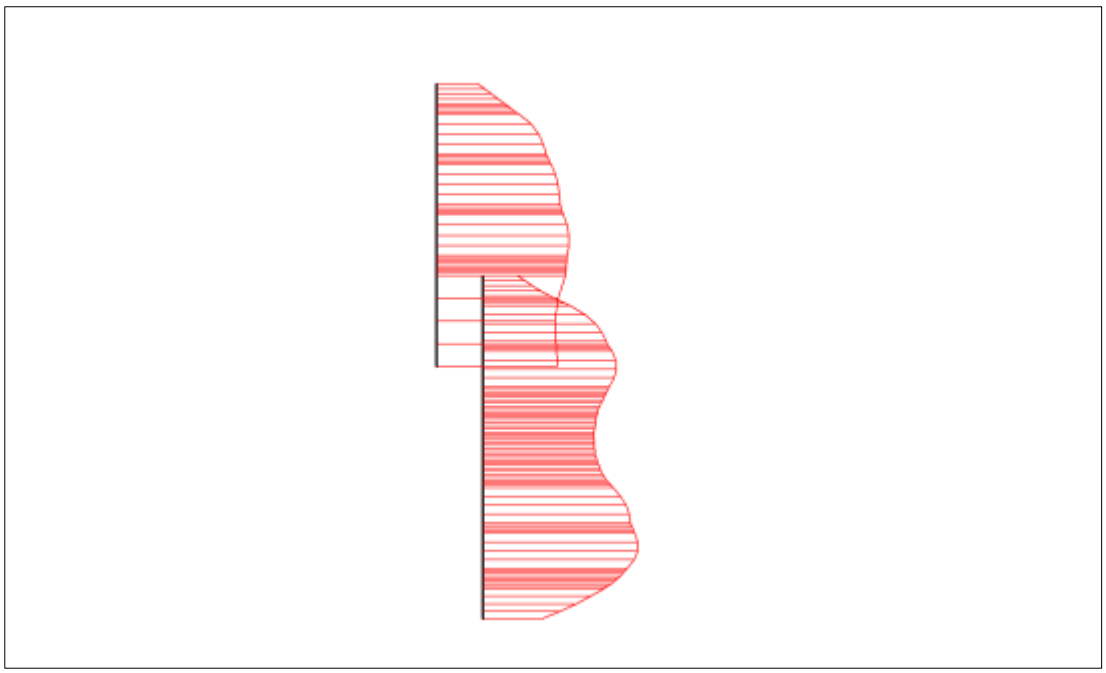

Figure 5.20 : Horizontal displacements in beam extreme value $33.11*10^{-3}$ m (phase:31).

Shear forces and bending moments occured in beam are given in figures 5.21 and 5.22, respectively. Reinforced concrete design for waler beams are done according to the maximum bending moment and the maximum shear force in beam; however it

was found to be unneccessary to design new waler beam for the new anchors. Therefore, waler beam construction was carried out according to the old project.

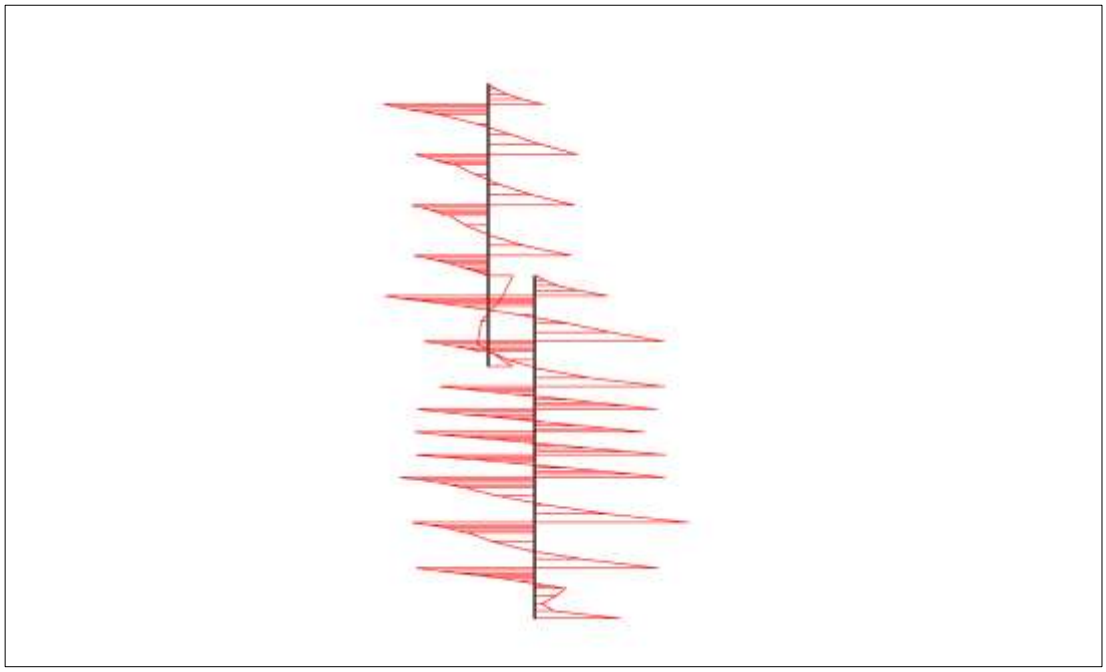

Figure 5.21 : Shear forces in beam extreme value -187.89 kN/m (phase:31).

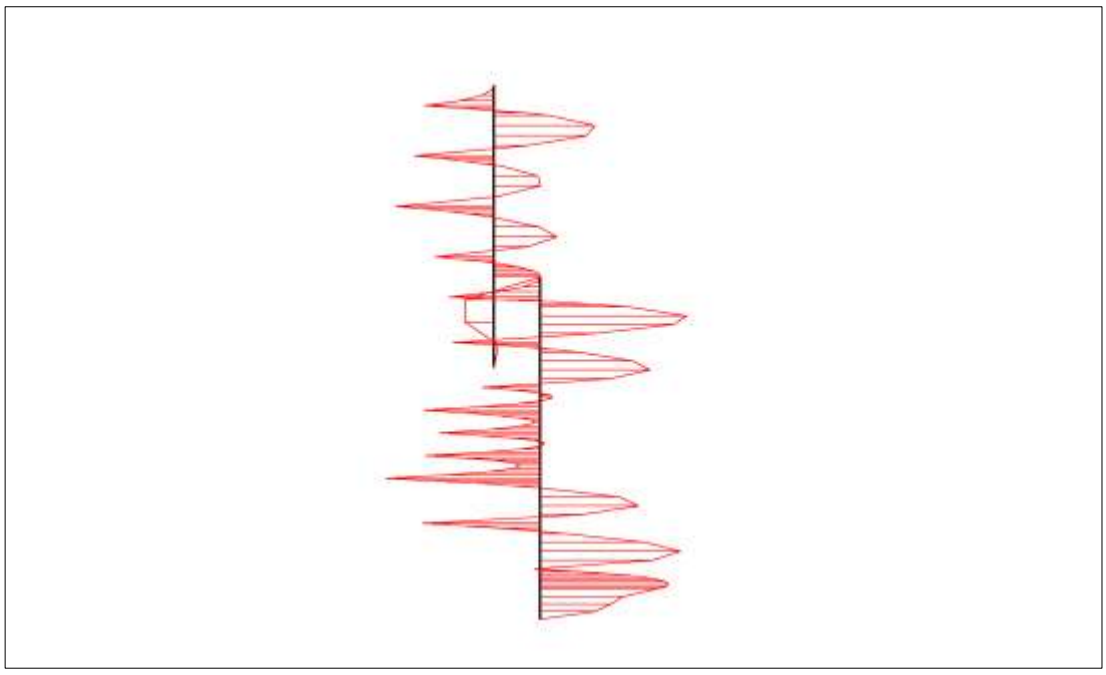

Figure 5.22 : Bending moments in beam extreme value 58.78 kNm/m (phase:31).

A cost analysis is also carried out within the scope of this thesis. A cost comparison between the old and the revised projects are given in Appendix H. The percentage of the increase in general cost is 8.52%. In addition to this cost analysis, also the cost of

crackmeters and the extra inclinometer measurements should be taken into consideration.

5.10 Influence of Soil Properties on Wall Displacements

In this section, by using the Hardening Soil Model in Plaxis 8.2, the development of the retaining wall displacements for different values of soil elastisity modulus as well as for different values of internal friction angle of soil are investigated.

5.10.1 Effect of elasticity modulus

The modulus of elasticity is an important soil parameter to measure the stiffness of soil or rock. The modulus of elasticity can be defined as the material resistance to being compressed or expanded. The modulus of elasticity is obtained from the slope of the stress-strain curve in the linearly elastic region. While the applied force overcomes the strength of soil, then failure occurs. It is known that the modulus of elasticity is a characteristic feature for the materials. According to Hooke's law, deformations are linear function of stress in perfectly elastic materails. On the other hand, rock material shows elasto-plastic behavior so that the stress-strain relationship of rock material is expressed by using different modulus of elasticity values E_{50}, E_{ur} and E_{oed} as given in the previous chapter. The modulus of elasticity in rocks is determined with the uniaxial compression tests. During the uniaxial compression test, the applied load is read from the manometer and the deformations are read from the 'strain gauge'. Moreover, it is essential to read both the axial deformation and the lateral deformation to determine the Poisson's ratio which represents the behavior of rock while tensioning and compression occurs.

In this chapter, how the elasticity modulus of soil affects the behavior of the retaining wall is investigated. Therefore, various elasticity modulus values are tried by holding the other soil and structure parameters as constant going through the geometry model given in Figure 5.5. 27 different values of elasticity modulus from 20 MPa to 150 MPa given in Table 5.15 were tried and horizontal displacements shadings and also horizontal displacements for various modulus of elasticity are given in Appendix I. Plaxis calculations show that the increasing value of elasticity modulus causes an increase in the soil strength so that the horizontal displacements in beam decrease.

Table 5.15 : Horizontal displacements for various elasticity modulus.

E_{50}^{ref} [Mpa]	E_{oed}^{ref} [Mpa]	E_{ur}^{ref} [Mpa]	U_x [cm]
20	20	60	6.77
25	25	75	5.66
30	30	90	4.96
35	35	105	4.34
40	40	120	3.96
45	45	135	3.66
50	50	150	3.39
55	55	165	3.18
60	60	180	3.03
65	65	195	2.82
70	70	210	2.59
75	75	225	2.54
80	80	240	2.42
85	85	255	2.32
90	90	270	2,21
95	95	285	2.12
100	100	300	2.04
105	105	315	1.99
110	110	330	1.88
115	115	345	1.84
120	120	360	1.81
125	125	375	1.76
130	130	390	1.75
135	135	405	1.70
140	140	420	1.66
145	145	435	1.63
150	150	450	1.58

According to the Plaxis calculations, it is seen that the displacement values decrease with increasing modulus of elasticity and the plot for the horizontal displacements corresponding to various modulus of elasticity are shown in Figure 5.23. Due to the Plaxis results, it can be said that while the modulus of elasticity of a rock material increases, the deformation of a given material resulting from the internal stresses will be reduced. Accordingly, it can be said that rock materials with a high E value is relatively more competent.

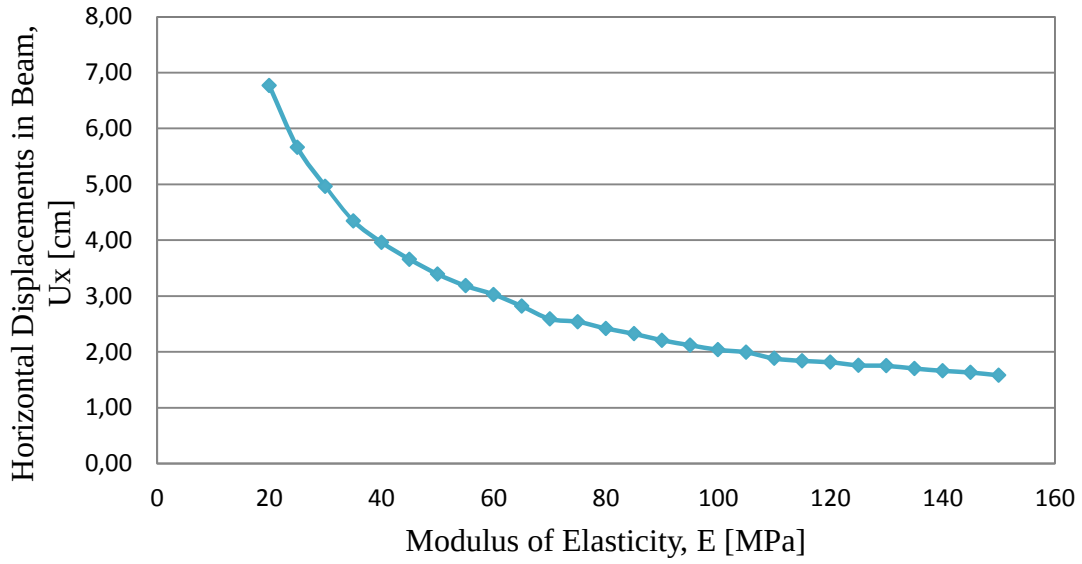

Figure 5.23 : Plot of horizontal displacements vs modulus of elasticity.

5.10.2 Effect of internal friction angle

The shear strength parameters of a soil can be determined in the laboratory by using direct shear test or triaxial test. According to the test results, Mohr-Coulomb failure envelope is obtained. The inclination of the Mohr-Coulomb failure plane is called as the internal friction angle and represented by φ. The internal friction angle can also be defined as a measure of soil or rock against to shear stress. There are a lot of different types of soil and rock with different geomechanical behaviors in nature. For this reason, it is come as no suprise that there are various internal friction angle values. The behavior of both sandy and clayey soils are shown in Figure 5.24. Sandy soils (cohesionless) have high internal friction angle. Sandy soils crumble easily due to have no cohesion. As shown in Figure 5.24(a), strength of sandy soil depends on the internal friction angle. Besides, clayey soils (cohesive) have low internal friction angle (Figure 5.24(b)).

Generally, it can be said that gravels and sandy soils have high values of internal friction angle and φ increases with increasing amounts of these materials in a soil. For sandy soils, the internal friction angle is based on the gradation, the density and shape of the particles and also independent from the water content. The internal friction angle of clayey soils depends on the water content and depending on the increased water content, saturated clay has a higher friction angle (Rahn, P. H., 2006).

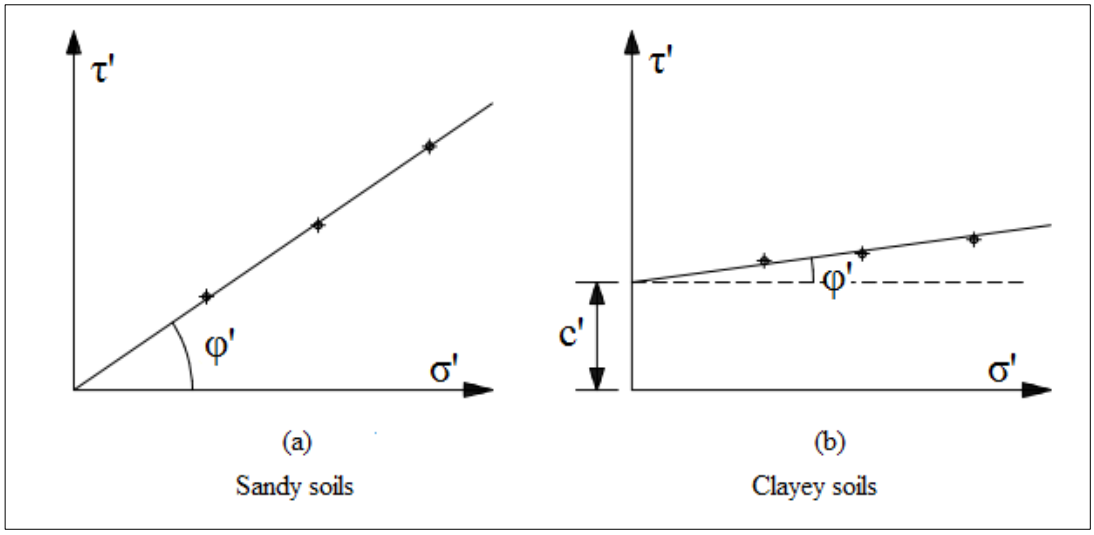

Figure 5.24 : Mohr-Coulomb failure envelopes for sandy and clayey soils

According to the literature, the angle of internal firction for loose sand ranges between 30^o~35^o, for medium sand 40^o and for dense sand the internal friction angle ranges between 35^o~45^o.

In this section, horizontal displacements in beam are investigated for various internal friction angles from 28^o to 42^o. The other material and structure parameters are assumed to be constant except the dilatancy angle. Plaxis offers for the angle of dilatancy equals to φ-30^o for soils $\varphi > 30^o$. In Table 5.16, both the angle of internal friction and the angle of dilatancy are given with horizontal displacements occured in beam according to Plaxis calculations.

Table 5.16 : Horizontal displacement values vs internal friction angle

Internal friction angle	φ [^{o}]	28	30	33	35	37	40	42
Angle of dilatation	ψ [^{o}]	0	0	3	5	7	10	12
Horizontal displacements in beam	U_x [cm]	13.87	10.29	6.64	5.20	4.17	3.05	2.81

Figure 5.25 is created by using Table 5.16. From the figure, it is seen that horizontal displacement values in beam are decreased when the internal friction angle value increases. This is because the strength of soil is generally increases with increasing values of internal friction angle.

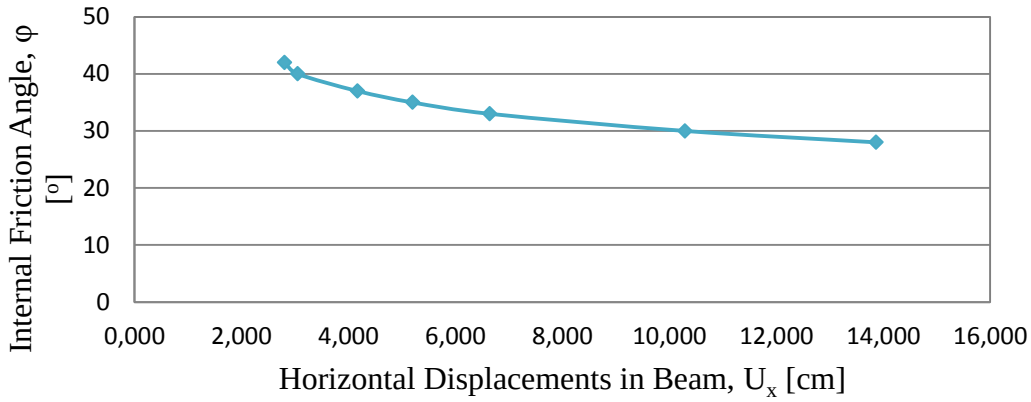

Figure 5.25 : Plot of horizontal displacements vs internal friction angles.

5.11 Influence of Soil-Structure Interaction on Wall Displacements

It is known that the structures interact with the ground in many geotechnical problems. To model this interaction between the ground and the structural element, interface elements are used. In Plaxis software, the degree of interaction is represented by R_{inter}. R_{inter} is related to interface strength which refers wall friction and soil/wall adhesion and soil strength parameters which refers cohesion and internal friction angle.

In this section, the effect of the interface reduction factor on horizontal displacements is investigated. The maximum horizontal displacements in beam, $U_{x,}$ varies between 4.70 cm and 3.97 cm when the interface reduction factor, R_{inter}, changes from 0.4 to 0.9 (Table 5.17).

Table 5.17 : Horizontal displacement values vs interface reduction factor

R_{inter}	[-]	0,9	0,8	0,7	0,6	0,5	0,4
Horizontal Displacements in Beam	[cm]	3,97	3,99	4,10	4,31	4,54	4,70

The plot for the horizontal displacements corresponding to interface strength reduction factor is given in Figure 5.26. According to these results, it can be said that there is not much difference between the horizontal displacement values when R_{inter} is changed. However, it gives more realistic results for the investigated area when R_{inter} approaches to 1. The interface reduction factor is taken as 1 by selecting the 'rigid' option for interface strength property while the interface does not have an

reduced strength compared to the surrounding soils' strength. This option is used for modelling the extended interfaces around the corners in stiff structures (Plaxis 2D Reference Manual, 2011).

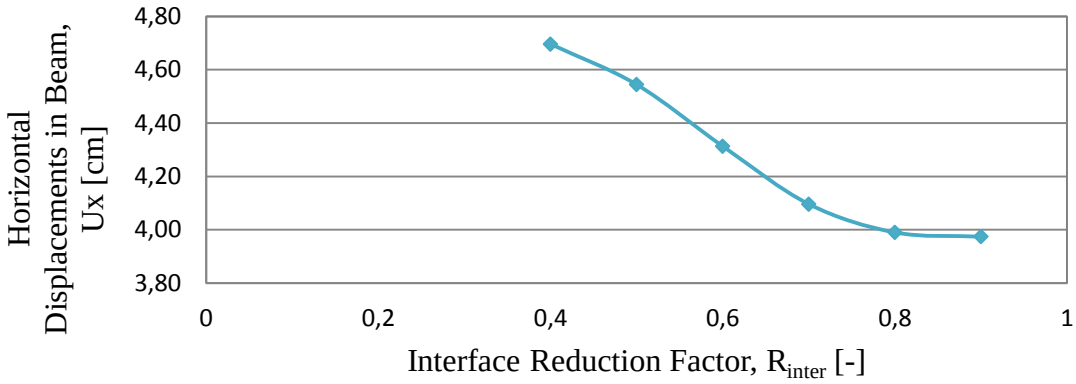

Figure 5.26 : Plot of horizontal displacements vs interface reduction factor.

The results taken from the Plaxis calculations show that while R_{inter} value approaches to 1 give more realistic results for the investigated model. Thus, it can be said that R_{inter} value is important for modelling the behavior of the structure. It is also indicated that R_{inter} is a characteristic value and should take various values for different types of soils. In this thesis, R_{inter} is assumed 0.95 for the simulation of the interaction between the greywacke and reinforced concrete pile. Inclinometer measurements and the literature given for the determination of the interface strength reduction factor in chapter 4 can be both used to verify that 0.95 is right value. In fact, R_{inter} for sand and concrete interaction is given in the range of 0.8 and 1.0 in the literature.

By considering these results, it can also be said that the load capacity of laterally loaded vertical retaining elements is related to interface behavior. The relative shear behavior in soil-pile interface and the development of the gaps between the pile and soil affects the stress distribution between the pile and soil (Uncuoğlu, 2009).

5.12 Influence of Anchor Properties on Wall Displacements

It is known that the rigidity of the retaining wall is related to the lateral support system properties. In the scope of thesis, behavior of a prestressed ground anchor wall is investigated so that in this section ground anchors are considered. In chapter 3, potential failure mechanisms of ground anchors are given. To prevent the failure

of the anchored systems, the design engineer can ring some changes in the anchor type, in the anchor sizes, in the anchor inclination, in the anchor spacing and also in the number of anchors. It must be noted that the design of a prestressed anchored wall must be carried out by both considering the safety and the economical conditions. In most cases, overdesigns are carried out for the applications for the safety, but sometimes by thinking overdesign it may be made unnecessary selections to improve the security of the system. Therefore the effects of the anchor bonded length and the anchor inclination and as well as the horizontal anchor spacings are investigated in this study and the results are given below.

5.12.1 Effect of anchor bonded length

A prestressed ground anchor is formed both of unbonded and bonded parts. A prestressing force is applied to the ground to prevent the potential failures in prestressed ground anchors. This force is firstly transferred with the unbonded part to the bonded part and then transferred from the bonded part to the ground. The bonded length cannot be less than 3 meters. In addition, bonded lengths for soils are chosen generally as 4.5~12 m and the bonded length should be minimum 7.5 m for the anchors in rock (FHWA-IF-99-015, 1999). Generally 8~10 m bonded lengths are used in practical terms.

The effect of anchor bonded length is investigated by using Plaxis version 8 in this section with different bonded lengths. All the soil and structure parameters are taken as constant except bonded lengths for the first construction stage. Various bonded lengths from 4 m to 12 m were tried and the results are given in Table 5.18. Hence, the chosen bonded length is enough for the system and lengthier bonded parts are not necessary considering costwise and time.

Table 5.18 : Wall displacements corresponding to different bonded lengths

Bonded length	L_b [m]	4,00	6,00	8,00	10,00	12,00
Horizontal displacements	U_x [cm]	3,68	3,57	2,41	2,44	2,44

It is seen from the table 5.18 that the lateral deformations in the retaining system have greater values as the bonded length is chosen smaller than 8 m. However, the

lateral deformations decrease when the bonded length is chosen as 8 m and there is not a significant change in the lateral deformations while the bonded length is increased to 12 m. The recommendations given in the standards for rock units must be kept in mind in the design phase. For the deep excavations carried out in sedimantary rocks, the bonded length should be chosen greater than 7.5 m considering safety and it should also be avoided unnecessary lengths considering cost. The deformed meshes and horizontal displacements for the first construction stage anchors with bonded lengths 8m, 10 m and 12 m are given in Figure 5.27, Figure 5.28 and Figure 5.29, respectively.

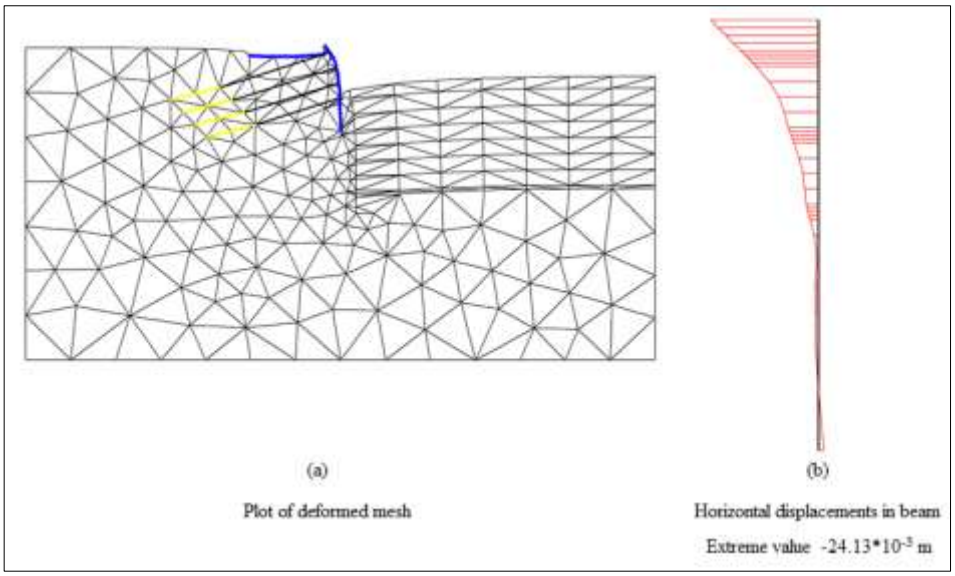

Figure 5.27 : Deformed mesh and horizontal displacements in beam for L_b=8m.

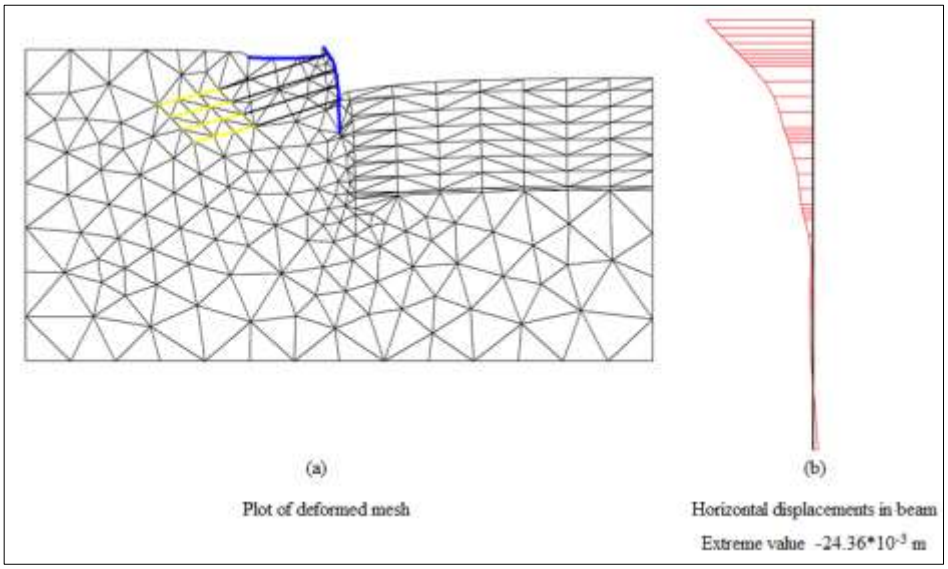

Figure 5.28 : Deformed mesh and horizontal displacements in beam for L_b=10m.

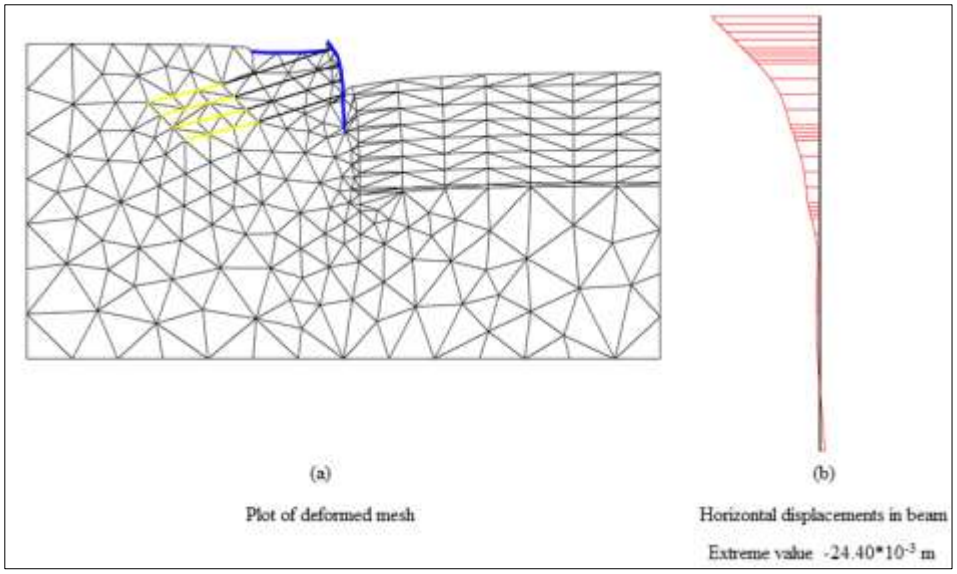

Figure 5.29 : Deformed mesh and horizontal displacements in beam for L_b=12m.

5.12.2 Effect of anchor inclination

The inclination of ground anchor is a very important issue for a successful design because it directly affects the stability of the retaining system. The friction forces can be increased by installing the ground anchors as possible as perpendicularly to the sliding surface. For instance, in the design, the anchor bonded length must be developed behind the potential failure plane to provide required design loads. However in some cases as in this project, anchors installed at wide angles larger than 45 degrees may cause the failure of the shoring system. Moreover, anchors installed at very acute angles less than or equal to 10 degrees induce grouting problems. Allowable limits for anchor inclination various 10^o to 45^o, but in general, in most cases 15^o or 30^o angle with the horizontal are preferred due to convenience of drilling. According to FHWA-IF-99-015(1999), the inclination of ground anchor is assumed to be 15^o with 12 m bonded length in soil or with 7.5 m bonded length in rock.

To see the influence of the anchor inclination on horizontal displacements in beam, various angles from 10 degrees to 45 degrees were tried in Plaxis 8.2 and the results are given in Table 5.19. It is seen from the table that the displacements increase with the increasing value of the anchor inclination. Anchors installed at angle 45 degrees caused failure of the system because the bonded length is not located behind the critical failure surface. From the table it can be said that for the investigation area the most suitable anchor inclination is 15 degrees.

Table 5.19 : Horizontal displacement values corresponding to anchor inclination.

Anchor Inclination	degrees [^{o}]	10	15	20	25	30	45
Horizontal displacements	U_x [cm]	4,11	3,96	4,13	4,74	5,78	fails

Plots of the horizontal displacements for various inclination degrees are given in Figure 5.30, Figure 5.31, Figure 5.32, Figure 5.33 and Figure 5.34. At each construction stage, stress-strain situations differ from each other. It can be easily seen from the figures given below, the location of the maximum displacement changes due to the anchor placement and some steps are more critical than others. For instance, in the investigated soil model, failure occurs at an angle of inclination 45^o. The failure of the shoring system may also cause the occurance of large deformations in the surrounding structures because of stress relief. Therefore, the right selection of the anchor inclination and the sizing of the retaining wall is very important not only for the safety of the excavation and also important for the safety of the surrounding structures.

Horizontal displacements calculated in beam element is decreased while the inclination angle of the ground anchor is increased from 10^o to 15^o as shown in Figure 5.30 and Figure 5.31.

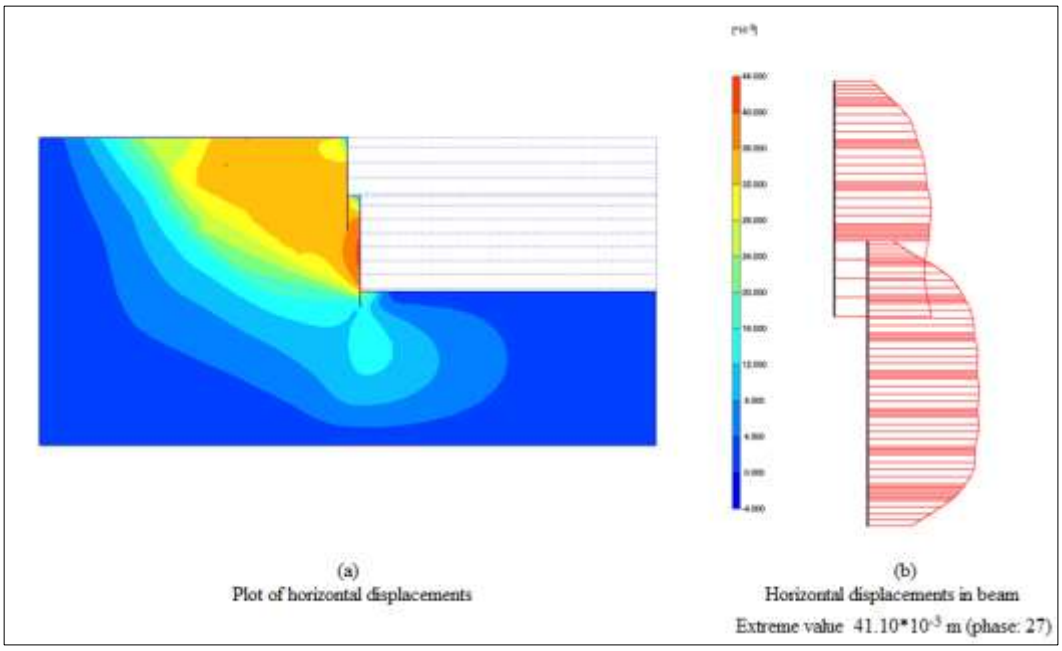

Figure 5.30 : Horizontal displacements in beam at 10^o inclination.

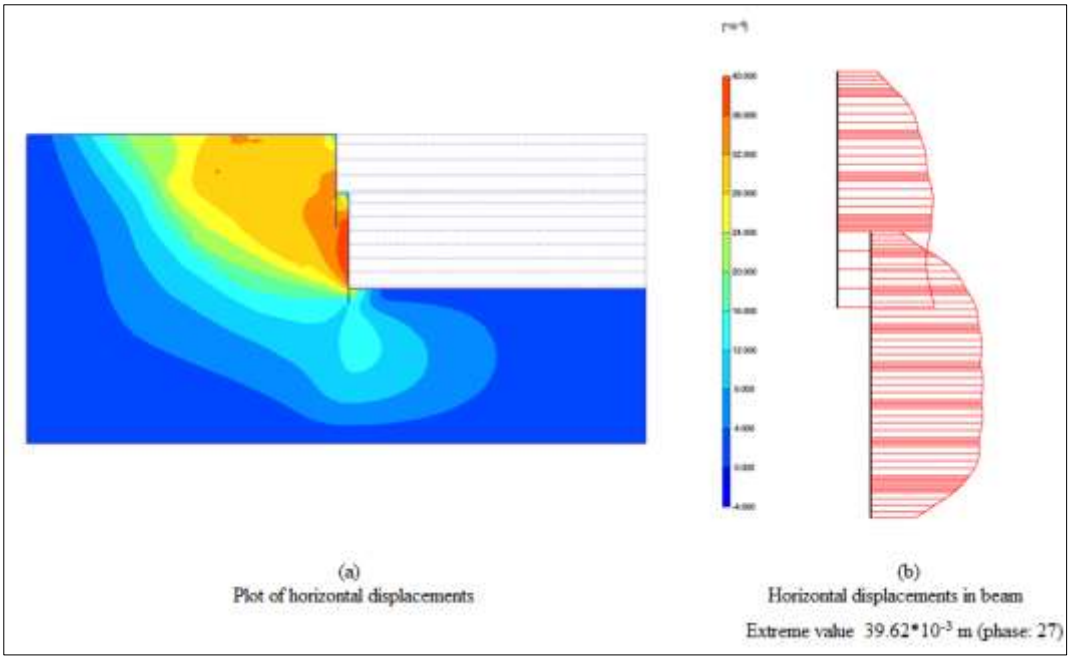

Figure 5.31 : Horizontal displacements in beam at 15^{o} inclination.

On the other hand, while the anchor inclination is increased from 20^{o} to 45^{o}, the horizontal displacement values are increased as shown in Figure 5.32., Figure 5.33 and Figure 5.34. Therefore, it cannot be said that the increasing of the angle of the anchor between the horizontal always increases the rigidity of the retaining wall. The inclination should be determined according to the type of soil, type of the project, type of the anchor, and also according to the location of underground structures, etc.

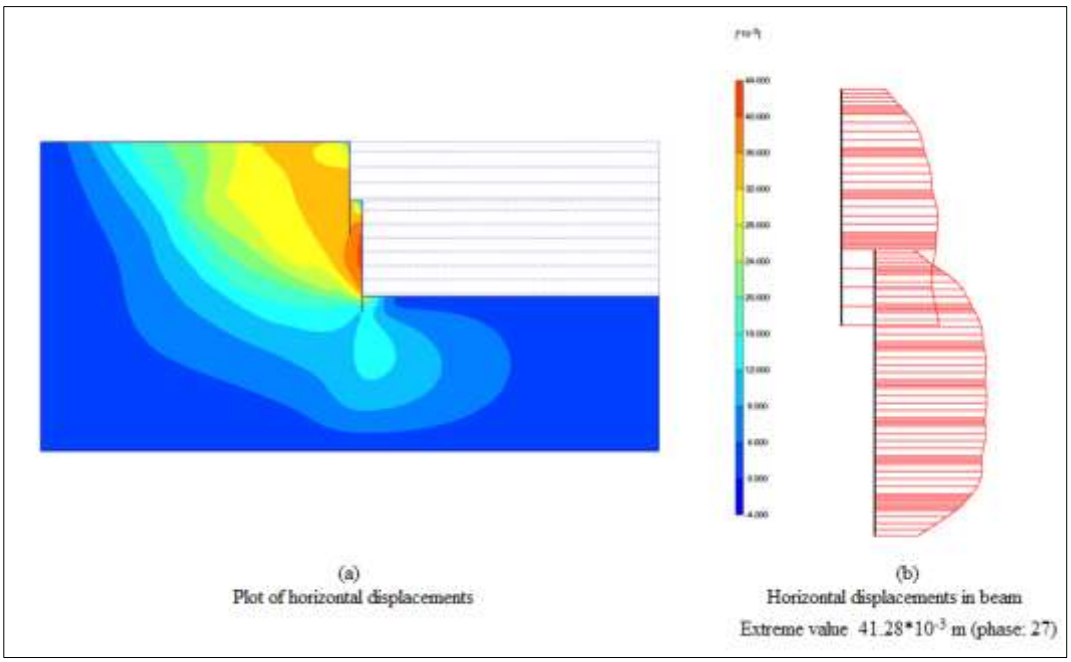

Figure 5.32 : Horizontal displacements in beam at 20^{o} inclination.

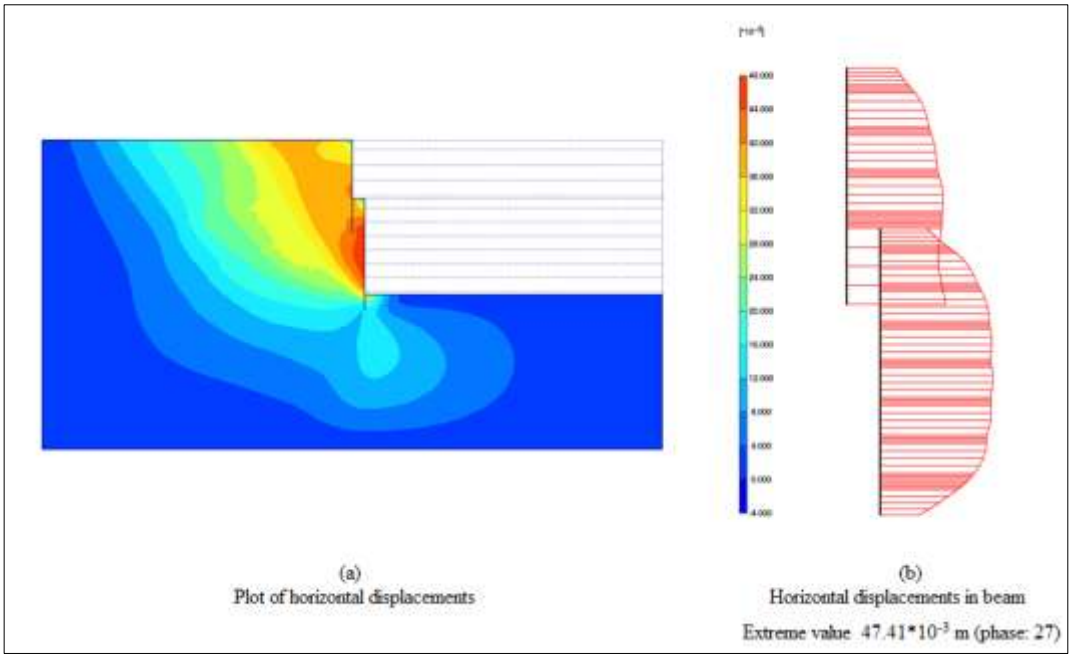

Figure 5.33 : Horizontal displacements in beam at 25^{o} inclination.

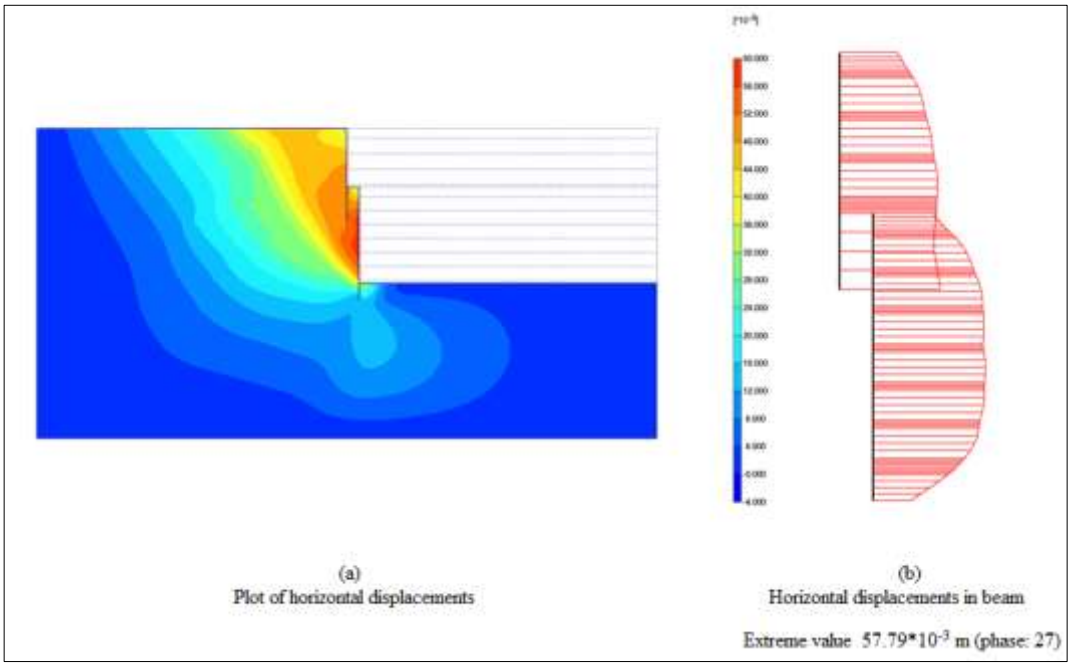

Figure 5.34 : Horizontal displacements in beam at 30^{o} inclination.

5.12.3 Effect of nominal strand diameter

Plaxis results for the same geometry model with different strand diameters are compared and the horizontal displacements in the vertical retaining element are given in Figure 5.35. The input for anchor and geogrid properties of various nominal diameter of strands (0.5", 0.6" and 0.7") is given in Table G.7 and Table G.8 in Appendix G. The minimum breaking strengths of 0.5", 0.6" and 0.7" nominal

diameter of strand are 183.7, 260.7 and 353.2 kN respectively (ASTM A416/A416M-02, 2002). According to the calculations, it is determined that the displacements in beam decrease with increasing diameter of strand.

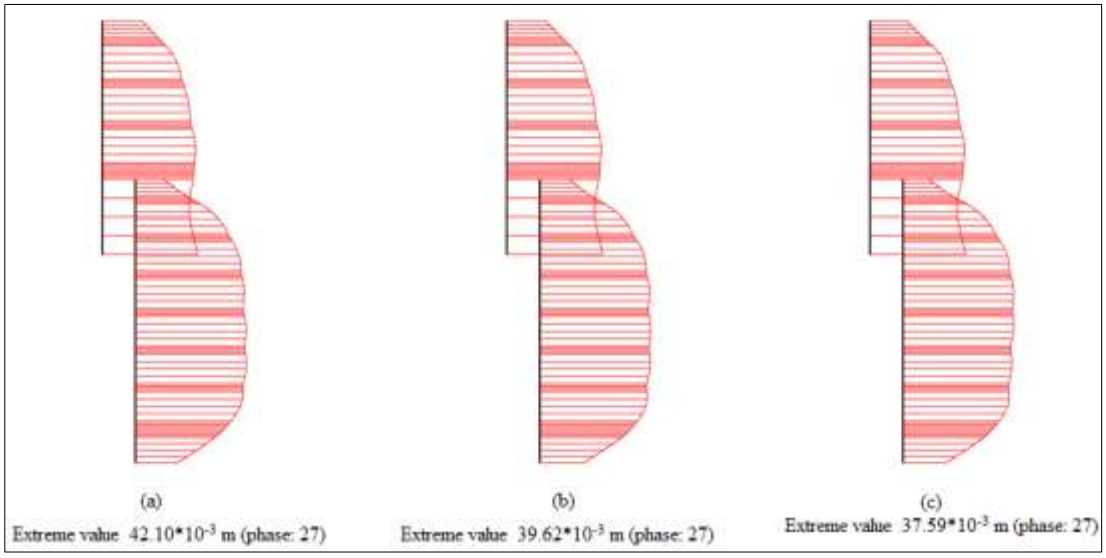

Figure 5.35 : Horizontal displacements in beam (a)for 0.5" strands (b)for 0.6" (c)for 0.7" strands.

As indicated in chapter 3, in geotechnical engineering practice 0.5 inch (12.70 mm) or 0.6 inch (15.24 mm) diameter strands with 7-wires that compliance with the standard ASTM A416/A416M are used. It must be noted the diamater of the strand affects the rigidity of the retaining system; however for some projects using 0.5 inch diameter strands can be sufficient. In addition, it is also possible to built the retaining system by using different diameters of strands for instance in the first stage 0.5 inch diamater strands can be used and in the second stage 0.6 inch diameter strands can be used. However, in the construction projects by considering the convenience of the installation and mass purchase of the construction materials one type of strand is usually preferred. Note that nowadays in geotechnical applications, smaller size diameters such as 0.5 inch and 0.6 inch strands are preferred.

5.12.4 Effect of horizontal anchor spacings

Determination for the horizontal anchor spacing is indicated in chapter 3. To see how the horizontal spacing of the ground anchors influences the retaining wall displacements, by using Plaxis software, calculations for different horizontal anchor spacings were done by taking the all other parameters and geometry of the model as

constant. The input values for horizontal anchor spacing and the outputs for horizontal displacements are given in Table 5.20.

Table 5.20 : Horizontal displacement values corresponding to horizontal anchor spacing.

Horizontal anchor spacing S_h, [cm]	Horizontal displacements in beam U_x, [cm]
100	3,65
110	3,70
120	3,77
130	3,80
140	3,89
150	3,96
160	4,01
170	4,06
180	4,11
190	4,17
200	4,31

The plot of horizontal displacements in beam corresponding to the horizontal anchor spacings is given in Figure 5.36.

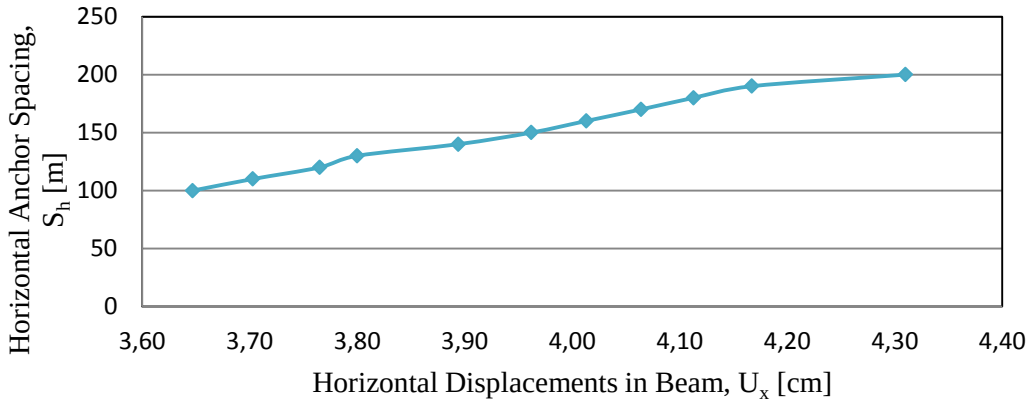

Figure 5.36 : Plot of horizontal displacements vs horizontal anchor spacing.

According to Plaxis results, horizontal displacements of the vertical beam element decrease with decreasing horizontal anchor spacing. In the site applications it may be hard to drill the anchors with a spacing of 1.3 m, 1.4 m etc. so that these amount are generally rounded off as 1.5 m, 2.0 m. In the investigated area, it is seen that the optimum value for ground anchor spacing is determined to be 1.5 m according to these results.

6. CONCLUSIONS AND RECOMMENDATIONS

The geotechnical engineering is one of the most important branches of civil engineering due to it is a comprehensive research subject that allows working of many diciplines together. Within the scope of this thesis, an anchored concrete pile wall that is a type of deep excavation support systems is discussed with an exhaustive literature and a case study. In the case study, the behavior of a prestressed anchored wall that used as a deep excavation support system in Hilton Istanbul Bomonti Hotel and Conference Center Project is analysed by using a numerical modeling software Plaxis. All of the calculation phases are defined as plastic calculations in this study. In all types of engineering, especially in civil engineering, it is important to design by considering both the economical and safety conditions with using scientific datas. Therefore, in last chapter it was also investigated the influence of some parameters on the safety and economy of the design.

As indicated above geotechnical engineering is a composed of so many diciplines. In the case study, firstly the geotechnical explorations carried out to determine the general properties of the soil in the investigated area are referred. Soil borings and also in-situ and laboratory tests must be done for the field before a deep excavation support system design. According to the field investigations, a geotechnical report is prepared as a pioneer for the design. The selection of the parameters is very important in the design because in finite element modeling wrong datas may cause undesirable results. In this study, the recommended soil profile in the geotechnical reports is used in finite element modeling.

One of the most significant point in engineering is to design a safe and also economical structure. Design of an engineering structure starts with preliminary design and continues with a numerical analysis. Before starting the construction of the shoring wall, The location of the existing adjacent structures, the location of roads and infrastructure facilities should all be determined carefully, because all the exsisting structures affect the design of the deep excavation support system. The engineer should avoid unnecessary sizes of the structural elements. For instance,

mini piles are used in the section investigated in this research. Also, a diaphragm wall can be constructed as vertical support element; however it has high cost. Hence mini piles are selected due to cost-effective instead of diaphragm wall. The small diameter piles must be connected back with the ground anchors to prevent horizontal displacements of the retaining system in deep excavations. Therefore, prestressed ground anchors were used as lateral support elements for mini piles.

The general soil profile of the investigated area is greywackes that is a type of sedimentary rocks. The stress-strain relationship of rock materials are represented by hyperbolic-shaped curve. Only very stiff, dense, cristalized and voidless igneous rock materials exhibits idealized elastic behavior. The hyperbolic-shaped curve shows different curvatures from the initial point to the failure line; hence different modulus of elasticity parameters are needed to designate this behavior. The most suitable soil model to represent this behavior in Plaxis is the Hardening Soil Model. The unloading responses of rock and the nonlinearity at stress levels below yield surface can be represented more realistic with HSM.

Design of structural elements under lateral forces is one of the significant topics in geotechnical engineering. This study is also set out to investigate the lateral earth pressure distributions in a braced excavation. The deep excavation support system investigated in this research is carried out near an important structure. Therefore, the retaining wall should be designed as no lateral movements occur in the wall which means that the earth pressure at rest coefficient should be considered in the lateral earth pressure calculations.

Considering the neighbouring structures such as Historic Bomonti Brewery, it has become a necessity to minimize the displacement during the design and the construction phases of the deep excavation support system. Therefore, during the construction phase, deep excavation support system and the neighboring structures have been monitored, and construction sequence has been coordinated in accordance with the results of instrumental monitoring. Prove tests have been applied to all ground anchors constructed within the shoring system. In order to observe horizontal displacements that maybe occur during the deep excavation in front of Historic Bomonti Brewery, 2 inclinometers IK-6 and IK-7 were installed behind the retaining wall before the excavation. Frequency of measurements is due to several reasons, the most important reason is the rate of movement. During the foundation excavation,

inclinometer readings were taken bi-weekly and a rapid increase in the measurements is observed in IK-7. During the site observations; settlements firstly were observed in neigbouring structure at 5^{th} construction stage as well. This is because of the increasing displacements in the shoring system. It is seen that the measurements taken from the inclinometers are in the range of calculated wall displacement amount; however, a rapid increase was observed. So that for safety, immediate preventions are decided to be taken. To observe this settlement cracks, crackmeters were placed vertically to the cracks on the historical building in addition to inclinometers on the shoring system. It was decided to built additional waler beams and new anchors with a total length of 30 meters between the 7^{th} and 8^{th} anchors and 8^{th} and 9^{th} anchors. By this additional waler beam construction, a partly reinforced concrete wall was created between the 7^{th} and 9^{th} excavation levels. During the staged excavation, readings were followed regularly both from crackmeters and inclinometers. It was observed that the displacements were decreased with the construction of additional structural elements and also with the start of the foundation construction of 7-storey carpark. In addition, inclinometer measurements taken from the inclinometers IK-6 and IK-7 show that maximum displacement values is at the same ranges with the finite element calculation results. It is known from the literature given in this thesis, the maximum horizontal displacement of the shoring wall is at a range of 0.2H% and according to this value the measured displacement values from the inclinometers didn't exceed the limitations. But it must be taken precautions while the geotechnical engineer see rapid increase in deformations in a short time. Meanwhile this situation emphasizes the importance of the instrumental observations during a staged construction analysis once again. In brief, the success of the shoring system built in Hilton Istanbul Bomonti Hotel and Conference Center is a natural result of team spirit as well as monitoring the system at all levels of the excavation carefully and if necessary to get the extra precautions.

According to the Plaxis results, horizontal displacements continue to the bottom of the excavation as the occurance of swelling at the bottom or the movement of the system as a whole. But in real, greywacke units don't show a behavior like this. However, inclinometer measurements show that displacements decrease with increasing depth and reach to zero value at the bottom of the excavation. Because displacement of the bottom of the inclinometer borehole is not reflected in the

inclinometer readings. Moreover, from the cumulative graphs it can be easily read that the maximum displacement occurred at 8~10 m depth from the surface; however Plaxis results gave a maximum displacement value at 18~22 m. The reason of this difference is that the inclinometer measurements are calculated by taking both the reading intervals and deflection angles, hence the translational movements as in site cannot be seen.

The deep excavations with a height over 3 meters must be supported by a retaining system.

The deep excavations in weathered rocks may cause some safety problems concerning to the dip direction of rock materials. Rock falls may occur during the deep excavation. Therefore, shotcrete application can be done between waler beams to avoid this risk.

It should not be forgotten that soil is an unknown material; sometimes in the soil borings some soil layers may be overlooked. This unknown soil layers may form shearing zones that cause sliding movements in the retaining system.

The constructed retaining system was not an impervious wall which means that the rainwater could drain between the mini piles. In addition to this consideration, the subsurface drainage can also be provided with horizontal drains also known as weep holes. Weep hole drills may be carried out at certain spacings 1~3m to prevent the high water pressure development as a result of the accumulation of water behind the retaining wall. For the investigated shoring system; drainage was carried out with the weep holes installed between 4^{th} and 5^{th} anchor levels. It must be noted that the usage of weepingpipes is important to prevent the block of the hole because of sedimantation of rock.

The deep excavation support system is designed as a two-staged construction. Prestressed ground anchors together with waler beams are used to support lateral loads in the mini-piled wall. ϕ25 cm diameter mini piles are used as vertical retaining element and placed with an interval of 0.50 cm. Concrete casting of mini piles can sometimes be problem; concrete placement cannot been carried out efficiently downwards. Mini pile construction was carried out in 2 stages to save space and to have an efficient concrete placement. In first stage of construction 14 m mini piles and in second stage construction 17 m mini piles are used. Furthermore, mini piles

are more advantageous than forepiles in terms of costwise. Mini pile installations must be done under the control of experienced geotechnical engineers. If the excavation is performed under water, the drilled zone must be drained out and the soil particles must be cleaned before pouring concrete for mini piles. In addition, whether concreting is not carried out carefully, during the excavation empty bores may be occur.

The most reliable results for anchor testing can be taken in 7 days. On the other hand, prestressing force can be adjusted in 3 days besides 7 days by using accelerating admixtures in cement grout.

The selection of the parameters used in the finite element program is very important for the accuracy of the analysis. Misspecified of parameters may cause wrong output datas. In last chapter of this thesis, the effects of some parameters used as input data in Plaxis software are investigated. Firstly, the importance of some soil properties as the modulus of elasticity and the internal friction angle are investigated. Due to the increase of the E_{ur} the displacement and the bending moments decreased. When the value of unloading-reloading modulus E_{ur} is changed from 60 MPa to 450 MPa, then the displacement decreases approximately 25%. As a result of the elasticity modulus analysis, it can be said that the deformations occurred in rock material decrease with increasing value of the elasticity modulus. Rocks with high modulus of elasticity behave more rigidity. Accordingly, the modulus of elasticity is directly related to the strength of rock material and rocks with high modulus of elasticity are relatively more compenent.

One of the most important soil strength parameter is the internal friction angle. In this thesis, various internal friction angle values for the same geometry model are tried to investigate how it affects the rigidity of soil. It can be said that in most cases for rock materials, the internal friction angle can be used to determine the rigidity of soil. However, these two assumptions related to the modulus of elasticity and the internal friction angle can be accepted trueness only for uniform soil models that does not have different formations inside.

After that the soil-structure interface is investigated. It is seen that the interface reduction factor inputed in finite element program is a characteristic value that changes according to the type of soil and the type of structure.

The bonded part of an anchor transfers the prestressing force to the ground; however the selection of the suitable bonded length is important. In our country, mostly 8~10 m bonded lengths are used. In chapter 5, the effect of anchor bonded length is investigated and it is seen that the chosen length is enough. Deformations in the retaining wall don't change significantly when the bonded length is increased. It only increases the cost.

Within the scope of this thesis, also the inclination of anchors, the nominal strand dimater and the horizontal anchor spacings effects on lateral displacements in beam are investigated and it can be said that the inclination of anchor also affects the stability of the system. The inclination angle is important for grout placement, but in some cases, selecting very large inclination angles may induce the failure of the system. This is because the anchor bonded part which carry the anchor loads and transfers to the soil or rock is out of the potential failure surface. In addition to this, the selection large inclination angles may be a problem for anchor drilling.

In the standards, the nominal diameter of ground anchors is given as 0.5 inch, 0.6 inch and 0.7 inch. For that reason, a numerical analysis is also carried out for the investigation of the effect of the nominal strand diameter on the horizontal displacements occur in the retaining system. The same geometry model is solved both for these three different diameters and it is seen that theer is not a significant difference in the displacements while using 0.7 inch diameter. The nominal strand diameter for ground anchors is generally chosen as 0.5 inch or 0.6 inch. The larger diameters are not preferred in slope protection works anymore so that for an anchored wall, the stability of the system should be increased by changing the number of anchors installed in stead of increasing the standard sized produced nominal diameters of anchor.

An another significant point in ground anchor installation is the determination of the anchor spacings. In this study, the effect of the horizontal anchor spacings is investigated and as a result of the calculations it is seen that choosing the horizontal intervals as 1.5 m is suitable for the investigated model. Generally in the site applications, the horizontal anchor spacings are not chosen greater than 2 meters and less than 1.2 meters. This is because for adjacent ground anchors, during the prestressing force adjustment, the stress bulbs occurred in grouted body of the anchors.

REFERENCES

Akbaş, M. (2010). Derin Kazıların Nümerik Analizi, *M.Sc. Thesis*, Yıldız Technical University, Istanbul.

Akçakal, Ö. (2009). Şev Stabilitesi Analizinde Geri Hesap Yöntemi ve Bir Vaka Analizi, *M.Sc. Thesis,* Istanbul Technical University, Istanbul.

Akgün, H., and Koçkar, M. K. (2004). Ilıksu Tünellerinin Jeoteknik Değerlendirmesi, *TMMOB İnşaat Mühendisleri Odası*, *Teknik Dergi,* Date retrieved: 22.04.2014, address: http://www.imo.org.tr/resimler/ dosya_ekler/392cb9658cce96d_ek.pdf?dergi=190

ASTM A416/A416M-02 (2002). Standard Specification for Steel Strand, Uncoated Seven-Wire for Prestressed Concrete, *American Society for Testing and Materials*, West Conshohocken, Pennsylvania.

ASSHTO (1996). Standard Specifications for Transportation Materials 16th Edition, *American Association of State Highway and Transportation Officials*, Washington, DC.

Bae, Y. (2007). Modelling Soil Behavior In Large Strain Resonant Column and Torsional Shear Tests, *PhD Thesis*, Utah State University, Utah.

BS 8081 (1989). British Standard Code of Practice for Ground Anchorages, *British Standard Institution,* London.

Bozkurt, M. (2010). Temel Çukuru İksa Sistemlerinin Sayısal Yöntemler İle Analizi, *M.Sc. Thesis,* Istanbul Technical University, Istanbul.

Brinkgreve, R.B.J. (1999). Beyond 2000 In Computational Geotechnics-10 Years of Plaxis, Balkema, Rotterdam, The Netherlands.

Coduto, D. P. (2006). Geoteknik Mühendisliği İlkeler ve Uygulamalar, Gazi Kitabevi, Ankara.

Caltrans. (2003). Bridge Design Specifications. *California Department of Transportation*, CA, USA.

Celep, Z. and Kumbasar, N. (2005). Betonarme Yapılar, Istanbul Technical University, Istanbul.

Celep, Z. (2007). Yapı Elemanı Olarak Yerinde Dökme Betonarme Kazıklar. *TMOBB İnşaat Mühendisleri Odası İstanbul Şubesi Yapı Tasarımı Kurs Notları,* Date retrieved: 20.12.2013, address: http://web.itu.edu.tr/celep/files/s1.pdf

Das, B. M. (1987). Theoretical Foundation Engineering, Developments in Geotechnical Engineering Vol 47, Elsevier Science Publishing Co., NY, USA.

Das, B. M. (2007). Principles of Foundation Engineering 6th Edition, Pws Publishing Co.

Das, B. M. (2008). Advanced Soil Mechanics 3rd Edition, Taylor&Francis, Inc., NY, USA.

Dayıoğlu, M. (2010). Derin Kazıların İncelenmesi ve Derin Kazı Uygulaması Üzerine Bir Örnek: Harbiye Kongre Merkezi Derin Temel Kazısı, *M.Sc. Thesis,* Istanbul Technical University, Istanbul.

DBYBHY (2007). Deprem bölgelerinde yapılacak binalar hakkında yönetmelik

DIN 4125 (1990). Ground Anchorages-Design, Construction and Testing, Deutches Institut für Normung.

EN1537 (2000). Execution of special geotechnical work, *European Standard,* CEN, Brussels.

Enar Engineers Architects & Consultants. (2007). Bomonti Uluslararası Kongre ve Turizm Yatırımları Projesi İstanbul İli, Şişli İlçesi, Şişli Merkez Mahallesi, Silahşör Caddesi No.1, 167 Pafta, 1018 Ada, 1 Parsel Bomonti Uluslararası Kongre ve Turizm Yatırımları Projesi Zemin Etüt Raporu İstanbul.

Ermanlar, L. (2009). Derin Kazılarda Sonucu Çevre Yapılarda Oluşan Deformasyonların Tahmini, *M.Sc. Thesis,* Yildiz Technical University, Istanbul.

FHWA-IF-99-015. (1999). Ground Anchors and Anchored Systems, Geotechnical Engineering Circular No.4, U.S. Department of Transportation, *Federal Highway Administration,* Washington DC.

FHWA-NHI-09-087. (2009). Corrosion/Degradation of Soil Reinforcements for Mechanically Stabilized Earth Walls and Reinforced Soil Slopes, U.S. Department of Transportation, *Federal Highway Administration,* Washington DC.

GCO Publication No. 1/90. (1990). Review of Design Methods for Excavation, *Geotechnical Engineering Office, Civil Engineering and Development Department,* Hong Kong.

Hayta, Ö. (2005). Finite Element Analysis of Tieback Wall Using Plaxis: A Case Study, *M.Sc. Thesis,* Bosphorus University, Istanbul.

ISRM. (1985). Suggested Method of Determination of Point Load Strength. *International Journal of Rock Mechanics and Mining Sciences and Geomechanics Abstracts*, V.22.

Kip, F. and Kumbasar, V. (1999). Zemin Mekaniği Problemleri, Çağlayan Kitabevi, Istanbul.

Koyuncu, S. (2006). Derin Kazı Problemlerinde Betonarme Perde ve Mini kazık Analizi, *M.Sc. Thesis,* Istanbul Technical University, Istanbul.

NAVFAC, DM-7.2. (1982). Foundations and Earth Structures Design Manual 7.2, *Department of the Navy*, Alexandria, VA.

Ou, C. (2006). Deep Excavation: Theory and Practice, Tylor and Francis Group Publishers, London, UK.

Öncü, G. (2009). Derin Kazılı İksa Sisteminde Oluşan Yer Değiştirmelerin Hesaplanarak Aletsel Gözlemlerle Karşılaştırılması, *M.Sc. Thesis*, Yıldız Technical University, Istanbul.

Özgen, E. (1984). İstinat Yapılarına Etkiyen Toprak Basınçları. *TMOBB İnşaat Mühendisleri Odası Türkiye Mühendislik Haberleri*, Date retrieved: 20.01.2014, address: http://www.e-kutuphane.imo.org.tr/pdf/3531.pdf

Plaxis Material Models Manual (2011).

Plaxis 2D Reference Manual (2011).

Podles, K., Rosso, R., Truty, A., and Zimmermann, T. (2010). Numerics in Geotechnics and Structures, Elmepress International, Lausanne, Switzerland.

Rahn, R.H. (2006). Mühendislik Jeolojisi: Çevresel Bir Yaklaşım, 2nd Edition, Gazi Kitabevi, Ankara..

Ranjan, G., and Rao, A.S.R. (2000). Basic and Applied Soil Mechanics, 2nd Edition, New Age International (P) Ltd. Publishers, New Delhi.

Sağlam, A. (2006). Derin Kazılarda Görülen Stabilite Problemleri ve İlgili Çözüm Kriterlerinin Belirlenmesi, *M.Sc. Thesis,* Sakarya University, Sakarya.

Sağlamer, A. (1985). Deep Excavations in Istanbul Greywacke, *Turkish Group of Soil Mechanics Symposium on Design of Supports to Deep Excavations*, Boğaziçi University, İstanbul.

Sivrikaya, O. and Toğrol, E. (2009). Arazi Deneyleri ve Değerlendirilmesi, Birsen Yayınevi, İstanbul.

Sütçüoğlu, M. (2009). A Case Study: A Deep Retaining System Construction With Prestressed Anchors, M.S. Thesis, Dokuz Eylül University, Izmir.

TS-648 (1980). Building Code for Steel Structures, Turkish Standard Institution, Ankara.

TS-699 (2009). Natural building stones - Methods of inspection and laboratory testing, Turkish Standard Institution, Ankara.

Uncuoğlu, E. (2009). Kohezyonsuz Zeminlerdeki Kazıkların Yatay Yük ve Moment Etkisi Altındaki Davranışlarının Analizi, *PhD Thesis*, Çukurova University, Adana.

[1] **Url-1** < *http://www.deepexcavation.com*>, date retrieved 25.10.2013.

Url-2 <*http://www.iaeg.info*>, date retrieved 25.11.2013.

USACE-EM 1110-2-1902. (2003). Slope Stability, Department of the Army, *U.S. Army Corps of Engineers Engineering and Design*, Washington DC.

ÜK, M. (2009). Derin Kazılar ve Derin Kazılara Bir Örnek: Flame Towers Projesi İksa Sistemi, *M.Sc. Thesis*, Istanbul Technical University, Istanbul.

Xanthakos, P. (1991). Ground Anchors and Anchored Structures, John Wiley & Sons, Inc., Canada.

Yüksel, F. (1990). Derin Kazılarda İksa Yöntemleri, *M.Sc. Thesis*, Istanbul Technical University, Istanbul.

APPENDICES

APPENDIX A: Maps
APPENDIX B: Boring Logs
APPENDIX C: Cross Sections
APPENDIX D: Project Renders
APPENDIX E: Photos
APPENDIX F: Inclinometer Measurements
APPENDIX G: Calculations for Structural Elements
APPENDIX H: Cost Analysis
APPENDIX I: Plot of Elasticity Modulus vs. Horizontal Displacements

APPENDIX A

Figure A.1 : Road map.

Figure A.2 : Project location (1).

Figure A.3 : Project location (2).

APPENDIX B

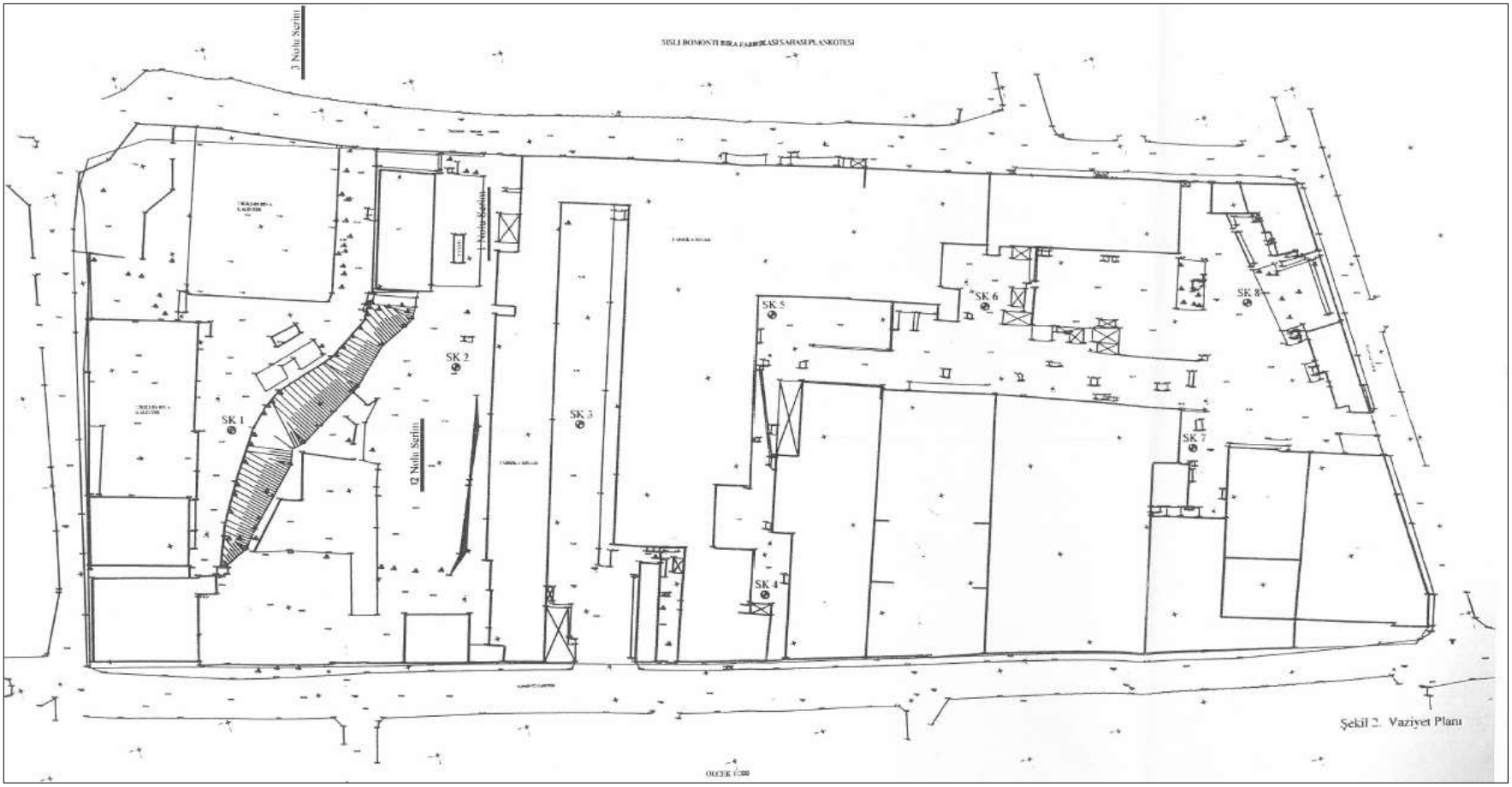

Figure B.1 : Layout plan and boring logs.

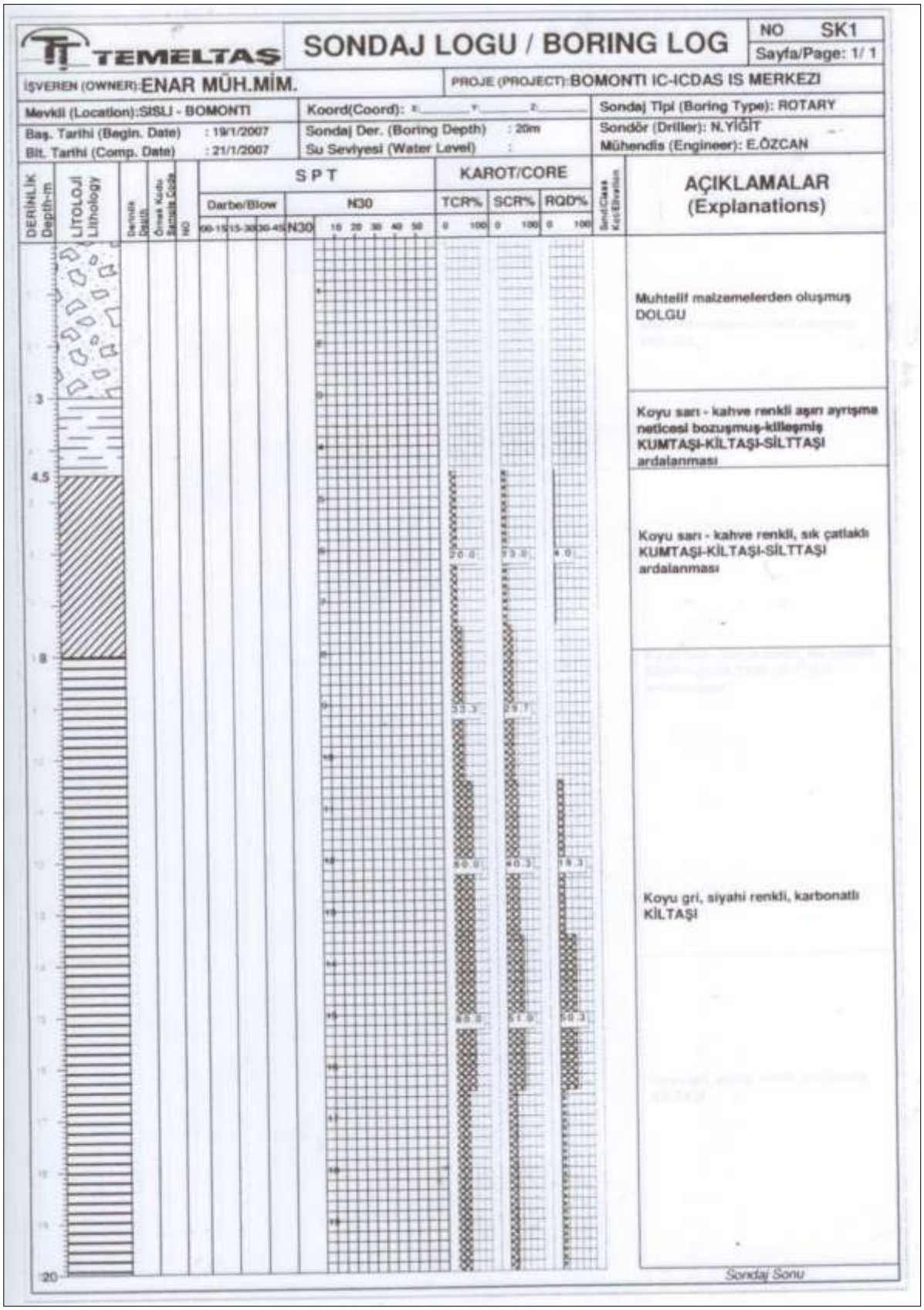

Figure B.2 : Boring log for SK1.

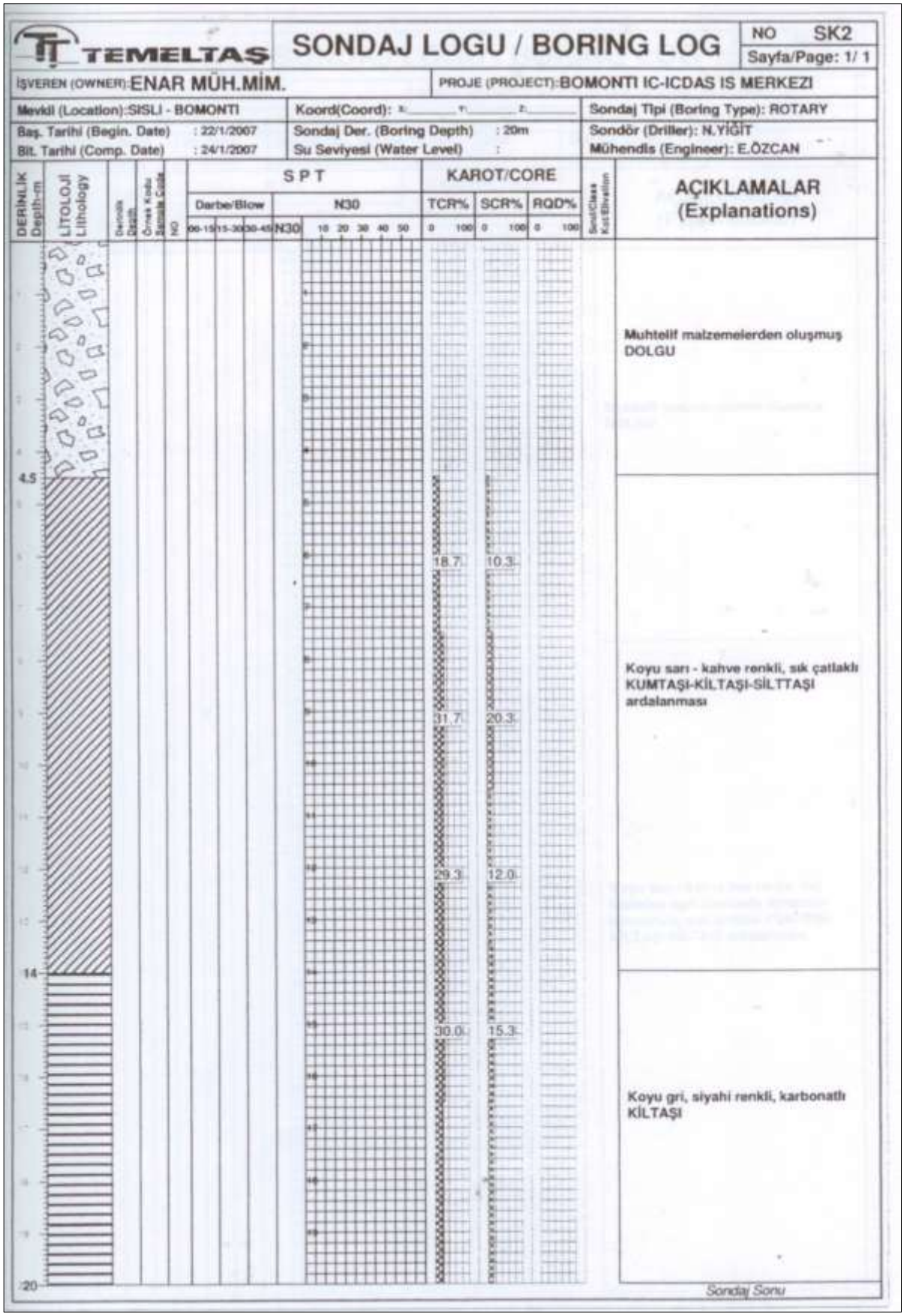

Figure B.3 : Boring log for SK2.

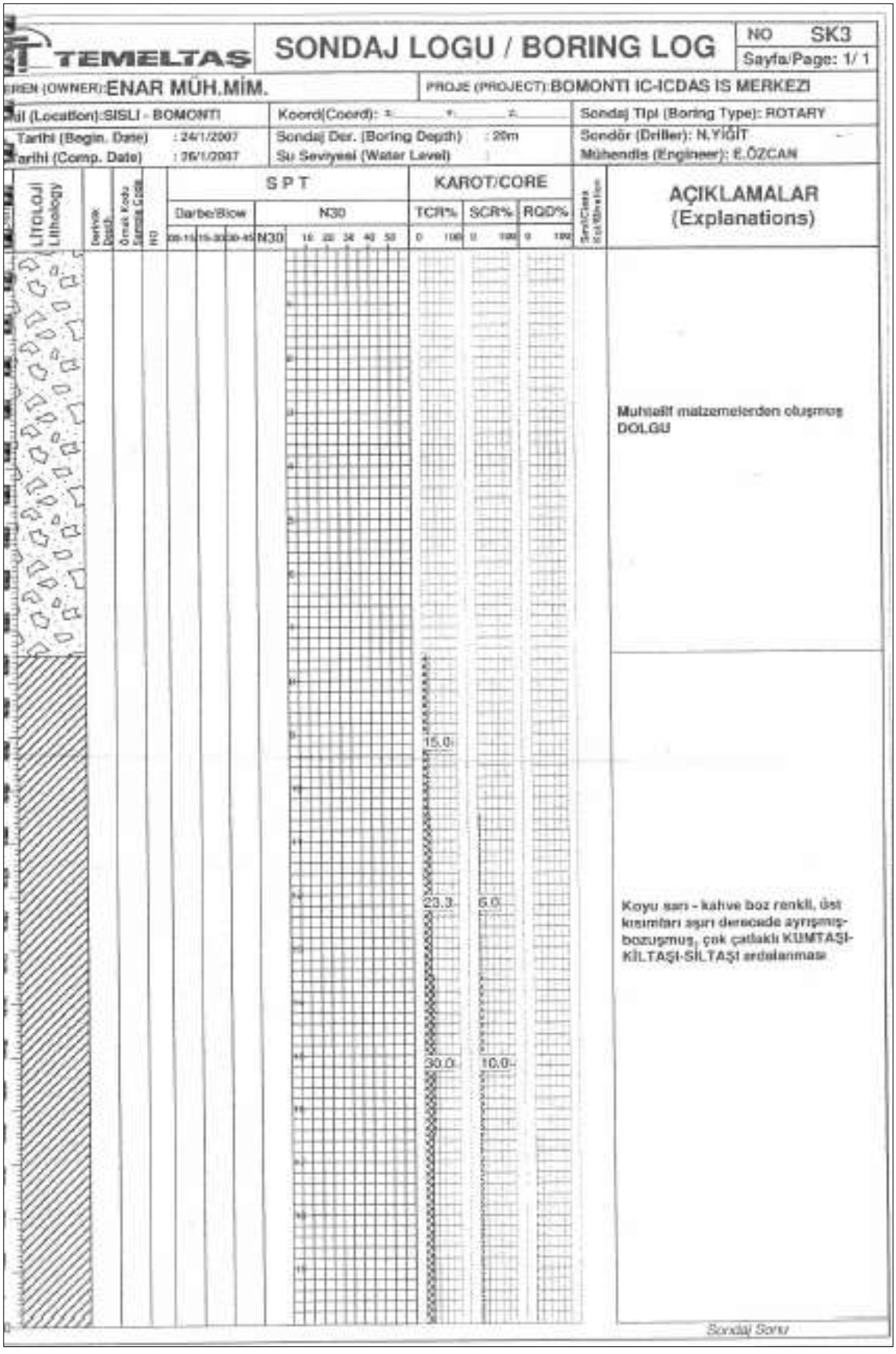

Figure B.4 : Boring log for SK3.

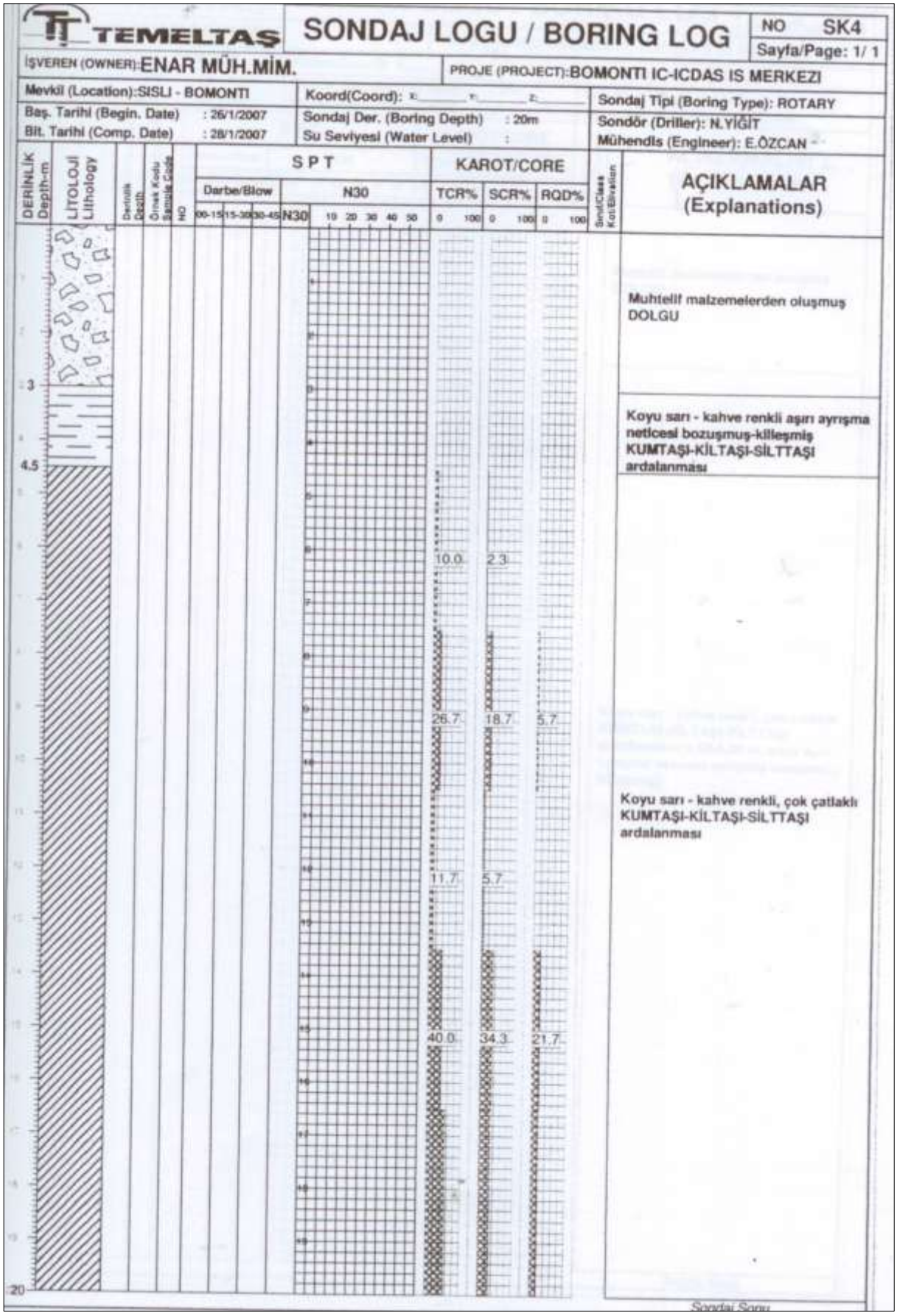

Figure B.5 : Boring log for SK4.

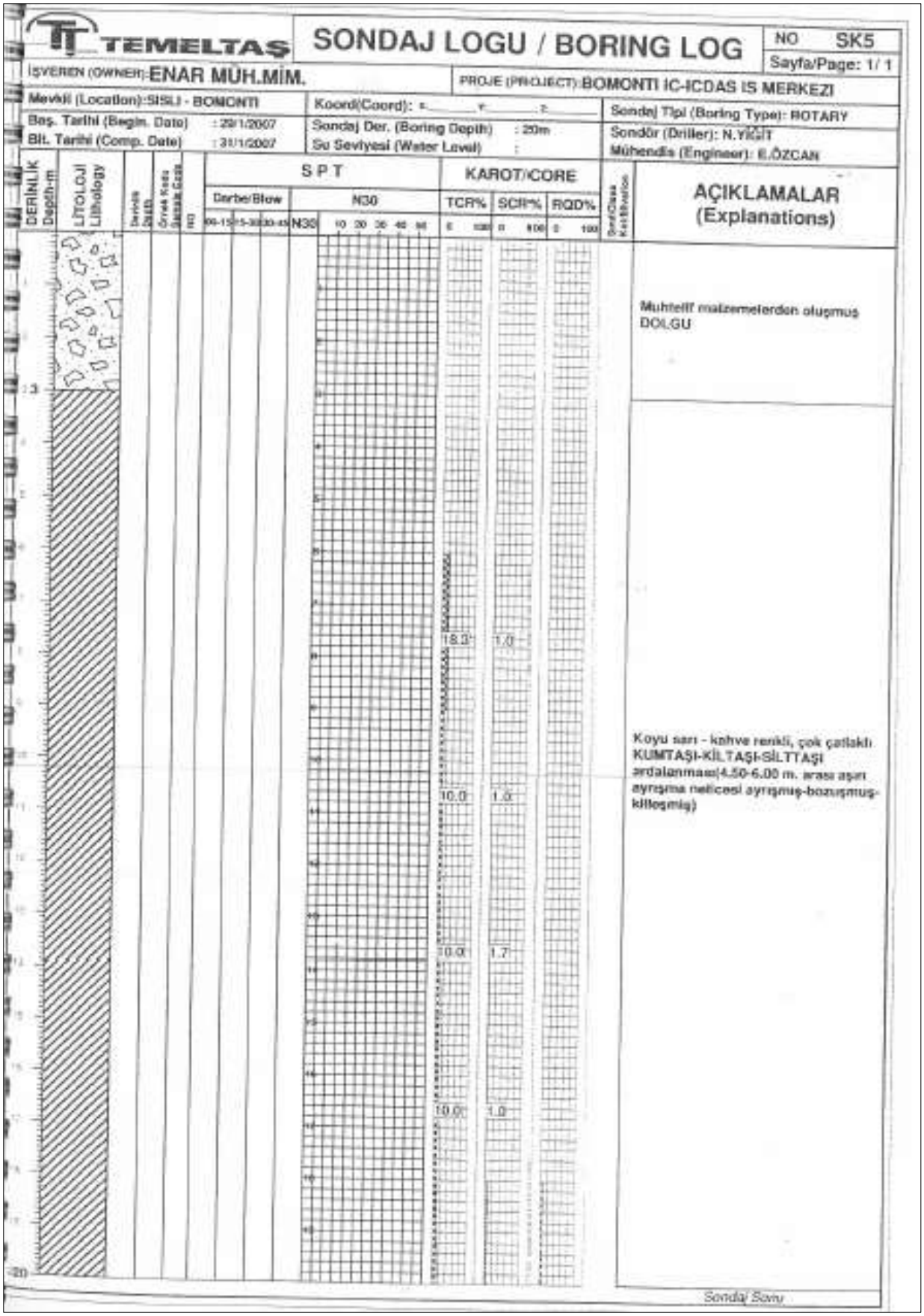

Figure B.6 : Boring log for SK5.

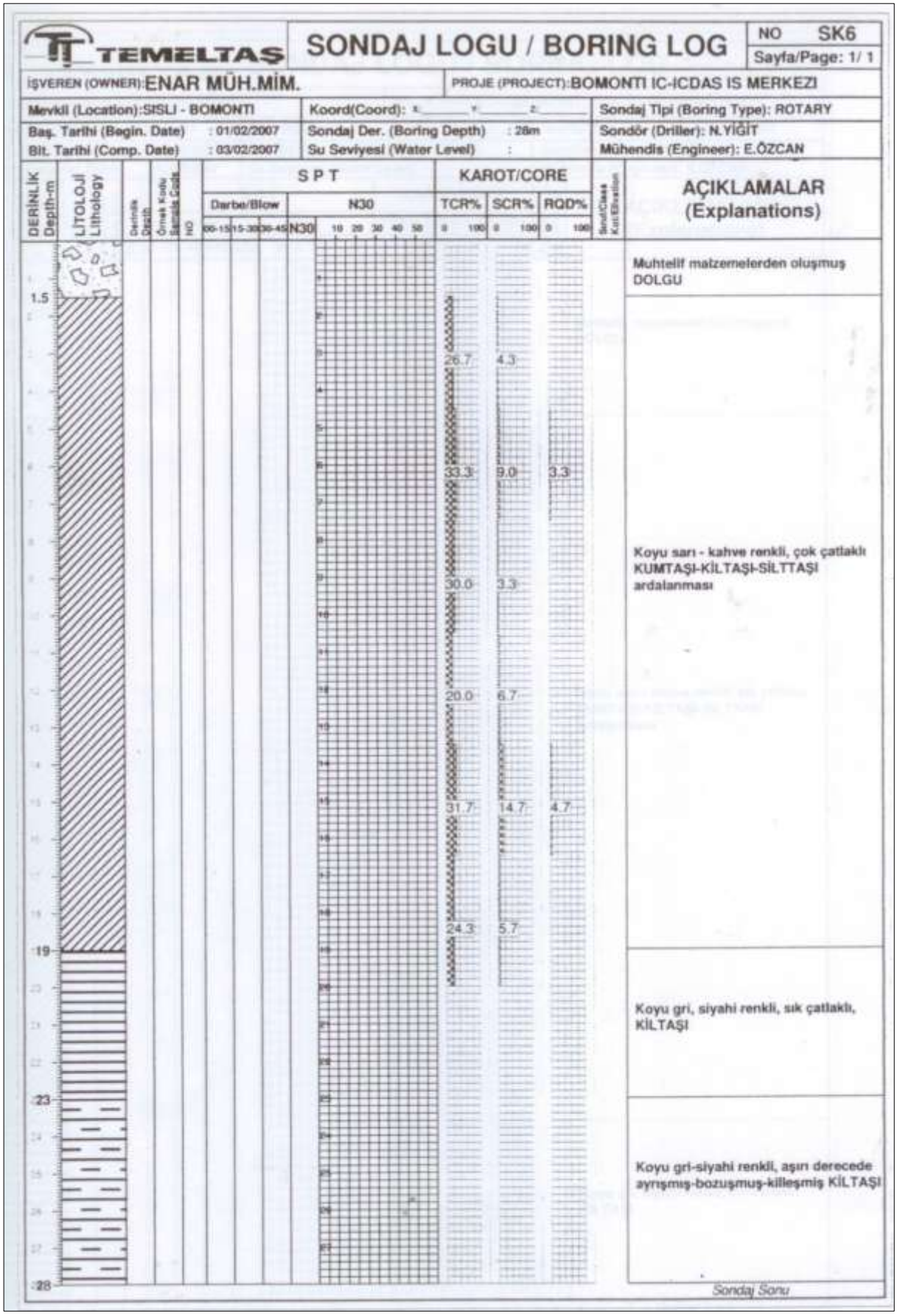

Figure B.7 : Boring log for SK6.

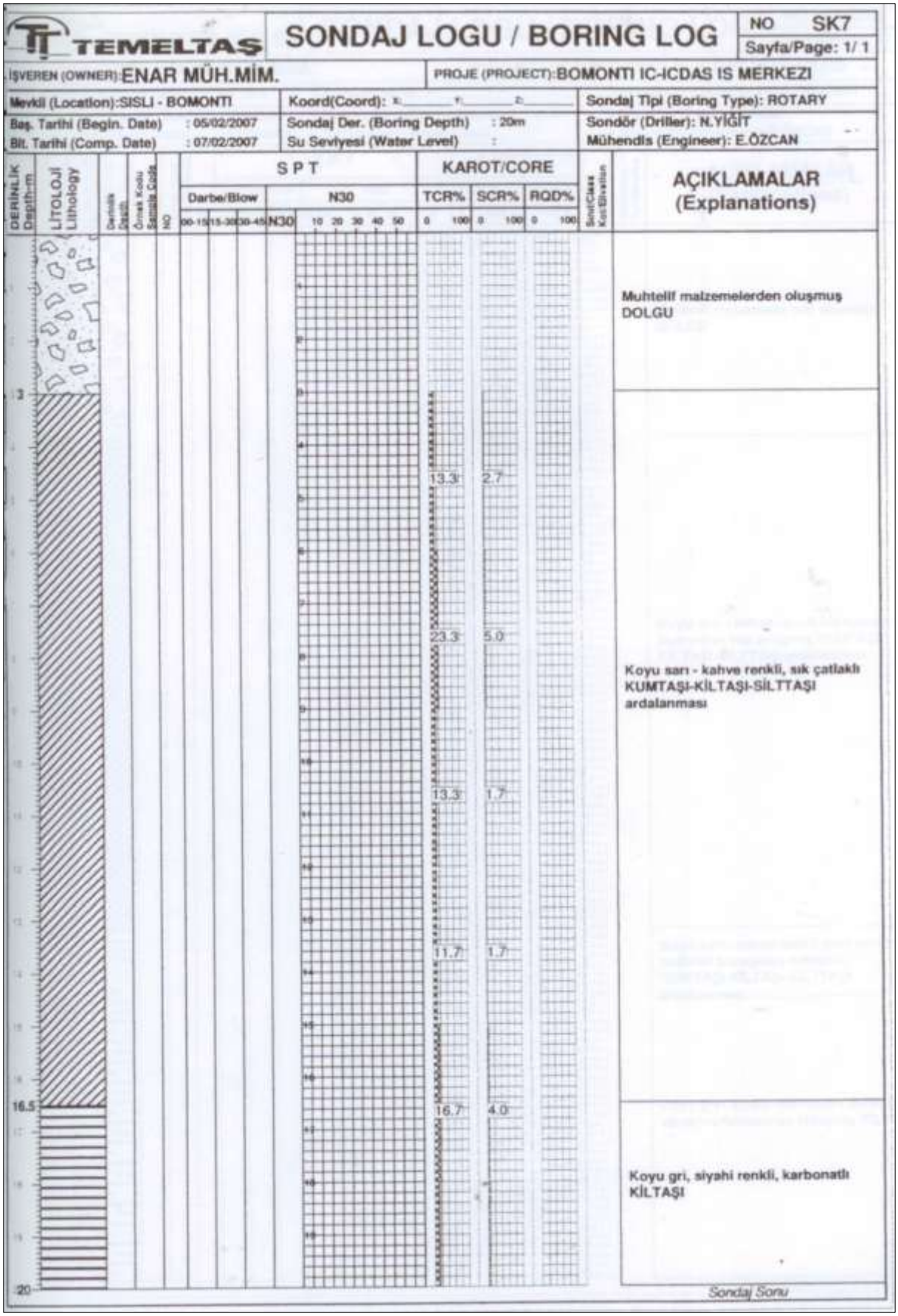

Figure B.8 : Boring log for SK7.

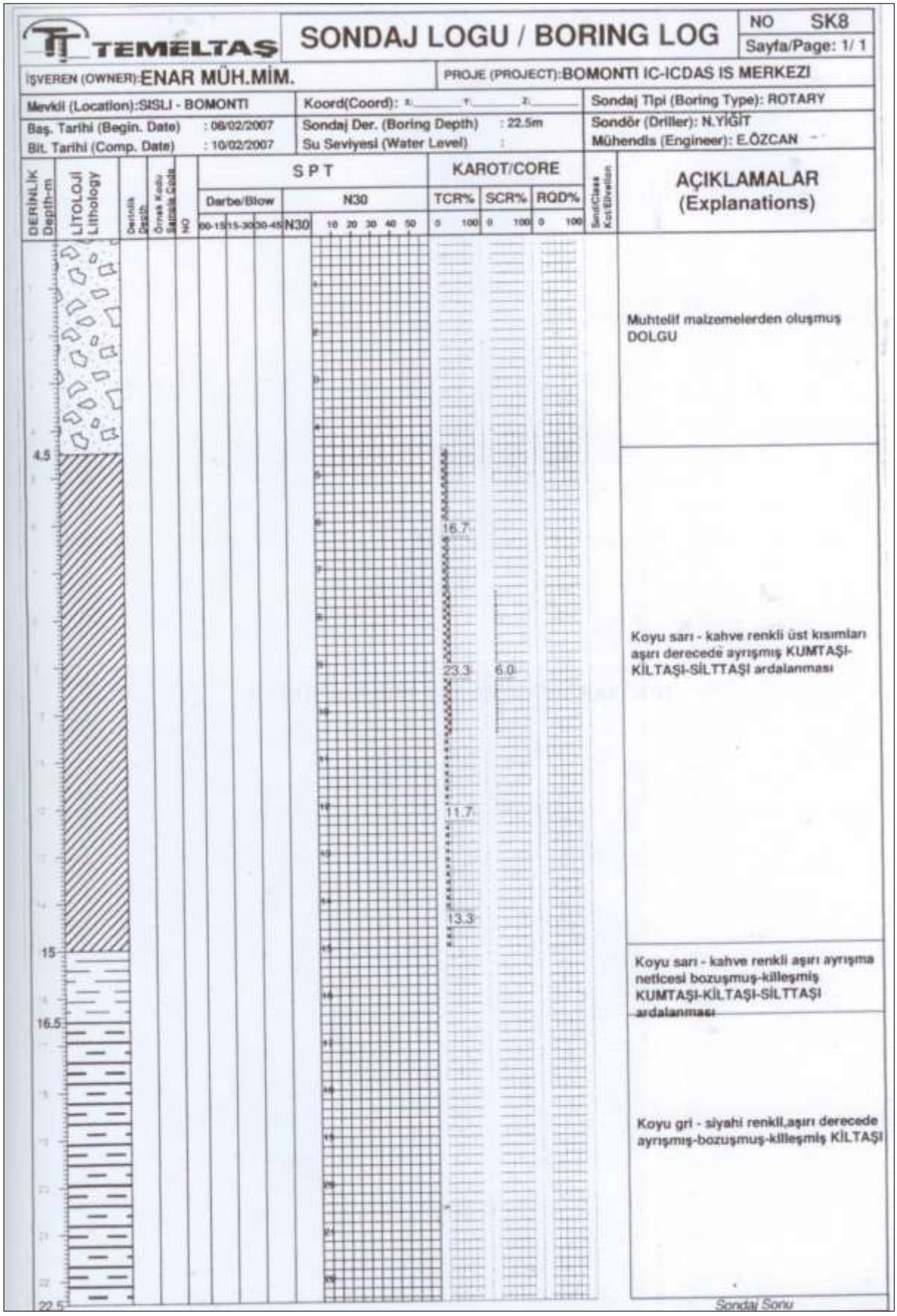

Figure B.9 : Boring log for SK8.

APPENDIX C

Figure C.1 : Preliminary design drawing.

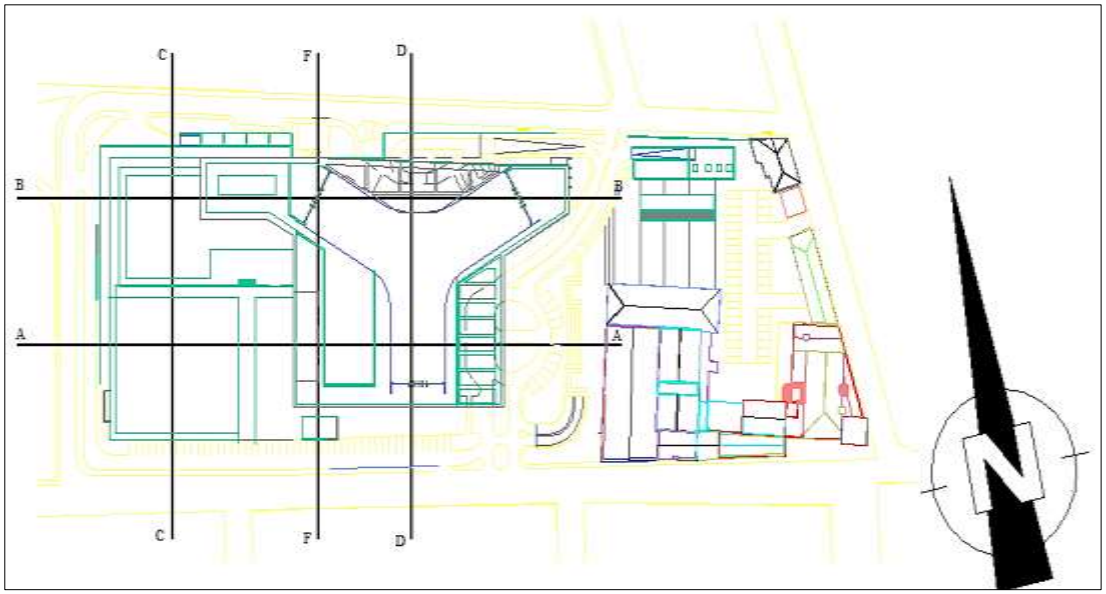

Figure C.2 : Key plan.

Figure C.3 : A-A cross-section of the investigated area.

APPENDIX D

Figure D.1 : Hilton Istanbul Bomonti Hotel and Conference Center render from Birahane Sokak.

Figure D.2 : Hilton Istanbul Bomonti Hotel and Conference Center perspective.

Figure D.3 : Hilton Istanbul Bomonti Hotel and Conference Center render from Silahşör Caddesi.

Figure D.4 : Hilton Istanbul Bomonti Hotel and Conference Center render from Silahşör Caddesi.

APPENDIX E

Figure E.1 : The Historic Bomonti Brewery in 2008 before restoration.

Figure E.2 : Excavation works for Hilton Istanbul Bomonti Hotel & Conference Center.

Figure E.3 : Staged construction in front of The Historic Bomonti Brewery.

Figure E.4 : Staged construction in front of The Historic Bomonti Brewery.

Figure E.5 : Aerial view of the site during reinforced concrete works.

Figure E.6 : Foundation works for 7-storey car park.

APPENDIX F

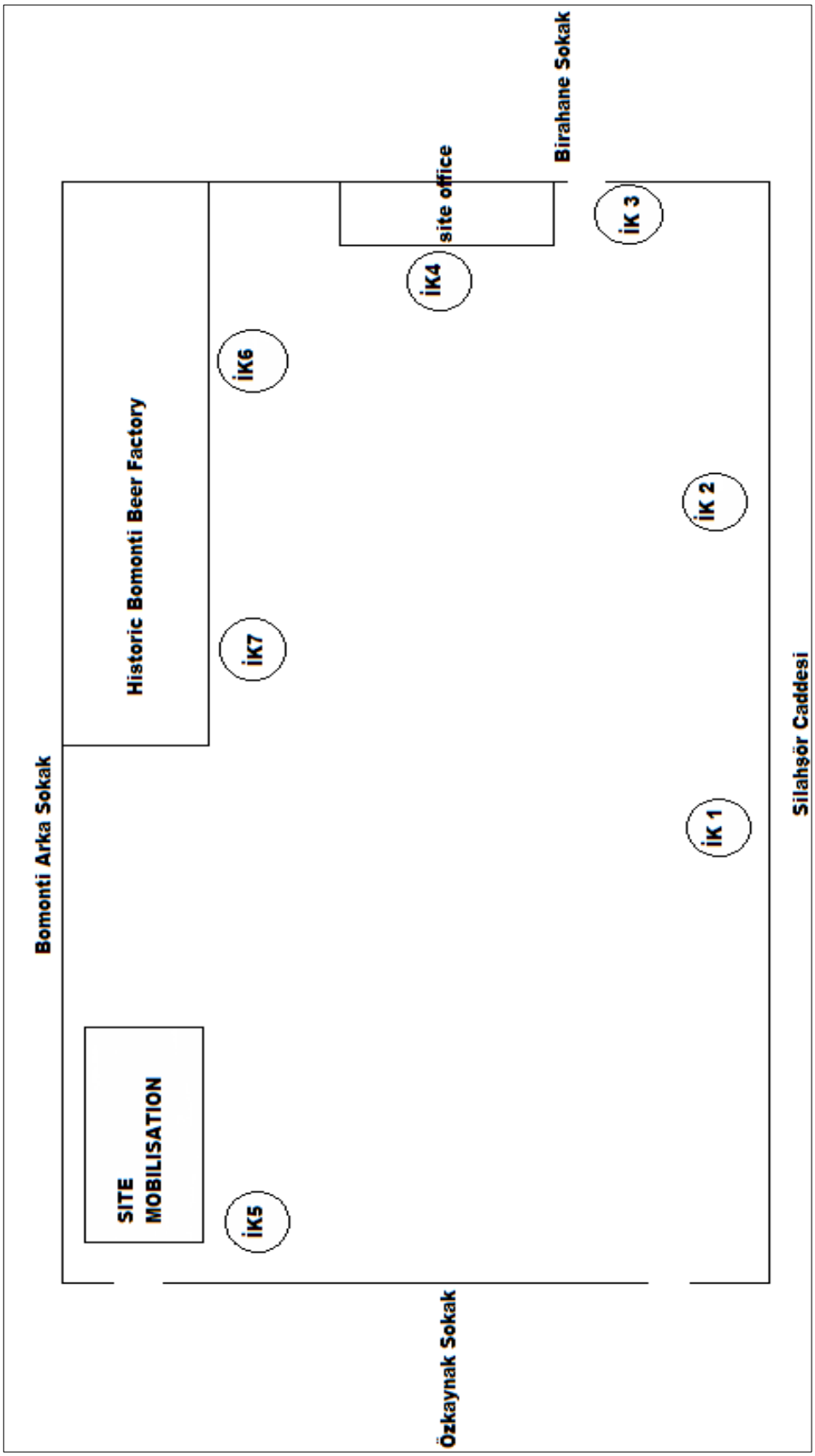

Figure F.1 : Placement of inclinometers.

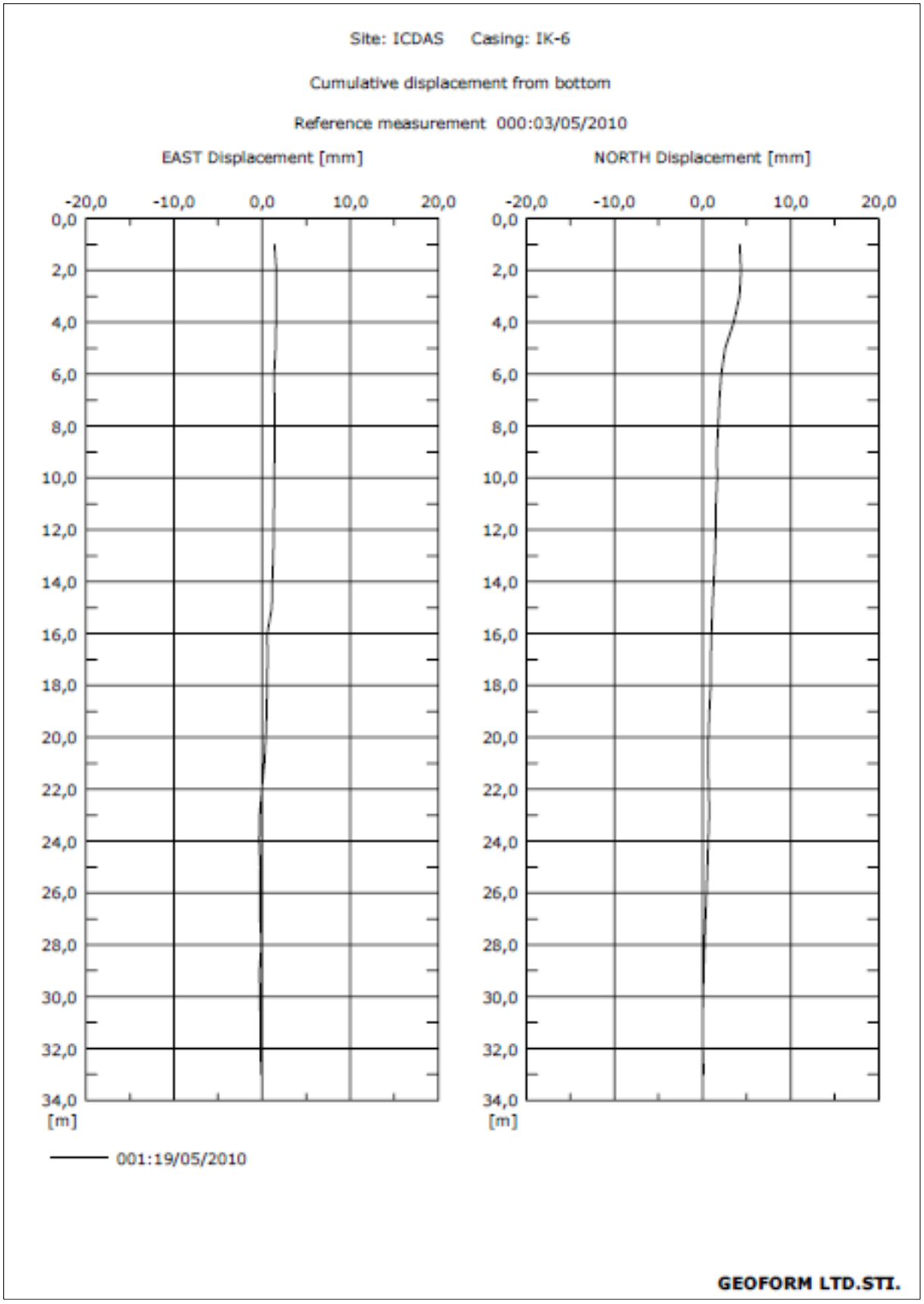

Figure F.2 : Inclinometer measurements for IK-6 in 19.05.2010.

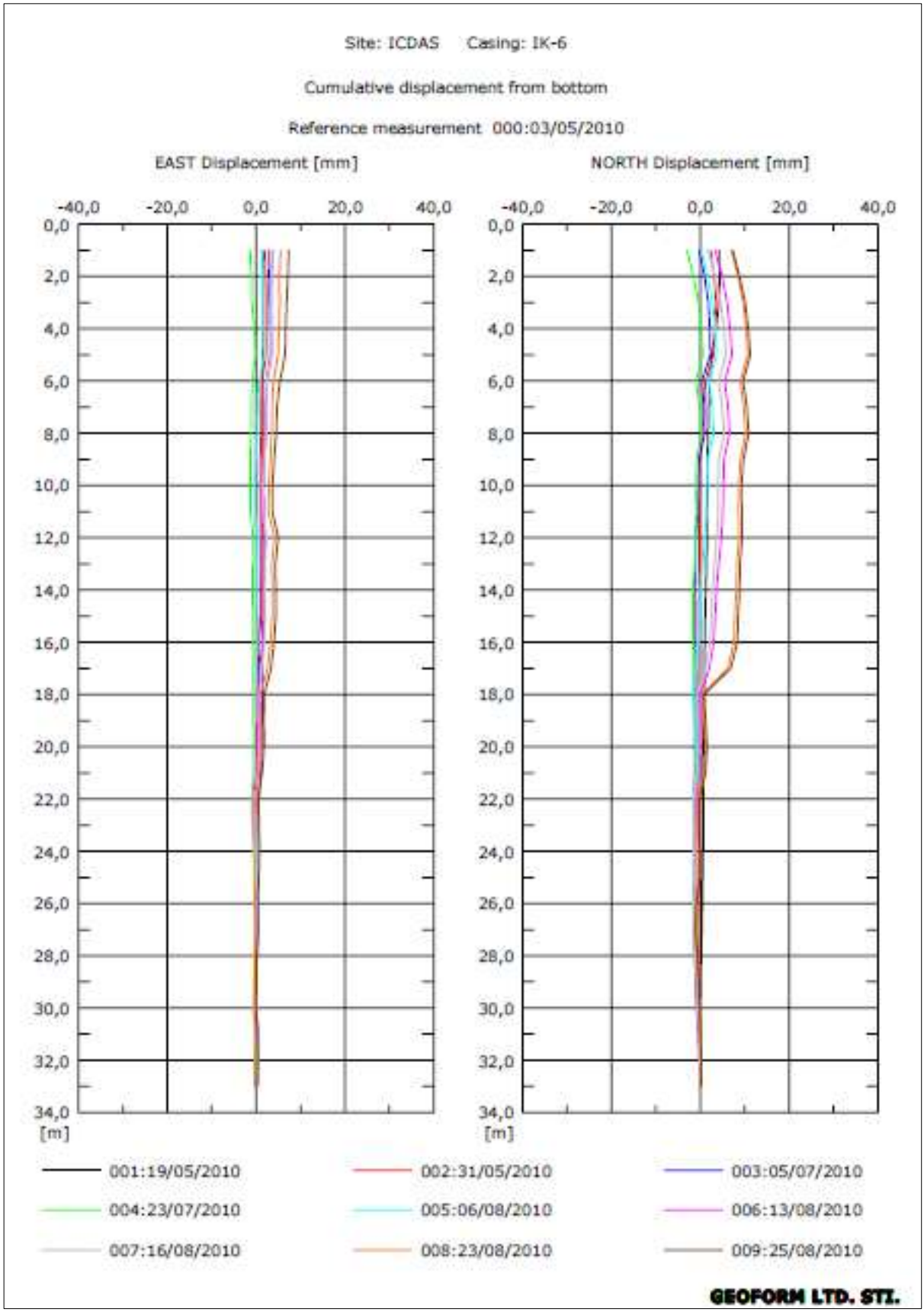

Figure F.3 : Inclinometer measurements for IK-6 in 25.08.2010.

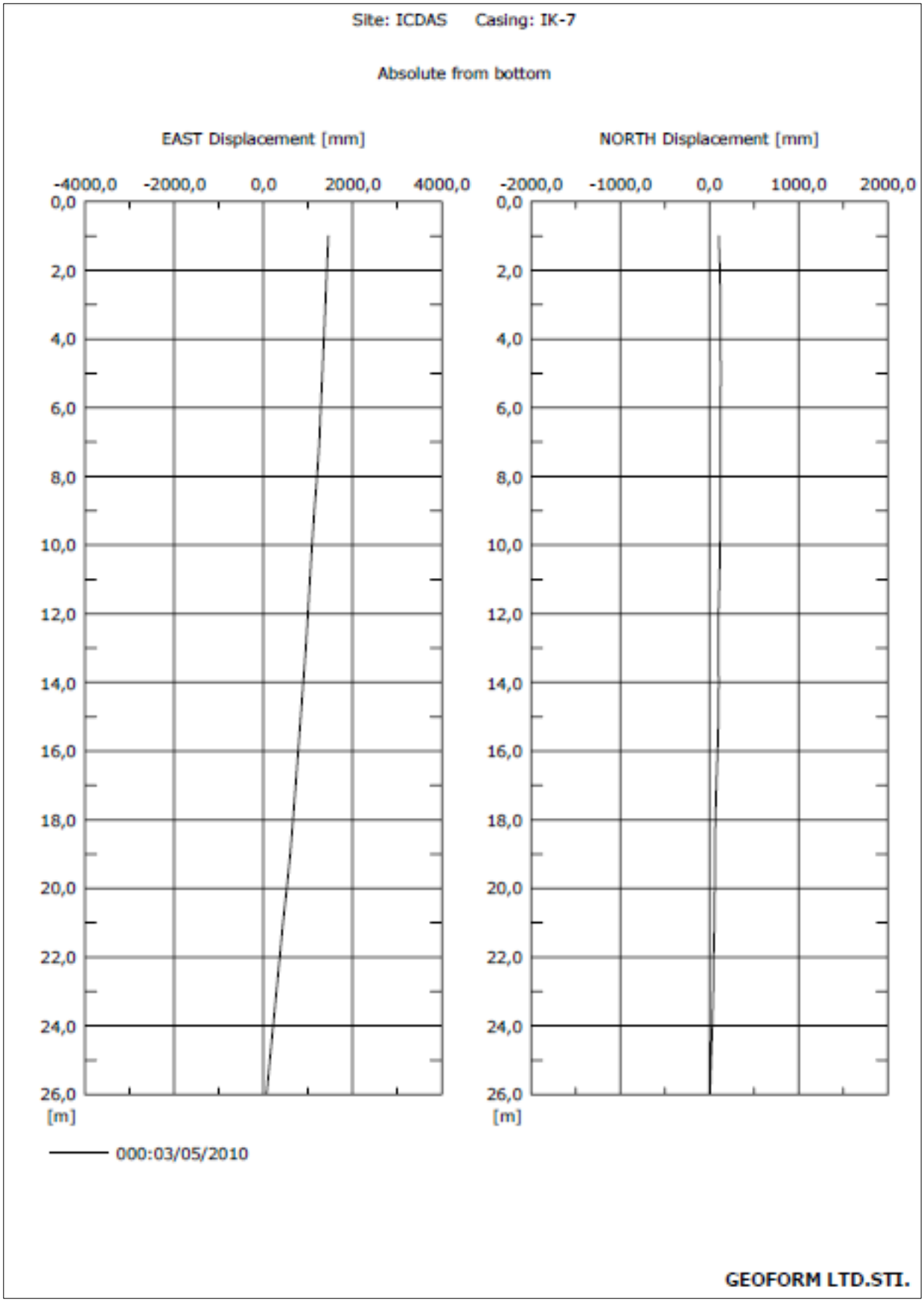

Figure F.4 : Inclinometer measurements for IK-7 in 03.05.2010.

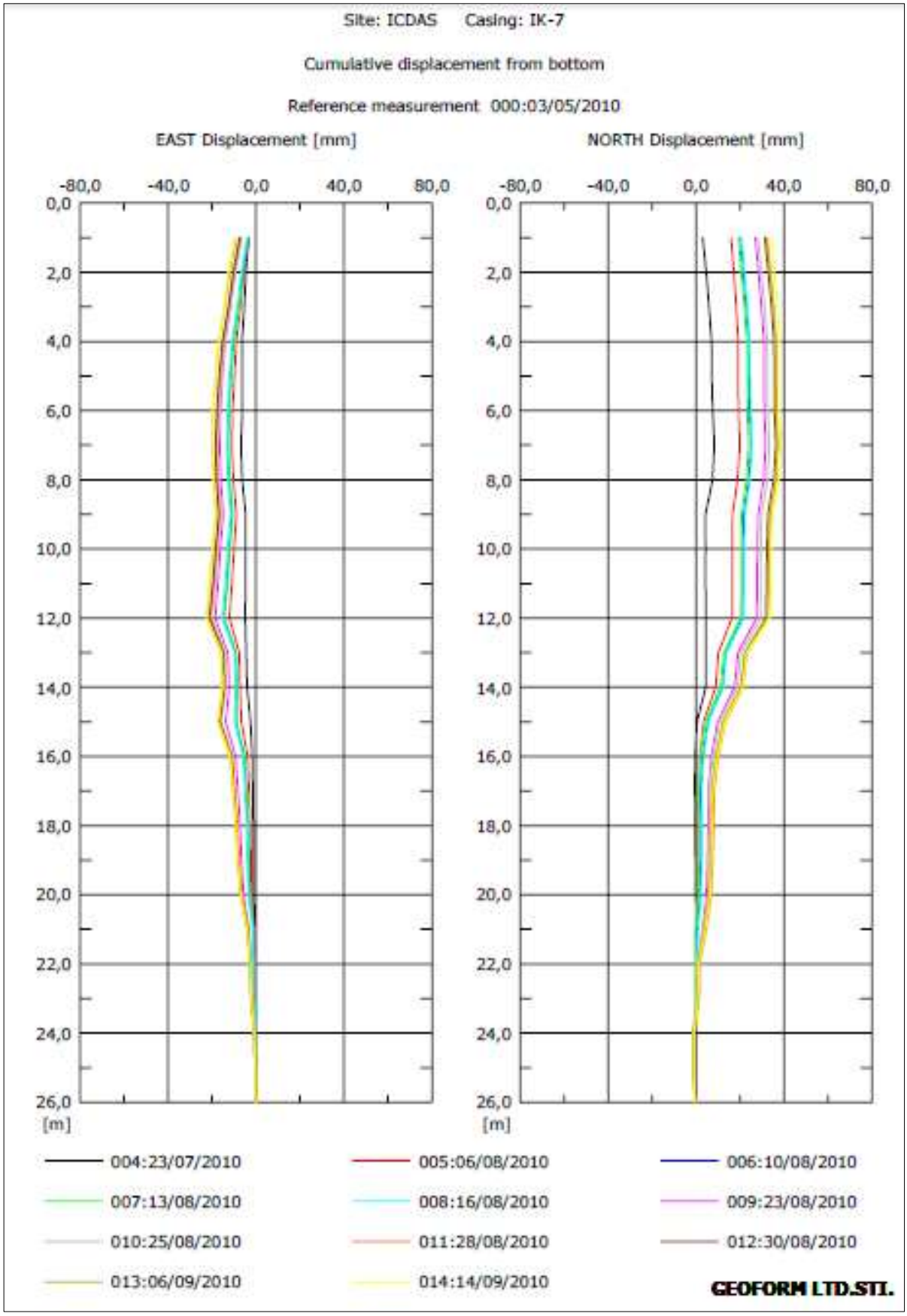

Figure F.5 : Inclinometer measurements for IK-7 in 14.09.2010.

APPENDIX G

I. Preliminary calculations for the deep excavation support system

Table G.1 : Pre-calculations for multi-levelled anchored pile wall.

IN FRONT OF HISTORIC BUILDING - 1st STAGE ANCHORS									
γ (kN/m^3)	22								
Ø (°)	37,5								
k_a	0,39								
q_s (kN/m^2)	45								
H_1 (m)	1,0								
H_2 (m)	2,5								
H_3 (m)	2,5								
H_4 (m)	2,5								
H_5 (m)	1,0								
H (m)	9,5								
S_h (m)	1,5								
p_e (kN/m^2)	57,13								
p_s (kN/m^2)	17,60								
TH_1 (kN/m)	149,08	α_1 (°)	15	S_{h1} (m)	1,5	DL_1 (kN)	231,51	PL_1 (kN)	289,39
TH_2 (kN/m)	186,80	α_2 (°)	15	S_{h2} (m)	1,5	DL_2 (kN)	290,09	PL_2 (kN)	362,61
TH_3 (kN/m)	186,80	α_3 (°)	15	S_{h3} (m)	1,5	DL_3 (kN)	290,09	PL_3 (kN)	362,61
TH_4 (kN/m)	129,21	α_4 (°)	15	S_{h4} (m)	1,5	DL_4 (kN)	200,64	PL_4 (kN)	250,81
M_1 (kNm/m)	22,55								
M_2 (kNm/m)	46,70								
M_3 (kNm/m)	46,70								
M_4 (kNm/m)	7,47								

IN FRONT OF HISTORIC BUILDING - 2nd STAGE ANCHORS									
γ (kN/m^3)	22								
Ø (°)	37,5								
k_a	0,39								
q_s (kN/m^2)	45								
H_1 (m)	1,0								
H_2 (m)	2,25								
H_3 (m)	2,25								
H_4 (m)	2,25								
H_5 (m)	2,25								
H_6 (m)	2,25								
H_7 (m)	2,25								
H_8 (m)	2,0								
H (m)	16,5								
S_h (m)	1,5								
p_e (kN/m^2)	98,21								
p_s (kN/m^2)	17,60								
TH_1 (kN/m)	213,35	α_1 (°)	15	S_{h1} (m)	1,5	DL_1 (kN)	331,31	PL_1 (kN)	414,14
TH_2 (kN/m)	260,56	α_2 (°)	15	S_{h2} (m)	1,5	DL_2 (kN)	404,62	PL_2 (kN)	505,78
TH_3 (kN/m)	260,56	α_3 (°)	15	S_{h3} (m)	1,5	DL_3 (kN)	404,62	PL_3 (kN)	505,78
TH_4 (kN/m)	260,56	α_4 (°)	15	S_{h4} (m)	1,5	DL_4 (kN)	404,62	PL_4 (kN)	505,78
TH_5 (kN/m)	260,56	α_5 (°)	15	S_{h5} (m)	1,5	DL_5 (kN)	404,62	PL_5 (kN)	505,78
TH_6 (kN/m)	260,56	α_6 (°)	15	S_{h6} (m)	1,5	DL_5 (kN)	404,62	PL_5 (kN)	505,78
TH_7 (kN/m)	241,26	α_7 (°)	15	S_{h7} (m)	1,5	DL_6 (kN)	374,65	PL_6 (kN)	468,31
M_1 (kNm/m)	32,44								
M_2 (kNm/m)	58,63								
M_3 (kNm/m)	58,63								
M_4 (kNm/m)	58,63								
M_5 (kNm/m)	58,63								
M_6 (kNm/m)	58,63								
M_7 (kNm/m)	58,63								

II. Reinforcement calculations for structural elements according to Plaxis results

Table G.2 : Calculation of reinforcement for mini pile.

LONGITUDINAL REINFORCEMENT DESIGN FOR MINIPILE								
Pile Diameter (cm)	Data	Internal forces according to Plaxis calculations		Forces on pile body (Pile spacing; 50 cm)		Design loads with factor of safety 1,6		
25	Section 1-1	M (kNm/m)	V (kN/m)	M (kNm/m)	V (kN/m)	M_d (kNm/m)	V_d (kN/m)	
		58,86	188,06	29,43	94,03	46,91	150,44	
Pile Diameter (cm)	Structural Steel Class		Concrete strength		Pile moment	m_r		
	Class	f_{yd} (Mpa)	Class	f_{cd} (Mpa)	M_d (kNm)	$M_d/0,25*\pi*D^3*k_1*f_{cd}$		
25	420	365,22	25	16,67	46,912	0,270		
ρ_m	$A_{schosen}$ (cm^2)	ρ_{min}	A_{smin} (cm^2)	ρ_{max}	A_{smax} (cm^2)	Pile reinforcement properties		
						Diameter (mm)	Number	Area A_s (cm^2)
0,65	12,38	0,01	4,91	0,03	14,73	18	5	12,72
						5ϕ18		

Table G.3 : Shear design for mini pile.

SHEAR REINFORCEMENT DESIGN FOR MINIPILE					
d_o (Pile diameter)	d' (Concrete cover)	D (Effective height)	Pile spacing	V_d,max	$V_{cr}=0.58*f_{ctd}*b_w*d$
mm	mm	mm	mm	kN/m	kN
250	25	200	500	94,03	37,52
A_c	A_{ck}	ϕ, chosen	A_{sw}	ρ_s $0,12*f_{ck}/f_{ywk}$	s_c $\pi*D*A_{sw}/\rho_s*A_{ck}$
mm^2	mm^2	mm	mm^2	-	mm
49087,39	31415,93	8	50,27	0,007	140,74
Link spacing- Middle part	S_{omax}	200 mm	Confinement zone	$s_c=s_o=D/5$	40 mm
	$S_{omax}=d_o/2$	125 mm		$s_c=s_o=80$ mm	80 mm
	$S_{omax}=12*\phi_l$	8 mm		s_{chosen}	50 mm
	s_{chosen}	100 mm		Link-->	ϕ8/10

Table G.4 : Calculation of reinforcement for cap beam.

REINFORCEMENT DESIGN FOR CAP BEAM									
Section No	Dimensions		A_c	ρ_{min}= 0,8	A_s min	Chosen reinforcement properties			
	b_w	h				A_s chosen	Diameter	Number	A_s
	cm	cm	cm^2	kN/m	cm^2	cm^2	mm	Number	cm^2
1	50	50	2500	0,80%	20,00	20,00	16	10	20,11

Table G.5 : Calculation for reinforcement in waler beam and shear design.

REINFORCEMENT DESIGN FOR WALER BEAM								
Section No	Dimensions		Anchor force	Anchor spacing, S	Moment, M $A_{max}*S^2/10$	Shear force, Q $A_{max}*S/2$	Design loads, FS=1.5	
	b_w	h	A_{max}				M_d	Q_d
	cm	cm	kN/m	m	kNm	kN	kNm	kN
2	70	35	347,400	1,5	78,165	260,55	117,2475	390,825
MATERIAL PROPERTIES						Conc' cover	ρ_m	0,02
Concrete	C25	γ_{mc}	1,50	fcd, Mpa	16,67	d', cm	m_d	0,05
Steel	S420	γ_{my}	1,15	fyd, Mpa	365,22	2,5	M_r	117,2475
A_s min (cm^2)		A_s max (cm^2)		A_s calc. (cm^2)	Chosen reinforcement properties			
$\rho_{min} \geq 0{,}8f_{ctd}/f_{yd}$	A_s min	ρ_{max}	A_s max	A_s	A_s chosen (cm^2)	Diameter (mm)	Number	A_s (cm^2)
0,25%	6,18	2,00%	49,00	12,63	12,63	18	5	12,72
V_d	V_{cr}	V_c	V_w	V_r	A_{sw}	Longitudinal reinforcement		
$A*L^2/2$	$0{,}65*f_{ctd}*b_w*d$	$0{,}80*V_{cr}$	$d/s*A_{sw}*f_{ywd}$	V_c+V_w	$n*A_o$	5ϕ18		
kN	kN	kN	kN	kN	cm^2	Shear reinforcement		
390,83	199,06	159,25	267,72	426,97	157,08	ϕ10/15		

III. Input properties for anchors and geogrids for various nominal diameters

Table G.6 : Anchor properties for various nominal diameter of strands.

Type of unbonded length	Number of strands	Diameter [inch]	Diameter [mm]	Cross section area of strand tendon [m^2]	Elasticity Modulus of steel, E [kN/m^2]	Axial stiffness, EA [kN]
3*0,5" node-to-node anchor	3	0,5	12,7	0,000126677	200.000.000	7,6006E+04
4*0,5" node-to-node anchor	4	0,5	12,7	0,000126677	200.000.000	1,0134E+05
3*0,6" node-to-node anchor	3	0,6	15,24	0,000182415	200.000.000	1,0945E+05
4*0,6" node-to-node anchor	4	0,6	15,24	0,000182415	200.000.000	1,4593E+05
3*0,7" node-to-node anchor	3	0,7	17,78	0,000248287	200.000.000	1,4897E+05
4*0,7" node-to-node anchor	4	0,7	17,78	0,000248287	200.000.000	1,9863E+05

Table G.7 : Grouted body properties for various nominal diameter of strands.

Type Bonded Length	Number of strands	Diameter [inch]	Elasticity Modulus of grout, E [kN/m^2]	Axial stiffness, EA [kN]	Axial stiffness of grout, EA [kN]	Total axial stiffness, EA [kN]	Lateral distance of anchor [m]	Total axial input value, EA [kN]
3*0,5" Geogrid-Grout	3	0,5	6.000.000	7,6006E+04	77.359	153.365	1,5	1,0224E+05
4*0,5" Geogrid-Grout	4	0,5	6.000.000	1,0134E+05	76.599	177.941	1,5	1,1863E+05
3*0,6" Geogrid-Grout	3	0,6	6.000.000	1,0945E+05	76.356	185.805	1,5	1,2387E+05
4*0,6" Geogrid-Grout	4	0,6	6.000.000	1,4593E+05	75.261	221.193	1,5	1,4746E+05
3*0,7" Geogrid-Grout	3	0,7	6.000.000	1,4897E+05	75.170	224.142	1,5	1,4943E+05
4*0,7" Geogrid-Grout	4	0,7	6.000.000	1,9863E+05	73.680	272.310	1,5	1,8154E+05

APPENDIX H

Table H.1 : Unit prices table.

Production type	Unit	Unit Price
3@0.6 inch anchor	m	13,00 TL
4@0.6 inch anchor	m	14,00 TL
Formwork installation	m^2	20,00 TL
Concrete	m^3	80,00 TL
Concrete cost of workmanship	m^3	10,00 TL
Rebar	ton	1000,00 TL
Rebar cost of workmanship	ton	120,00 TL

Table H.2 : Cost analysis for the anchors of the old project.

Cost Analysis for Prestressed Ground Anchor								
Construction stage	L_t [m]	Spacing [m]	Number of anchors	Total length per anchor [m]	Prestressing length [m]	Number of strands	Unit price	Total length [m]
1	28,00	1,5	52	1456	1,25	3	*13,00 TL*	*1457,25*
2	26,00	1,5	52	1352	1,25	3	*13,00 TL*	*1353,25*
3	24,00	1,5	52	1248	1,25	3	*13,00 TL*	*1249,25*
4	22,00	1,5	52	1144	1,25	3	*13,00 TL*	*1145,25*
5	26,00	1,5	49	1284	1,25	4	*14,00 TL*	*1285,22*
6	24,00	1,5	49	1185	1,25	4	*14,00 TL*	*1186,45*
7	22,00	1,5	49	1086	1,25	4	*14,00 TL*	*1087,68*
8	20,00	1,5	49	988	1,25	4	*14,00 TL*	*988,92*
9	18,00	1,5	49	889	1,25	4	*14,00 TL*	*890,15*
10	16,00	1,5	49	790	1,25	4	*14,00 TL*	*791,38*
11	14,00	1,5	49	691	1,25	4	*14,00 TL*	*692,62*
						TOTAL [m]		*12127,41667*
						TOTAL COST		*164.579 TL*

Table H.3 : Cost analysis for the anchors of the revised project.

Cost Analysis for Prestressed Ground Anchor								
Construction stage	L_t [m]	Spacing [m]	Number of anchors	Total length per anchor [m]	Prestressing length [m]	Number of strands	Unit price	Total length [m]
1	28,00	1,5	52	1456	1,25	3	*13,00 TL*	*1457,25*
2	26,00	1,5	52	1352	1,25	3	*13,00 TL*	*1353,25*
3	24,00	1,5	52	1248	1,25	3	*13,00 TL*	*1249,25*
4	22,00	1,5	52	1144	1,25	3	*13,00 TL*	*1145,25*
5	26,00	1,5	49	1284	1,25	4	*14,00 TL*	*1285,22*
6	24,00	1,5	49	1185	1,25	4	*14,00 TL*	*1186,45*
7	22,00	1,5	49	1086	1,25	4	*14,00 TL*	*1087,68*
7-8	30,00	1,5	49	1482	1,25	4	*14,00 TL*	*1482,75*
8	20,00	1,5	49	988	1,25	4	*14,00 TL*	*988,92*
8-9	30,00	1,5	49	1482	1,25	4	*14,00 TL*	*1482,75*
9	18,00	1,5	49	889	1,25	4	*14,00 TL*	*890,15*
10	16,00	1,5	49	790	1,25	4	*14,00 TL*	*791,38*
11	14,00	1,5	49	691	1,25	4	*14,00 TL*	*692,62*
						TOTAL [m]		*15092,91667*
						TOTAL COST		*206.096 TL*

Table H.4 : Cost analysis for the waler beams according to the old project.

Cost Analysis for 70x35 cm Waler Beams						
SECTION LENGTH [m]	CONCRETE C30/35 [m^3]	FORMWORK [m^2]	REBAR TOTAL LENGTH [m]		REBAR (ton)	
			Ø10/15 (Stirrups)	Ø18 (Longitudinal reinforcement)	Ø10	Ø18
309,46	75,82	216,62	309,46	337,31	0,191	0,674
518,53	127,04	362,97	518,53	565,19	0,320	1,129

Rebar cost	***2.314 TL***
Rebar labor cost	***278 TL***
Concrete cost	***16.229 TL***
Concrete labor cost	***2.029 TL***
Formwork cost	***11.592 TL***
TOTAL	***32.441 TL***

Table H.5 : Cost analysis for the waler beams according to the revised project.

Cost Analysis for 70x35 cm Waler Beams After Revision						
SECTION LENGTH [m]	CONCRETE C30/35 [m^3]	FORMWORK [m^2]	REBAR TOTAL LENGTH [m]		REBAR (ton)	
			Ø10/15 (Stirrups)	Ø18 (Longitudinal reinforcement)	Ø10	Ø18
309,46	75,82	216,62	309,46	337,31	0,191	0,674
518,53	127,04	362,97	518,53	565,19	0,320	1,129
148,15	36,30	103,71	148,15	161,48	0,091	0,323

Rebar cost	***2.728 TL***
Rebar labor cost	***327 TL***
Concrete cost	***19.132 TL***
Concrete labor cost	***2.392 TL***
Formwork cost	***13.666 TL***
TOTAL	***38.245 TL***

Table H.6 : Cost analysis for the cap beams.

Cost Analysis for 50x50 cm Cap Beams						
SECTION LENGTH [m]	CONCRETE C30/35 [m³]	FORMWORK *for one side* [m²]	REBAR TOTAL LENGTH [m]		REBAR (ton)	
			Ø10/15 (Stirrups)	Ø16 (Longitudinal reinforcement)	Ø10	Ø16
77,37	19,34	38,68	77,37	84,04	0,048	0,133
74,08	18,52	37,04	74,08	80,75	0,046	0,127

Rebar cost	***353 TL***
Rebar labor cost	***42 TL***
Concrete cost	***3.029 TL***
Concrete labor cost	***379 TL***
Formwork cost	***1.514 TL***
TOTAL	***5.318 TL***

Table H.7 : Cost estimation for Ø25mini piles.

Cost Estimation for Ø25cm Minipiles								
PILE LENGTH [m]	NUMBER OF PILES	DRILLING LENGTH [m]	CONCRETE C25/30 [m³]	REBAR [m]			REBAR [ton]	
				Ø10 (Stirrups)	Ø18 (Long. Rebar. with overlap.)	Ø18 (Long. Rebar) (loses+overlap.)	Ø10	Ø18
14	155	2274,678	111,60139	27779,18	47085,83	51794,42	17,140	103,485
19	148	2955,792	145,01855	36001,24	61184,89	67303,38	22,213	134,472

Rebar cost	***277.310 TL***
Rebar labor cost	***33.277 TL***
Concrete cost	***20.530 TL***
Concrete labor cost	***2.566 TL***
TOTAL	***333.683 TL***

Table H.8 : Cost comparison table.

Production type	Old Project	Revised Project	Difference
Mini piles	333.683,00 TL	333.683,00 TL	0,00 TL
Cap beam	5318,00 TL	5.318,00 TL	0,00 TL
Ground anchors	164.579,00 TL	206.096,00 TL	41.517,00 TL
Waler beams	34.441,00 TL	38.245,00 TL	3.804,00 TL
Weep hole drilling 4.-5. waler beams		37,03 TL	37,03 TL
Shotcrete between 1.-2. waler beams		234,00 TL	234,00 TL
Shotcrete between 2.-3. waler beams		234,00 TL	234,00 TL
	TOTAL INCREASE IN COST		**45.826,03 TL**
	% INCREASE IN COST		**8,52%**

APPENDIX I

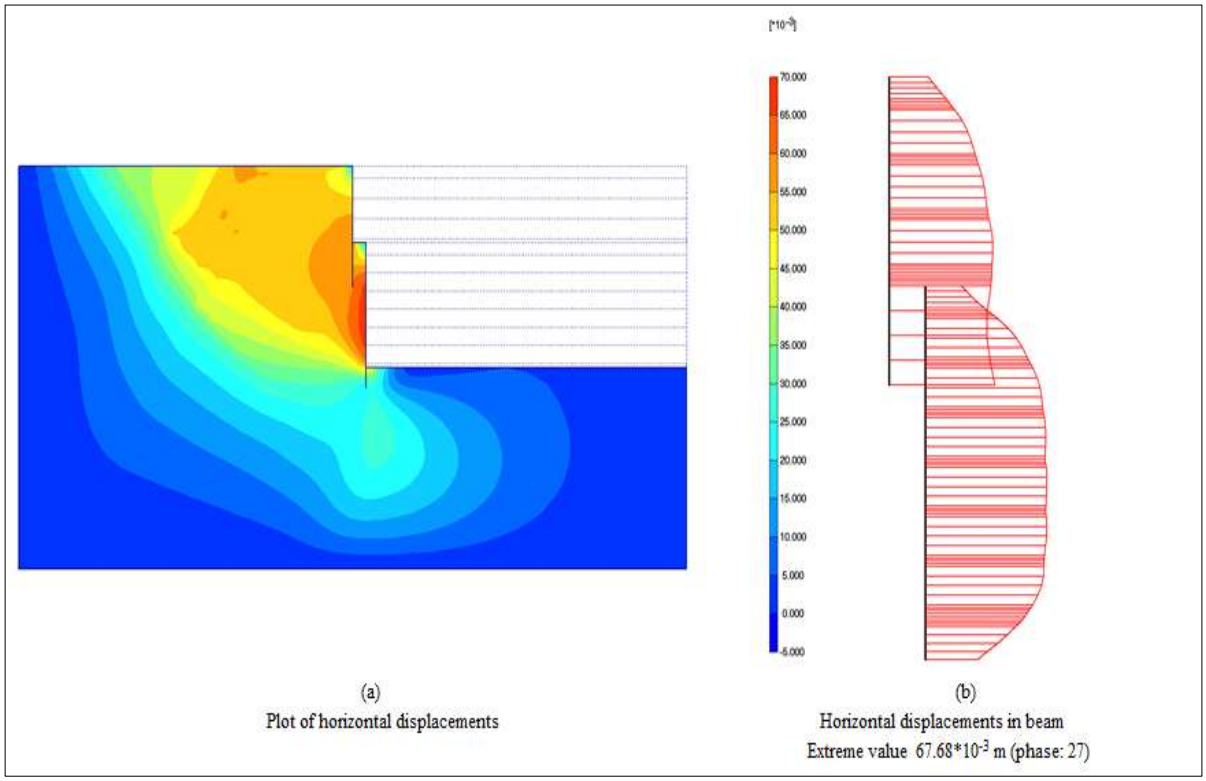

Figure I.1 : Horizontal displacements in beam for E=20 MPa.

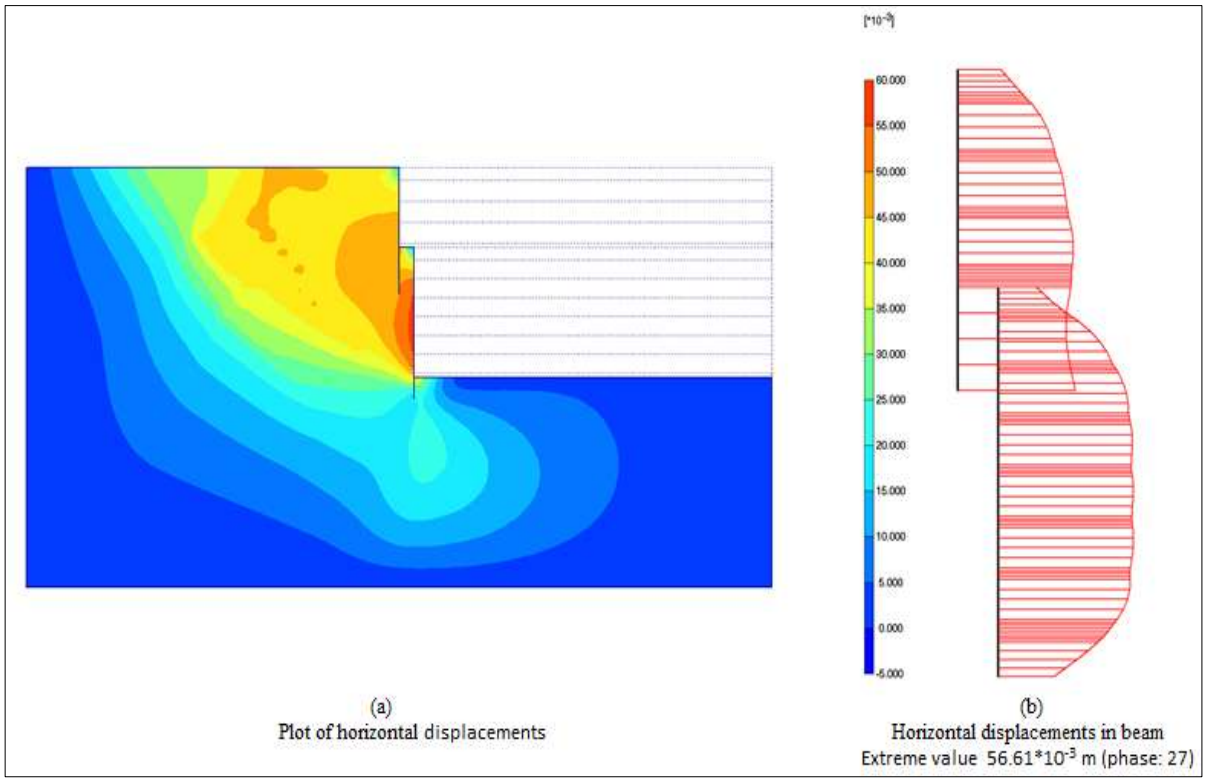

Figure I.2 : Horizontal displacements in beam for E=25 MPa.

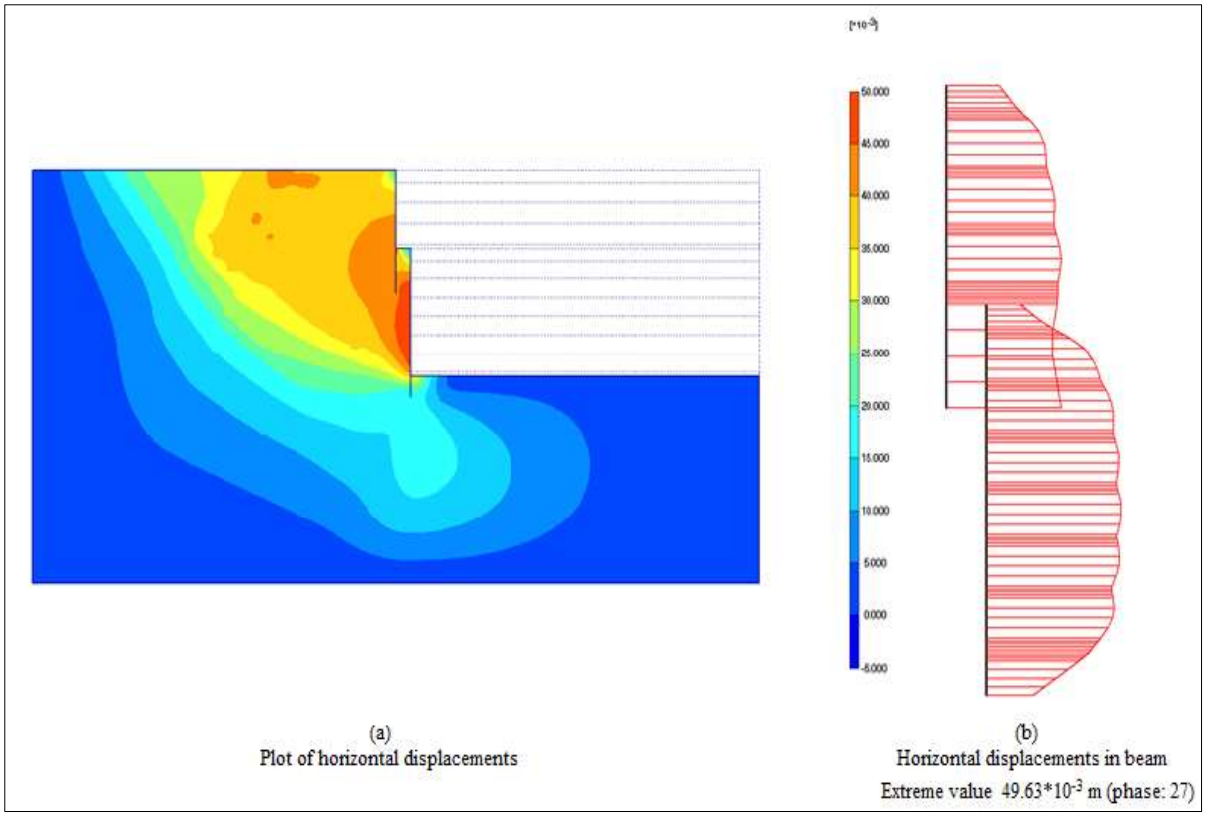

Figure I.3 : Horizontal displacements in beam for E=30 MPa.

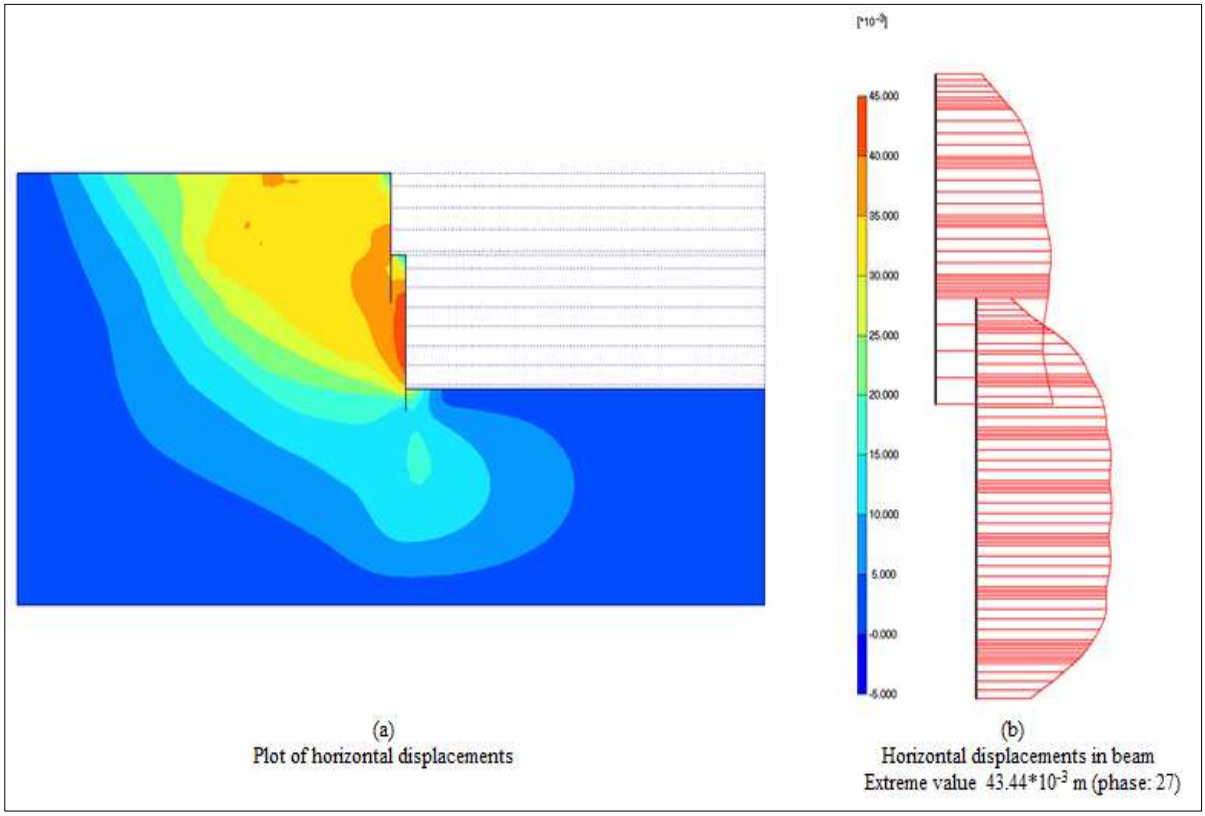

Figure I.4 : Horizontal displacements in beam for E=35 MPa.

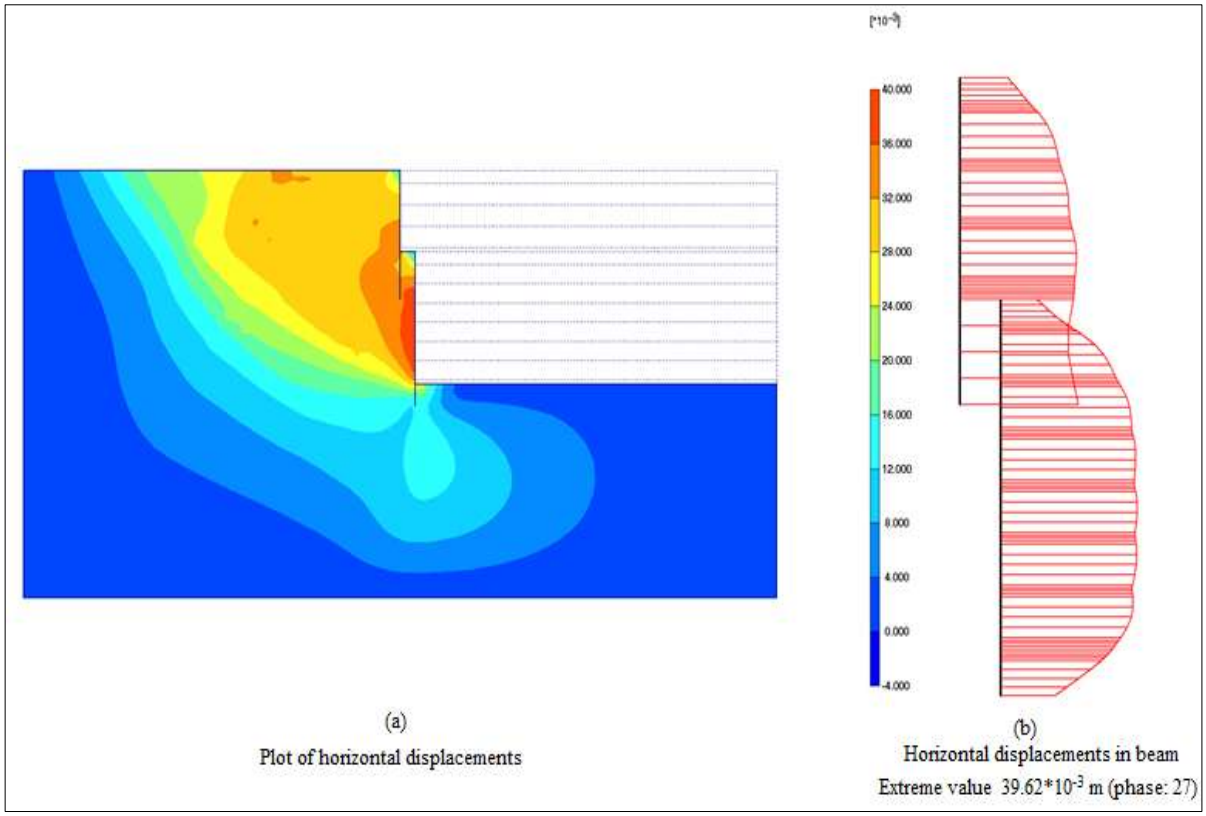

Figure I.5 : Horizontal displacements in beam for E=40 MPa.

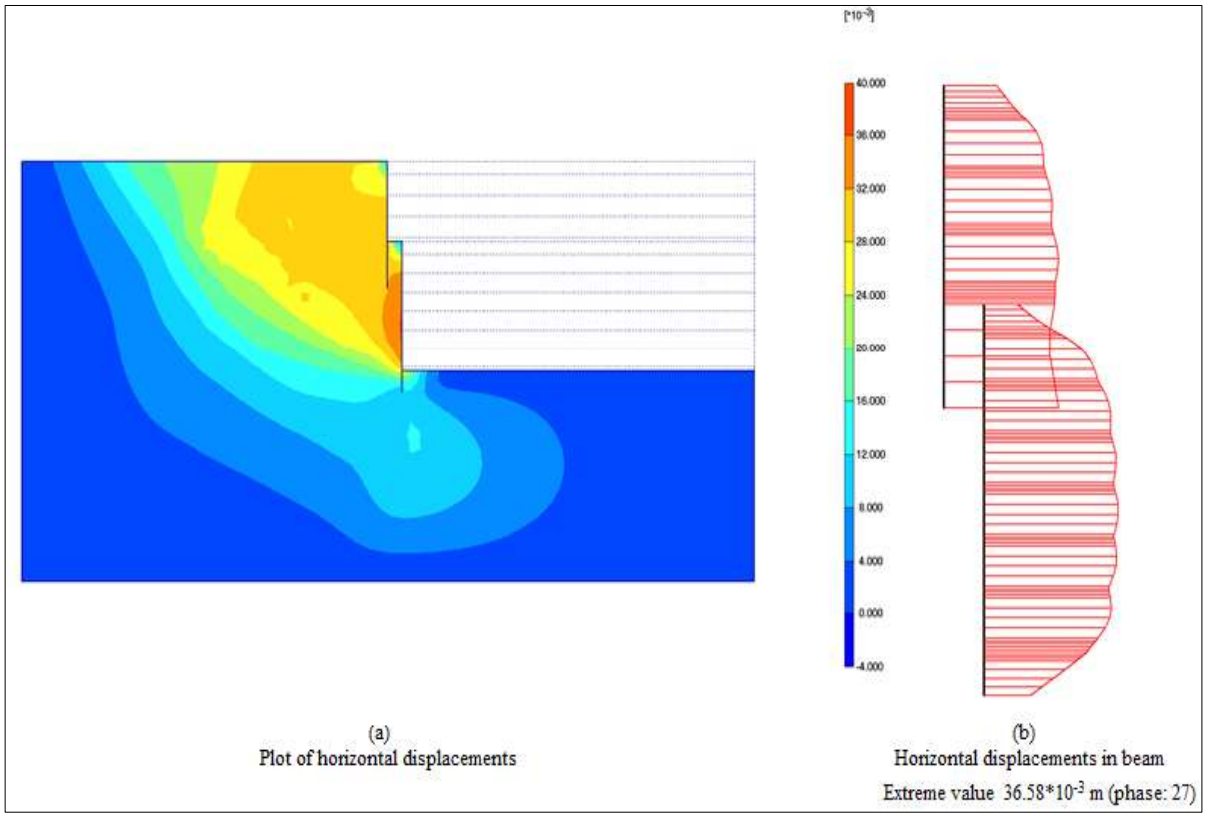

Figure I.6 : Horizontal displacements in beam for E=45 MPa.

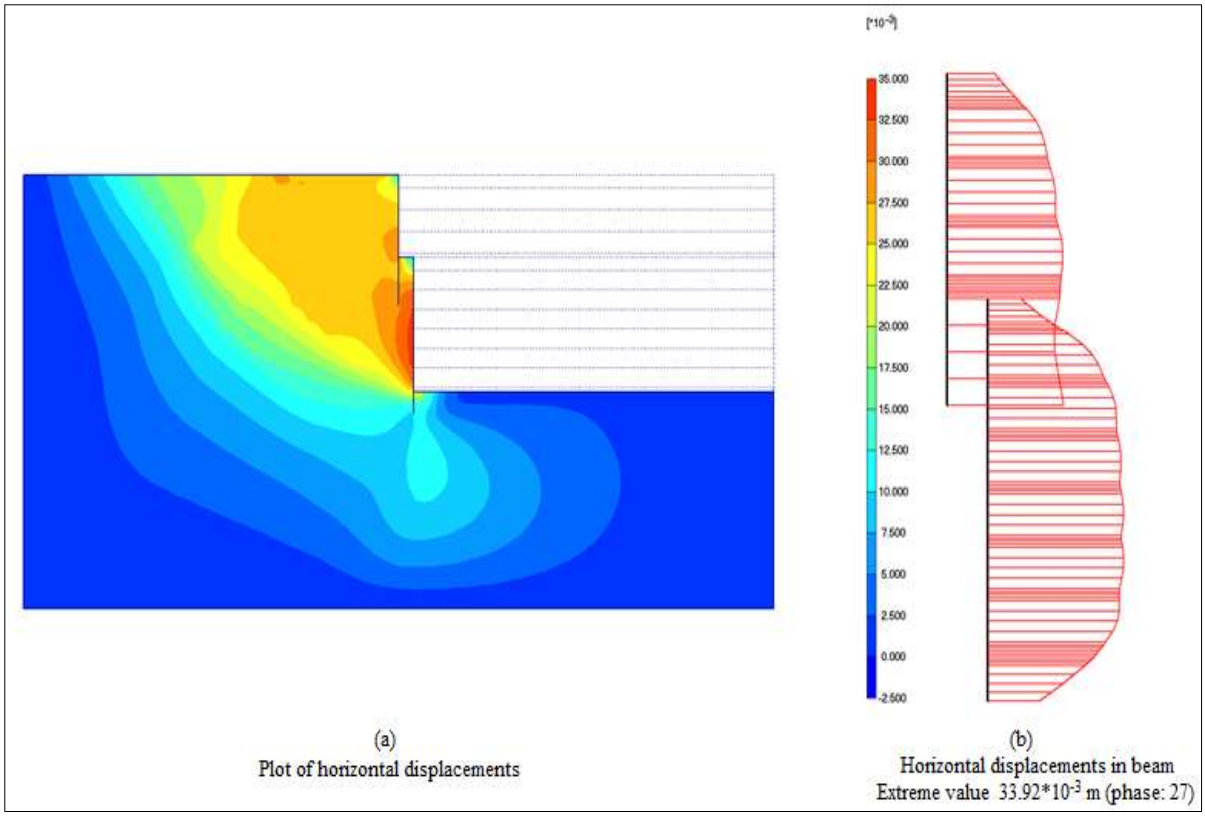

Figure I.7 : Horizontal displacements in beam for E=50 MPa.

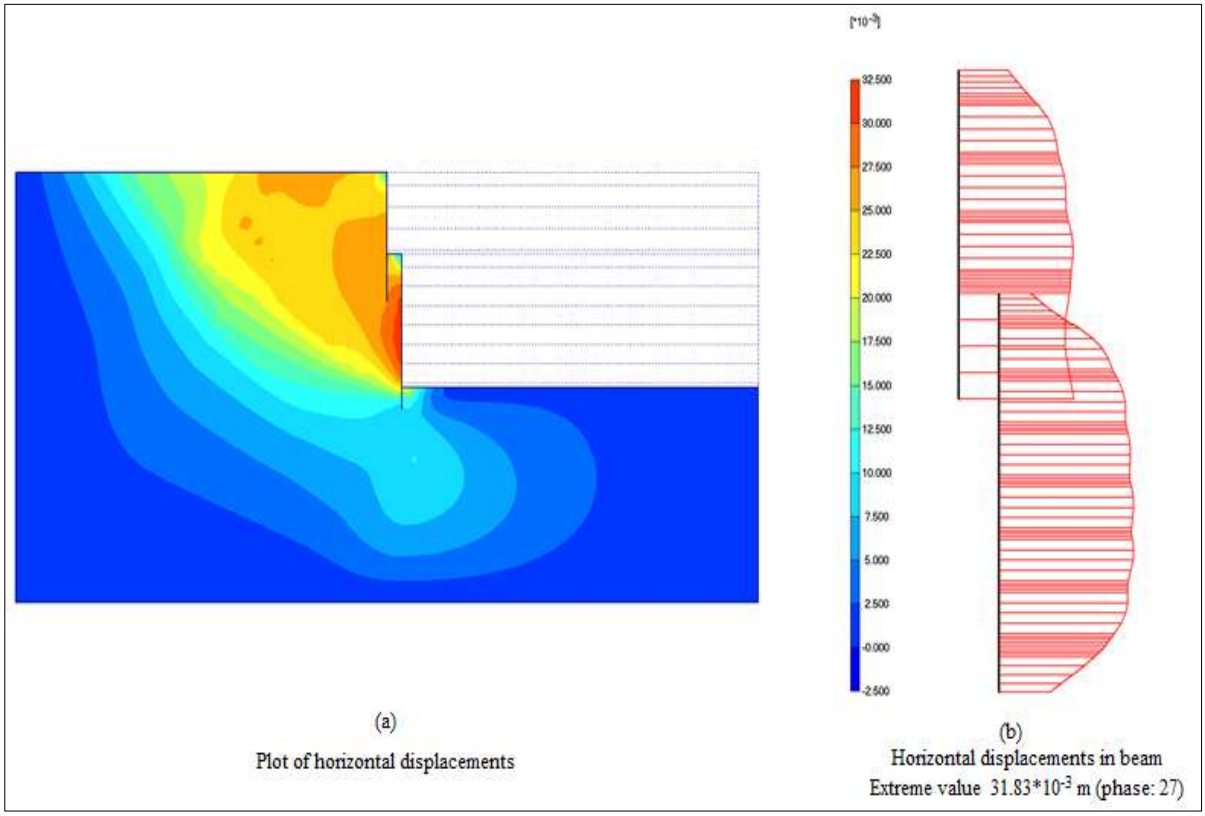

Figure I.8 : Horizontal displacements in beam for E=55 MPa.

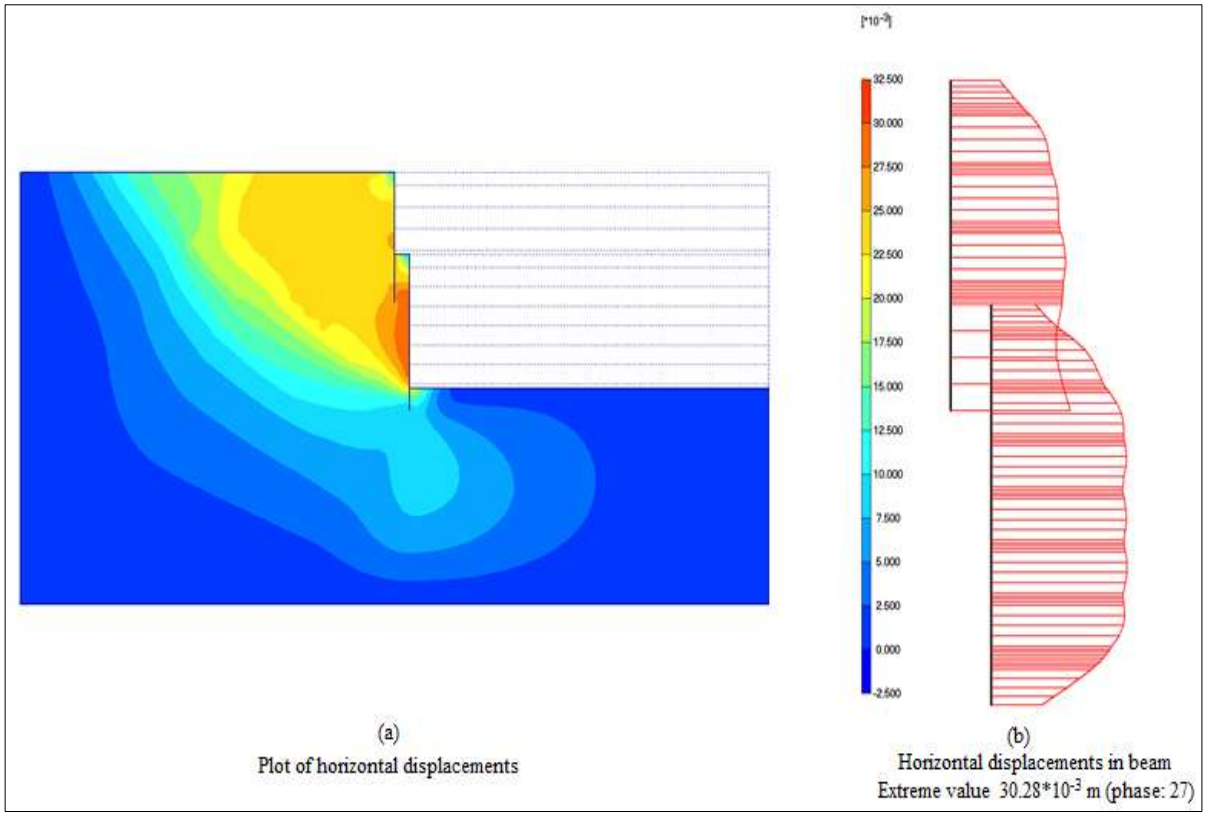

Figure I.9 : Horizontal displacements in beam for E=60 MPa.

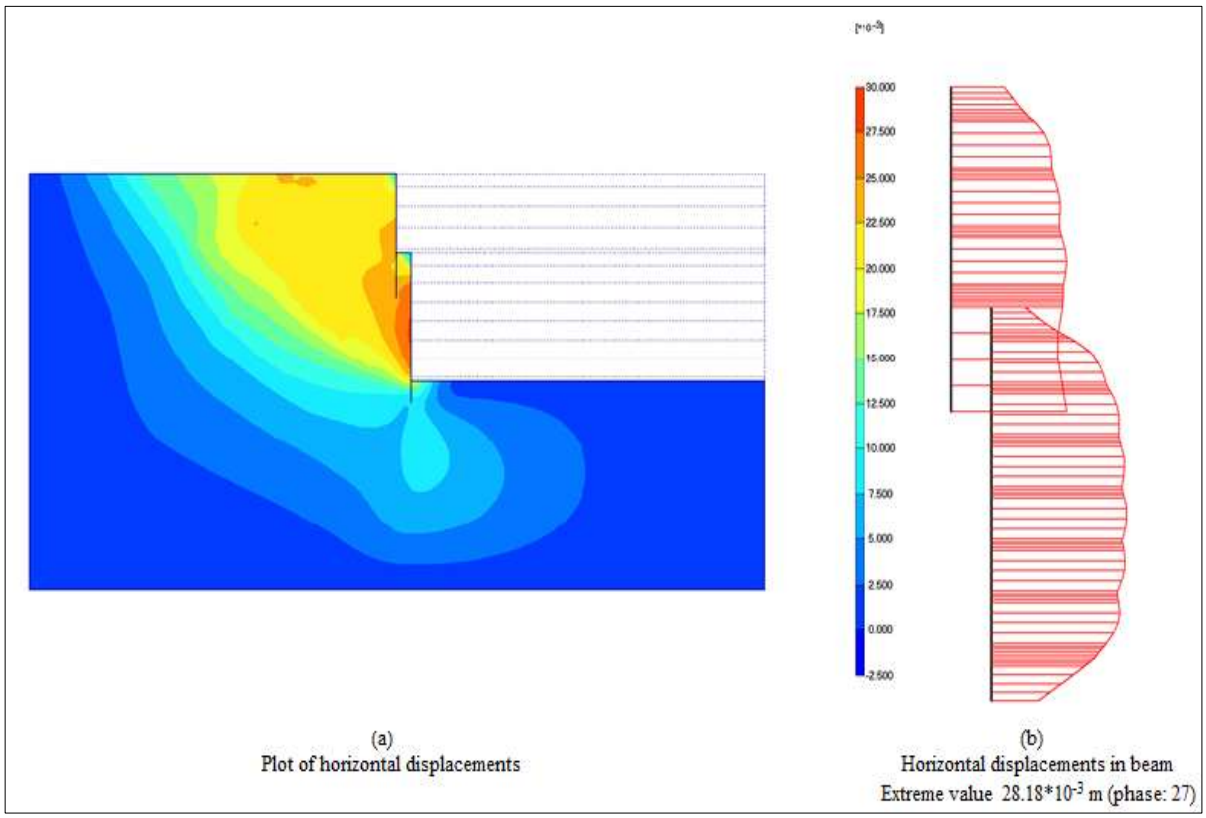

Figure I.10 : Horizontal displacements in beam for E=65 MPa.

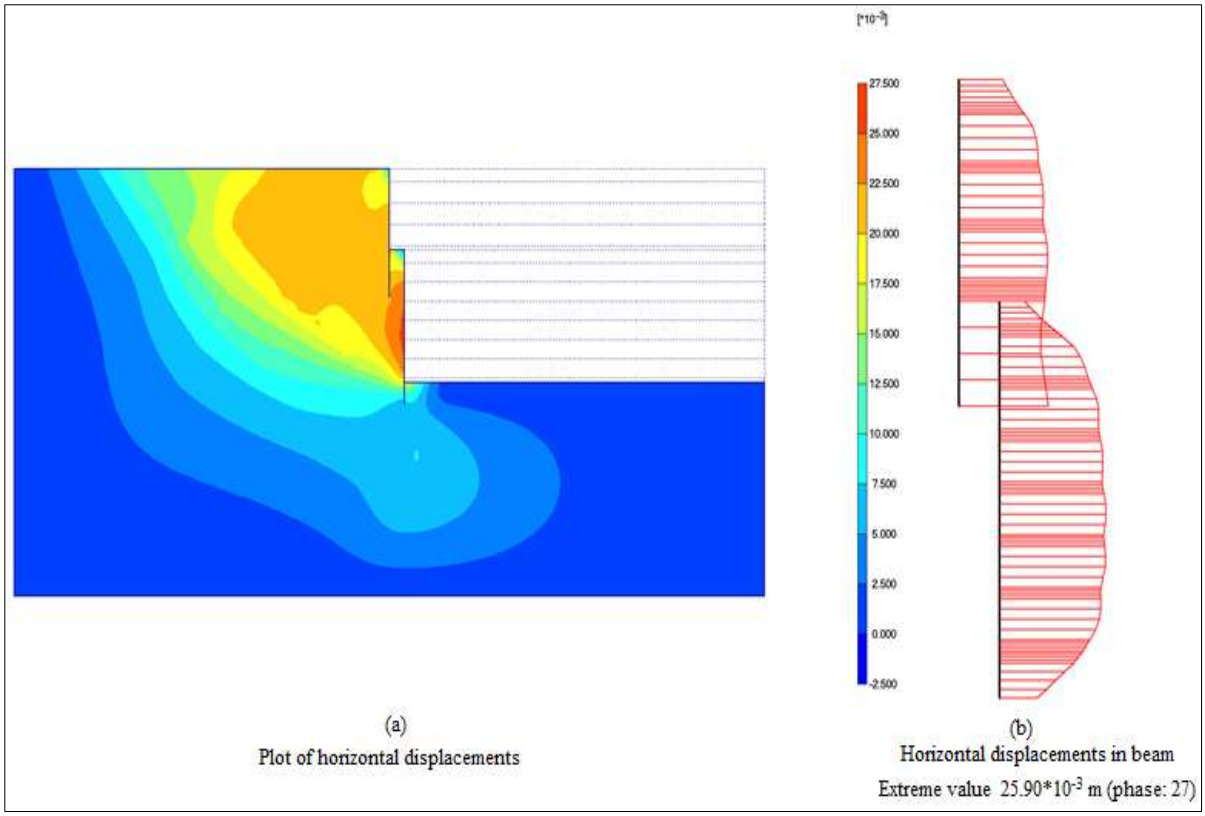

Figure I.11 : Horizontal displacements in beam for E=70 MPa.

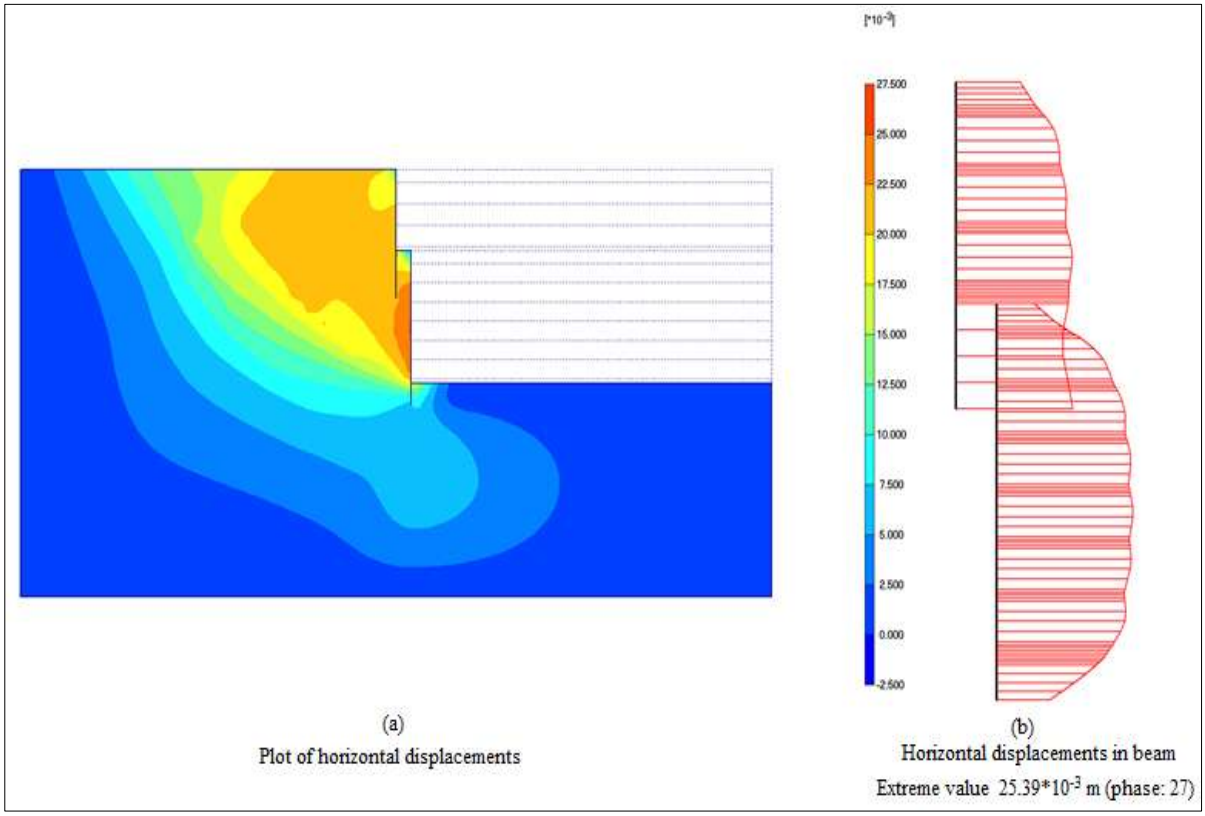

Figure I.12 : Horizontal displacements in beam for E=75 MPa.

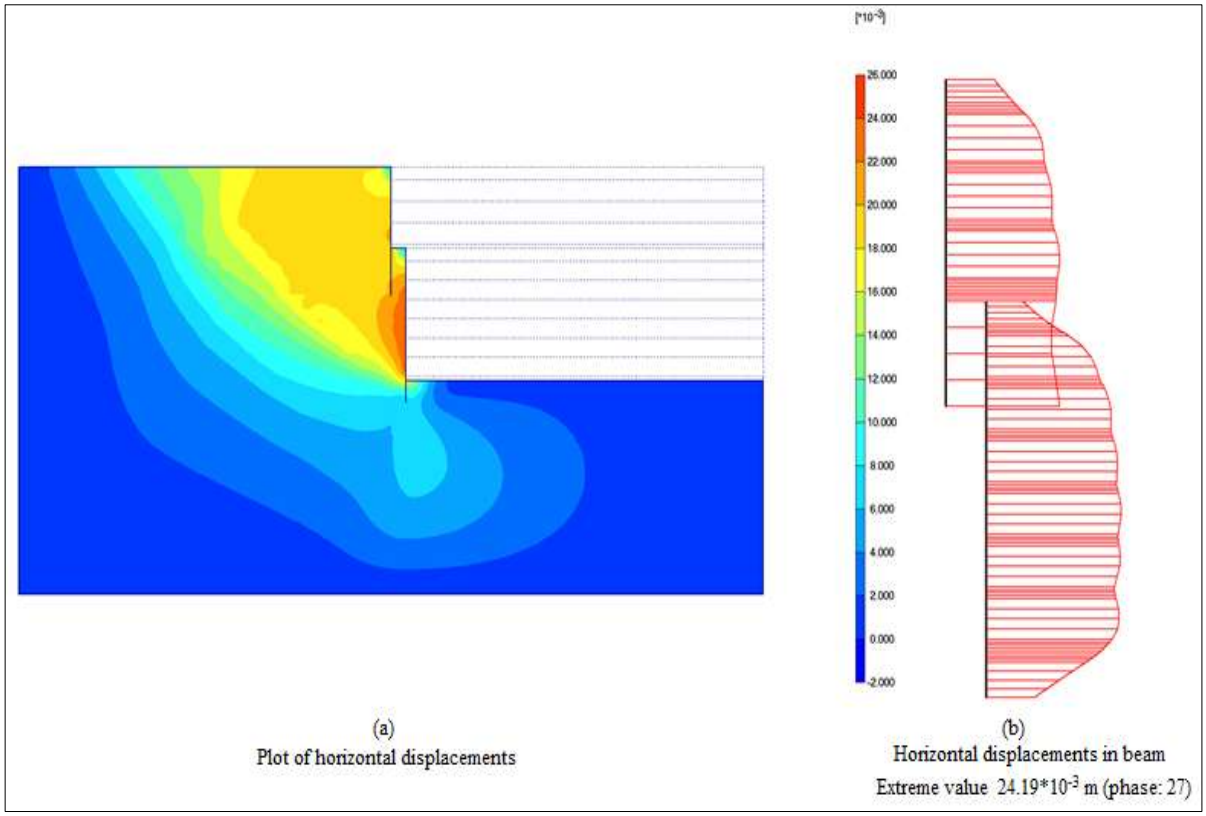

Figure I.13 : Horizontal displacements in beam for E=80 MPa.

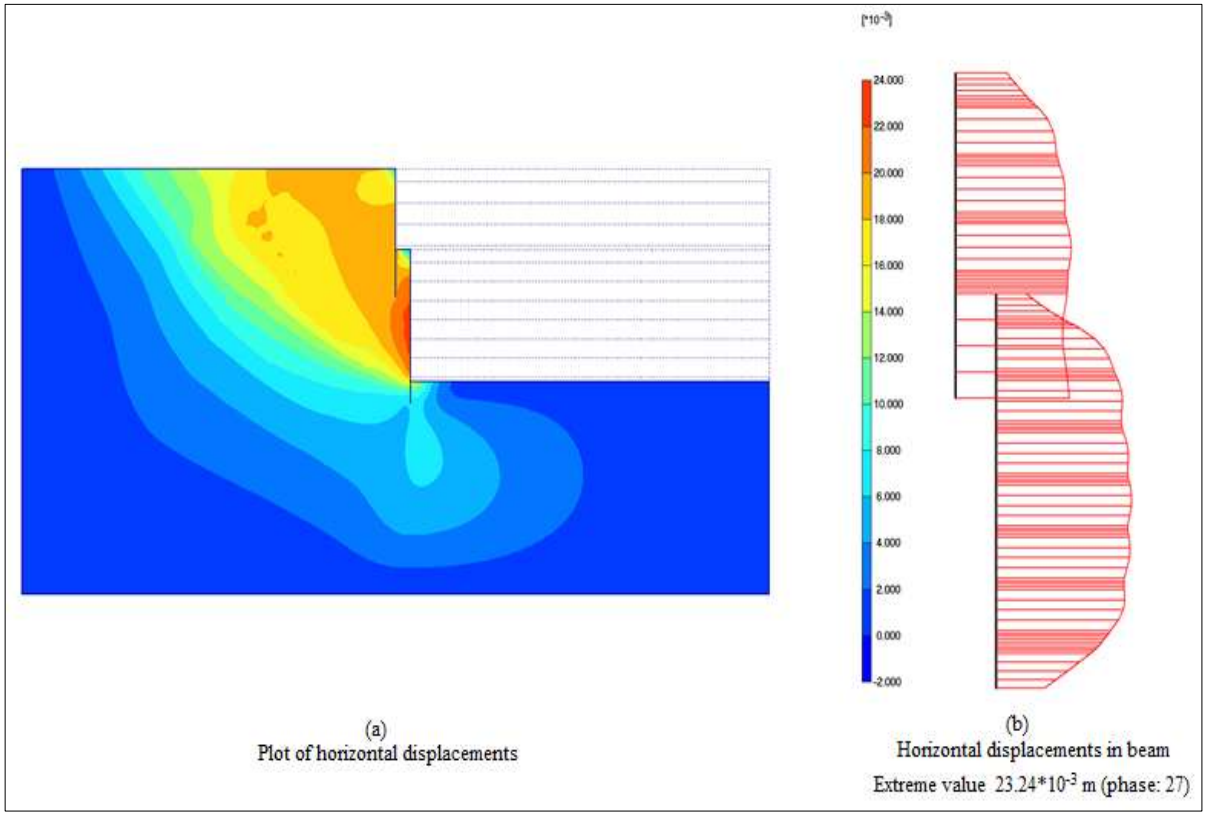

Figure I.14 : Horizontal displacements in beam for E=85 MPa.

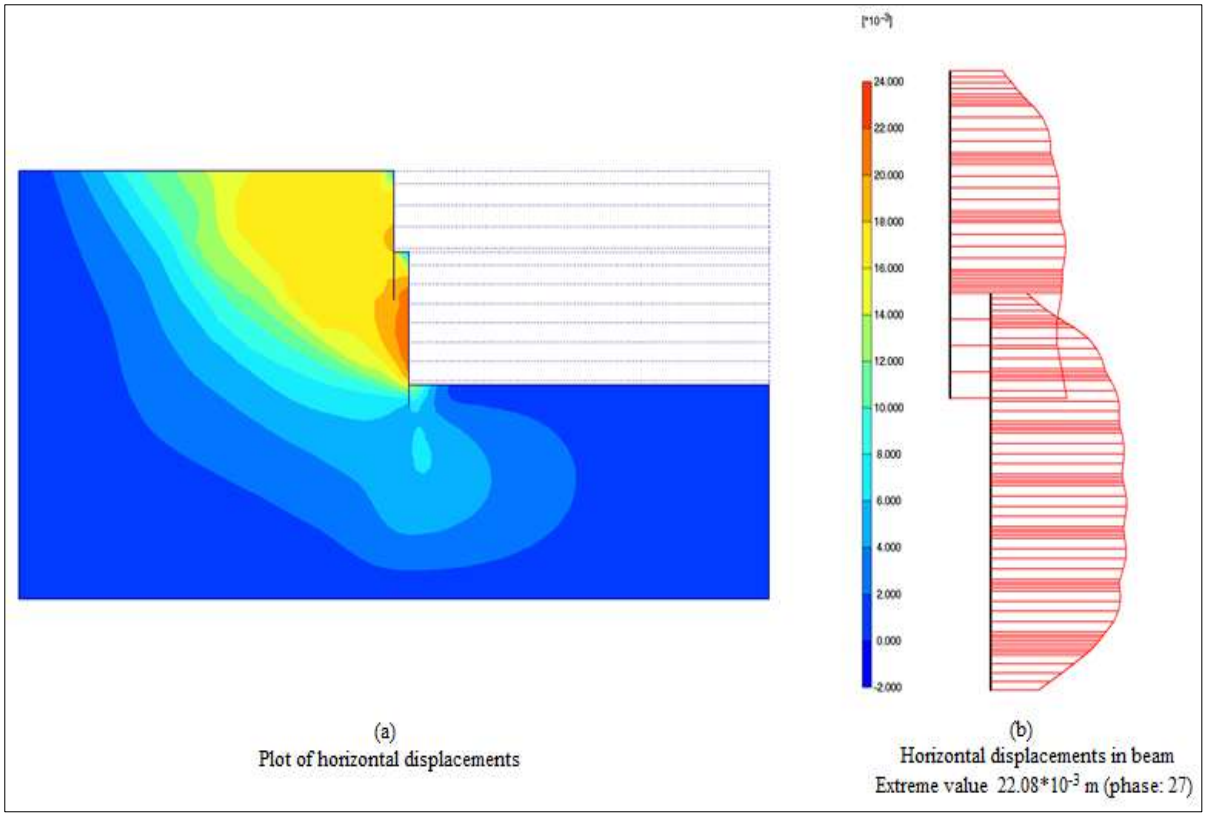

Figure I.15 : Horizontal displacements in beam for E=90 MPa.

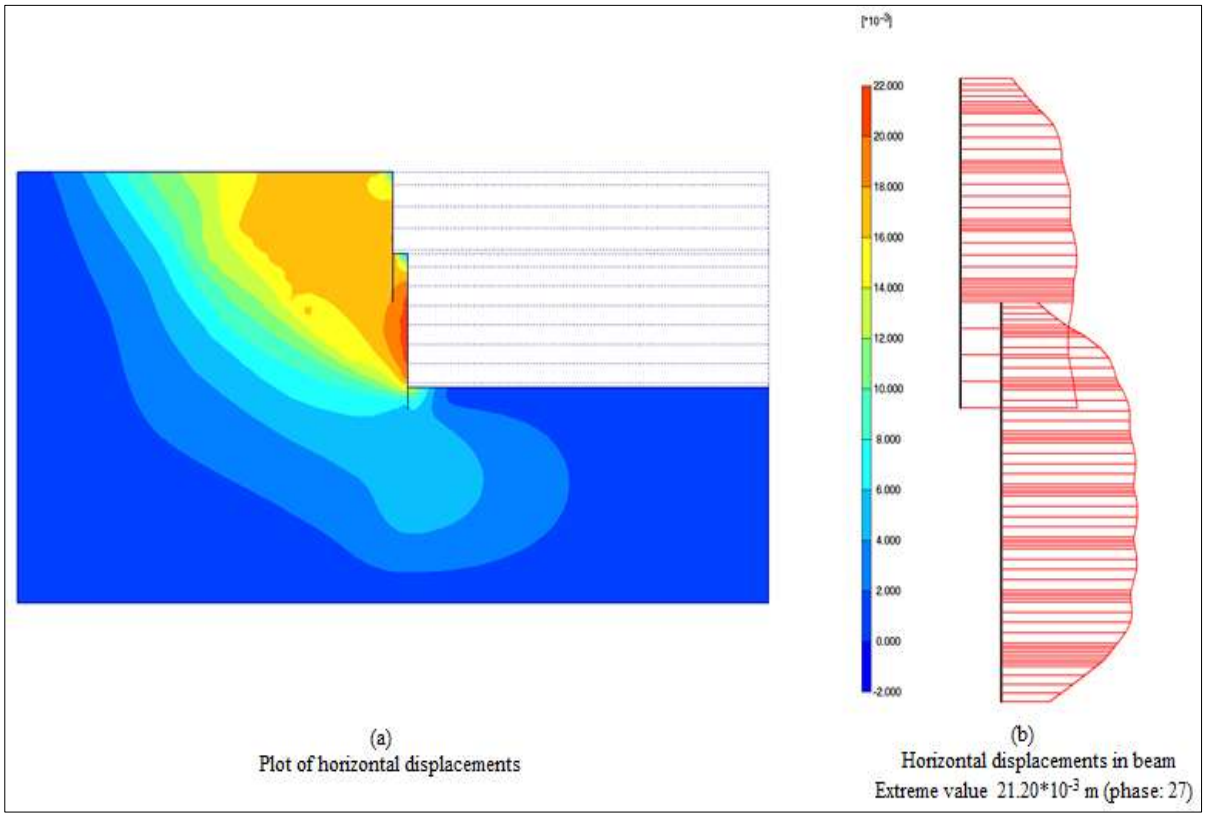

Figure I.16 : Horizontal displacements in beam for E=95 MPa.

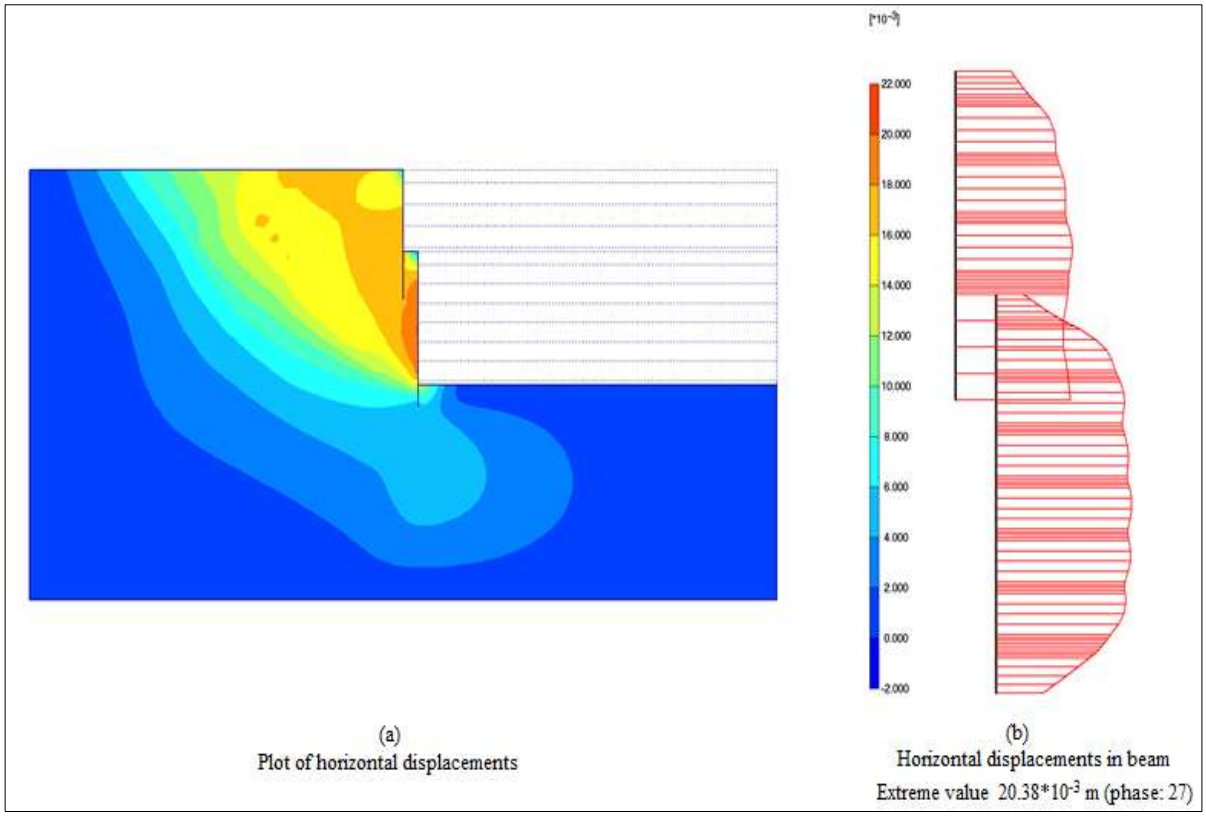

Figure I.17 : Horizontal displacements in beam for E=100 MPa.

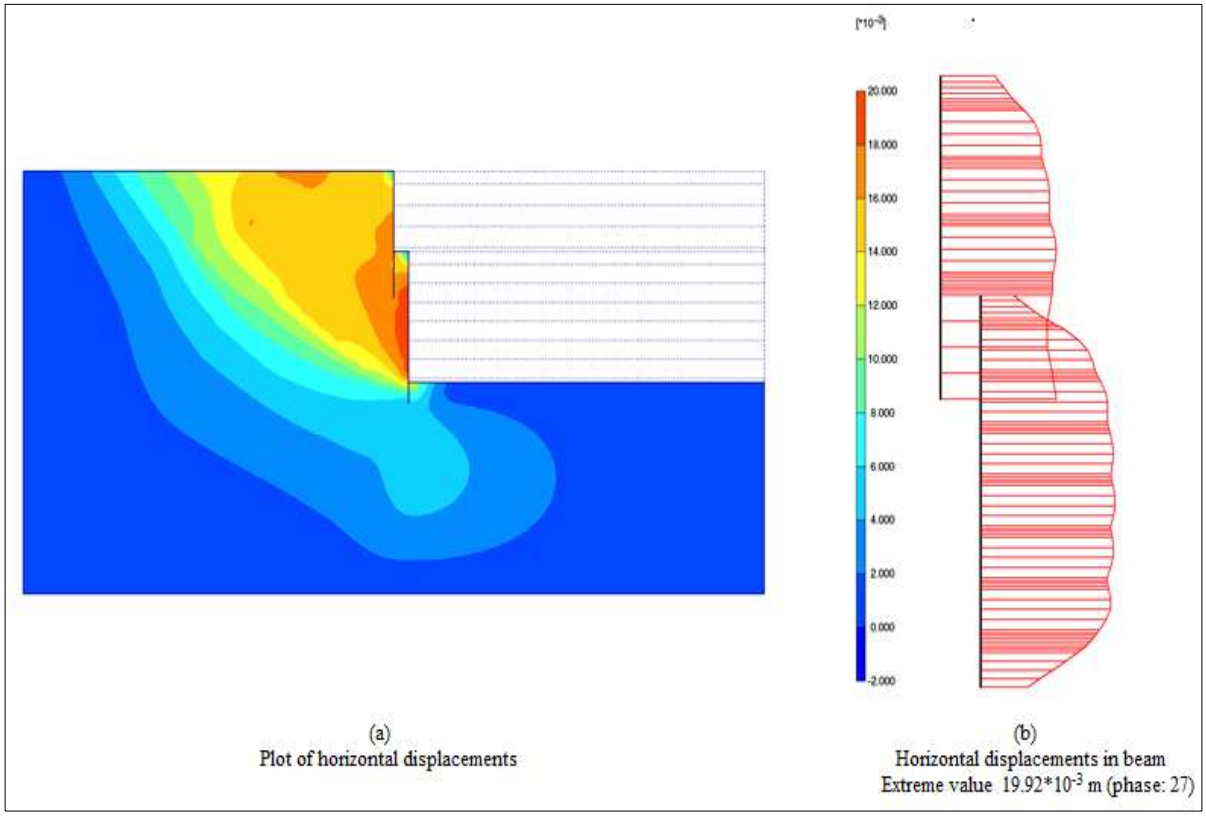

Figure I.18 : Horizontal displacements in beam for E=105 MPa.

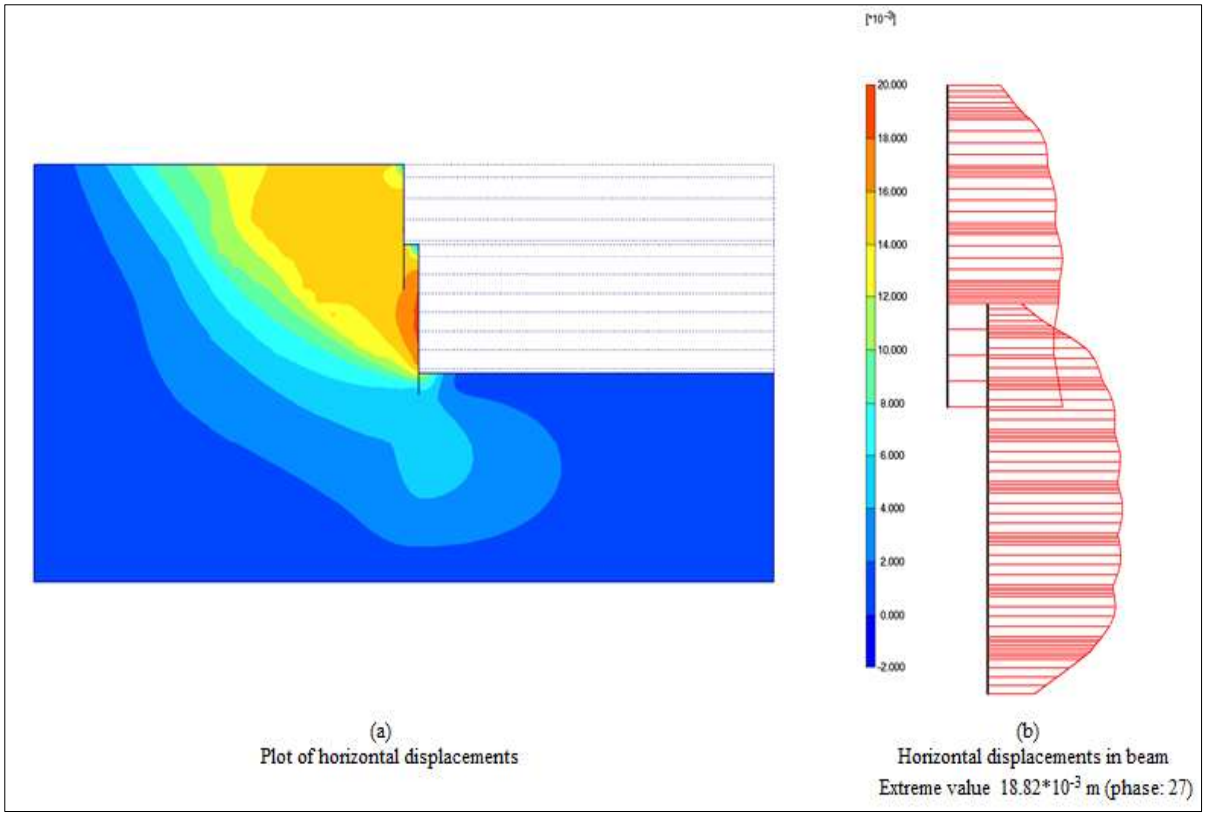

Figure I.19 : Horizontal displacements in beam for E=110 MPa.

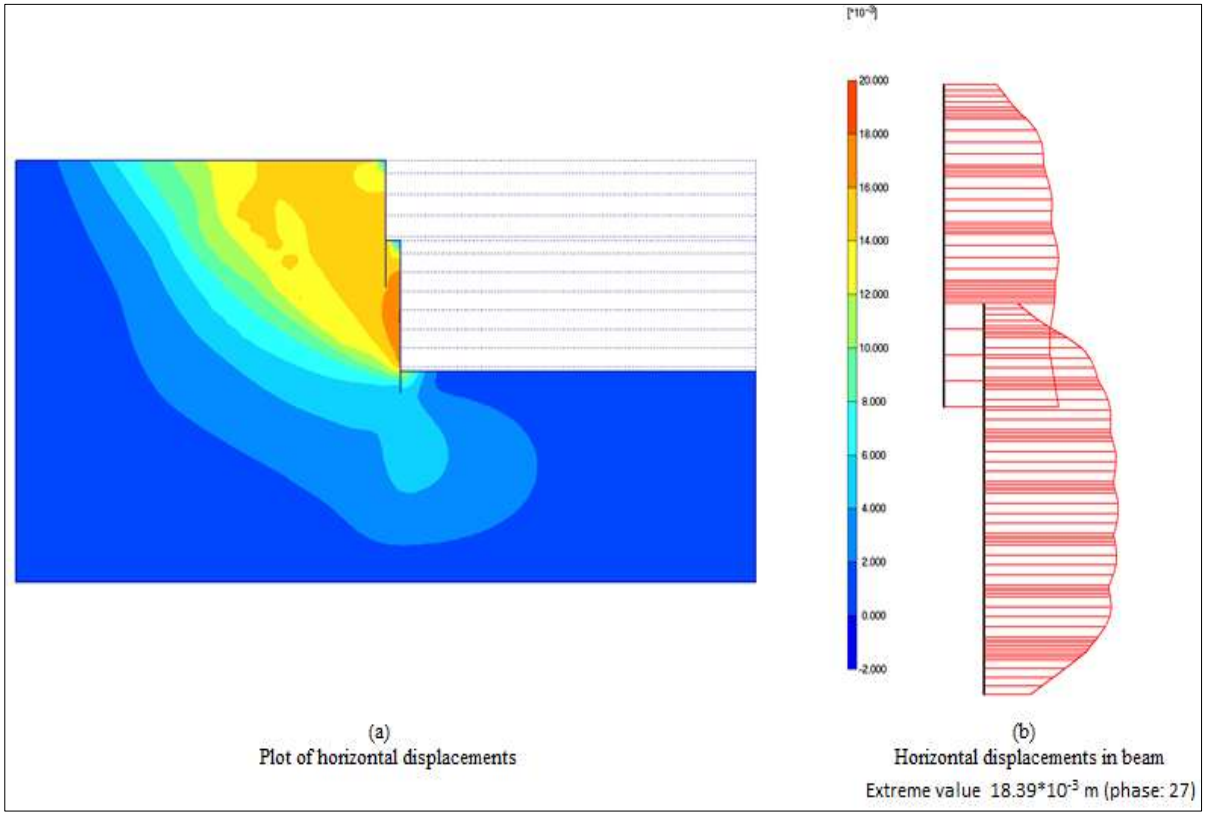

Figure I.20 : Horizontal displacements in beam for E=115 MPa.

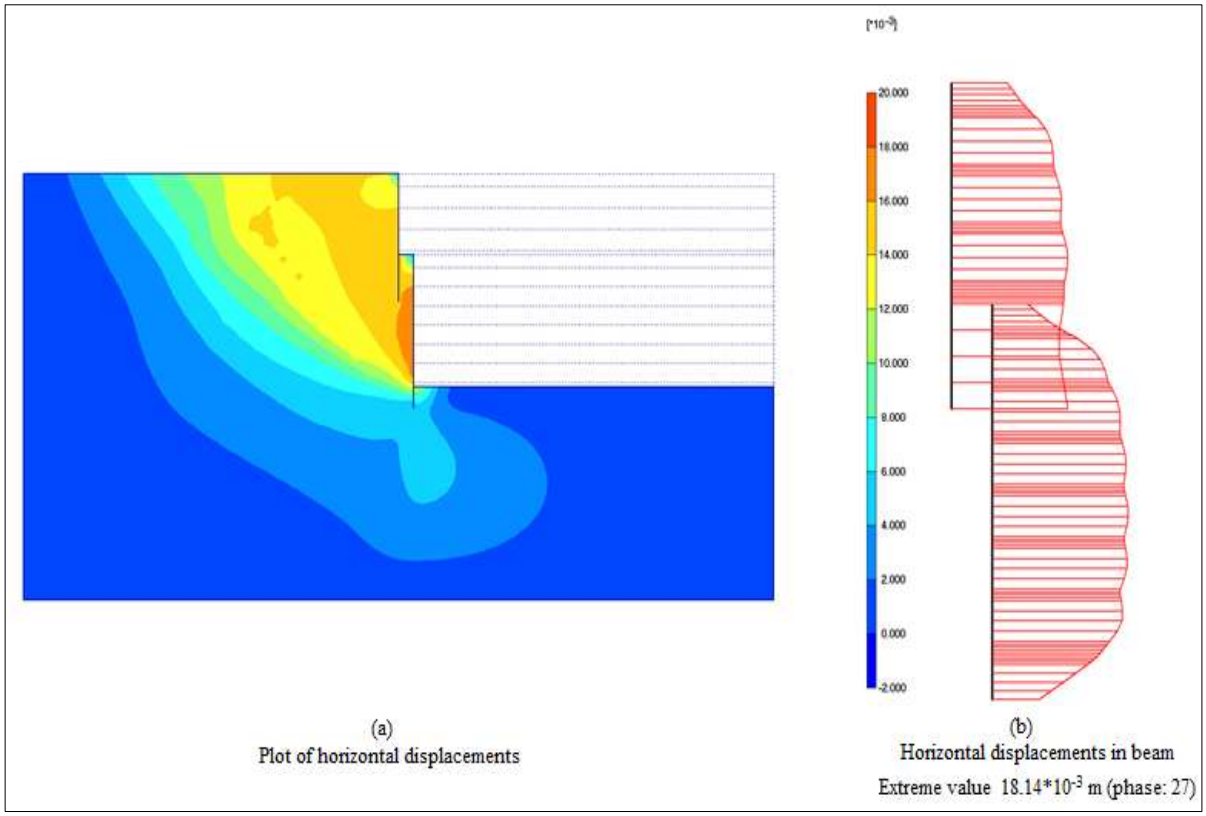

Figure I.21 : Horizontal displacements in beam for E=120 MPa.

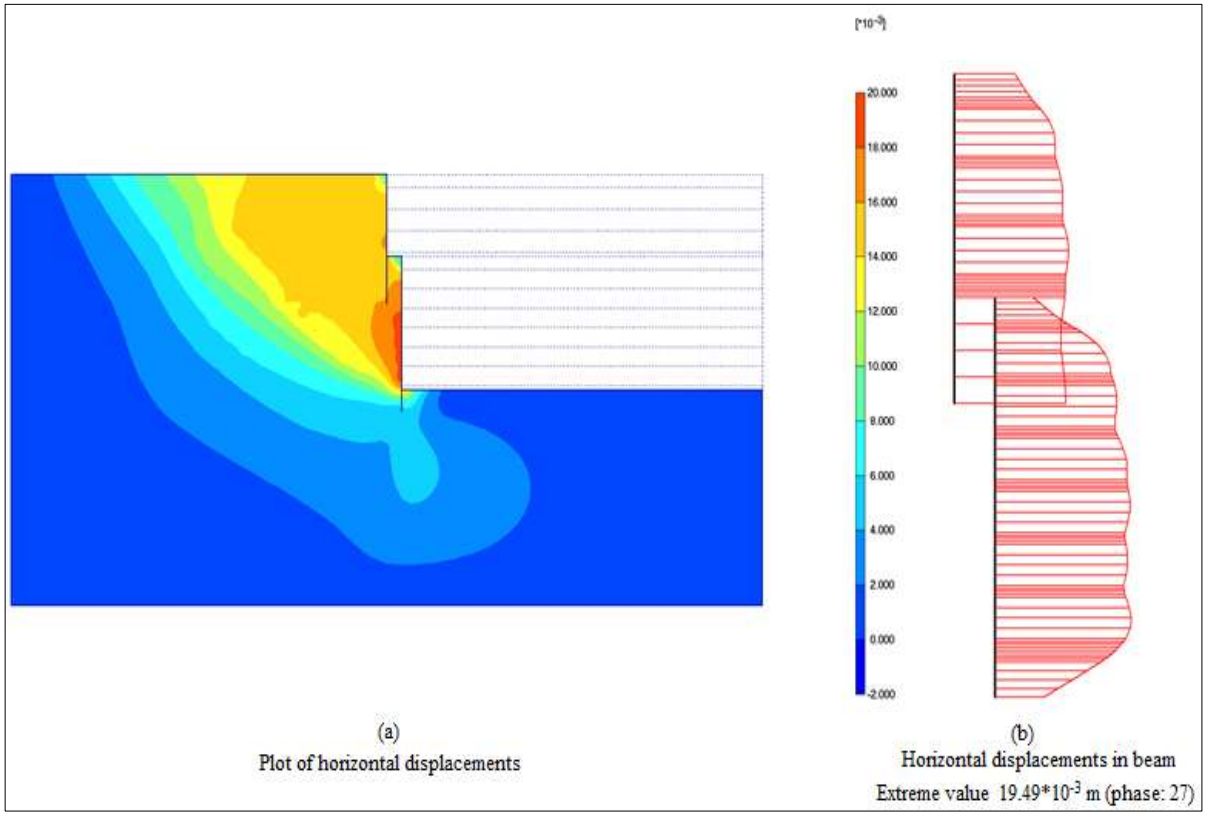

Figure I.22 : Horizontal displacements in beam for E=125 MPa.

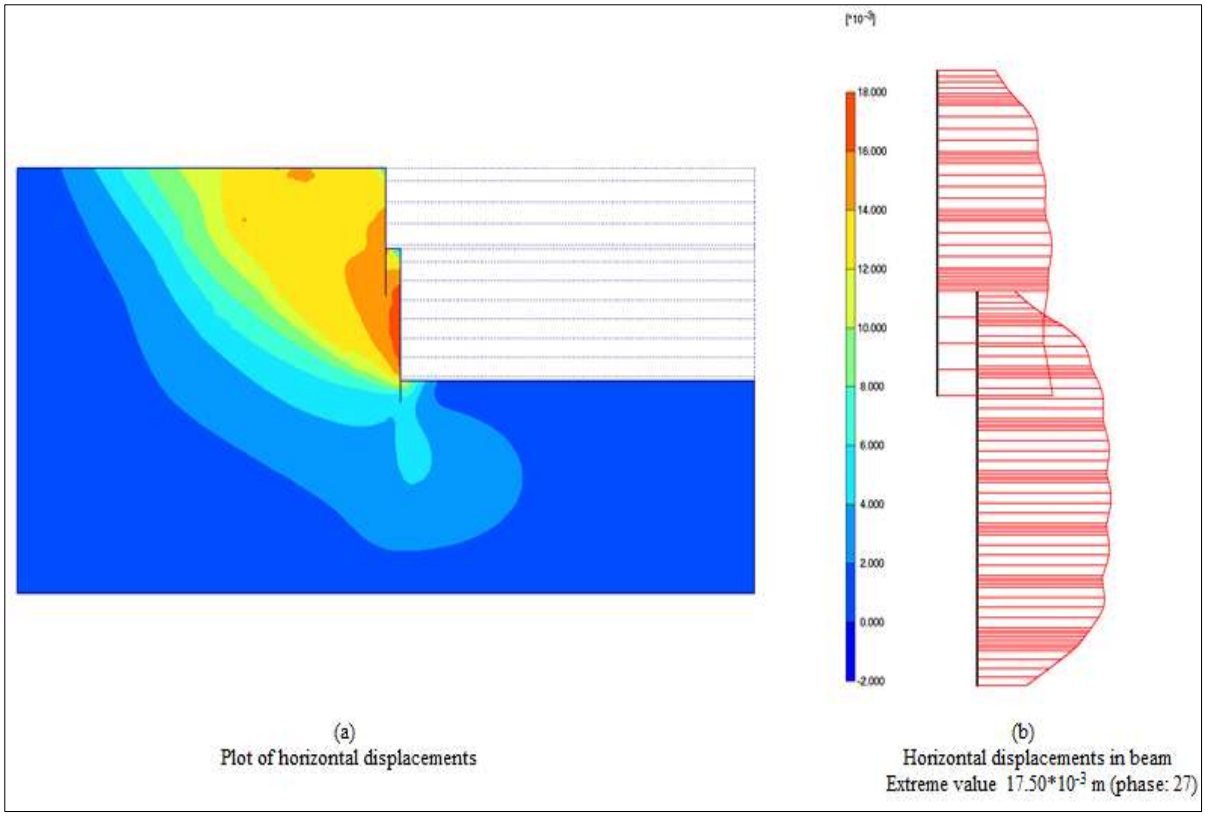

Figure I.23 : Horizontal displacements in beam for E=130 MPa.

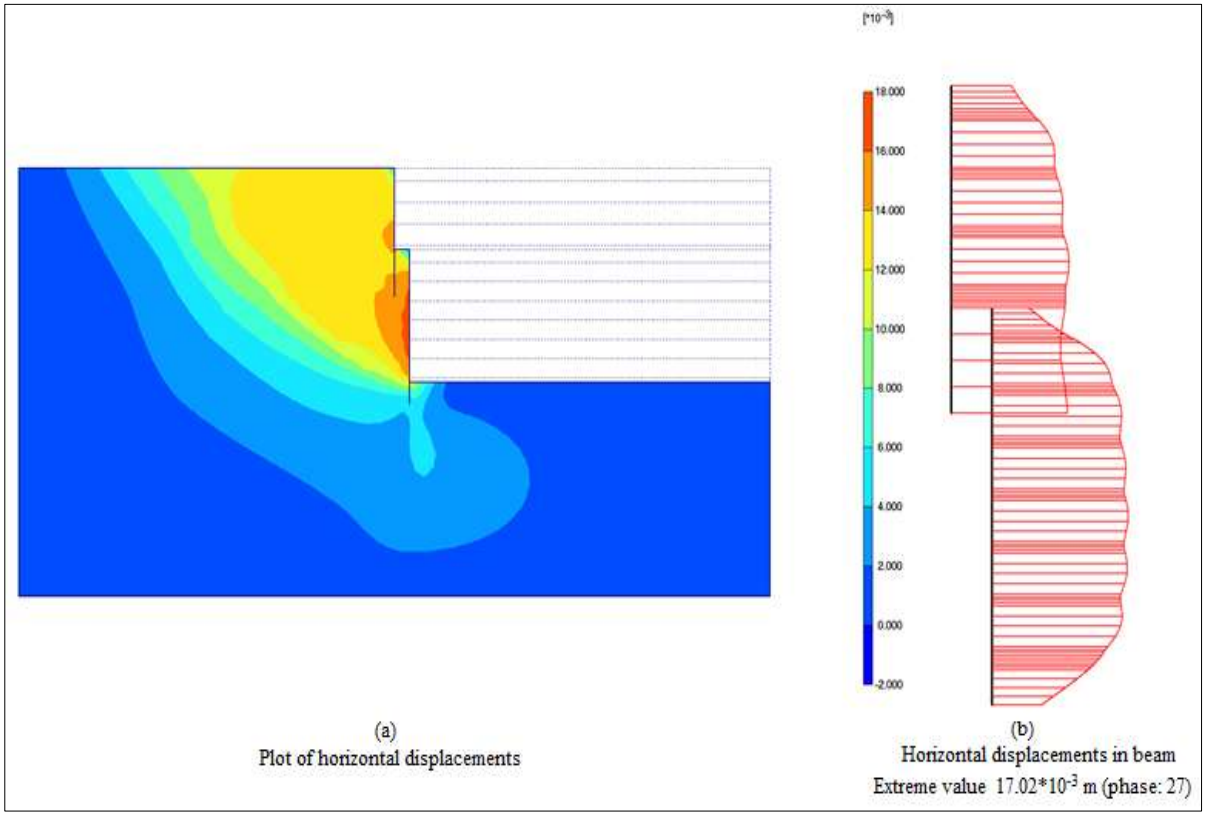

Figure I.24 : Horizontal displacements in beam for E=135 MPa.

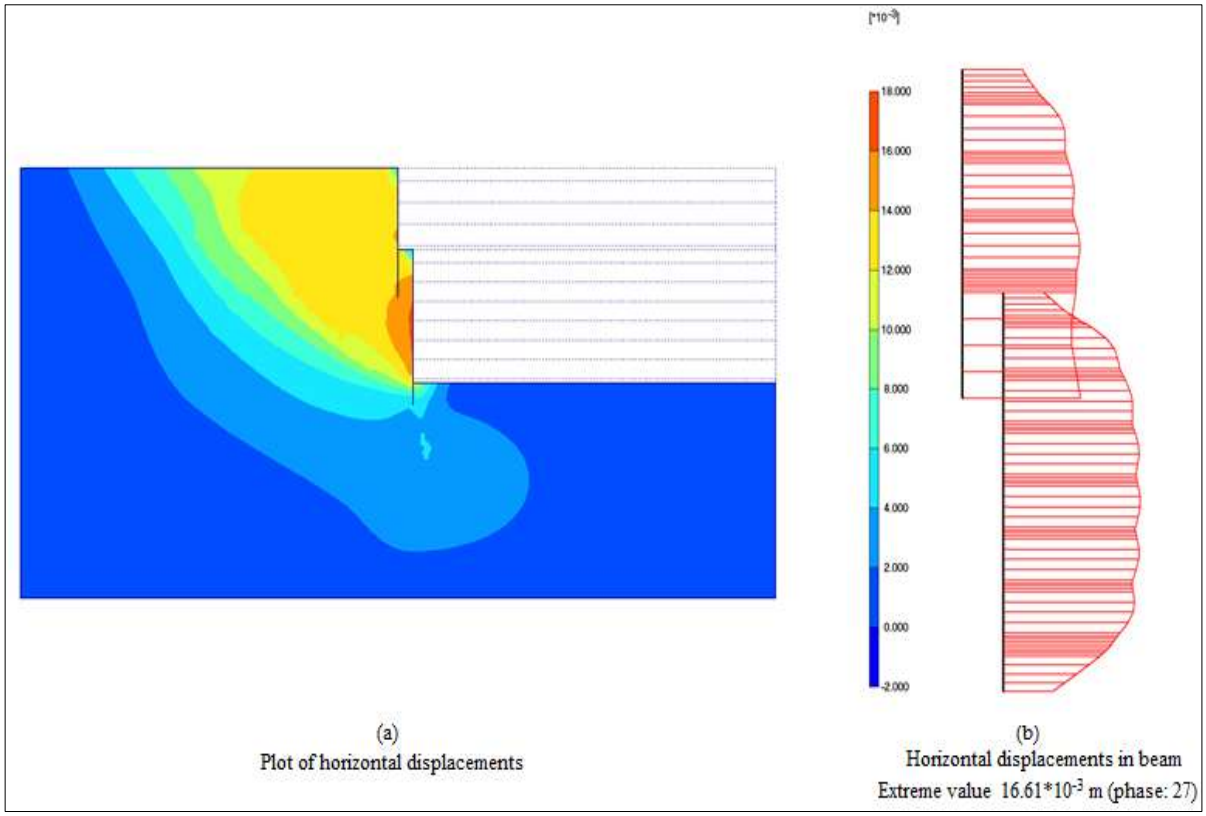

Figure I.25 : Horizontal displacements in beam for E=140 MPa.

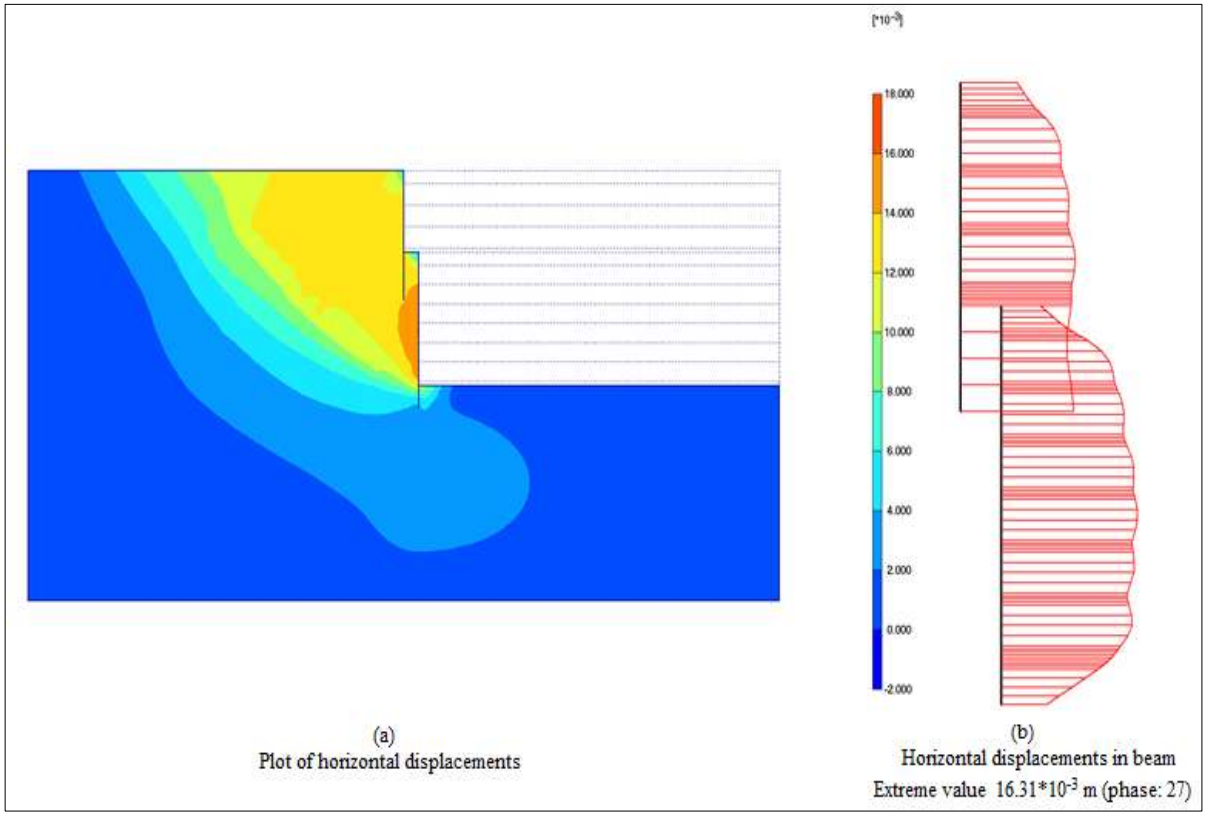

Figure I.26 : Horizontal displacements in beam for E=145 MPa.

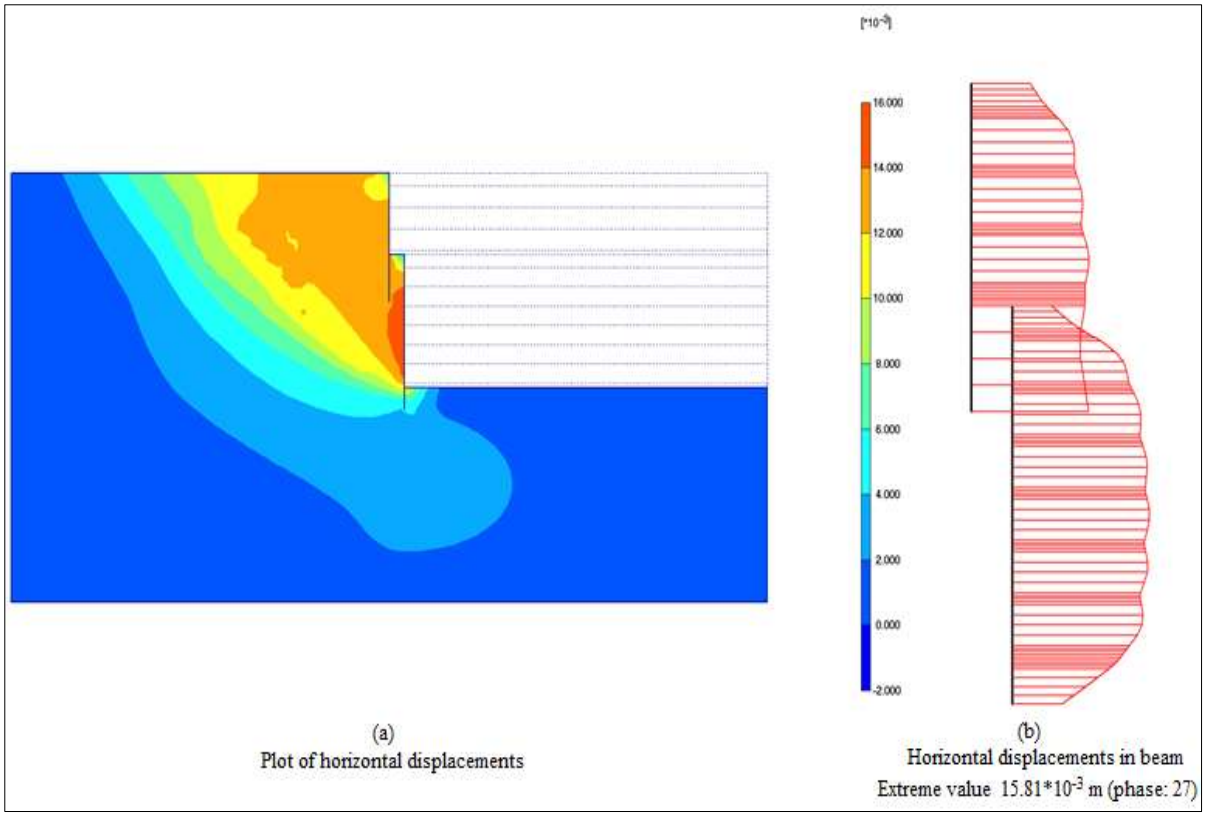

Figure I.27 : Horizontal displacements in beam for E=150 MPa.

CURRICULUM

VITAE

Name Surname: Ece AKTAN

Place and Date of Birth: Istanbul, 1987

B.Sc.: Istanbul Technical University Civil Engineering Faculty

Professional Experience and Rewards:

- Civil/Site Engineer, B.Sc., Northern Marmara Motorway and 3rd Bosphorus Bridge Project, IC İçtaş – Astaldi JV., Istanbul, Turkey, 10.2013-present
- Civil/Site Engineer, B.Sc., Hilton Istanbul Bomonti Hotel and Conference Center Project, IC Holding Ictas Construction Co., Istanbul, Turkey, 03.2010-10.2013.
- Intern for rough construction works in Hilton Istanbul Bomonti Hotel and Conference Center Project, Ictas Construction Co., İstanbul, 2008.
- Intern for finishing works in Bosphorus Houses Project, Polat Construction Industry & Trade Inc., İstanbul, 2007.